2(mix)

01

III

E7.4-10632
CR-138742

WHEAT:

ITS WATER USE, PRODUCTION AND DISEASE DETECTION AND PREDICTION

COMPLETION REPORT

1974

(E74-10632) WHEAT: ITS WATER USE, PRODUCTION AND DISEASE DETECTION AND PREDICTION Completion Report (Kansas State Univ.) 238 p HC $15.00 CSCL 02C G3/13

N74-27795
THRU
N74-27800
Unclas
00632

1060C

05

238

KANSAS ENVIRONMENTAL AND RESOURCE
STUDY: A GREAT PLAINS MODEL

Wheat: Its Water Use, Production and Disease
Detection and Prediction

Edward T. Kanemasu
Evapotranspiration Laboratory
Kansas State University
Manhattan, Kansas 66506

February 5, 1974
Completion Report
Report No. 2263-3

Prepared for
NATIONAL AERONAUTICS AND SPACE
ADMINISTRATION

GODDARD SPACE FLIGHT CENTER

GREENBELT, MARYLAND 20771

TECHNICAL REPORT STANDARD TITLE PAGE

1. Report No. 2263-3	2. Government Accession No.	3. Recipient's Catalog No.
4. Title and Subtitle: Wheat: Its Water Use, Production and Disease Detection and Prediction		5. Report Date: February 5, 1974
		6. Performing Organization Code
7. Author(s) E. T. Kanemasu, D. Lenhert, C. Niblett H. Manges, and M. G. Eversmeyer		8. Performing Organization Report No.
9. Performing Organization Name and Address: Kansas State University Manhattan, Kansas 66506		10. Work Unit No.
		11. Contract or Grant No. NAS5-21822
12. Sponsoring Agency Name and Address: NASA-GSFC Greenbelt, Maryland — Richard Stonesifer		13. Type of Report and Period Covered: Completion
		14. Sponsoring Agency Code

15. Supplementary Notes

16. Abstract

In this report are discussed (1) the effects of wheat disease on water use and yield, and (2) the use of ERTS-1 imagery in the evaluation of wheat growth and in the detection of disease severity.

Leaf area index was linearly correlated with ratios MSS4:MSS5 and MSS5:MSS6. In an area of severe wheat streak mosaic virus infected fields, correlations of ERTS-1 digital counts with wheat yields and disease severity levels were significant at the 5% level for MSS bands 4 and 5 and band ratios of 4/6 and 4/7.

Data collection platforms were used to gather meteorological data for the early prediction of rust severity and economic loss.

17. Key Words (Selected by Author(s))	18. Distribution Statement
Wheat, disease, water use, leaf area index	

19. Security Classif. (of this report)	20. Security Classif. (of this page)	21. No. of Pages	22. Price*

*For sale by the Clearinghouse for Federal Scientific and Technical Information, Springfield, Virginia 22151.

TABLE OF CONTENTS

TABLE OF CONTENTS (Continued)

LIST OF FIGURES

LIST OF TABLES

LIST OF TABLES (Continued)

Page

N74-27796

1.0 INTRODUCTION

This report includes data for the 1972 (October, 1971 to June, 1972) and 1973 (October, 1972 to June, 1973) growing season for winter wheat in Kansas. Obviously, there was no ERTS-1 imagery for the 1972 wheat crop since the satellite was launched July 23, 1972. However, under the PEIS (Pre-ERTS Investigator Support), we obtained three U-2 flights over our test areas (March 21, April 26 and June 6, 1972). The imagery was taken during the NASA-Ames to Wallop Island ferry trips. U-2 flight lines for each date differed and made chronological comparison of a given test area impossible; however, we were able to detect virus infected wheat fields on U-2 color infrared film. A systematic analysis of U-2 data was not possible because ground observations and U-2 flight lines did not always coincide. Since the actual U-2 film was not received until 3 months after the harvest, we could not generate the necessary ground truth.

In addition to the U-2 flights, the University of Kansas-CRINC (Center for Research, Inc.) provided three low altitude flights with a Cessna 182 equipped with four Hasselblad cameras. Cessna flight coverage was selected from ground observations of wheat fields. Diseased and healthy fields in the same frame were compared as to the date of planting, variety, disease severity, fertility, topography and crop rotation. In comparing many of healthy and diseased fields, a common denominator was crop rotation. For example, soil borne mosaic virus was more severe on fields that were cropped with wheat the previous year.

The 1973 Kansas wheat crop produced a record 381,000,000 bu with an average yield of 37.0 bu per acre which is attributed to a 10% increase over 1972 in both harvested acres and yield. Part of the increase in yield can be attributed to abundant soil moisture because of ample precipitation and the absence of severe disease epidemics over the state. The abnormally high precipitation adversely affected this project by (a) reducing water stress, (b) producing cool weather which affects disease infestation, and (c) association with clouds which affect quality of the imagery.

Efforts were concentrated in two of the five test areas: Finney County (Garden City) and Riley County (Manhattan), (Fig. 1.1). The Finney county site had a large area infected with wheat streak mosaic virus (WSMV). Riley county was the location of the data collection systems (DCS) and the plots for the energy balance determinations. We obtained 5 ERTS-1 observations for the WSMV area and 7 observations for the irrigated and nonirrigated wheat fields in Finney county. In addition, 8 observations were obtained for Riley county. Because of cloud cover during U-2 flights, no U-2 imagery was available for the entire 1973 wheat crop. Two sets of U-2 imagery were obtained after the wheat harvest.

Objectives of the investigation were: (a) to evaluate the effect of water stress, disease, and leaf area on the reflectance characteristics of wheat, (b) to evaluate disease losses in terms of yield and water use, and (c) to predict disease severity and economic loss.

In this report, the water use of irrigated and nonirrigated wheat and of healthy and diseased wheat are discussed in Chapter 2 (objective a and b). Data handling and reduction of ERTS-1 imagery is reported in a separate chapter (Chapter 3). The use of ERTS-1 imagery to determine leaf area, crop growth and disease severity is given in Chapter 4 and 5 (objective a and b). Prediction of disease severity and economic loss (objective c) by the use of ERTS-1 data collection systems is reported in Appendix A. Appendix C contains a detailed electronic description of the data collection interface

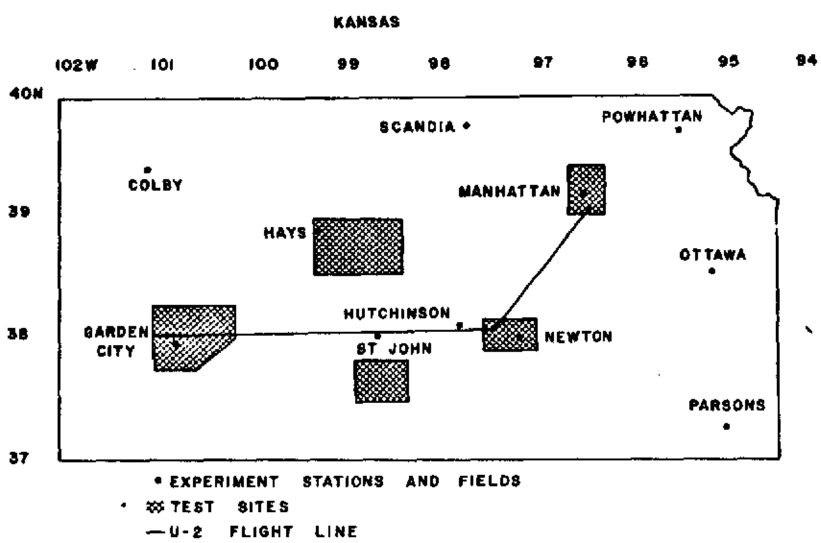

Fig. 1.1 Map of test areas in Kansas.

system. The results of ground measurements of the spectral reflectance of sorghum, soybean and wheat are provided in Appendix B. As a result of the ERTS-1 project, a Master's Thesis was written and is provided as Appendix D. Appendices E, F, G and H are related to data handling and reduction phases of the project.

The investigators wish to express appreciation to the National Aeronautics and Space Administration for supporting this project.

Soils on the two fields are classified as a Ulyssess-Richfield silt loam with 1.5 percent organic matter and a pH of 6.9. A particle size analysis indicated the soils contained about 50 percent silt and 20 percent clay.

Field A, which had been summer fallowed since July 1971, was planted to Scout winter wheat on September 15, 1972. Seeding rate was 29 kg per hectare in rows spaced 25.4 cm apart. The wheat was completely headed by May 24, 1973 and a yield of 2689 kg per hectare harvested on July 5, 1973.

As field B had been in wheat the previous season, it was preirrigated. Ninety kg per hectare of nitrogen were applied as anhydrous ammonia prior to planting and 50 kg per hectare of Eagle winter wheat were seeded on September 22, 1972, in rows 30.48 cm apart. Two irrigations of 3.05 cm each were applied through a center pivot sprinkler system on May 23 and June 2, 1973. Wheat harvest was completed on July 5 and the yield was 3496 kg per hectare.

According to Variety Tests with Fall-Planted Small Grains (1971), Eagle wheat is a selection of Scout with nearly identical vegetative characteristics. Reflectance measured by the MSS system aboard ERTS-1 should be independent of winter wheat variety, Scout or Eagle.

Data Collection

Fields A and B were both divided into four equal sized square plots with a sampling area in the center of each plot. Two additional sampling areas were established in field A where the corners of the field were double drilled. The sampling areas were sub-divided into one meter square plots. Leaf area index and soil moisture were measured within one day of each pass of ERTS-1 on one plot of each sampling area selected at random.

Leaf area was determined by measuring the length and breadth of each leaf from randomly selected plants. Area of each individual leaf was calculated from the equation (Teare and Peterson, 1971):

$$LA = 0.813X - 0.64 \tag{2.1}$$

where:

LA = Leaf area, cm^2

X = Product of length times breadth of leaf, cm^2

Total leaf area on each one meter square plot was calculated by multiplying number of plants times average plant leaf area. Leaf area index was taken as the ratio of total leaf area to the land surface area.

Soil samples were taken from the surface and at the following increments of depth: 0 to 15, 15 to 30, 30 to 60, 60 to 91, 91 to 121, 121 to 152, and 152 to 182 cm. The samples were weighed, dried in an oven at 105°C until they reached a constant weight and reweighed. Soil moisture was calculated and expressed as percent on a dry weight basis.

Bulk density, field capacity and the permanent wilting point for Ulyssess-Richfield silt loam were obtained from the Garden City Experiment Station.

Meteorological data from the area were collected for use in the ET model. Maximum and minimum temperatures, dew point temperatures and wind run were obtained from the Garden City Experiment Station. Solar radiation was obtained from the Dodge City Weather Service and rainfall was measured near the field site.

Data Analysis

Digital counts in each MSS band and various combinations of bands were compared by multiple regression techniques with leaf area index and available soil moisture.

Using an IBM 360/50 digital computer, estimates of the water use by wheat from the ET model developed by Jensen et al. (1971) were compared with changes in measured soil moisture.

RESULTS

Although ERTS-1 passed over the field site every 18 days, clear atmospheric conditions were encountered on only 6 flight days during the period from wheat seeding to wheat harvest. Table 2.1 gives weather conditions on each flight date and the schedule of data collection. Data for July 7 were excluded from the analyses because the wheat crop had been harvested.

Prediction of Leaf Area Index

Tables 2.2 and 2.3 give digital counts of MSS data for bands 4, 5, 6 and 7 and ratios of 4 to 5, 4 to 7 and 5 to 7 along with measured LAI for fields A and B. The regression equations for predicting LAI are:

$$LAI = -0.15MSS4 + 5.41 \quad , \quad R^2 = 0.80 \qquad (2.2)$$

$$LAI = -0.065MSS5 + 2.66 \quad , \quad R^2 = 0.86 \qquad (2.3)$$

$$LAI = 1.94MSS6 - 9.37 \quad , \quad R^2 = 0.20 \qquad (2.4)$$

$$LAI = 0.15MSS7 - 3.53 \quad , \quad R^2 = 0.53 \qquad (2.5)$$

$$LAI = 2.92MSS4/5 - 2.63 \quad , \quad R^2 = 0.95 \qquad (2.6)$$

$$LAI = -1.22MSS5/7 + 2.08 \quad , \quad R^2 = 0.85 \qquad (2.7)$$

where

LAI = Leaf area index

MSS = Digital counts for numbered band or ratio

R^2 = Regression coefficient

For each equation there is some minimum or maximum value of the digital counts or ratios beyond which LAI goes negative and the results are meaningless.

Table 2.1 Weather conditions during satellite pass over test fields.

Date	Weather Condition	Data Acquired[a]
September 4, 1972	Cloudy	
September 22, 1972	Clear	X
October 10, 1972	Partly Cloudy	
October 28, 1972	Cloudy	
November 15, 1972	Cloudy	
December 3, 1972	Partly Cloudy	
December 21, 1972	Partly Cloudy	
January 8, 1973	Cloudy	
January 26, 1973	Cloudy	
February 13, 1973	Rain	
March 3, 1973	Foggy	
March 21, 1973	Clear	X
April 8, 1973	Heavy Snow	
April 26, 1973	Rain	
May 14, 1973	Clear	X
June 1, 1973	Clear	X
June 19, 1973	Clear	X
July 7, 1973	Clear	X

[a]Indicates both ERTS-1 and field data taken.

Table 2.2. Digital counts of MSS data and LAI for field A.

Date		MSS4	MSS5	MSS6	MSS7	MSS4/5	MSS4/7	MSS5/7	LAI[b]
9/22/72	Mean	34.75	37.89	38.64	19.55	0.918	1.779	1.939	0.00
	S.D.[a]	1.41	1.90	2.18	0.86	0.040	0.068	0.080	0.00
3/21/73	Mean	33.26	32.29	45.87	25.25	1.031	1.318	1.280	0.37
	S.D.	1.28	1.58	1.74	0.69	0.040	0.055	0.069	0.10
5/14/73	Mean	29.74	24.50	48.11	28.08	1.218	1.064	0.877	0.97
	S.D.	1.69	2.12	1.79	1.66	0.066	0.101	0.104	0.26
6/1/73	Mean	33.43	29.48	52.32	29.87	1.138	1.121	0.990	0.89
	S.D.	1.72	2.42	1.84	1.04	0.062	0.083	0.104	0.25
6/19/73	Mean	41.14	49.33	55.26	28.70	0.835	1.436	1.722	0.00
	S.D.	1.62	2.07	1.49	0.92	0.033	0.074	0.090	0.00
7/7/73	Mean	59.46	78.53	77.68	36.36	0.758	1.636	2.161	0.00
	S.D.	2.14	4.25	2.72	1.49	0.030	0.061	0.115	0.00

[a]Standard deviation.
[b]Average of six sampling points.

Table 2.3. Digital counts of MSS data and LAI for field B.

Date		MSS4	MSS5	MSS6	MSS7	MSS4/5	MSS4/7	MSS5/7	LAI[b]
9/22/73	Mean	37.05	40.41	40.96	20.78	0.919	1.786	1.947	0.00
	S.D.[a]	1.62	2.54	2.37	1.02	0.038	0.094	0.128	0.00
3/21/73	Mean	33.54	32.99	41.47	22.57	1.019	1.488	1.463	0.44
	S.D.	1.09	1.91	2.15	0.96	0.049	0.073	0.088	0.07
5/14/73	Mean	27.63	19.22	56.66	36.78	1.454	0.760	0.532	1.53
	S.D.	1.60	2.68	3.56	3.18	0.132	0.109	0.129	0.39
6/1/73	Mean	26.93	20.03	48.66	31.61	1.355	0.858	0.638	1.23
	S.D.	1.32	2.23	3.43	2.54	0.111	0.083	0.094	0.36
6/19/73	Mean	36.68	37.94	52.00	29.97	0.971	1.227	1.270	0.00
	S.D.	1.21	3.11	2.05	1.56	0.060	0.079	0.131	0.00
7/7/73	Mean	54.46	73.87	77.48	38.24	0.739	1.425	1.932	0.00
	S.D.	2.30	4.37	3.39	1.31	0.033	0.060	0.100	0.00

[a]Standard deviation.
[b]Average of four sampling points.

The regression coefficients for all the LAI prediction equations except equation (2.4) were statistically significant at the 0.05 level. For the individual bands, 4 and 5 were better predictors of LAI. While ratios of band 4 to band 5 and band 5 to band 7 were good predictors of LAI, the ratio of band 4 to band 5 had the higher regression coefficient. Figure 2.1 shows measured LAI as a function of the ratio of digital counts in band 4 and band 5.

Prediction of Soil Moisture

Available soil moisture for plant use was taken as the difference between soil moisture at sampling and at the permanent wilting point. Table 2.4 gives available soil moisture for fields A and B at depths of 0 to 15, 0 to 30, 0 to 60, and 0 to 91 cm. The negative values are due to errors in the assumption of soil moisture percentage at permanent wilting point as the soil profile probably did not become that dry. Rather than adjust soil moisture percentage by changing the permanent wilting point percentages, the available soil moisture values were left negative. The only effects of this action are that the constants in the regression equations may be in error but the form of the equations will remain the same and the regression coefficients are not affected.

Linear regression equations to predict available soil moisture from digital counts in the individual MSS bands and various band ratios were developed from digital counts in Tables 2.2 and 2.3 and available soil moisture in Table 2.4. Data for field B on March 21 were excluded from the analyses because of rain between flight of ERTS-1 and soil measurements. Only band 6 predicted available soil moisture at the 0.10 level of significance. The equations for available soil moisture in the 0 to 15 cm zone, AV_{15}, and in the 0 to 91 cm zone, AV_{91}, were:

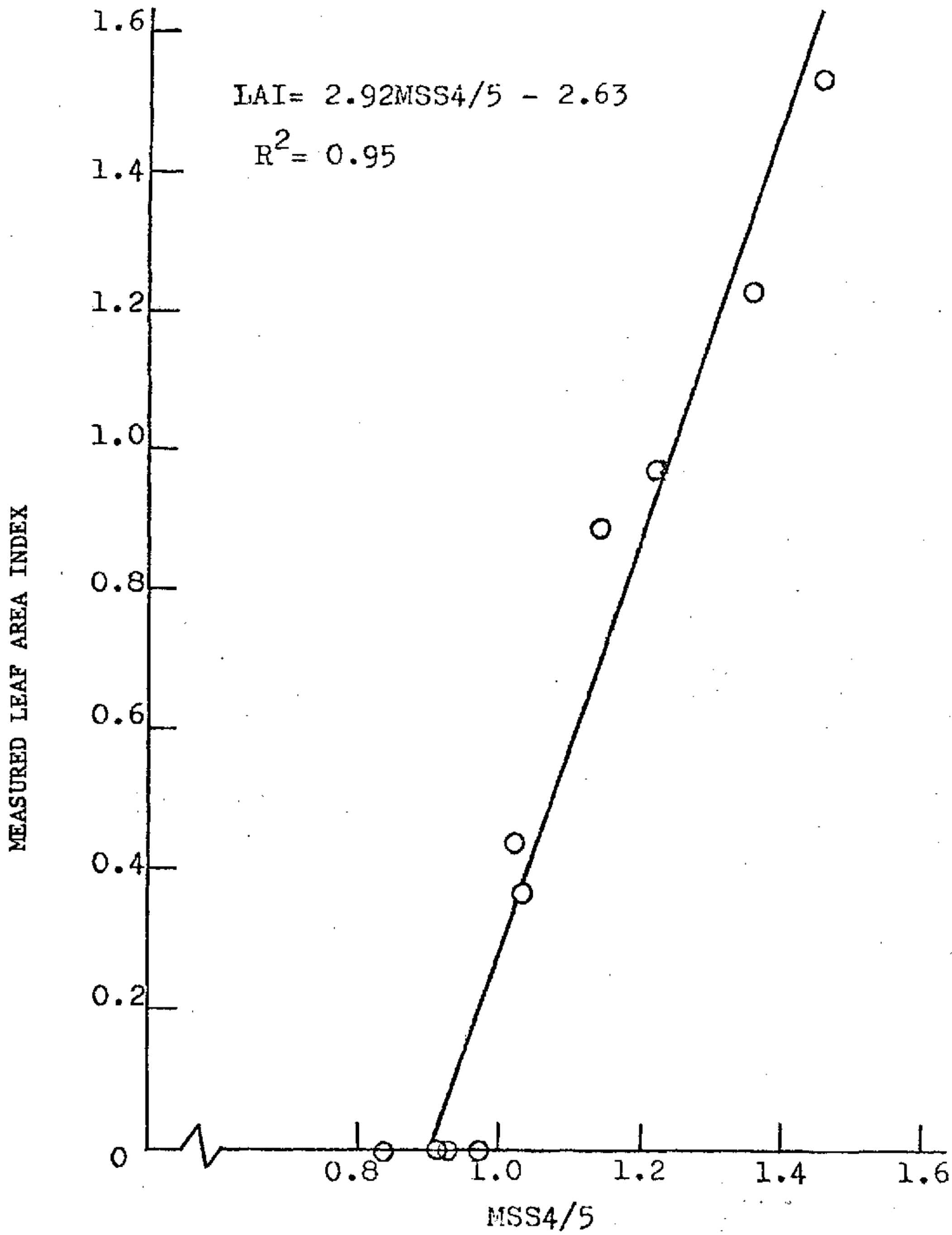

Figure 2.1. Relationship between measured LAI and ratio of digital counts in band 4 to band 5.

Table 2.4. Available soil moistures (cm of water).

Date	Soil Depth-cm 0-15	0-30	0-60	0-91
	FIELD A (DRYLAND)			
9/22/72	0.66	1.37	2.59	3.29
3/21/73	0.66	1.50	3.13	4.33
5/14/73	0.19	0.40	1.24	2.38
6/1/73	-0.26[a]	-0.34	-0.14	0.23
6/19/73	-0.63	-0.99	-1.46	-2.02
	FIELD B (IRRIGATED)			
9/22/72	0.61	1.00	1.58	1.70
3/21/73	0.73	1.71	3.38	4.48
5/14/73	0.52	0.67	1.35	2.16
6/1/73	0.85	1.20	1.44	1.51
6/19/73	-0.37	-0.78	-1.12	-1.57

[a]Negative available soil moisture because soil moisture at permanent wilting point was lower than that measured at the Garden City Branch Experiment Station.

$$AV_{15} = 7.52 - 0.15MSS6 \quad , \quad R^2 = 0.35 \tag{2.8}$$

$$AV_{91} = 30.31 - 0.60MSS6 \quad , \quad R^2 = 0.33 \tag{2.9}$$

Measured LAI was added as an independent variable and multiple regression equations developed to predict soil moisture. The resulting equations for available soil moisture in the 0 to 15 cm zone, AV_{15}, and the 0 to 91 cm zone, AV_{91}, which had a significant regression coefficient at the 0.05 level, were:

$$AV_{15} = 11.73 - 1.88\ LAI - 0.31MSS4 \quad , \quad R^2 = 0.93 \tag{2.10}$$

$$AV_{15} = 5.14 + 0.76\ LAI - 0.11MSS6 \quad , \quad R^2 = 0.80 \tag{2.11}$$

$$AV_{15} = 4.85 + 1.56\ LAI - 0.20MSS7 \quad , \quad R^2 = 0.79 \tag{2.12}$$

$$AV_{91} = 21.99 + 3.03\ LAI - 0.46MSS6 \quad , \quad R^2 = 0.73 \tag{2.13}$$

$$AV_{91} = 18.1 + 5.60\ LAI - 0.71MSS7 \quad , \quad R^2 = 0.84 \tag{2.14}$$

As LAI was highly correlated with the ratio of counts in band 4 to band 5, equation (2.6) was substituted into equations (2.10) and (2.14) for predicting available soil moixture, The resulting equations were:

$$AV_{15} = 16.67 - 5.49MSS4/5 - 0.31MSS4 \tag{2.15}$$

and

$$AV_{91} = 3.37 + 16.35MSS4/5 - 0.71MSS7 \tag{2.16}$$

Figure 2.2 shows the comparison of available soil moisture predicted by equations (2.15) and (2.16) with measured available soil moisture.

Predicting Water Use

As no usable data were collected by ERTS-1 from the time wheat was seeded until March 21, 1973, water use calculations were made from that date until just prior to wheat harvest. Table 2.5 gives precipitation

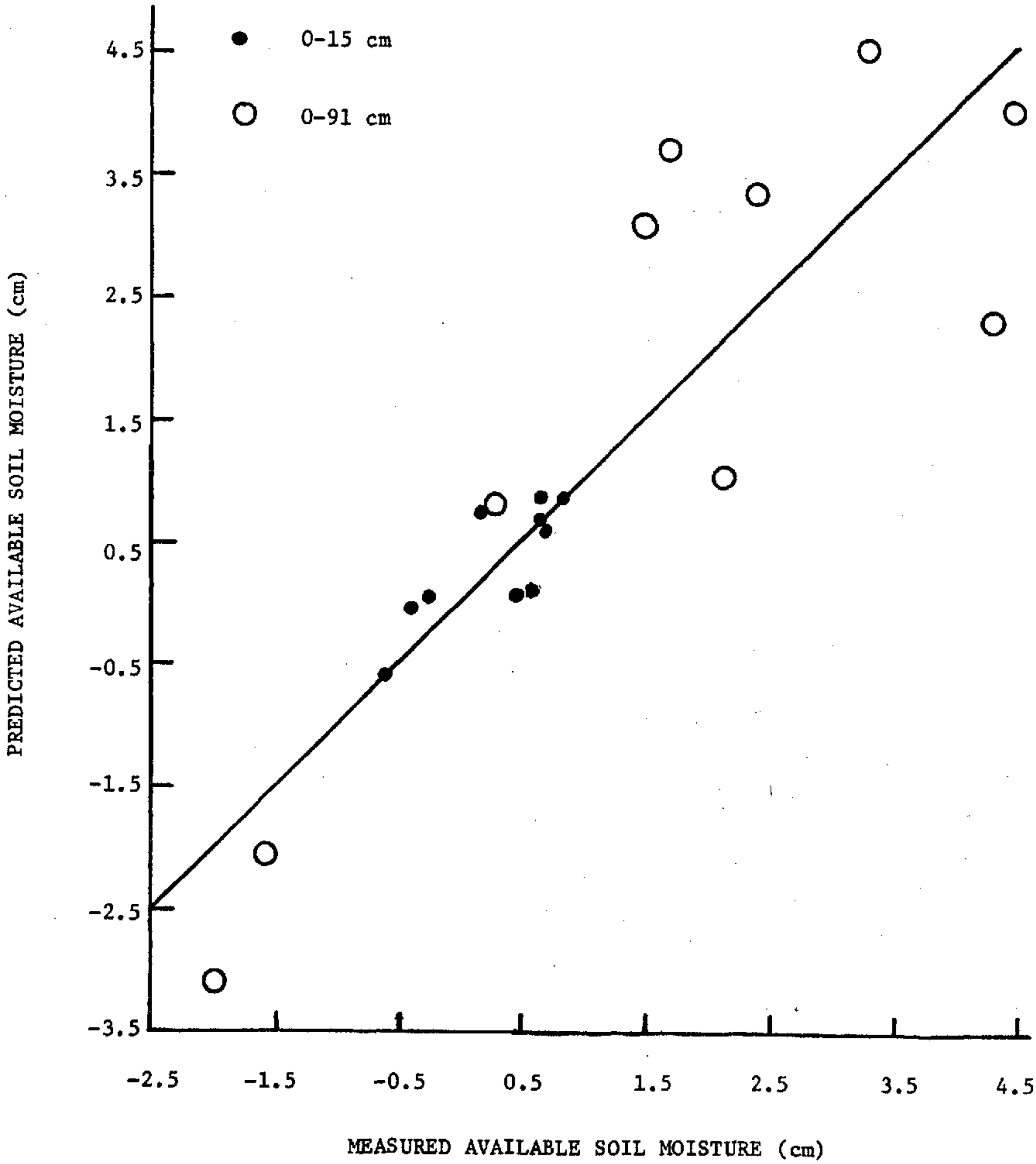

Figure 2.2. Comparison of measured and predicted available soil moisture.

Table 2.5. Precipitation and irrigation at the test sites.

Date	Precipitation cm	Irrigation (Field B) cm
3/23/73	1.10	
3/27/73	0.70	
3/30/73	1.00	
4/7/73	0.25	
4/24/73	0.80	
5/7/73	1.25	
5/23/73		3.05
6/2/73		3.05
6/28/73	0.90	

measured by a local farmer near the test site and irrigation water applied to field B during the latter period. The irrigations were carried out over about a 3 day period and the total amount credited to the center day of the period.

The ET model as developed by Jensen <u>et al</u>. (1971) was used to predict soil moisture depletion on both wheat fields using their suggested crop coefficients. Measured soil moisture depletion was entered into the computer program for March 21, 1973. The wheat crop coefficients were:

$$Y = 0.233 - 0.0114X + 0.000484X^2 - 0.00000289X^3 \quad (2.17)$$

and

$$Y = 1.022 + 0.00853D - 0.000726D^2 + 0.00000444D^3 \quad (2.18)$$

where:

Y = Wheat crop coefficient

X = Percent of period between seeding and 100 percent crop cover

D = Days after 100 percent crop cover

Table 2.6 gives the measured and predicted soil moisture depletion and water use for fields A and B where measured soil moisture depletion is the difference between field capacity for the 182 cm soil profile sampled and the measured soil moisture level. The ET model over-predicted soil moisture depletion and water use for the period March 21 to June 1 and greatly underpredicted soil moisture depletion and water use for the period June 1 to June 19. Soil moisture depletion and water use for the entire period were under-predicted by the ET model.

A new crop coefficient for the ET model was computed from a multiple regression analysis using LAI measurements from field A. The new crop coefficient equations were:

Table 2.6. Measured and predicted soil moisture depletion and water use.

Date	Soil Moisture Depletion - cm				Water Use for Period - cm			
	Measured[a]	Jensen[b]	Revised 1[c]	Revised 2[d]	Measured[a]	Jensen[b]	Revised 1[c]	Revised 2[d]
				FIELD A (DRYLAND)				
3/21/73	17.65	-----	-----	-----	-----	-----	-----	-----
5/14/73	19.84	25.07	19.35	-----	7.29	12.52	6.80	-----
6/1/73	27.74	31.24	27.86	-----	7.90	6.17	8.51	-----
6/19/73	37.52	32.16	34.65	-----	9.78	0.92	6.79	-----
Total	-----	-----	-----	-----	24.97	19.61	22.10	-----
				FIELD B (IRRIGATED)				
3/21/73	19.28	-----	-----	-----	-----	-----	-----	-----
5/14/73	23.44	26.14	20.80	26.52	9.26	11.96	6.62	12.34
6/1/73	27.15	29.24	26.56	32.66	6.76	6.15	8.81	9.19
6/19/73	37.77	27.61	31.52	37.90	13.67	4.68	8.01	8.29
Total	-----	-----	-----	-----	29.69	22.79	23.44	29.82

[a]Field measurements of soil moisture depletion.

[b]Wheat crop coefficient suggested by Jensen et al. (1971).

[c]Wheat crop coefficient from LAI of field A.

[d]Wheat crop coefficient from LAI of field B.

$$Y = 0.005 + 0.0165X - 0.000467X^2 + 0.00000402X^3 \quad (2.19)$$

and

$$Y = 0.998 - 0.00297D - 0.000747D^2 \quad (2.20)$$

Predicted soil moisture depletion and water use are given in Table 2.6 for fields A and B using the revised crop coefficients in the ET model. Predicted water use for the period was within 2.87 cm or about 10 percent of measured water use for field A and is within the accepted accuracy for the ET model. Predicted soil moisture depletion for field A compared very closely with measured values on May 14 and June 1 but was low on June 19 when wheat was nearing maturity. The ET model with a revised crop coefficient based upon LAI for field A under-predicted water use for field B.

As the ET model utilizing LAI as the crop coefficient from dryland wheat successfully predicted water use on field A, LAI from irrigated wheat was used as the crop coefficient to predict water use on field B. The crop coefficient equations were:

$$Y = 0.0109X - 0.000288X^2 + 0.00000333X^3 \quad (2.21)$$

and

$$Y = 1.52 - 0.000834D^2 \quad (2.22)$$

Table 2.6 gives the predicted soil moisture depletion and water use for field B using the revised crop coefficient in the ET model. Predicted soil moisture depletion and water use were about equal to measured values on June 19. However, there was considerable variation between measured and predicted values on May 14 and June 1.

DISCUSSION

Limited data were collected during this study because of cloud cover during many passes of ERTS-1. However, it appears that the MSS system has the potential for predicting water use of growing crops.

One possible method for predicting water use is from available soil moisture predicted from reflectance measurements. Water use would be the difference between available soil moisture on succeeding days. As the MSS system only sees the earth's surface, soil moisture would be predicted from its effects on the soil surface and growing vegetation.

Kondrat'yev (1965) reported that albedo varies between soils. The variability was attributed to different soil color, soil moisture content, organic matter content and soil particle size with soil moisture content the most important factor. Bowers (1971) found that reflectance increases as soil moisture decreases and concluded that reflectance techniques are precise enough to measure surface moisture. However, due to the effects of other soil factors on reflectance, a calibration will be necessary for each soil type.

There are several factors which influence reflectance from growing vegetation. According to David (1969), a water deficit in the soil will result in increased reflectance. Severe nitrogen deficiencies also increase reflectance (Remote Sensing, 1970). Leaf reflectance is affected by variety and relative maturity of the crop (Remote Multispectral Sensing in Agriculture, 1970). There are other factors including soil salinity, plant diseases and mineral deficiencies which may affect reflectance from vegetation. Whether soil moisture can be accurately predicted by the MSS system depends upon the relationships between soil moisture, vegetative growth and factors affecting reflectance.

Only band 6 showed potential for predicting available soil moisture by a linear relationship with digital counts. The addition of a second band or band ratio which correlated with LAI improved the accuracy of available soil moisture prediction.

Water use of growing vegetation can be predicted from ET models. The MSS system, through prediction of LAI, has the potential to supply the numerical values of the crop coefficient equations for winter wheat developed from LAI measurements. Although LAI is greater for irrigated wheat than for dryland wheat, the curves have the same general shape as shown in Figure 2.3. Additional research is needed to determine the correct relationship between LAI and crop coefficient. When this relationship can be expressed mathematically, the MSS system will be capable of supplying the crop coefficient for ET models.

Practical use of data collected by ERTS-1 or similar vehicles is dependent upon timely acquisition and processing of the data. To be useful in water resources management, the data should be available within 24 hours of flight time. One potential use of the data is in irrigation scheduling.

SUMMARY

To effectively manage water on agricultural lands, daily water use of crops must be known. We hypothesized that the MSS system aboard ERTS-1 could provide data for predicting water use of winter wheat.

A linear relationship was found between digital counts in band 6 and available soil moisture at 0 to 15 and 0 to 91 cm depths. Prediction of available soil moisture was improved by adding the ratio of band 4 to band 5, which predicted LAI, as a second independent variable. Daily water use is the change in available soil moisture on successive days.

Crop coefficient equations, based upon LAI, were developed for use in an ET model to predict daily water use of dryland and irrigated wheat. Predicted water use for the period March 21 to June 19, 1973, was within accepted accuracy for ET models.

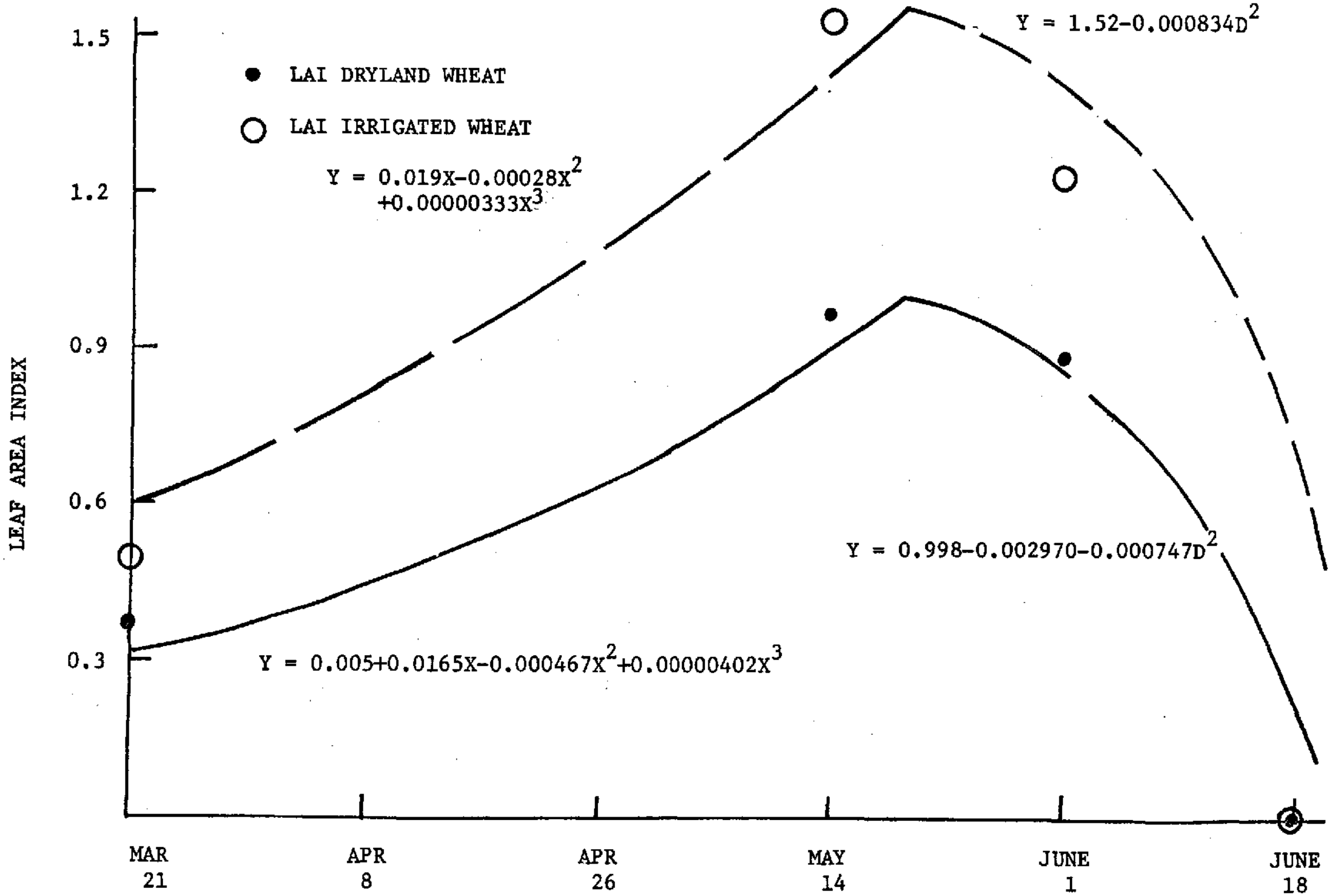

Figure 2.3. Crop coefficient curves for winter wheat.

As only limited MSS data were collected because of excessive cloud cover, additional research is needed to verify and extrapolate the results of this study to fields with different soil types.

2.2 Water Loss from Diseased and Healthy Wheat

The patterns of water use in healthy and diseased wheat are important to both basic and applied research in terms of a clearer understanding of the epidemiology and of management practices that will reduce economic effects due to the disease. By accurately determining the water use of healthy and diseased crops and predicting yield reductions due to disease, we can provide the grower with information so that he can intelligently decide whether he should allow the diseased wheat to attain maturity or plow under the diseased wheat and replant a following crop. In western Kansas, wheat and other crops (i.e. soybean and sorghum) yields are largely determined by the availability of water; therefore, the earlier the grower decides to replant, the greater the conservation in soil moisture and a more likelihood of a successful crop.

Procedure

Five fields, Erichsen (commercial, healthy), Hartner (commercial, healthy), rust-infected, wheat streak mosaic virus-infected and control (healthy), were planted to *Triticum aestivum* L. cv. Scout in late September 1972. Cropping descriptions for the five fields are given in Table 2.7. From the amount of water stored in the soil profile and the precipitation, the seasonal water use can be estimated. Soil moisture samples were determined weekly (in some cases, inclement weather prevented weekly measurements) at 15-cm increments in a 150-cm profile.

Table 2.7. Cropping descriptions of five wheat fields.

Field	Soil Texture	Seeding Rate Kg/ha	Row Spacing cm	Harvested plants per m^2
Erichsen	Silty clay loam	96	20.3	856
Hartner	Silt loam	101	20.3	872
Rust-infected	Silty clay loam	84	17.8	959
Wheat streak mosaic	Silty clay loam	84	17.8	1125
Control	Silty clay loam	84	17.8	1144

Hourly estimates of the evapotranspiration rate (ET) were determined by the surface energy balance,

$$ET = (R_n - G)/(1 + \beta) \qquad (2.23)$$

where R_n and G are the flux densities of net radiation and soil heat, respectively. The Bowen ratio (β) is determined by $\gamma\ \Delta T/\Delta e$ where γ is the psychrometric constant and ΔT and Δe are the gradients of temperatures and vapor pressure above the canopy. Temperatures and water vapor pressures were determined with wet and dry bulb thermocouple psychrometers where the wick of the wet bulb was composed of a porous ceramic tube. Net radiation was determined with a hemispherical shielded radiometer located 3.0 meters above ground. Soil heat flux were determined with heat flux plates (5-cm depth) and calorimetrically. The sensors were scanned every 10 minutes and recorded on punch tape. The instruments and data acquisition system are described by Brun et al. (1972).

Stomatal resistance, R_s, was determined with a diffusion porometer described by Kanemasu et al. (1969) and given by

$$1/R_s = 1/R_{ab} + 1/R_{ad} \qquad (2.24)$$

where R_{ab} and R_{ad} are the resistances of the abaxial and adaxial surfaces of the leaves. Leaf-water potential was estimated by pressure bomb technique (Barr, 1968). In both the stomatal resistance and leaf-water potential determinations, three upper canopy leaves were measured at near midday.

Results and Discussion

Figure 2.4 shows the water loss (determined by soil moisture) and the precipitation pattern. The amount of water loss from all five fields were quite similar; the water loss for the Hartner field being the largest.

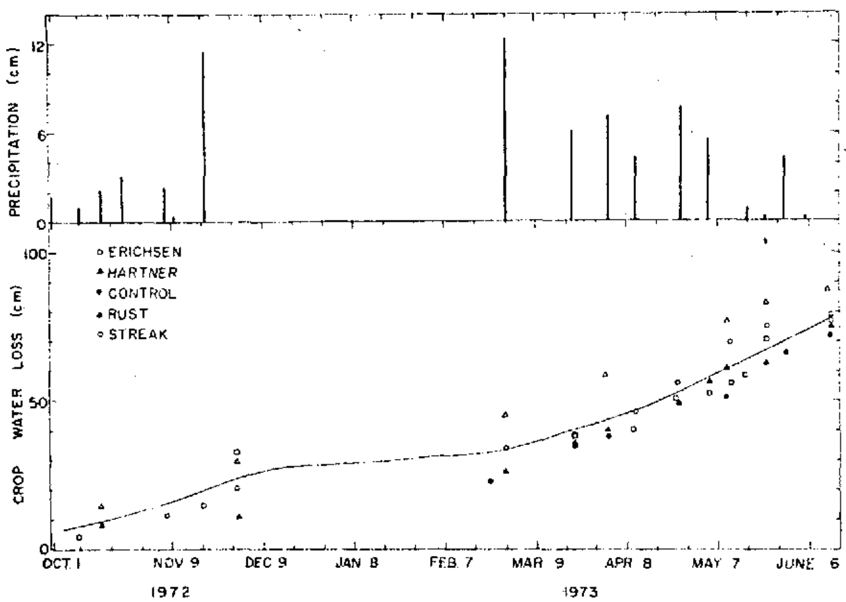

Figure 2.4 Crop water use from five wheat fields and precipitation pattern for the general area.

This could be attributed to the lighter textured soil (silt loam) and the heavy rains (72 cm compared to the 30 year normal of 51 cm) which would be conducive to large drainage rates below the root zone. The average seasonal water loss for the five fields was 78.83 ± 5.89 cm. Nearly one-half of this amount being lost after dormancy (late March). By predicting the yield reductions 30 days in advance (e.g. predicting the economic loss from April 23 to 29 meteorological data[1]), a grower could conserve up to 15 cm of water (assuming about 7-cm loss through evaporation) by plowing under his diseased crop; this soil water would then be available for the following crop.

Figures 2.5, 2.6, and 2.7 show the hourly energy balance terms for May 4, May 19, and June 15, respectively. The rust infection and the control fields have nearly identical fluxes of net radiation and evapotranspiration. However, the soil heat flux was approximately 50% greater for the control than for the rust-infected. On May 19 net radiation was greater for the control but the evapotranspiration was slightly greater for the rust-infected (Fig. 2.6). On June 15 (hard-dough stage, Table 2.8) the evapotranspiration rates were similar for the two fields but the net radiation was greater for the control than for the rust-infected.

Although there was a greater heat load on the control field, as indicated by the net radiation, evapotransporation was greater in the rust-infected field at time when rust spores were strongly evident (May 19) on the leaves. The greater ET rate would suggest a lower stomatal resistance on rust-infected leaves which was confirmed by data presented in Fig. 2.8 (c.f. May 19).

---

[1]Appendix A. ERTS-1 Data Collection System Used to Predict Wheat Disease.

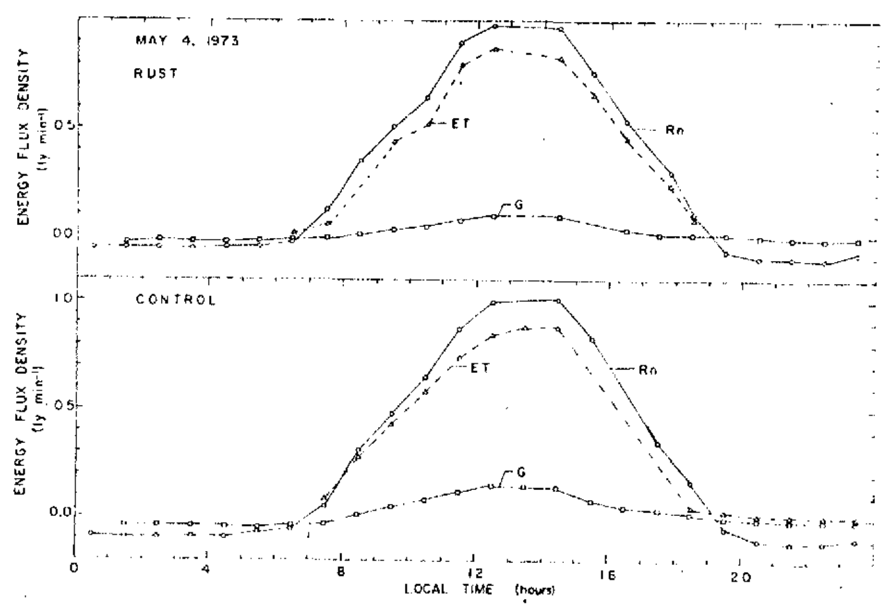

Figure 2.5 Trends in the hourly energy balance of rust and control (healthy) wheat for May 4, 1973. ET = evapotranspiration, Rn = net radiation, and G = soil heat flux.

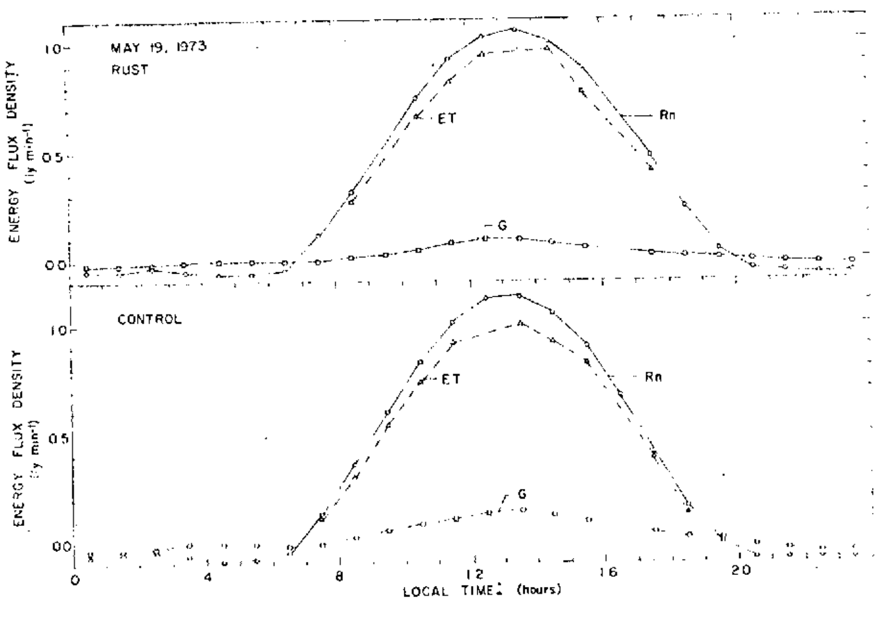

Figure 2.6 Trends in the hourly energy balance of rust and control (healthy) wheat for May 19, 1973. ET = evapotranspiration, Rn = net radiation and G = soil heat flux.

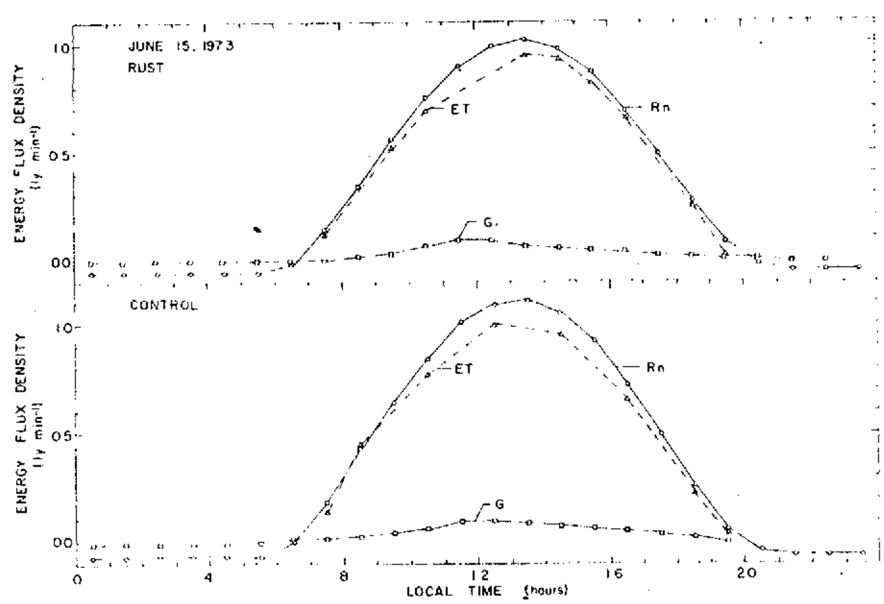

Figure 2.7 Trends in the hourly energy balance of rust and control (healthy) wheat for June 15, 1973. ET = evapotranspiration, Rn = net radiation, and G = soil heat flux.

Table 2.8. Physiological calendar for wheat

Date	Identifying Characteristics
September 23	planted
April 21	early joint
May 1	boot
May 8	heading
May 18	flowering
May 30	milk stage
June 6	soft dough
June 15	hard dough

Table 2.9. Yield data for test wheat fields.

Field	Yield (bu/Acre) kg/ha	1000 Kernal weight gm
Erichsen	(36.3) 2566	33.0
Hartner	(41.7) 2892	31.1
Rusted	(28.4) 2616	33.4
Streak (WSMV)	(36.7) 2621	33.7
Control (healthy)	(40.0) 2729	33.3

Lower stomatal resistances enhance diffusion of both water vapor (ET) and carbon dioxide (photosynthesis). The larger stomatal resistances of the wheat streak mosaic virus (WSMV)-infected plants indicate a loss of turgor pressure by the epidermal leaf tissue (decrease in leaf-water potential). Fig. 2.9 shows the lower leaf-water potential of WSMV -infected compared to the control. Rust-infected leaves had a lower leaf-water potentials later in the growing season (May 29 to June 5). The unfavorable water balance of the diseased plants was reflected in the yields (Table 2.9).

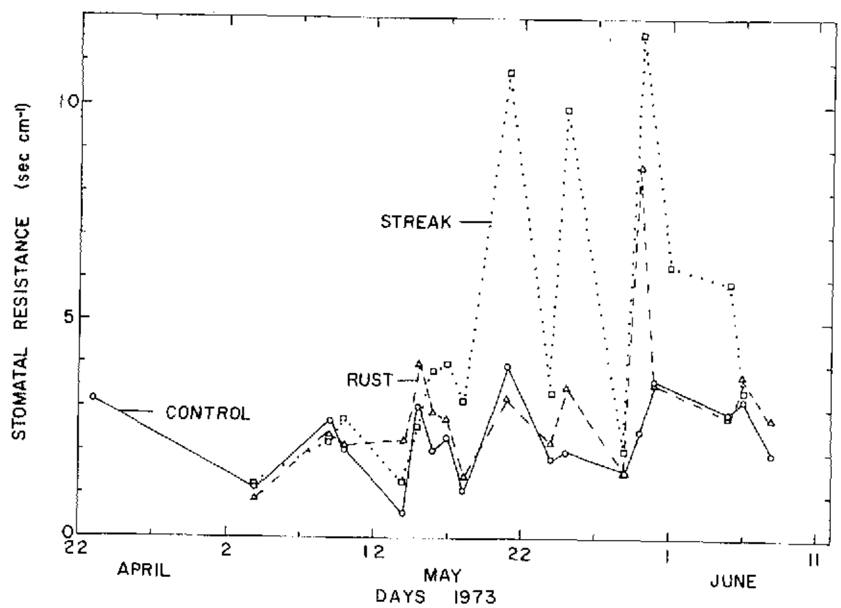

Figure 2.8 Daily trends in stomatal diffusion resistance of control, rust-infected and wheat streak mosaic virus (WSMV)-infected wheat leaves.

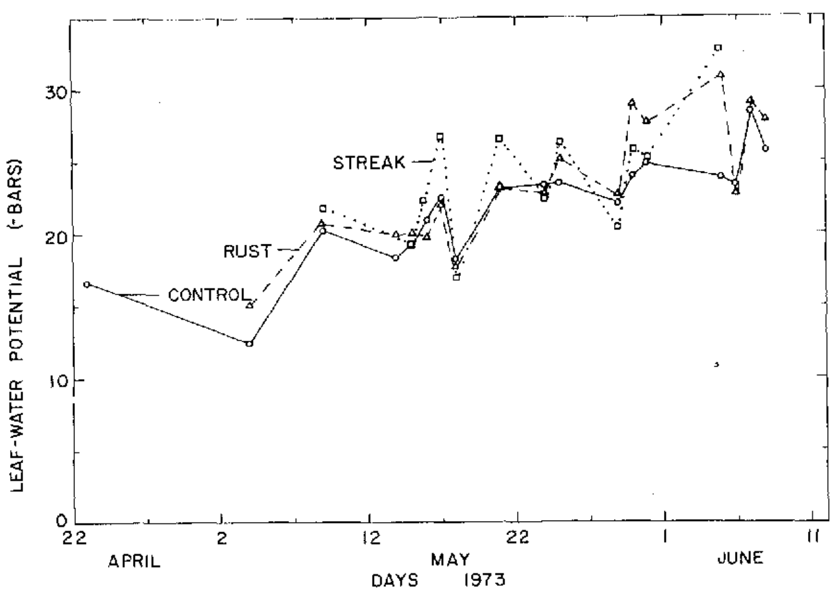

Figure 2.9 Daily trends in the leaf-water potential of control, rust-infected and (WSMV)-infected wheat leaves.

3.0 DATA REDUCTION

3.1 General Data Handling Method

Initially we requested a standing order for 9" by 9" positive transparencies of MSS4 and MSS5 of each of the two fixed test areas (Riley county and the irrigated and nonirrigated fields in Finney county) and the high probability wheat streak mosaic virus (WSMV) areas of Kansas. Upon receipt of the transparencies they were examined for lack of clouds over the test areas and general suitability for further data reduction. Initially, several dates were examined and cataloged before determining which transparency would be used for further data processing. Later in the project when more frequent data were required and the anticipated arrival of the computer compatible tapes (CCT's) was approximately three months after date of the overflight, it was decided to order tapes as soon as possible in order to minimize the delays.

Upon receipt of these tapes, the transparencies were used to determine the desired test area and the tapes were then sent to the Remote Sensing Laboratory at the University of Kansas so that the desired area could be stripped off onto another tape and a gray-scale map was generated (Fig. 3.1). Since the second tape was organized in a band by band structure, a third tape was generated organized on a point basis. The computer maps were then put together for the location of the test areas by line and cell numbers. Numerous methods were attempted for locating the test fields (including the use of U-2 data); however, the best method was to use a clear piece of acetate over the entire area. This was laid over the computer maps and all

Figure 3.1 Computer Generated Gray Scale Map

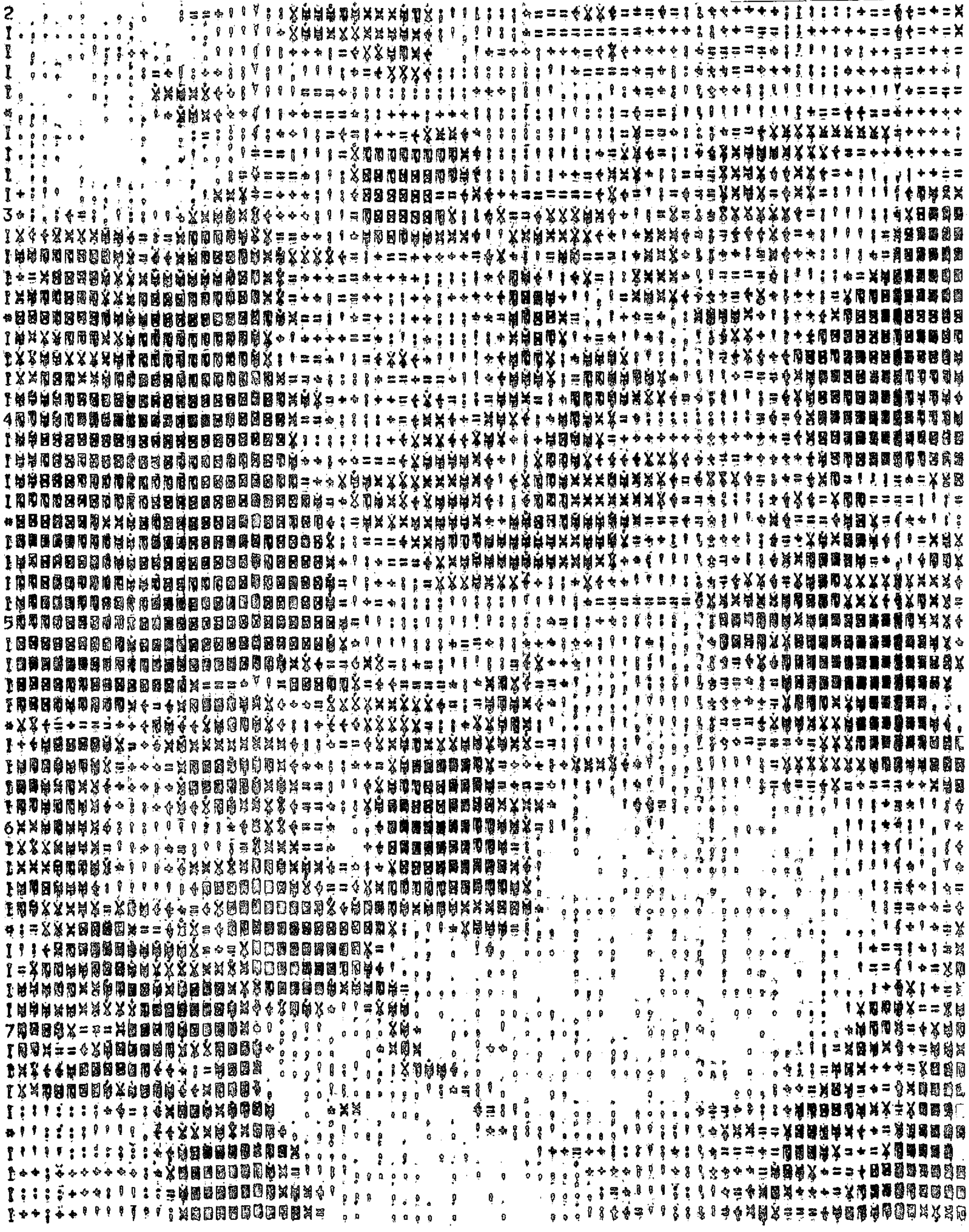

pertinent identifiable points sketched on the acetate with a grease pencil. One of the most difficult tasks was the consistent identification of a test field on the maps.

For the Riley county test fields the U-2 transparencies were projected over the computer maps in order to approximate the location of the fields. There were several identifying points that were initially thought to be identifiable on each date but were not. After the initial location had been verified by several people familiar with the test sites, the acetate sheet was used to identify the area on succeeding dates.

For the Finney county test fields the most useful identifying marks for a large area were the county mile lines (roads every mile). Knowing their approximate spacing, a best fit to these mile lines was drawn on the computer map and again, by using several people familiar with the test area, an original layout of the test fields was made. It must be emphasized that one major check in this process must be the discussion of more than one trained person as to the location of a specific field and even then errors occur. The acetate overlay reduced the time in locating the fields on succeeding dates, especially in the case of the WSMV test area of Finney county with its over fifty fields. It should be noted that the N-S mile lines are much easier to locate than the E-W ones.

After locating the fields, the corners of a straight line approximation to the field were recorded by line and cell number and key punched. These were used to pick the data for a specific field from the point-oriented computer tapes. In order to check the locating of the field, two methods were used. First the points taken from a specific file were displayed as a "1" on a printout with all other points as a "0" which allowed for the detection of many small errors. This was made easier by the fact that each file contained the data for a 64 by 64 block or area. However, the most useful method turned out to be the use of a Calcomp plot of the boundary of all fields on a specific data. These boundaries were generated using the identical data cards. Different dates could be overlaid and differences in size and location easily detected. An error of a hundred lines was detected in one case, 64 cells in another, and one line or cell in several cases. At this stage the data for each of the test areas were handled differently; however for each area one common program was run which indicated the mean, minimum, maximum, standard deviation, correlation coefficient, and histograms of each of the MSS bands, the difference of bands 6 and 4, 7 and 4, 6 and 5, 7 and 5 (where band 7 had been multiplied by 2 to make the ranges of all band 128) and the ratios of bands 4 and 5, 4 and 6, 4 and 7, 5 and 6, and 5 and 7. An example of this printout is shown in Figure 3.2. This particular printout will be discussed later in this chapter.

3.2 Special Computer Programs Generated

General Program

A number of special computer programs were generated to assist in the location of the fields and in the data reduction for each field. The most frequently used program found the means, minimums, maximums, standard deviation, correlation coefficients and histogram. The input to this program consisted of the tape to be used, the inset or points to be discarded around each field, and the boundary data for each field (line and cell number for each corner). A program listing is given in Appendix E. A sample of the output is shown in Figure 3.2. This sample is for one entire file of data for tape number 1294-16521 which covered the WSMV region of Finney county on May 13, 1973. A total number of 114,688 points

	MSS4	MSS5	MSS6	MSS7	MSS6-4	2MSS7-4	MSS6-5	2MSS7-5	MSS4/5	MSS4/6	MSS4/7	MSS5/6	MSS5/7
MEANS	4[illegible].7[illegible]3	30.221	53.925	28.819	13.291	16.932	14.773	18.414	1.064	0.759	1.465	0.734	1.426
MINIMUMS	3.000	15.000	14.000	4.000	-81.000	-81.000	-13.000	-28.000	0.057	0.048	0.091	0.187	0.283
MAXIMUMS	127.000	92.000	101.000	62.000	68.000	92.000	79.000	106.000	4.421	3.630	8.167	1.455	5.500
STD DEV	8.009	11.101	6.620	6.056	10.370	15.821	13.482	19.191	0.213	0.190	0.449	0.233	0.532

CORRELATION COEFFICIENTS

	MSS4	MSS5	MSS6	MSS7	MSS6-4	2MSS7-4	MSS6-5	2MSS7-5	MSS4/5	MSS4/6	MSS4/7	MSS5/6	MSS5/7
MSS4	0.99993	0.94927	0.19978	-0.24612	-0.66772	-0.67150	-0.64288	-0.64593	-0.17846	0.61923	0.73404	0.60702	0.68633
MSS5		0.99999	0.03981	-0.39067	-0.66690	-0.73008	-0.81621	-0.81293	-0.71980	0.57540	0.70238	0.79374	0.85501
MSS6			0.99994	1.08103	0.77015	0.72913	0.68277	0.66268	0.46649	-0.78685	-0.44292	-0.69921	-0.40011
MSS7				0.99998	0.80924	0.84461	0.79913	0.82079	0.47714	-0.70033	-0.79543	-0.72589	-0.77385
MSS6-4					0.99999	0.96098	0.90894	0.90073	0.42796	-0.78735	-0.87282	-0.77271	-0.81534
2MSS7-4						0.99999	0.94092	0.95870	0.51507	-0.79819	-0.89028	-0.81804	-0.86930
MSS6-5							0.99999	0.98084	0.65607	-0.72457	-0.92792	-0.87215	-0.91034
2MSS7-5								0.99999	0.66090	-0.74501	-0.83859	-0.87118	-0.91945
MSS4/5									0.99998	-0.12229	-0.22785	-0.45898	-0.49960
MSS4/6										0.99997	0.87929	0.89895	0.79660
MSS4/7											0.99998	0.84124	0.92070
MSS5/6												0.99998	0.92045
MSS5/7													0.99999

Figure 3.2

are covered. It is interesting to note that only 3 quantities have a normalized cross correlation of less than 0.2 and these are MSS band 4 and MSS band 6 which have a correlation of 0.20, MSS band 5 and MSS band 6 with a value of 0.04, and the ratios of MSS 4/5 and MSS 4/6 with a correlation of -0.12 which is probably due to the low correlation between bands 5 and 6.

Calcomp CONTUR Subroutine

A Calcomp, contour-generating program was developed which is a very efficient program running in from 1/3 to 1/10 the time of other programs tested. The algorithm utilized 4 adjacent points requiring data which is equally spaced in the X direction and the Y direction but not necessarily the same spacing. This program was used to attempt to define the location of fields and specific targets for location; however this method did not meet with much success. This program can be easily modified to cross hatch a region between two or more given contours by modification of program to intercept the branch out when it is determined that the contour does not cross the rectangle. The computer subroutine, brief description and flow chart are given in Appendix F.

Enhancing Category Variation

A series of computer programs were written to implement a method of taking vector data and reducing it to a single number for ease of plotting. Data from unwanted categories would be near zero, and the data from the desired category would have maximized variation about some number. The proof of the algorithm is given in Appendix G. The computer programs are given in Appendix H. The first computes the eigenvectors and eigenvalues using a set of sample data. The second program computes the variation of data when the test eigenvectors are inputed.

3.3 CCT Data Used

Table 3.1 gives a listing of the observation numbers of each of the tapes used for each of the test areas. The Riley county test field did not receive coverage from May 10, 1973 until July 4, 1973 due to cloud coverage even though it was in the overlap and was covered on two consecutive days each period. An almost three month period was missed in late fall for the irrigated and non-irrigated fields of Finney county due to cloud coverage.

3.4 Data Reduction Recommendations for Other Investigators

The following are a summary of our recommendations to investigators utilizing ERTS CCT's.

1. Print a computer gray-scale map of the area. Be sure to include at least a 3 mile buffer all the way around a small test area to aid in location. If possible include large man-made objects such as airports, interstate highways, water bodies, etc.
2. On the first attempt to locate the field have as many people as possible that are familiar with the test area go over the tentative location. If possible, have them try to locate it without any information as to where others have placed it and then collectively discuss the location.
3. After the initial location is defined, make an acetate overlay including the pertinent characteristics such as large dark areas, sharp boundaries, etc. MSS5 seems the best suited for this. Use this overlay to place the location of the test areas on later dates. Even then it is useful to have others duplicate your overlay. There will be a few point variation from date to date

Table 3.1. Computer compatible tapes used in the project.

Observation Number	Satellite Pass Date	Comments
Riley County Test Area		
1022-16391	14 Aug 72	Before Planting
1058-16392	19 Sep 72	
1237-16345	17 Mar 73	
1256-16403	5 Apr 73	
1274-16403	23 Apr 73	
1291-16344	10 May 73	
1328-16400	15 Jun 73	Clouds obscured field
1346-16395	4 Jul 73	After Harvest
Irrigated and Non-Irrigated Test Area Finney County		
1061-16564	22 Sep 72	
1132-16514	5 Dec 72	On edge of tape
1240-16523	22 Mar 73	1
1295-16573	14 May 73	
1312-16520	1 Jun 73	
1330-16515	19 Jun 73	1
1348-16514	7 Jul 73	After Harvest 1
Wheat Streak Mosaic Virus Test Area Finney County		
1240-16523	22 Mar 73	1
1294-16521	13 May 73	
1313-16520	1 Jun 73	
1330-16515	19 Jun 73	1
1348-16514	7 Jul 73	After Harvest 1

1-Used for both Finney County Test Areas due to magnification and other optical errors but a local region of possibly 4 to 10 square miles does not change appreciably.

4. Provide cross checks on your locations whenever possible, such as test field boundaries overlaid on reflectance contours. If more than one test area is in the view, their relative positions should remain constant between dates.

4.0 EFFECT OF CROP GROWTH ON ERTS-1 MSS RESPONSE

Determination of crop growth from spacecraft has received considerable attention by agriculturists[2]. Such efforts have been brought about by the increasing awareness of shortages in food and fiber production. In a given area, agronomic crops develop and mature at somewhat predictable rates and abnormal growth patterns are exhibited when the photosynthetic process is interupted or reduced (e.g. disease, insects, nutrition, drought or flooding). Therefore, the monitoring of crop growth can provide valuable information on the prediction of production.

Plants appear green to the human eye because the relatively large reflection in the green wavelength (500 nm). This relatively high reflectance in the visible wavelengths can be attributed to the strong absorptance of blue (450 nm) and red (500 nm) wavelengths by plant pigments, namely, chlorophyll. More characteristic of healthy plant leaves than the low reflectance in the visible wavelengths (400-700 nm) is the high reflectance (about 50 percent) and transmittance (40 percent) to near infrared (700-1300 nm) radiation. Because of this optical characteristic, leaves stacked on top of one another exhibit greater near infrared reflectance as the leaf layer increases; therefore, near infrared reflectance has important consequence in indicating differences in vegetation density (Allen and Richardson, 1968).

The reflected radiation stream from a crop canopy is composed of rays reflected from the vegetation and from the soil surface. The surface, which dominates the scene reflectance depends upon percentage of crop cover. For many crops, especially row crops, there is a good correlation between percentage

[2] Symposium on significant results obtained from ERTS-1. NASA SP-327. March 5-9, 1973. NASA-GSFC.

cover and leaf area index (leaf area to ground area); however as the percentage approaches 100 (about 85%) large increases in leaf area index can occur with slight changes in percent cover. Since the spectral reflectance of soil differs from that of chlorophyll-containing tissue, vegetation density can be deduced from the signal strength of reflected rays in the visible and near infrared wavelengths. Kanemasu (Appendix B) suggests that ratio of the reflectances in wavelengths of MSS4 and MSS 5 is less than unity when soil exposure dominates the scene and tends to follow the leaf area index while Wiegand et al. (1973) states "the photosynthetic potential of green plants cannot be deduced directly from the photosynthetically active wavelengths" (MSS4 and 5). However, the apparent inconsistency in the two studies may be due to the MSS4:MSS5 ratio being sensitive at low LAI (<2) while the MSS6 and 7 bands being more sensitive at high LAI (>2). At low LAI, the soil reflective properties in the visible wavelengths dominate while at high LAI the leaf reflective properties in the near infrared wavelengths dominate.

METHODS AND MATERIALS

Four commercial wheat fields were used in study. Table 4.1 shows their location and cropping description.

Plant samples for leaf area determination were collected at frequent intervals (usually 10 days) throughout the growing season. Samples in two of the fields (Hartner and Erichsen) were measured with an optical planimeter while the leaf area of samples from the other two fields were determined with an empirical equation using leaf width and length (equation 2.1).

Table 4.1. Location and cropping description of the Riley county fields (Hartner and Erichsen) and the irrigated and non-irrigated wheat fields in Finney county.

Location	Row Spacing (cm)
Hartner - 39° 08' N, 96° 37' W	20.3
Erichsen - 39° 07' N, 96° 35' W	20.3
Irrigated - 38° 8.5' N, 101° 4.9' W	30.5
Nonirrigated - 38° 9.6' N, 101° 5.9' W	25.4

Data reduction

The greater the digital count in each band, the greater the radiance. Maximum digital counts for MSS4, 5 and 6 is 127. The radiance (mw cm^{-2} sr^{-1} μm^{-1}) is given by

$$E = \text{(digital counts) (maximum radiance)}/127 \tag{4.1}$$

where the maximum radiance for 4, 5 and 6 are 24.8, 20.0 and 17.6, respectively.

The radiance for MSS7 is

$$E_7 = \text{(digital counts) (15.3)}/63 \tag{4.2}$$

Hence, conversion factors (mw cm^{-2} sr^{-1} μm^{-1} $counts^{-1}$) for digital counts in bands MSS4, 5, 6, and 7 to radiance are 0.19528, 0.15748, 0.13858, and 0.24286. The radiance, E, measured above earth's atmosphere, has been affected by the optical properties of the atmosphere.

Satellite reflectance is the ratio of the radiance, E, to the irradiance (incoming radiation flux above atmosphere). In order to compare satellite reflectance with ground reflectance, the spectral transmission of the atmosphere must be determined. The transmission of atmosphere becomes increasingly important to surfaces with low reflectances where errors can overwhelm low signal strength.

Assuming equal atmospheric transmission for MSS4 and 5, we can describe the reflectance ratio of MSS4 and 5 as

$$\frac{R_4}{R_5} = \frac{E_4}{I_4}\left(\frac{E_5}{I_5}\right)^{-1} \tag{4.3}$$

where I_4 and I_5 are the incident radiation fluxes in the wavelengths of MSS4 and MSS5. Assuming (I_5/I_4) equals 0.8696 (Smithsonian Meteorological Tables), equation (4.3) can be rewritten in terms of the conversion factors

$$\frac{R_4}{R_5} = \frac{(\text{Counts } 4)}{(\text{Counts } 5)} \frac{(0.19528)}{(0.15748)} (0.8696) = \frac{\text{Counts } 4}{\text{Counts } 5} (1.078) \qquad (4.4)$$

Similar relationships can be derived for the other combination of the reflectance ratios; however, caution should be used since the assumptions are not completely valid. The reflectance ratio of MSS4:MSS5 is slightly larger than the ratio of their digital counts. In this report, we will use digital count ratios and not attempt to estimate reflectance ratios.

RESULTS

Table 4.2 shows (a) the digital counts for MSS4, 5, 6, and 7, (b) the difference in digital counts, (c) the ratio of the digital counts, and (d) their standard deviations for the eight ERTS-1 observations on two Riley county wheat fields. Linear regression equations were calculated for the correlation of leaf area index (LAI) and percent cover (P.C.) with the 13 digital parameters listed in Table 4.2. The regression equations for the pooled data (both fields) are summarized in Table 4.3 for the September to May observations.

The lowest correlation coefficients were obtained directly from the MSS bands while the highest correlation coefficients were the difference between two bands, MSS6-5 and MSS (2 x 7)-5; however, band differences have high standard deviations. In general, the linear correlations were high whenever two bands were combined either by ratio or difference. Of the band ratios used, the poorest correlations were MSS4/6, and 4/7. It is significant that the MSS4/5, which consists of bands confined to the visible wavelengths, is one of the better indicators of crop growth.

Table 4.4 shows the pixel correlation coefficients between the MSS bands for the Hartner field. A positive correlation existed between bands

Table 4.2a. Mean digital counts and standard deviations for ERTS-1 observations of Hartner field.

Observation No.	NSS4	MSS5	MSS6	MSS7	6-4	(2x7)-4	6-5	(2x7)-5	4/5	4/5	4/7	5/6	5/7
1022-16391	41.46	44.82	49.91	24.14	8.46	6.82	5.09	3.46	.95	.83	1.73	.90	1.88
August 14, 1972	(4.86)[a]	(8.92)	(2.64)	(1.70)	(3.62)	(7.02)	(7.57)	(11.13)	(.11)	(.08)	(.26)	(.16)	(.43)
1058-16392	34.74	37.48	37.39	17.65	2.65	.57	-.09	-2.17	.93	.93	1.98	1.00	2.14
Sept. 19, 1972	(3.83)	(4.20)	(2.43)	(1.43)	(3.59)	(4.11)	(4.14)	(5.31)	(.12)	(.10)	(.23)	(.11)	(.29)
1076-16393	35.04	36.38	38.17	19.17	3.13	3.29	1.79	1.96	.97	.92	1.83	.95	1.90
Oct. 7, 1972	(3.30)	(5.26)	(2.99)	(1.24)	(2.25)	(3.45)	(3.30)	(4.73)	(.07)	(.06)	(.17)	(.09)	(.24)
1237-16345	30.41	28.46	36.55	19.32	6.14	8.23	8.09	10.18	1.07	.83	1.58	.78	1.48
March 17, 1973	(1.74)	(2.30)	(2.06)	(1.39)	(2.49)	(3.34)	(3.16)	(3.92)	(.07)	(.06)	(.15)	(.08)	(.18)
1256-16403	29.96	27.18	40.77	22.14	10.82	14.32	13.59	17.09	1.12	.74	1.37	.67	1.26
April 5, 1973	(2.75)	(4.89)	(2.73)	(2.10)	(4.28)	(6.05)	(6.48)	(8.30)	(0.11)	(.10)	(.225)	(.15)	(.35)
1274-16403	27.90	22.80	44.45	25.10	16.55	22.30	21.65	27.4	1.25	.63	1.12	.51	.92
April 23, 1973	(3.16)	(5.04)	(1.40)	(1.59)	(2.80)	(5.70)	(4.66)	(7.53)	(.12)	(.06)	(.21)	(.11)	(.28)
1291-16344	30.17	22.11	48.89	27.89	18.72	25.61	26.78	33.67	1.37	.62	1.08	.45	.79
May 10, 1973	(1.69)	(1.91)	(2.19)	(1.08)	(2.11)	(2.73)	(2.29)	(2.79)	(.06)	(.03)	(.07)	(.04)	(.07)
1346-16395	37.0	39.75	46.25	22.90	9.25	8.80	6.50	6.05	.93	.80	1.62	.87	1.76
July 4, 1973	---[b]	(3.46)	(4.87)	(2.47)	---	---	(5.69)	(6.30)	---	---	---	(.11)	(.24)

[a](Standard deviation)

[b]Discontinuity in telemetry

Table 4.2b. Mean digital counts and standard deviations for ERTS-1 observations of Erichsen field.

Observation No.	MSS4	MSS5	MSS6	MSS7	6-4	(2x7)-4	6-5	(2x7)-5	4/5	4/6	4/7	5/6	5/7
1022-16391	26.06	21.13	27.88	13.75	1.81	1.44	6.75	6.38	1.24	1.01	2.13	.82	1.75
August 14, 1972	(1.98)[a]	(1.36)	(8.98)	(5.70)	(7.20)	(9.65)	(8.47)	(10.91)	(.08)	(.24)	(.62)	(.22)	(.57)
1058-16392	30.54	28.21	29.33	13.83	-1.21	-2.88	1.125	- .54	1.09	1.05	2.24	.97	2.07
Sept. 19, 1972	(2.11)	(3.08)	(2.85)	(1.86)	(3.04)	(3.79)	(3.51)	(4.23)	(.07)	(.11)	(.31)	(.12)	(.30)
1076-16393	22.40	19.18	18.69	9.41	-3.69	-3.56	- .49	- .36	1.18	1.23	2.48	1.04	2.10
Oct. 7, 1972	(1.58)	(2.51)	(3.54)	(2.38)	(2.48)	(3.80)	(2.09)	(3.27)	(.10)	(.17)	(.46)	(.11)	(.30)
1256-16403	23.57	17.93	26.14	14.64	2.57	5.71	8.21	11.36	1.33	.92	1.65	.70	1.27
April 5, 1973	(2.21)	(3.03)	(2.96)	(2.34)	(4.33)	(5.80)	(5.24)	(6.69)	(.12)	(.16)	(.33)	(.17)	(.33)
1274-16403	25.77	17.82	41.59	24.59	15.82	23.41	23.77	31.35	1.48	.64	1.10	.45	.78
April 23, 1973	(2.31)	(3.97)	(6.28)	(4.78)	(7.82)	(10.92)	(9.68)	(12.77)	(.18)	(.15)	(.34)	(.18)	(.35)
1291-16344	27.82	18.12	50.44	29.32	22.62	30.82	32.32	40.53	1.55	.57	.99	.37	.66
May 10, 1973	(1.09)	(1.74)	(7.78)	(5.74)	(7.57)	(11.28)	(8.95)	(12.68)	(.15)	(.10)	(.23)	(.10)	(.21)
1346-16395	49.0	59.47	62.00	30.33	13.00	11.66	2.53	1.20	.82	.79	1.62	.96	1.96
July 4, 1972	---[b]	(2.45)	(2.73)	(1.84)	---	---	(1.55)	(2.70)	---	---	---	(.02)	(.09)

[a] (Standard deviation)

[b] Discontinuity in telemetry

Table 4.3a. Linear regression equations of leaf area index (LAI) and digital counts from MSS 4, 5, 6, and 7 taken from 6 ERTS-1 observations of Erichsen and Hartner fields.

Linear Regression Equation	Correlation Coefficient
LAI = -0.081 (MSS 4) + 3.333	-.308
LAI = -0.101 (MSS 5) + 3.414	-.704
LAI = 0.072 (MSS 6) - 1.824	.734
LAI = 0.126 (MSS 7) - 1.717	.838
LAI = 0.095 (MSS 6-4) - .001	.910
LAI = 0.071 [MSS (2 x 7)-4] - .028	.937
LAI = 0.074 (MSS 6-5) - .128	.958
LAI = 0.058 [MSS (2 x 7)-5] - .107	.962
LAI = 4.148 (MSS 4/5) - 4.195	.918
LAI = -3.946 (MSS 4/6) + 4.095	-.815
LAI = -1.696 (MSS 4/7) + 3.472	-.864
LAI = -3.665 (MSS 5/6) + 3.400	-.945
LAI = -1.565 (MSS 5/7) + 2.952	-.920

Table 4.3b. Linear regression equations of percent cover (PC) and digital counts from MSS 4, 5, 6, and 7 taken from 6 ERTS-1 observations of Erichsen and Hartner fields.

Linear Regression Equation	Correlation Coefficient
PC = -3.457 (MSS 4) + 137.492	-.410
PC = -3.142 (MSS 5) + 115.858	-.729
PC = 2.579 (MSS 6) - 63.474	.717
PC = 4.573 (MSS 7) - 59.997	.843
PC = 3.364 (MSS 6-4) + 4.214	.915
PC = 2.465 [MSS (2 x 7)-4] + 4.403	.942
PC = 2.536 (MSS 6-5) + 2.100	.967
PC = 1.953 [MSS (2 x 7)-5] + 3.318	.968
PC = 131.342 (MSS 4/5) - 123.603	.892
PC = -146.141 (MSS 4/6) + 152.736	-.869
PC = -61.194 (MSS 4/7) + 128.859	-.900
PC = -123.929 (MSS 5/6) + 122.025	-.963
PC = -52.937 (MSS 5/7) + 107.027	-.952

Table 4.4. Correlation coefficients between the various MSS bands for the Hartner field.

Date	4 vs 5	4 vs 6	4 vs 7	5 vs 6	5 vs 7	6 vs 7
August 14	.90	.65	-.41	.59	-.51	.01
September 19	.41	.39	.26	.30	-.10	.66
October 7	.88	.72	.30	.78	.42	.69
March 17	.60	.14	-.03	-.04	-.17	.73
April 5	.87	-.21	-.47	-.38	-.64	.75
April 23	.91	.44	-.59	-.38	-.63	.23
May 10	.79	.41	.01	.36	.06	.68
July 4	.13	.09	.09	.09	-.09	.86

4 and 5 and between 6 and 7. The lowest positive correlation existed between a visible band (4 or 5) and a near-infrared band (6 or 7). This relationship results because vegetation absorbs strongly in the visible and reflects strongly in the near-infrared wavelengths.

Radiometric response. Fig. 4.1 shows the scene radiance from a single wheat field at various growth stages. In general, as the plants develop, radiance in bands 4 and 5 decrease while bands 6 and 7 increase. The higher radiance at LAI = 0 than at LAI = .14 may be due to soil moisture differences (Appendix B). The stubble field (post harvest) shows a high reflectance in the visible (MSS 4 and 5) and in the near infrared wavelengths (MSS 6 and 7).

Finney County Fields. In the Finney county area, leaf area indices were determined periodically on an irrigated and a nonirrigated wheat field (c.f. section 2.1). The Riley county (Hartner and Erichsen fields) and Finney county (irrigated and non-irrigated fields) data were pooled and linear regression equations were determined for the various band ratios (Table 4.5). The MSS4 to MSS5 ratio gave the highest correlation coefficient with the MSS 5 to MSS6 ratio having a slightly lower correlation coefficient.

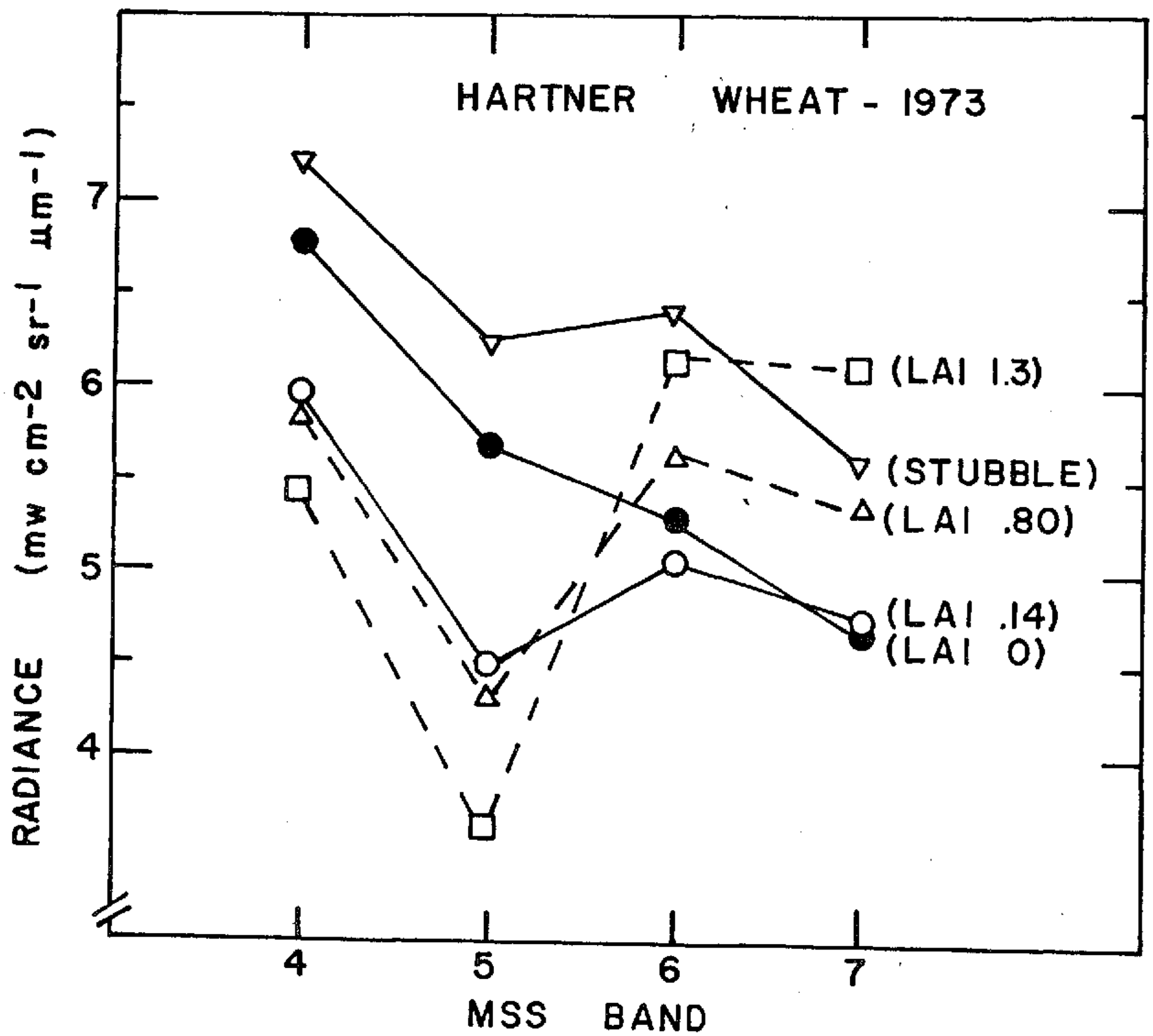

Fig. 4.1. Radiometric response of ERTS-1 bands for Hartner wheat field during 1973 growing season.

Table 4.5. Linear regression equations of pooled LAI and MSS digital count data from Hartner and Erichsen fields (Riley county) and irrigated and non-irrigated fields (Finney county).

Linear Regression Equation	Correlation Coefficient
LAI = 3.305 (MSS4/5) - 3.089	.92
LAI = -3.395 (MSS4/6) + 3.275	-.72
LAI = -1.384 (MSS4/7) + 2.650	-.73
LAI = -3.034 (MSS5/6) + 2.804	-.90
LAI = -1.307 (MSS5/7) + 2.402	-.87

5.0 DETECTION OF DISEASE SEVERITY AND ECONOMIC LOSS

ERTS-1 imagery was processed to determine the satellite's usefulness in the early detection and estimation of wheat disease severity and economic loss. The experimental site was a 450 square mile area of Finney and Gray counties which contained healthy and wheat streak mosaic virus (WSMV)-infected wheat fields. A detailed map of this area was prepared and the crop and its condition was determined in every field. The following severity ratings were used:

0 = Healthy, No WSMV infection (very green)

1 = Trace WSMV infection (few yellow plants)

2 = Moderate WSMV infection (whole field slightly yellow)

3 = Severe WSMV infection (whole field very yellow)

With farmers permission, four random samples (a sample = 16 square foot plot) were harvested from each of 54 fields. Samples were threshed for yield determination, and four yield groups were assigned:

A = 13.8 - 20.00 Bushels/Acre

B = 20.1 - 25.0 Bushels/Acre

C = 25.1 - 30.0 Bushels/Acre

D = 30.1 - 41.6 Bushels/Acre

Grey scale maps of the site were prepared for MSS Band 5 for each clear date (March 20, May 13, May 31 and June 18, 1973). Test fields were readily identified using center-pivot irrigators, airports and peculiar field shapes for registration. Digital data for the four MSS bands on each data were processed manually or by machine for each field. To minimize border effects a boundary of one data point around the edge of each field was discarded.

Means were determined for digital counts on all MSS bands and ratios of the bands. These means were tabulated relative to yield (Table 5.1) and disease severity (Table 5.2). Correlation coefficients for MSS digital counts versus yield and MSS digital counts versus severity were determined. None of these relationships was significant at the 1% level, but 11 of 72 relationships were significant at the 5% level. Of these, eight occurred in the 5/31/73 data. On this date a negative correlation existed between yield and MSS bands 4 and 5, with a positive correlation between yield and the MSS 4/5 band ratio (Table 5.3, Fig. 5.1-C). A significant negative correlation existed (barely) on 5/31/73 between yield and the MSS 4/6 and 4/7 band ratios (Table 5.3). MSS band 6 was correlated with yield on 3/20/73 (Table 5.3). MSS band 7 never showed a correlation with yield at the 5% level (Table 5.3).

Similar correlations occurred between MSS digital counts and disease severity. For 5/31/73 a positive correlation existed between severity and MSS band 4 and for the MSS 4/6 and 4/7 band ratios (Table 5.4, Fig. 5.2-C). A higher positive correlation existed on 6/18/73 between MSS bands 4 and 5 and severity (Table 5.4, Fig. 5.2-D). There was no significant correlation between MSS bands 6 or 7 and severity (Table 5.4).

Significant correlations between MSS digital counts and wheat yields or disease severity were demonstrated only for the 5/31/73 and 6/18/73 data. The negative correlation between yield and digital counts for MSS bands 4 and 5 on 5/31/73 (Fig. 5.1-C) is reasonable and probably resulted from premature coloration of the crop, greater reflectance by the soil due to thinning of the crop or both. WSMV prematurely colors and thins the crop. Positive correlations between severity and digital counts for MSS bands 4 and 5 on 5/31/73 and 5/18/73 (Fig. 5.2-C,D) are also plausible for the same reasons.

We have correlated ERTS-1 imagery with ground truth for both wheat yield and disease severity with significant correlation obtained at the 5% level. Also, in both cases the effects of the disease are being detected near the end of the crop season rather than the disease *per se* being detected early in the season. It is reasonable to assume that a disease sufficiently severe to reduce yields by over 50% and readily detectable by eye should have been more readily detected and quantified by ERTS-1. However, WSMV was most obvious from very late March to May 1 when no ERTS-1 imagery was available due to inclement weather. Therefore, although we report some positive results on the quantitative effects of the disease, we were unable to adequately test the ERTS-1 system for early detection and estimation of severity and yield reduction in wheat due to wheat streak mosaic virus.

Table 5.1. Means of MSS digital counts in relation to wheat yields.

Date	Yield Group	Yield	MSS Band 4	5	6	7	MSS Band Ratio 4/5	4/6	4/7	5/6	5/7
3/20/73	A	17.2	25.8	22.4	29.7	16.2	1.2	0.9	1.6	0.8	1.4
	Std. Dev.	2.4	0.7	1.1	2.8	1.9	0.0	0.1	0.2	0.1	0.2
	B	22.8	27.0	24.3	29.8	15.8	1.1	0.9	1.7	0.8	1.6
	Std. Dev.	1.4	1.7	2.9	1.5	1.2	0.1	0.1	0.2	0.1	0.3
	C	28.3	26.4	22.8	31.9	17.3	1.2	0.8	1.5	0.7	1.3
	Std. Dev.	1.3	1.5	3.1	3.6	2.6	0.1	0.1	0.2	0.1	0.3
	D	35.7	26.8	23.6	31.9	17.5	1.2	0.8	1.6	0.8	1.4
	Std. Dev.	3.6	2.6	4.4	3.3	2.1	0.1	0.1	0.2	0.1	0.3
5/13/73	A	17.5	34.4	29.7	49.7	27.3	1.2	0.7	1.3	0.6	1.1
	Std. Dev.	2.5	2.7	3.6	6.8	4.6	0.1	0.1	0.2	0.1	0.2
	B	23.3	35.5	30.6	54.8	30.7	1.2	0.7	1.2	0.6	1.1
	Std. Dev.	1.0	3.8	5.7	7.4	5.2	0.1	0.1	0.3	0.1	0.3
	C	28.0	34.7	29.3	54.0	31.1	1.2	0.7	1.2	0.6	1.0
	Std. Dev.	1.3	2.8	4.6	6.4	5.1	0.1	0.1	0.2	0.1	0.3
	D	36.3	34.7	29.7	52.0	29.4	1.2	0.7	1.3	0.6	1.1
	Std. Dev.	3.9	6.4	8.7	12.3	8.3	0.1	0.2	0.6	0.2	0.5
5/31/73	A	17.1	37.0	35.6	53.0	29.3	1.1	0.7	1.3	0.7	1.2
	Std. Dev.	2.2	2.3	3.3	5.4	3.2	0.0	0.1	0.1	0.1	0.2
	B	22.9	35.4	33.2	53.0	30.1	1.1	0.7	1.2	0.6	1.1
	Std. Dev.	1.3	3.5	6.1	2.7	2.8	0.1	0.1	0.2	0.1	0.3
	C	27.6	32.6	29.2	51.6	30.6	1.2	0.6	1.1	0.6	1.0
	Std. Dev.	1.4	3.9	6.1	3.1	2.9	0.1	0.1	0.2	0.1	0.2
	D	36.9	32.6	28.9	52.6	31.3	1.2	0.6	1.1	0.6	1.0
	Std. Dev.	3.6	3.9	7.2	2.6	3.3	0.1	0.1	0.3	0.2	0.4
6/18/73	A	17.6	42.5	48.1	53.1	27.3	0.9	0.8	1.6	0.9	1.8
	Std. Dev.	1.9	4.7	6.3	5.2	2.7	0.0	0.1	0.2	0.1	0.2
	B	22.9	41.4	45.8	53.3	28.0	0.9	0.8	1.5	0.9	1.7
	Std. Dev.	1.3	3.2	2.8	4.1	2.4	0.0	0.1	0.1	0.1	0.2
	C	27.3	38.5	42.5	52.3	28.3	0.9	0.7	1.4	0.8	1.5
	Std. Dev.	1.4	3.3	5.4	3.0	1.1	0.0	0.0	0.1	0.1	0.2
	D	36.7	39.6	43.8	51.6	27.5	0.9	0.8	1.5	0.9	1.6
	Std. Dev.	3.5	3.0	4.3	2.5	1.3	0.0	0.0	0.1	0.1	0.2

Table 5.2. Means of MSS digital counts in relation to disease severity

Date	Severity Group	Yield	MSS Band 4	MSS Band 5	MSS Band 6	MSS Band 7	MSS Band Ratio 4/5	4/6	4/7	5/6	5/7
3/20/73	0	26.2	27.1	24.4	30.1	16.2	1.1	0.9	1.7	0.8	1.5
	Std. Dev.	6.8	1.9	3.4	3.1	2.1	0.1	0.1	0.2	0.1	0.3
	1	32.4	26.2	22.6	32.4	18.0	1.2	0.8	1.5	0.7	1.3
	Std. Dev.	4.9	2.1	3.6	4.4	3.0	0.1	0.1	0.2	0.1	0.3
	2	27.5	27.0	24.0	30.1	16.1	1.1	0.9	1.7	0.8	1.5
	Std. Dev.	7.1	2.2	3.7	1.5	1.2	0.1	0.1	0.2	0.1	0.3
	3	20.8	26.0	22.6	31.0	17.1	1.2	0.8	1.5	0.7	1.3
	Std. Dev.	6.3	0.8	1.4	1.4	1.1	0.0	0.0	0.1	0.1	0.1
5/13/73	0	28.2	35.6	31.6	51.5	28.8	1.2	0.7	1.3	0.6	1.2
	Std. Dev.	6.2	3.8	6.3	5.3	4.3	0.1	0.1	0.3	0.1	0.3
	1	31.8	31.6	25.3	48.8	28.3	1.3	0.7	1.3	0.6	1.0
	Std. Dev.	5.2	3.7	4.8	13.1	9.2	0.1	0.2	0.7	0.2	0.5
	2	28.0	36.1	30.9	57.1	32.6	1.2	0.6	1.2	0.6	1.0
	Std. Dev.	7.9	4.6	6.5	7.5	5.8	0.1	0.1	0.3	0.1	0.3
	3	22.7	35.8	30.8	53.5	29.6	1.2	0.7	1.2	0.6	1.1
	Std. Dev.	6.2	4.2	5.1	7.5	4.2	0.1	0.1	0.1	0.1	0.1
5/31/73	0	26.6	32.5	29.0	52.8	31.4	1.2	0.6	1.1	0.6	1.0
	Std. Dev.	7.1	4.4	6.8	3.7	3.1	0.1	0.1	0.2	0.1	0.3
	1	32.2	33.8	31.2	51.8	30.3	1.1	0.7	1.2	0.6	1.1
	Std. Dev.	5.1	4.6	8.1	3.5	3.6	0.1	0.1	0.3	0.2	0.4
	2	27.5	35.1	32.2	53.6	30.7	1.1	0.7	1.2	0.6	1.1
	Std. Dev.	7.8	3.6	6.4	2.5	2.5	0.1	0.1	0.2	0.1	0.3
	3	20.0	35.8	34.0	51.5	28.6	1.1	0.7	1.3	0.7	1.2
	Std. Dev.	3.8	1.4	2.3	3.6	2.6	0.0	0.1	0.1	0.1	0.2
6/18/73	0	26.6	38.8	42.7	51.2	27.6	0.9	0.8	1.4	0.8	1.6
	Std. Dev.	7.1	3.7	5.6	3.7	2.2	0.0	0.1	0.2	0.1	0.3
	1	32.2	39.7	44.1	52.7	28.1	0.9	0.8	1.4	0.8	1.6
	Std. Dev.	5.1	3.1	4.3	2.5	1.2	0.0	0.0	0.1	0.1	0.2
	2	27.5	40.8	45.3	52.9	27.9	0.9	0.8	1.5	0.9	1.6
	Std. Dev.	7.8	2.8	2.9	3.7	2.1	0.0	0.1	0.1	0.1	0.2
	3	22.1	42.5	47.6	53.5	27.8	0.9	0.8	1.5	0.9	1.7
	Std. Dev.	5.7	4.7	6.0	4.4	1.7	0.0	0.0	0.1	0.1	0.1

Table 5.3. Correlation coefficients - MSS digital counts vs. wheat yields

	MSS Band				MSS Band Ratio				
Date	4	5	6	7	4/5	4/6	4/7	5/6	5/7
3/20/73	.18	.14	.32*	.30	-.02	-.18	-.18	-.09	-.10
5/13/73	-.02	-.01	-.07	-.03	.09	.13	.13	.08	.09
5/31/73	-.39*	-.34*	-.06	.21	.34*	-.31*	-.31*	-.30	-.29
6/18/73	-.23	-.24	-.16	-.01	.12	-.17	-.21	-.20	-.22

*Significant at 5% level.

Correlation coefficients with a minimum of 40 degrees of freedom: 1% = .393
5% = .304
10% = .257

Table 5.4. Correlation coefficients - MSS digital counts vs. disease severity

	MSS Band				MSS Band Ratio				
Date	4	5	6	7	4/5	4/6	4/7	5/6	5/7
3/20/73	-.13	-.10	.01	-.01	.04	-.13	-.10	-.12	-.10
5/13/73	.10	.02	.20	.16	.04	-.13	-.11	-.14	-.12
5/31/73	.32*	.27	-.05	-.28	-.29	.32*	.32*	.27	.28
6/18/73	.35*	.35*	.22	.03	-.18	.25	.27	.29	.28

*Significant at 5% level.

Correlation coefficients as above.

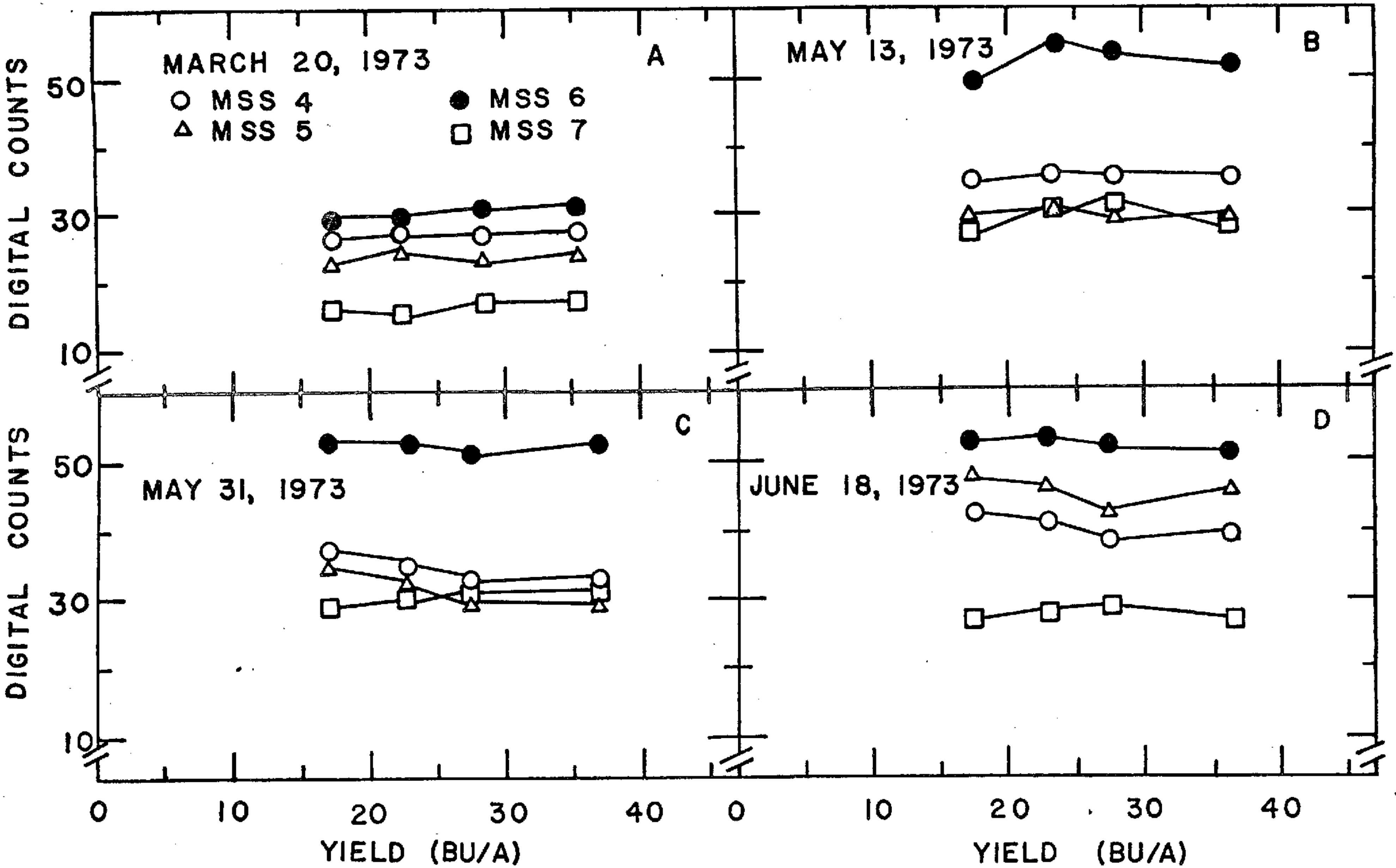

Fig. 5.1. Temporal variations in the relationship between mean digital counts and wheat yield.

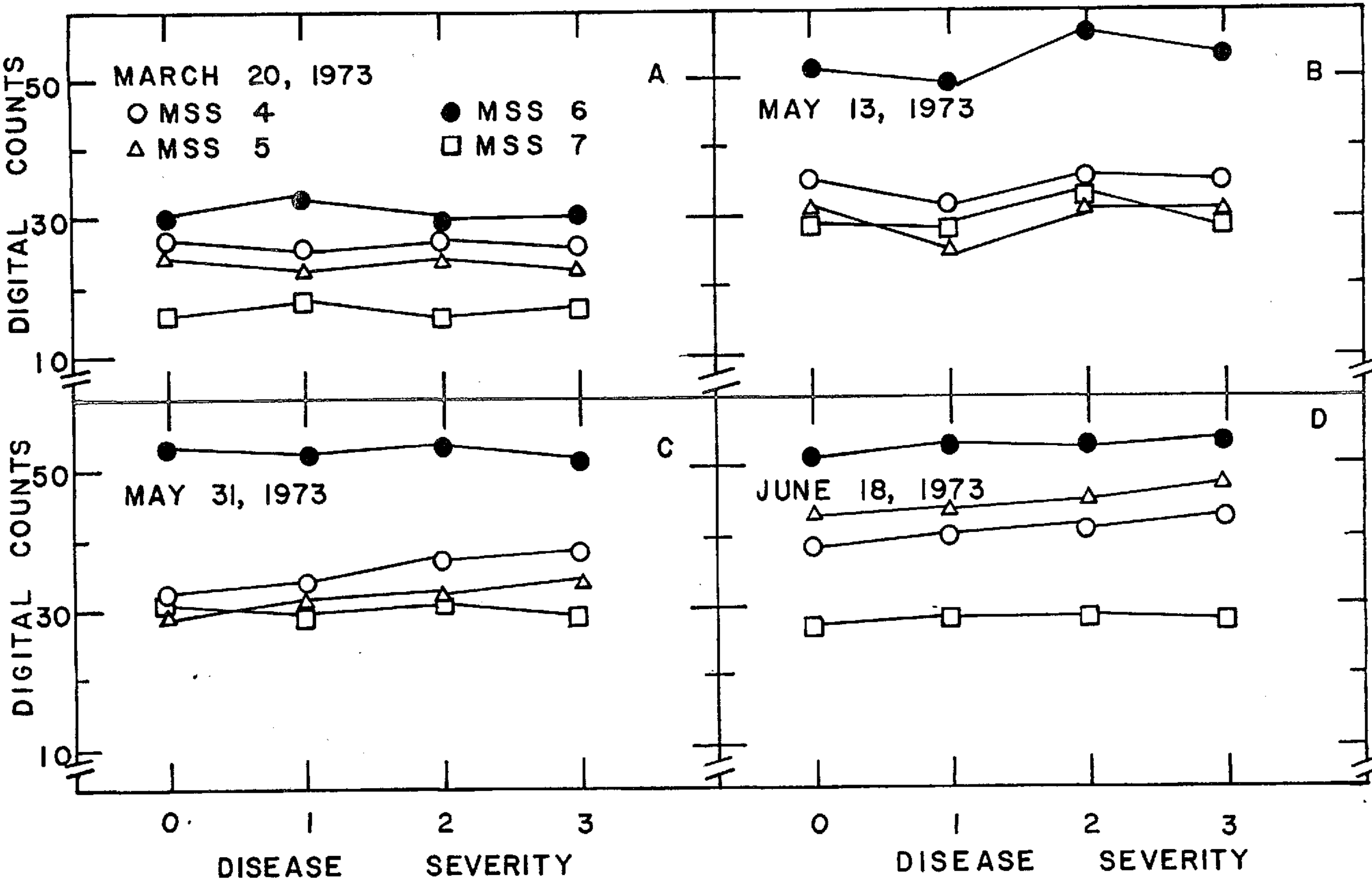

Fig. 5.2. Temporal variations in the relationship between mean digital counts and WSMV severity.

6.0 LITERATURE CITED

1. Allen, W. A. and A. J. Richardson. 1968. Interaction of light with a plant canopy. Jour. Apt. Soc. Amer. 58:1023-1028.

2. Barr, H. D. 1968. Determination of water deficits in plant tissues. In: Water deficits and plant growth. Vol. 1. (ed.) T. T. Kozlowski. Academic Press. New York. p. 235-368.

3. Bowers, S. A. 1971. Reflection of radiant energy from soils. Kansas State University Library, Manhattan, Kansas.

4. Brun, L. J., E. T. Kanemasu, and W. L. Powers. 1972. Evapotranspiration from soybean and sorghum fields. Agron. Jour. 64:145-148.

5. David, W. P. 1969. Remote sensing of crop water deficits and its potential applications. Texas A & M University Remote Sensing Center Technical Report RSC-06.

6. Jensen, M. E., J. L. Wright and B. J. Pratt. 1971. Estimating soil moisture depletion from climate, crop and soil data. Trans. Amer. Soc. Agr. Eng. 14(5):954-959.

7. Kanemasu, E. T., G. W. Thurtell, and C. B. Tanner. 1969. Design, calibration and field use of a stomatal diffusion porometer. Pl. Physiol., Lancaster, 44:881-885.

8. Kondrat'yev, K. Y. 1965. Actionomentry NASATT F9712. National Aeronautics and Space Administration, Washington, D.C.

9. List, R. J. 1949. Smithsonian Meteorological T.bles. Smithsonian Institution Press. Washington, D.C.

10. Remote Multispectral Sensing in Agriculture. 1970. Purdue University Agricultural Experiment Station Bulletin 873.

11. Remote Sensing. 1970. National Academy of Sciences, Washington, D.C.

12. Teare, I. D. and C. J. Peterson. 1971. Surface area of chlorophyll-containing tissue of the inflorescence of triticum aestivum 1. Crop Sci. 2(5):627-628.

13. Variety Tests with Fall-Planted Small Grains. 1971. Kansas State University Agricultural Experiment Station Report 180.

14. Wiegand, C. L., H. W. Gausman, J. A. Cuellar, A. H. Gerbermann and A. J. Richardson. 1973. Vegetation density as deduced from ERTS-1 MSS response. Proc. ERTS-1 Symposium. December 10-13, 1973.

7.0 CONCLUSIONS

A computer-based model of estimating evapotranspiration for irrigation scheduling requires a crop coefficient curve. The leaf area index (LAI) of wheat appears to provide a reasonable estimate of a wheat-crop coefficient and can be deduced from MSS digital data. The ratio of any two MSS bands (digital counts) are linearly correlated with LAI ($r > .70$); the ratios of MSS4:MSS5 and MSS5:MSS6 appear to best simulate LAI ($r > .90$). In addition, these linear regression equations are useful for estimating LAI of wheat on fields other than which the equation were derived.

The soil moisture in the roo zone of wheat was estimated with reasonable success from MSS7 and MSS4:MSS5; however, the relationship is not unique and would depend upon soil type. This preliminary work needs further investigation.

The early detection of wheat streak mosaic virus using the available ERTS-1 imagery for 1973 was not possible. At the time of greatest visual difference between healthy and disease wheat, no ERTS-1 imagery was available because of cloud cover. However, we attempted a later detection of disease severity using the May 13, 1973 imagery but no significant correlation of disease severity to band digital count was found. The May 31, 1973 imagery showed a higher degree of significance (5% level) of digital counts versus severity and digital counts versus yield. This relationship was attributed to the premature yellowing and thinning of diseased wheat.

Our use of data collection platforms (DCP) to predict disease severity was successful and appears to have potential applications. The implementation of the DCP did not create a major maintenance problem.

8.0 FUTURE RESEARCH NEEDS

Currently we are at the stage of development where it is feasible to monitor large agricultural areas and identify the crop type and stage of development. However, further study is required for the detection and evaluation of disease and water stress. These physiological stresses are of major importance in their effect on crop yield. As with most agricultural programs, the timeliness of the observations is extremely critical.

N74-27797

Appendix A

ERTS-1 Data Collection Systems Used to Predict Wheat Disease Severities

ERTS-1 DATA COLLECTION SYSTEMS USED TO PREDICT WHEAT DISEASE SEVERITIES[1]

E. T. Kanemasu, H. Schimmelpfennig, E. Chin Choy,
M. G. Eversmeyer and D. Lenhert[2]

ABSTRACT

The feasibility of using the data collection system on Earth Technology Satellite-1 to predict wheat leaf rust severity and resulting yield loss was tested.

Ground-based data-collection platforms (DCPs), placed in two commercial wheat fields in Riley County, Kansas, transmitted to the satellite such meteorological information as maximum and minimum temperature, relative humidity and hours of free moisture. Meteorological data received from the two DCPs from April 23 to 29 were used to estimate the disease progress curve. Values from the curve were used to predict the percentage decrease in wheat yields resulting from leaf rust. Actual decrease in yields was obtained by applying a zinc and maneb spray (5.6 kg/ha) to control leaf rust, then comparing yields of the controlled (healthy) and the noncontrolled (rusted) areas. In each field a 9% decrease in yield was predicted by the DCP-derived data; actual decreases were 12% and 9%.

---

[1] Contribution No. 1387, Agronomy Department, Evapotranspiration Laboratory, and Contribution No. 595, Department of Plant Pathology, Kansas Agricultural Experiment Station, Kansas State University in cooperation with the United States Department of Agriculture. National Aeronautics and Space Administration provided partial support for this research. Date received ________________.

[2] Assistant Professor of Microclimatology, Electronic Technician, Research Associate, Research Plant Pathologist, USDA, ARS, NCR, and Associate Electrical Engineer, Department of Electrical Engineering, Engineering Experiment Station, Kansas State University, Manhattan, Kansas 66506.

INTRODUCTION

Epidemiological investigations have shown that the severity of wheat leaf rust (*Puccinia recondita* Rob. ex Desm f. sp. *tritici*) and subsequent loss in yield can be predicted (Eversmeyer and Burleigh, 1970; Burleigh et al., 1972a; Burleigh et al., 1972b). Such predictions would be most important for determining curative measures to reduce economic loss.

In the above mentioned investigations, stepwise multiple regression techniques were used to identify biological and meteorological variables useful in explaining variation in wheat leaf rust severities 7, 14, 21, and 30 days after the date of prediction (DP) and the relationship between those predicted severities and yield loss. Equations in the form $Y_i = K_i + b_1 x_{1i} + \ldots + b_n x_{ni}$ were formulated and tested. Variables which they reported to be most significant in the successful prediction of wheat leaf rust development were: leaf rust severity on DP, growth stage of wheat on the date predicted, average hours of free moisture during seven days prior to DP, number of days or precipitation greater than or equal to 0.25 mm during seven days prior to DP, a fungal growth function, and fungal infection function. The equations predicted leaf rust severity in test plots within ± 1, 3, and 12%, 14, 21, and 30 days in advance, respectively. They studied the relationship between leaf rust severity at several wheat growth stages and yield loss and constructed general equations to predict percent loss.

Successful prediction of disease losses for large remote areas would require continuous gathering of meteorological and biological data on widely separated fields, which using routine instrumentation would require an enormous maintenance capability. The recent launching (July 23, 1972) of Earth Resources Technology Satellite-1 (ERTS-1) has permitted the use of spacecraft to collect data from ground-based transmitters placed in remote areas; in turn the satellite can retransmit data to one of three prime receiving stations: Goldstone, California; NASA Test and Training Facility; and Fairbanks, Alaska. (Detailed information can be found in the Data Users Handbook)[3].

The satellite's data collecting capability offers a unique opportunity to test and evaluate the use of information gathered by data collection platforms to predict epidemics of wheat leaf rust.

MATERIALS AND METHODS

Two data-collection platforms (DCP) -- furnished by NASA as part of an ERTS-1 experiment (site 1, 39°07'N, 96°35'W; site 2, 39°08'N, 96°35'W) -- were located in two Riley County (Kansas) commercial fields (40 acres each) of wheat (*Triticum aestivum* L. cv. Scout). Site 1 and site 2 fields were a silty clay loam and silt loam, respectively. Both fields were planted to wheat in late September in 20-cm rows. The DCPs were installed by December 1, 1972 and were operational until July 23, 1973.

The data collection platform (DCP) is an automatic, data-relay terminal that accepts 8 channels of either analog or digital data from user-furnished electronics (sensor interfaces). Every 3 minutes the DCP interrogates the 8 input channels and transmits the data, regardless of the satellite's position. The satellite passed close enough to the Riley County DCPs to receive the transmission with a ± 1 hour period at 1030

[3]Available through General Electric, Space Division, Valley Forge Space Center, P. O. Box 8555, Philadelphia, Penn. 19101.

and 2230 local time. Because many of our sensors required interrogation at other times, we designed a sensor interface that interrogates sensors at the proper time, then digitally stores the data for transmitting later. (A detailed description of the interface appears in a NASA report)[4].

The power supply (storage batteries) was enclosed in a box separate from the rest of the DCP to prevent corrosion by acid fumes. The transmitter and interface were enclosed in a double wooden box.

Table 1 gives sensor data transmitted and received by the satellite during the two periods of each day that the satellite was within DCP range. Information on channels 1 through 4 was obtained primarily for input into the disease prediction equations; the visible and near infrared reflectance data (channels 5-8) were used to analyze crop growth.

Relative humidity was measured by a sulfonated polystyrene sensor (PCRC-11, Phys-Chemical Research Corp.), and soil moisture was estimated by gypsum soil moisture blocks (CEL-WFD, Beckman Instruments). The signal conditioning consisted of an AC ohmmeter and a logarithmic amplifier for linearization. Free moisture was detected by measuring the AC resistance change of a bifilar array exposed to the atmosphere. When wetted, the electrical resistance of the array decreases and the resistance of the array was determined with a level-detecting AC ohmmeter. Air temperatures (maximum, minimum, and instantaneous) were determined by thermalinear thermistors (YSI 700, Yellow Spring Instruments). Maximum and minimum temperatures stored in the interface memory were compared with the current temperature every 3 minutes and updated. Visible (590 to 720 nm) and

---

[4]Report No. 2263-3, Kansas Environmental and Resource Study: A Great Plains Model. January, 1973. NASA.

near infrared (730-1000 nm) radiation streams were measured using silicon photocells filtered on their respective wavelengths ranges. (Details on sensors and signal conditioning can be found in a NASA report)[4].

The relative humidity and temperature sensors were located in small ventilated weather shelters. The weather shelters were positioned at least 35 m from the edge of the field. Early in the season, the sensors were maintained at a height of about 30 cm above the soil surface but, as the plants developed, the shelters were raised to keep the sensors near the top of the canopy. The free moisture sensors were maintained at mid-canopy height. The photocells were located on stands approximately 2.5 m above the soil surface.

Beginning April 25, weekly applications of a zinc and maneb spray (5.6 kg/ha) were made on four randomly selected 2.2 m^2 areas (healthy) near each DCP for control of wheat leaf rust. Grain yields were obtained by harvesting four 1.5 m^2 plots from the sprayed areas and four adjacent 1.5 m^2 areas on which leaf rust was not controlled. Leaf rust severity estimates were made at the time of spray application using the modified Cobb scale (Peterson 1948).

RESULTS

The DCP can be used to collect and transmit data with minimal maintenance. Two 12V storage batteries, used to power the system, were replaced every four weeks, when they needed recharging. At the same time, sensors were routinely checked. Occasional down-time was experienced due to an electrical storm or rodents chewing transmission cables.

Data (IBM cards) were received from NASA 5 to 14 days after transmission to the satellite. Normally, 8 to 12 transmissions were received by the satellite each day from each DCP (Fig. 1). Figs. 2 and 3 show typical meteorological information acquired by the DCP.

Maximum and minimum temperatures and hours of dew occurring each day as recorded by the two DCPs for the seven day period April 23 to 29 were used together with other biological data taken in the test fields to predict leaf rust severities that would be expected on May 6, 13, 20, 29, near each DCP. These predicted severities were used in the leaf rust loss equations to predict the percent reduction in wheat yields to be expected due to leaf rust development. Using meteorological data obtained from the DCPs a 9% decrease in wheat yields due to leaf rust was predicted for each site, and compared favorably with actual decreases in yield of 9% and 12% (Table 2). Actual yield reductions were obtained by comparison of yields of the controlled (healthy) and the noncontrolled (rusted areas).

The manpower required for obtaining data in remote areas could be minimized by use of DCPs. Our results indicate DCP-derived data can be effectively used in existing disease prediction equations.

REFERENCES

1. Burleigh, J. R., A. P. Roelfs, and M. G. Eversmeyer. 1972a. Phytopathology 62:944-946.
2. __________, M. G. Eversmeyer, and A. P. Roelfs. 1972b. Phytopathology 62:947-953.
3. Eversmeyer, M. G. and J. R. Burleigh. 1970. Phytopathology 60:805-811.
4. Peterson, R. F., A. B. Campbell, and H. E. Hannah. 1948. Can. J. Res. 26:496-500.

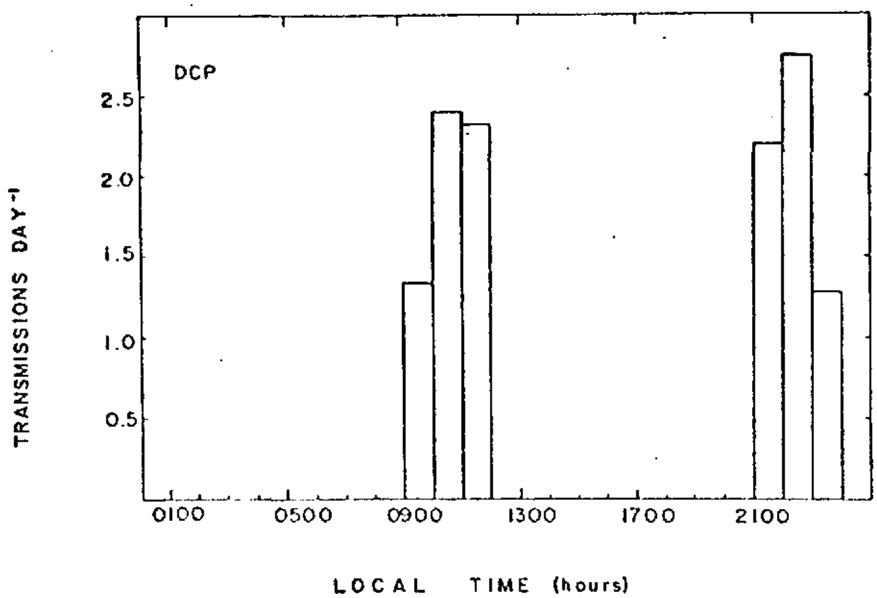

Fig. 1. Average daily transmissions received from DCPs in Riley County wheat fields by the satellite, December, 1972.

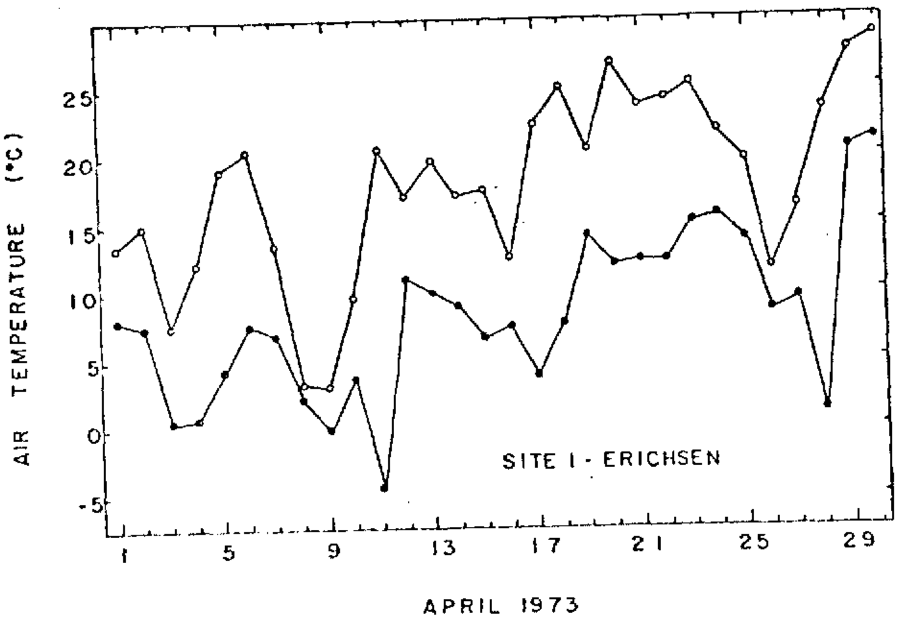

Fig. 2. Maximum and minimum air temperature in a wheat canopy as transmitted by the DCP.

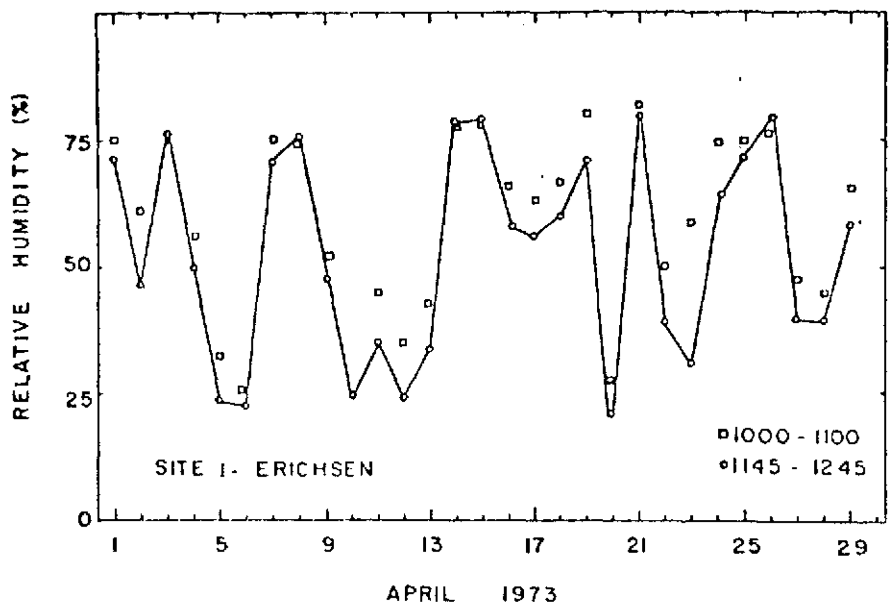

Fig. 3. Relative humidity in a wheat canopy as transmitted by the DCP.

Table 1. Data from DCPs in Riley County wheat fields transmitted at the two periods.

CHANNEL	9:00-11:00 TRANSMISSION	21:00-23:00 TRANSMISSION
1	instantaneous relative humidity	instantaneous soil moisture
2	cumulative hours free moistures	cumulative hours free moisture
3	minimum temperature 00:00-11:30	maximum temperature 11:30-00:00
4	instantaneous temperature	instantaneous temperature
5	instantaneous incoming visible	14:00 incoming visible
6	instantaneous reflected visible	14:00 reflected visible
7	instantaneous incoming infrared	14:00 incoming infrared
8	instantaneous reflected infrared	14:00 reflected infrared

Table 2. Leaf rust severity estimates, wheat yields and percentages loss observed in commercial fields from which DCP data were obtained.

Location	Rep.	April 26 GS[1/]	April 26 %DS[2/]	May 18 GS	May 18 %DS	May 25 GS	May 25 %DS	June 4 GS	June 4 %DS	June 11 GS	June 11 %DS	kg/ha	% Loss actual	% Loss predicted
ERICHSEN														
Healthy	1	EJ	0	H	.5	A	.5	M	1	SD	3	2913		
	2	EJ	0	H	.5	A	.5	M	1	SD	3	2887		
	3	EJ	0	H	.5	A	.5	M	1	SD	3	2911		
	4	EJ	0	H	.5	A	.5	M	1	SD	3	2975		
	Ave.											2921	12.3	9.2
Rusted	1	EJ	0	H	.5	A	.5	M	20	SD	40	2627		
	2	EJ	0	H	.5	A	.5	M	20	SD	40	2690		
	3	EJ	0	H	.5	A	.5	M	20	SD	40	2424		
	4	EJ	0	H	.5	A	.5	M	20	SD	40	2511		
	Ave.											2562		
HARTNER														
Healthy	1	EJ	0	H	.5	A	.5	M	.5	SD	.5	3135		
	2	EJ	0	H	.5	A	.5	M	.5	SD	.5	3050		
	3	EJ	0	H	.5	A	.5	M	.5	SD	.5	3227		
	4	EJ	0	H	.5	A	.5	M	.5	SD	.5	3143		
	Ave.											3139	9.3	9.1
Rusted	1	EJ	0	H	.5	A	.5	M	15	SD	30	2882		
	2	EJ	0	H	.5	A	.5	M	15	SD	30	2762		
	3	EJ	0	H	.5	A	.5	M	15	SD	30	2891		
	4	EJ	0	H	.5	A	.5	M	15	SD	30	2854		
	Ave.											2847		

1/ Growth stage; EJ (early joint); H (heading); A (anthesis); M (milk); SD (soft dough)

2/ disease severity

N74-27798

Appendix B

Seasonal Reflectance Patterns of Wheat, Sorghum and Soybean

SEASONAL CANOPY REFLECTANCE PATTERNS OF WHEAT, SORGHUM AND SOYBEAN[1]

by

E. T. Kanemasu[2]

ABSTRACT

Reflectance characteristics of agronomic crops are of major importance in the energy exchanges of a surface. In addition, unique reflectance patterns may be an aid in crop identification by means of remote sensing. Our study suggests that the ratio of the reflectances of the 545-nm to the 655-nm wavebands provides information about the viewed surface, regardless of the crop. The reflectance ratio is less than unity early and late in the growing season. For all crops studied, the ratio closely followed crop growth and development and appeared to be more desirable than the near-infrared reflectance as an index of growth.

---

[1]Contribution No. 1385 Evapotranspiration Laboratory, Agronomy Department, Kansas Agricultural Experiment Station, Kansas State University, Manhattan, Kansas 66506. This study was partially supported by the National Aeronautics and Space Administration. Received ______________.

[2]Assistant Professor of Microclimatology, Evapotranspiration Laboratory, Department of Agronomy, Kansas State University, Manhattan, Kansas 66506.

INTRODUCTION

Canopy reflectance patterns are important to the radiative balance of a crop and as possible discrimination features for remote sensing applications. Individual leaf reflectance can provide valuable information after a canopy cover becomes complete. However, in most cases the condition of the viewed surface is not known and discrimination analysis must be performed on canopy-reflectance data that may not be easily interpreted from leaf-reflectance data.

This study focused on determining canopy-reflectance patterns that would allow the surface condition to be determined.

METHODS AND MATERIALS

Two fields each of wheat (Triticum aestivum L. cv. Scout), sorghum (Sorghum bicolor L. Moench Pioneer var. 846) and soybeans (Glycine max L. cv. Clark 63) were selected in a bottomland area where one field was a dark-colored, silty clay loam (lat. 39°08'N, long. 96°37.5'W) and the other a light-colored, silt loam (lat. 30°08'N, long. 96°37'W).

Growing conditions were considered normal (compared to previous seasons) and adequate soil moisture was maintained by precipitation and irrigation. Specific growth stages and leaf area indices (leaf area to ground area) were recorded periodically. All the plants within a half square meter area were taken to the laboratory and leaf area was determined with an optical palnimeter.

To determine the spectral hemispherical reflectance of the canopy, the sensor head of a portable spectral radiometer (LI-187, Lambda Instrument Co.) was pointed upward and downward. The spectroradiometer has 9 full-scale ranges from 0.3 to 3000 watts m^{-2} (μm^{-1}). The sensor head (8.2-cm diameter) consists of seven miniature sensors covering the visible and near infrared wavelengths (Table 1). The D, F, and G sensors (545, 655, and 750 nm) closely correspond to Earth Resources Technology Satellite (ERTS-1) bands 4, 5, and 6. During the measurements the sensor head was positioned approximately 1.5 to 2.0 meters above the canopy. Azimuthal direction was kept constant relative to the sun; the observer always faced the sun. Measurements were taken only on clear days.

RESULTS AND DISCUSSION

During a significant part of a crop's growing season, bare soil is exposed. As the plant grows, less soil is exposed and the soil's reflectivity becomes less important in overall canopy reflectance. In our study soil reflectance was strongly influenced by the surface moisture (% by weight) of the silty clay loam (Fig. 1). The near-infrared wavelength band was the most sensitive to surface moisture. The longer the wavelength, the higher was the reflectance, a relationship which was consistent with the findings of other investigators (Bowers and Hanks, 1965).

Fig. 2 shows the midday spectral reflectances for wheat, sorghum, and soybeans at growth stages early, middle, and late in the season. The highest reflectance was in the near infrared at midseason. In addition, at that time reflectance was greater at 545 nm than at 655 nm; the reverse was true early and late in the season. That suggests that the ratio of the reflectances at 545 and 655 may be an indicator of soil exposure early in the season and of crop maturity late in the season.

The effect of solar elevation on reflectance usually hinders the interpreting of surface conditions from reflectance data (Suits, 1972). Therefore, the effect of sun angle on the reflectance ratio must be known before reflectance data can be interpreted correctly. Fig. 3 shows the ratios of 545 and of 655 nm reflectance with solar elevation for wheat, sorghum, soybeans, and bare soil. For each canopy, the ratio remained constant with increased solar elevation. For a mature crop, the ratio was about 1.3; for a bare soil, about 0.8. The near-infrared reflectance for wheat and sorghum decreased with increased solar elevation; but that for soybeans varied somewhat, perhaps because leaf angles changed with solar elevation (Fuchs et al. 1972).

Because the reflectance ratio apparently is not influenced by solar elevation, reflectance ratios for wheat, soybeans, and sorghum can be compared over a large portion of the growing season without serious error due to changes in sun angle. The results of such measurements are shown in Fig. 4. Fig. 4a shows that the wheat on the light-colored soil had higher near-infrared reflectance than that of the dark-colored soil (early in the season); the near-infrared reflectance did not start to increase until the late-joint growth stage. The reflectance ratio apparently followed the leaf area index curve (Fig. 5a). The ratio increased above unity at a leaf area index of about 1.0 and remained above unity during maximum growth, then decreased below unity at maturity (leaf area index < 1.0). The reflectance ratio was greater for the field with the greater leaf area index. Similarly, Fig. 4b shows the same trends in the near-infrared reflectance and the reflectance ratio for soybeans. At 120 days after planting, the soybean leaves yellowed from an infection of bacterial pustule and the reflectance ratio decreased to less than one on the infected soybeans. Thus, the reflectance ratio may serve as an indicator of physiological stress, such as brought about by disease, insects, drought or by normal maturation of the plant.

Measurements on narrow-row (46 cm) and wide-row (92 cm) sorghum (grown on dark-colored soil) which were made over the entire growing season (Fig. 4c), showed the effect of canopy cover more clearly. Plant density was maintained at 17 plants per square meter in each field (2 ha). The close-row spacing closed its canopy early in the season while the wide-row canopy never completely closed; both fields had similar leaf area indices. Near-infrared reflectance varied greatly early in the season, presumably because of changes in surface-moisture content. The reflectance ratio of the narrow-row sorghum increased to above unity at a leaf area index of about 1.0 (Fig. 5b) which also corresponded to near 90% cover (visual estimate); the wide row sorghum did not reach a ratio of unity until a leaf area of 2.5 (approximately 85% cover). The reflectance pattern for the sorghum (76-cm rows) on the light-colored field (not shown) closely followed that of the wide-row sorghum, illustrating that reflectance ratio may follow percentage cover more closely than leaf area index. The reflectance ratio decreased to below unity late in the season, even though the leaf area index was greater than one. The percentage cover at that time was about 60%.

Table 2 shows the linear regression equations derived from Figs. 4 and 5. They were obtained from single-field measurements for soybeans and sorghum (because leaf-area measurements were incomplete on the light-colored field); for wheat, data from three fields were pooled. The percentage cover was continuously estimated only for the wheat fields. Neither reflectance ratio nor near-infrared reflectance (NIR) offered a unique equation for relating reflectance to leaf area index (LAI) for all crops. The correlation coefficients were highest for soybeans and lowest for wheat. Where data from several wheat fields were examined the correlation coefficient was greater for the ratio than for the near-infrared reflectance.

This study suggests that the reflectance ratio of the 545- to 655-nm wavelengths may serve as benchmarks for crop growth and possibly for indicating percentage cover. When the ratio is less than unity, soil reflectance dominates canopy reflectance. When the crop matures, the ratio decreases to less than one. The ratio apparently is a better indicator of crop growth than is the 750 nm reflectance. The reflectance ratio alone does not appear to discriminate between crop species, but should be a valuable parameter when used with other recognition processes. The two wavelengths involved in the ratio correspond to multispectral scanner bands 4 and 5 (MSS4 and MSS5) of ERTS-1. A study is underway to test the feasibility of using the ratio of MSS4 and MSS5 for wheat growth and disease detection.

REFERENCES

1. Bowers, S. A. and R. J. Hanks. (1965). Soil Sci. 100:130-138.

2. Fuchs, M., G. Stanhill, and A. G. Waanders. (1972). Israel J. Agr. Res. 22:63-75.

3. Suits, G. H. (1972). Remote Sens. of Env. 2:175-182.

Table 1. Optical characteristics of the spectral radiometer

Sensor	Center wavelength (nm)	Band width (nm)
A	415	40
B	450	32.5
C	500	45
D	545	35
E	600	40.2
F	655	45
G	750	80

Table 2. Linear regression equations and correlation coefficients for wide-row and narrow-row sorghum, wheat and soybeans. LAI is leaf area index; NIR is near-infrared reflectance.

	Linear regression equation	Correlation coefficient
Sorghum (wide-row)	LAI = 10.93 x (ratio)- 8.37	0.89
	LAI = 0.26 x (%NIR) - 2.70	0.84
Sorghum (narrow row)	LAI = 9.18 x (ratio)- 6.90	0.80
	LAI = 0.23 x (%NIR) - 3.24	0.87
Wheat	LAI = 5.06 x (ratio)- 4.07	0.75
	LAI = 0.13 x (%NIR) - 1.67	0.64
	% cover = 109.88x(ratio)-63.71	0.87
	% cover = 2.85x(%NIR) -19.24	0.72
Soybean	LAI = 13.67 x (ratio)- 11.28	0.96
	LAI = 0.296 x (%NIR)- 5.10	0.98

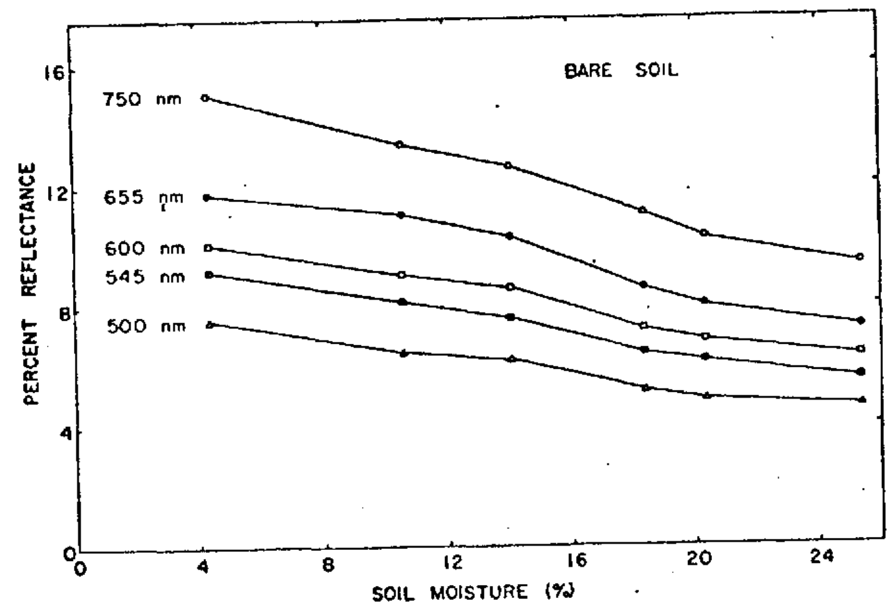

Fig. 1. Effect of surface soil moisture (% by weight) on spectral reflectance of a silty clay loam soil. Measurements were taken at midday.

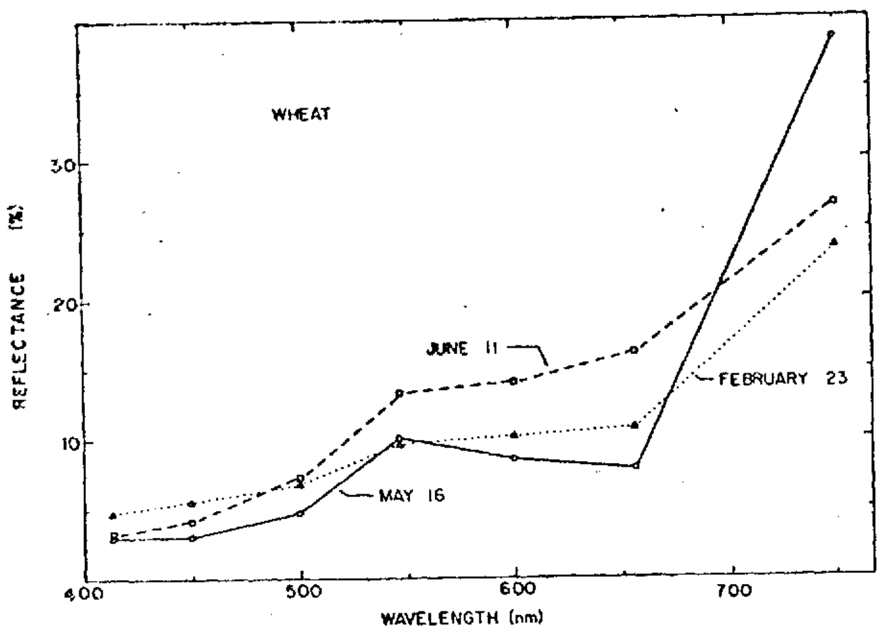

Fig. 2a. Spectral reflectance of wheat on February 23, 1973 (dormancy), May 16 (heading), and June 11 (hard dough).

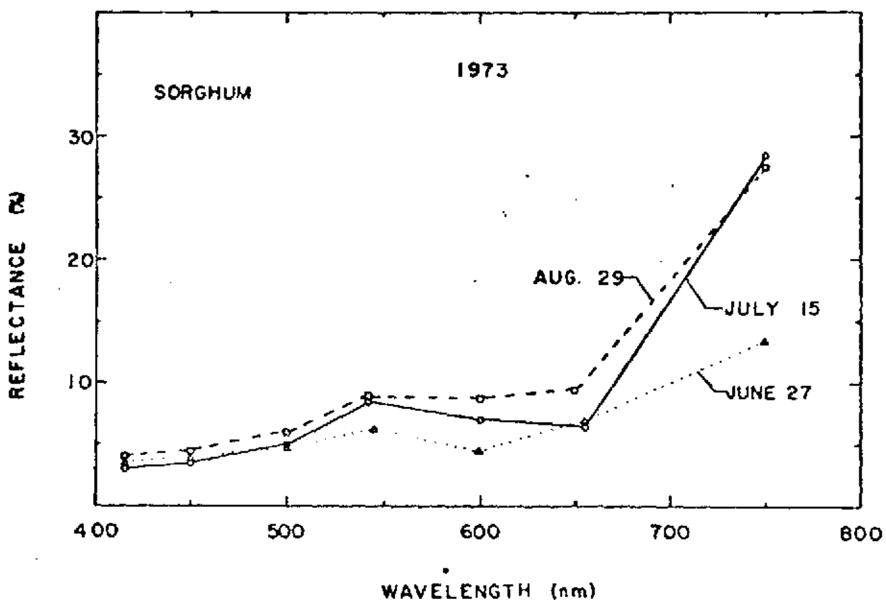

Fig. 2b. Spectral reflectance of sorghum on June 27 (five leaves), July 15 (nine leaves), and August 29 hard dough).

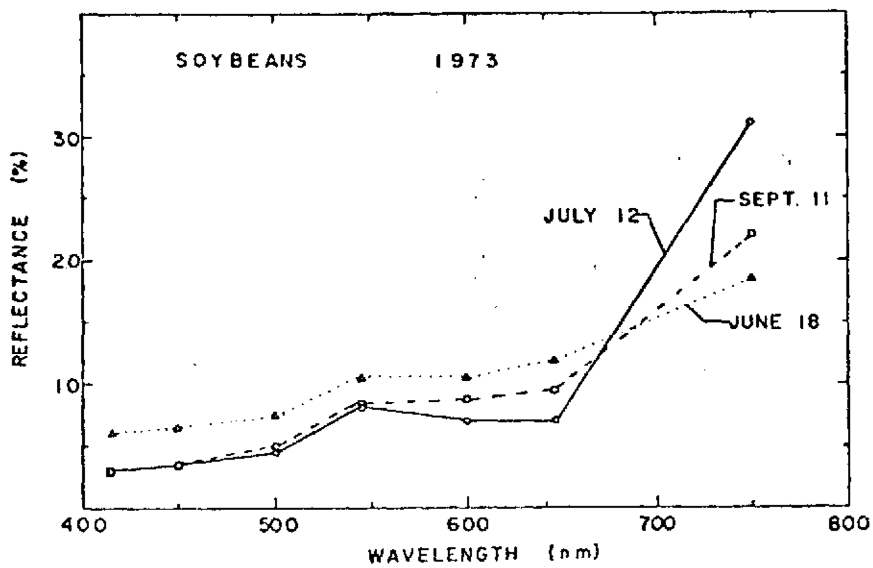

Fig. 2c. Spectral reflectance of soybean on June 18 (four trifoliate leaves), July 12 (podding), and September 11 (greenbean stage).

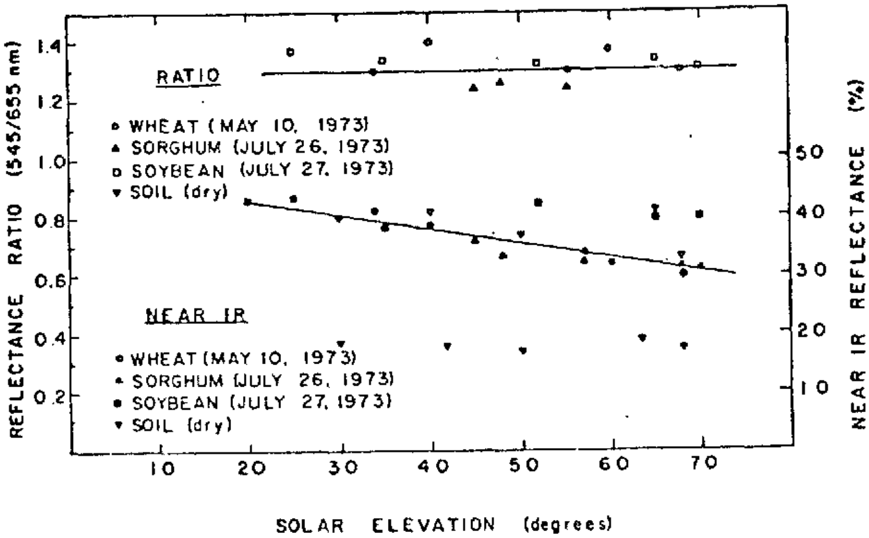

Fig. 3. Effect of solar elevation (0-horizon) on the reflectance ratio of the 545 to 655 nm waveband and on the near infrared reflectance (750 nm) of wheat (boot stage), sorghum (early heading), soybean (late podding), and dry silty clay loam.

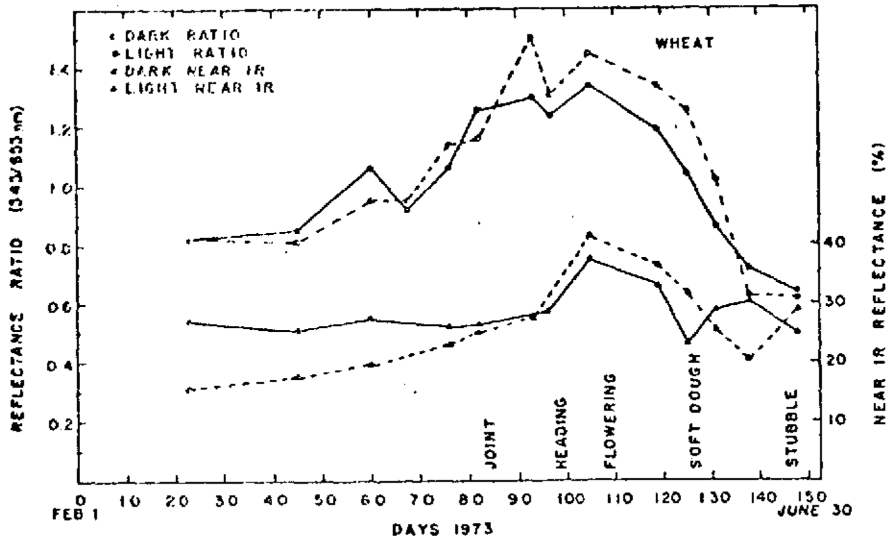

Fig. 4a. Seasonal trends in the reflectance ratio and near infrared reflectance of a silty clay loam wheat field (dark-colored) and a silt loam wheat field (light-colored).

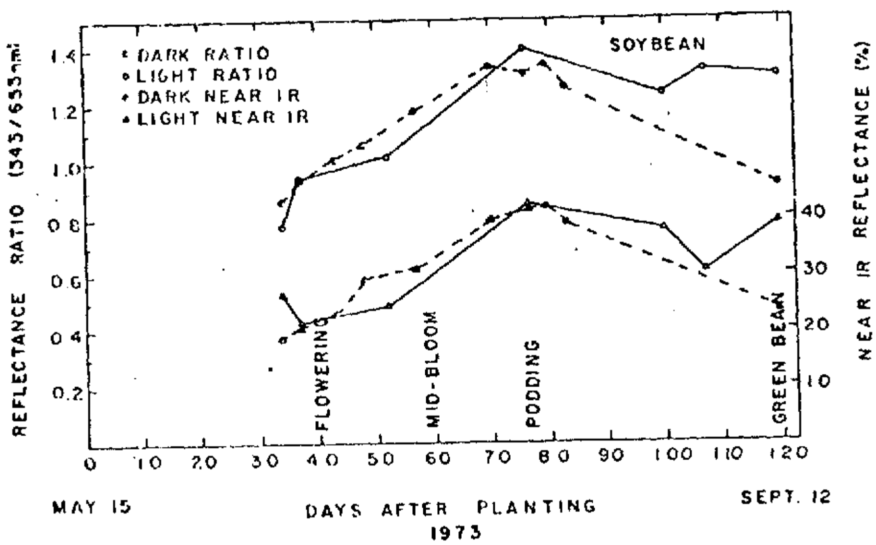

Fig. 4b. Seasonal trends in the reflectance ratio and near infrared reflectance of a silty clay loam soybean field (dark) and a silt loam field (light).

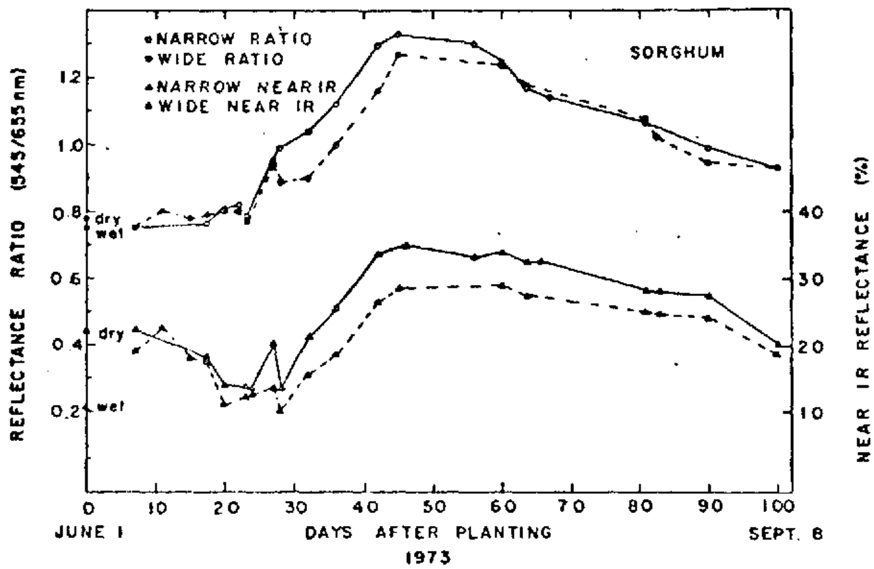

Fig. 4c. Seasonal trends in the reflectance ratio and near infrared reflectance of narrow and wide row sorghum on a silty clay loam soil. The wet and dry data points represent bare soil measurements.

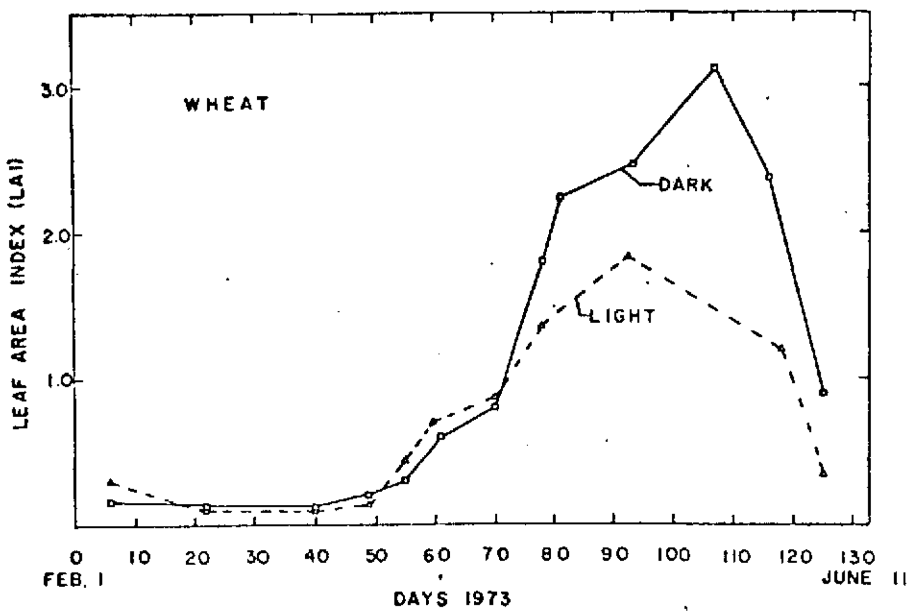

Fig. 5a. Seasonal trends in the leaf area index (LAI) of wheat on the silty clay loam field (dark) and on the silt loam field (light).

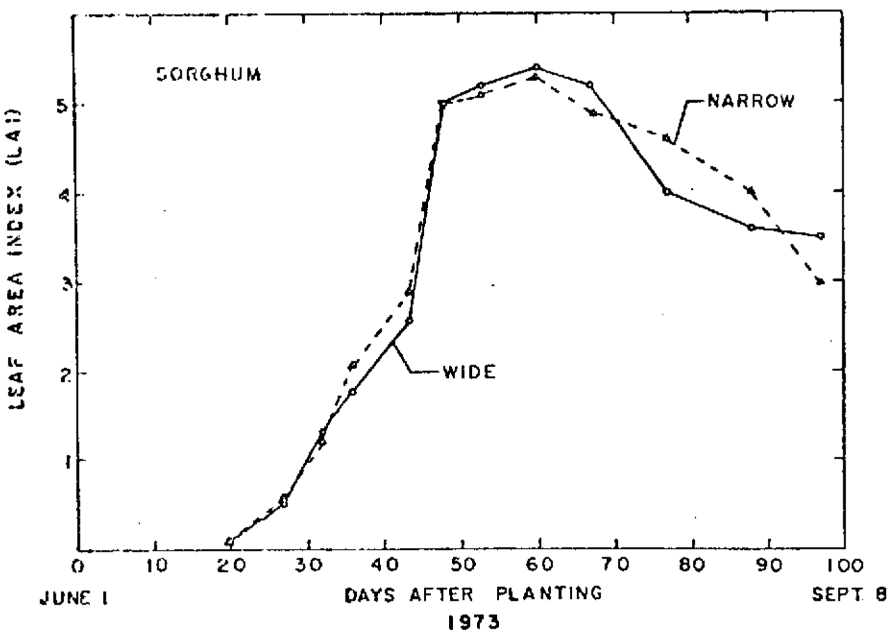

Fig. 5b. Seasonal trends in leaf area index of the wide- and narrow-row sorghum.

N74-27799

Appendix C

Flexible DCP Interface

FLEXIBLE DCP INTERFACE[1]

by

H. Schimmelpfennig and E. T. Kanemasu[2]

ABSTRACT

A user of an ERTS data collection system (DCS) must supply the sensors and signal-conditioning interface. The electronic interface must be compatible with the NASA-furnished data collection platform (DCP). We describe here a "universal" signal-conditioning system for use with a wide range of environmental sensors.

The interface is environmentally and electronically compatible with the DCP and has operated satisfactorily for a complete winter wheat growing season in Kansas.

---

[1]Contribution No. 1397, Agronomy Department, Evapotranspiration Laboratory, Kansas Agricultural Experiment Station, Kansas State University, Manhattan, Kansas 66506. This study was partially supported by the National Aeronautics and Space Administration. Received ____________.

[2]Electronic Technician and Assistant Professor of Microclimatology, Evapotranspiration Laboratory, Department of Agronomy, Kansas State University, Manhattan, Kansas 66506.

INTRODUCTION

The Data Collection Platform (DCP) is a field-deployable, automatic, data-relay terminal that can be located in remote areas to gather information for specific applications or to complement imagery information received from the ERTS system. The DCP (which consists of an electronic unit, an antenna assembly, and an interconnecting cable) accepts sensor input data. The accepted data can be in the format of eight analog inputs; eight 8-bit, serial-digital inputs; eight, 8-bit, parallel-digital inputs; or combinations of these formats. To gather these data, the user must supply a power source, sensors and signal-condition system for his specific requirements[3].

The data collection platform interface (DCPI), described here, is a "universal" signal-conditioning system that accepts inputs from 8 sensors of almost any type and interfaces them to the DCP. The DCPI contains power supplies, control logic, memory, and signal-conditioning modules for each sensor. An alteration in a signal-conditioning function can be easily affected by inserting the proper module in the DCPI. Modules can perform a variety of signal conditioning functions such as amplifying, linearizing, integrating, totaling counts, sample-hold, and comparing previous readings. Appendix A lists the sensor and signal-conditioning system used in our wheat study.

TECHNICAL DESCRIPTION

Figure 1 is a functional block diagram of the DCPI. Two 12-volt car batteries power both the DCP and DCPI. Time between recharging the battery

---

[3] Earth Resources Technology Satellite Data Collection Platform Field Installation, Operation and Maintenance Manual. NASA. Goddard Space Flight Center.

is dependent on the particular function modules; for our study, it was about 2 months under average conditions.

The 24-hour clock sends time data (in 10 minute increments) to the modules. The main controller sequentially interrogates the signal-conditioning modules and controls the data storage cycle. The analog to digital converter converts analog to digital data for storage in the memory.

The 64-bit memory stores the data from the 8 sensors (8 bits for each sensor). Data are transferred to the DCP for transmission, or back to the modules for comparison to current data.

Light emitting diodes on the instrument panel monitor the data and provide information during routine field inspections. The DCP transmits at 3-minute intervals 24 hours a day. The TRANSMIT CLOCK from the DCP shifts 64 data bits (8 per sensor) from the memory to the transmitter. After the transmission, the DCPI scans the eight channels and stores any new data in the memory. The logic flow in a scan cycle is best illustrated by specific example, like maximum-minimum temperature.

Example Logic Flow. At the start of a scan, the main controller turns on the power supply and, after a 5-second delay, interrogates channel 1. Following interrogation, logic control shifts from the main controller to the interrogated module, which then connects itself (via a set of CMOS switches) to the 10 control-buss lines. Assume that the sensor is a temperature sensor and the module is designed to find the maximum air temperature during the day. The maximum temperature module converts the resistance of the temperature sensor to a properly scaled, analog voltage, and then generates a START OF CONVERSION (SOC) command, causing the ANALOG-

TO-DIGITAL CONVERTER (ADC) to convert the analog voltage from the module (ADO) line to digital data. After the digital conversion, the ADC generates an END-OF-CONVERSION (EOC) signal informing the module that the conversion process is complete.

Previous maximum temperature is stored both in an 8-bit, parallel output shift register on the module and also in the main memory. These digital data are converted (at the module) to analog and compared with current temperature. Two cases present themselves: (1) the present temperature is higher than the maximum or (2) the present temperature is lower than the maximum.

<u>Case 1</u>. The module sets the DATA, REPLACE-SAVE (D, R-S) line to REPLACE and generates a START-OF-STORE (SOST) command. The main controller accepts the command and generates an 8-pulse, shift-clock train (SHFT CLK). The SHFT CLK shifts the digital data from the ADC to the input of the memory and shifts the memory 8 places, thus transferring the new data into memory. The DIGITAL DATA in (DDI) line transfers the new temperature reading from the ADC to the module using the SHFT CLK signal for synchronization.

<u>Case 2</u>. The module sets the D, R-S line to SAVE and generates an SOST command. The main controller again generates SHFT CLK. The replace-save switch at the memory input is now set at SAVE and the memory cycles the stored data, leaving them unchanged in memory.

At the end of the storage cycle the main controller generates an END-OF-STORE (EOST) command, which resets a latch on the maximum temperature, and then interrogates Channel 2. The same type of control chain now occurs with module 2. This sequence continues until all 8 channels have been scanned.

Digital data also can be gated from the module to the main memory. Module 2, hours of free moisture, would set the DATA, ANALOG-DIGITAL (D,A-D) line to digital. Digital data gated by SHFT CLK proceeds from the module on the DIGITAL-DATA-OUT (DDO) line, through the analog-digital switch, directly to the memory. The replace-save function is operable in the digital as well as the analog data mode.

The sequence of INT, SOC, EOC, SOST, and EOST is repeated for each module. After the last module is interrogated, the interface turns off everything except the continuous power.

Control Cards A1 and A2 (Figs. 2 and 3).

The DCPI control section includes two circuit cards, A1 and A2. A1 contains the 64-bit memory and most of the control logic. A2 contains the analog-to-digital converter and display drivers.

At the start of a DCP transmission the DATA GATE drops low and remains for its 80 ms warmup-transmit cycle. Q1, Q2, and Q5 interface between the 5-volt DCP TTL logic and the 12-volt DCPI CMOS logic. U10D turns on V_x, a 5-volt supply for Q5 (needed during transmit only).

If a manual scan is not in progress, the LOW at the output of U9D is gated through U13B to the mode control on the 64-bit memory (U12). U12 is now in the recirculate mode and, when clocked, its data bits will leave $\bar{Q}$, through U17 to the DCP.

At the end of the transmission U18 latches turning on a 5-volt supply (V_5) and the main ± 15-volt supply (V_S). After a 5-second warmup, counter U26 is reset and advanced to channel 1, sending a HIGH interrogate signal to module 1. Module 1 returns its analog data (if any) to the analog-to-digital converter on control card A2. Module 1 next returns a high SOC command to the ADC. The network of U3, U4, and U5 provides a delay, after the analog signal reaches the LH0042 buffer amplifier, before the A to D conversion can start. This network also assures that SOC commands from two consecutive modules will be "see" as two HIGHS, not one long continues HIGH.

Upon completing the A to D conversion, the ADC returns an EOC pulse to the module. When ready, the module sets the D, A-D line to 1 if it is to send digital data for storage. It sets the D, S-R (DATA, SAVE-REPLACE) to 0 or 1 depending if the new data (either from the ADC or digital data from the module) are to be retained. Next, the module returns a START OF STORE (SOST) command. The 8-pulse, shift gene ator (U19, U15, U20) sends 8-clock pulses to the memory (U12); the modules; and on card A2 to U1, the ADC to serial shift register, and to U5, the memory-to display shift register. U24 gates the digital data from the ADC shift register or the module to the memory. When the storage cycle is complete, an END OF STORE (EOST) signal is sent back to the module and U26 is advanced to interrogate the next module. After the last module has been interrogated, U14B resets latch U18A, turning off the power supplies and ending the scanning cycle.

The scanning cycle can be run under manual control to observe data and control states at each important step, thus facilitating trouble shooting.

Pressing the MANUAL SCAN START button sets latch U18B, which blocks out interferring signals from the DCP transmitter and SOST signals from the modules. U18A latches on and U26 advances to interrogate module 1. Panel LED's now display the output of the analog to digital converter, whether the data in memory will be saved or replaced, and whether analog or digital data from the module will be stored. Pressing the STEP button starts the store cycle. The LED's now display the memory contents for channel 1: either the new channel 1 data, or the previous channel 1 data which have been retained. Pressing the STEP button again advances U26 to channel 2. Switching the DCAN, MEMORY CYCLE switch to the MEMORY CYCLE position locks the memory in the recirculate mode, thus allowing a review of the memory contents unaltered by a scan cycle.

TIME CLOCK (Fig. 4).

A crystal-controlled clock sends 24-hour time information to each module. This enables the modules to operate on time dependent data.

Crystal-controlled oscillator U1 runs at 27.96 KHz. U4 and U8 divide this frequency down to 1 pulse per 10 minutes. U3, U6, and U10 give time outputs in 10-minute increments through 24 hours. The time outputs are bussed in parallel to all the modules.

U7 gives a 14:00 signal to the four radiation modules to avoid adding identical decoding circuitry to the four modules.

MODULES

RADIATION MODULES (Fig. 5).

The radiation module is designed for silicon photocells. U1 is a current-to-voltage converter. R1 sets the gain. U2 is a buffer for the 100-second, RC network R7, C2.

A time signal to Pin 9 causes the 14:00 data to be retained in memory for the evening transmission. From 00:00 to 13:59 the DCP transmits instantaneous data.

MAXIMUM-MINIMUM-INSTANTANEOUS TEMPERATURE (Fig. 6).

This module is divided into two circuit cards and supplies data to two channels. The module outputs instantaneous temperature on one channel. The other channel is the maximum temperature between 11:30 and 23:59, or the minimum temperature between 00:00 and 11;30. Unless a front passes through, the true maximum and minimum temperatures are transmitted.

U8 and U9 form a linear thermistor thermometer using a YSI (Yellow Spring Instruments) thermalinear network. When Pin 19 is interrogated, instantaneous temperature is sent to the controller, which converts the instantaneous analog signal to digital data. The digital data are passed back on 10 parallel lines to the input of 10-bit latch.

The returning EOC signal strobes U26, latching SAVE-REPLACE LATCH U6A and U6B if a new maximum or minimum is present. This enters the new maximum or minimum in U3. The DAC converts this to analog data. When the next channel is scanned, U4B passes the maximum or minimum to the controller.

RELATIVE HUMIDITY AND SOIL MOISTURE (Fig. 7).

This module transmits relative humidity from 00:00 to 13:59 and soil moisture from 14;00 to 23:59.

U1 is a 1200-Hz oscillator. U1C gives a high pulse during the last 1/4 of the 300-Hz square wave at the output of U2B. U3's output is a ± 1 volt square wave which drives the RH and SM sensors through DC blocking tantalum capacitor pairs. U4 and U5 convert current through the sensor to voltage.

The output of U4 and U5 is a square wave with a high spike on the front. The spike width is proportional to the lead wire capacitance and is an error term.

U6 and U7 are precision full-wave rectifiers. U8 C and D and U9 form a sample-hold circuit that eliminates all but the last 1/4 of the wave form. This technique gets rid of the lead-wire capacitance error. U8A and -B gate the RH or SM data to the next stages, depending on time of day.

LOG AMP is a logarithmic amplifier, which straightens the RH and SM curves. U10 and U11 add offset and gain to put the signal in the final form.

The relative humidity sensor works over a 2,000 ohm to 2 megohm range. Soil moisture is read over a 200-ohm to 20,000-ohm range.

HOURS FREE MOISTURE (Fig. 8).

The presence of dew or rain is sensed by the lowered resistance of a bifilar grid. U1 drives a 27 Hz square-wave through the sensor and R1, R2. C1, C2, and R4 rectify and filter the output. Operational amplifier U2 compares this signal with a fraction of the logic supply.

If the sensor is wet, a 36.621 ms/cycle signal from the time clock is gated into 20-stage ripple counter U3 and U4. The last 8 bits of the counter total 256 bits at 5 minutes per bit. Hours of free moisture are obtained by subtracting successive transmissions.

POWER SUPPLIES (Fig. 9).

Two 12-volt storage batteries are the main power source. The DCP requires 24 volts and the DCPI 12 volts (Fig. 9).

Continuous 12-volt power runs all the CMOS logic in the DCPI. A 12 volt to ± 15 volt converter supplies continuous operational amplifier power if needed (Fig. 9). During a transmission, a 5-volt supply turns on to interface the CMOS to TTL. During a scan, a high power 12-volt to ± 15-volt converter supplies power to the operational amplifiers, while a high power 5-volt supply powers the ADC and some TTL logic in the DCPI.

APPENDIX C1

DCP SENSOR AND SIGNAL CONDITIONING CHARACTERISTICS

CH 1. Relative humidity and soil moisture

Position: in the canopy

Sensor: Type, Relative Humidity PCRC-11 sulfonated polystyrene (Phys-Chemical Research Corp.)

Span: 0-100% RH ± RH

Accuracy: ± 1% RH

Position: 30-cm depth

Sensor: Type, soil moisture block CEL-WFD (Beckman Instruments)

Accuracy: 2% of reading

Signal Conditioning: Type, Lead-wire, capacitance-eliminating, AC ohmmeter with log amplifier for linearization.

CH 2. Hours of free moisture (dew and rain)

Position: above canopy

Sensor: Type, Bifilar array on printed-circuit board (G-10 epoxy base)

Signal Conditioning: Type, level-detecting, AC ohmmeter Accuracy, ± 20 MS per change of sensor state with no additional cumulative error.

CH 3. Maximum and minimum temperature

Position: at top of canopy

Sensor: Type, YSI series 700 thermalinear thermistor probe. (Yellow Springs Instruments)

Signal Conditioning: Type, digital storage of max (min) and analog comparison with present temperature.

Accuracy: ± 0.25°C

CH 4. Instantaneous temperature

Position: at top of canopy

Sensor type and accuracy: same as channel 3.

Signal conditioning: Type, thermalinear thermistor bridge

Accuracy: ± 0.15°C.

CH 5. Incoming visible radiation

Position: approximate 2m above soil surface

Sensor: Type, silicon photocell SBC 255

Instrument: (1) cosine corrected head

(2) 6 mm heat adsorbing glass (KG-3)

(3) diffusing plastic

(4) wratten 26 filter

Response: 590 to 720 nm

Construction: Built by E. T. Laboratory

Signal Conditioning: Type, Signal averaging filter

Accuracy: ± 0.3%

Response time: 10 to 90% - 220 seconds

CH 6. Reflected visible

Same as Ch 1 except sensor is faced downward

CH 7. Incoming near-infrared radiation

Position: 1.5 m above soil surface

Sensor: Type, Silicon photocell

Instrument: (1) cosine corrected head

(2) diffusing plastic

(3) wratten 88A

Construction: Built by E. T. Laboratory

Response: 730 to 1000 nm

CH 8. Reflected near infrared

Same as Ch 3 except sensor faced downward.

APPENDIX C2

PARTS LIST FOR CONTROL BOARDS A1 AND A2

U2 - Noninverting buffer, RCA CD4050AE
(schematic shows this as an inverting buffer)

U12 - 64-bit shift register, RCA CD4031AE

U17, U18, U20 - dual flip-flop, RCA CD4013AE

U19 - counter, RCA CD4022AE

U26 - counter, RCA CD4017AE

R1, R4 - 180K and R2, R40 - 120K

R3, R11, R12, R14, $17, $19, $27, $28, $35, $37, $38 - 100K

R5, R6 - 390K

R7, R8, R9 - 82K

R10 - 39K

R13 - 12K

R16, R18, R26, R29, R34, R39 - 1.2K

R21 - 470K

R23 - 1K

R24 - 68K

R25, R30, R31 - 270K

R32 - 560K

R33 - 220K

R41, R42 - 1.5M

C1, C6, C7, C8, C10, C11, C12 - .01μF

C2, C3 - 10μF

C4, C5 - 470 pF

C9 - .002 μF

Notes: (1) All digital logic parts are RCA COSMOS except where noted differently on schematics

(2) COMOS CD4016AE transmission gates are shown as

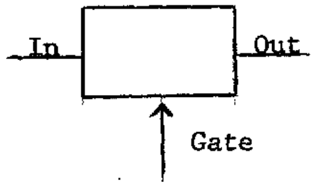

(3) NPN transistors are 2N222A

PNP transistors are 2N2907A

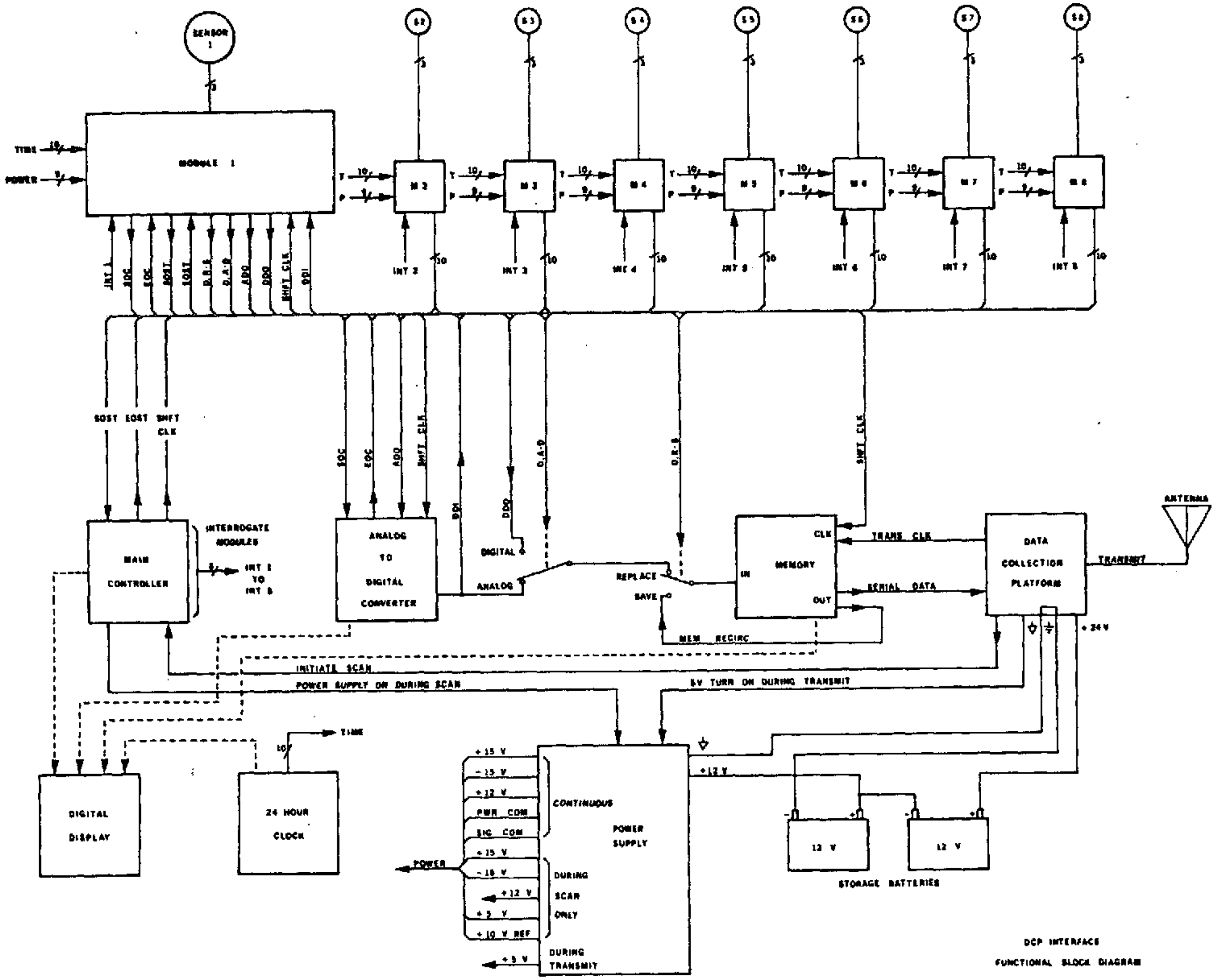

Fig. 1. DCP Interface Functional Block Diagram

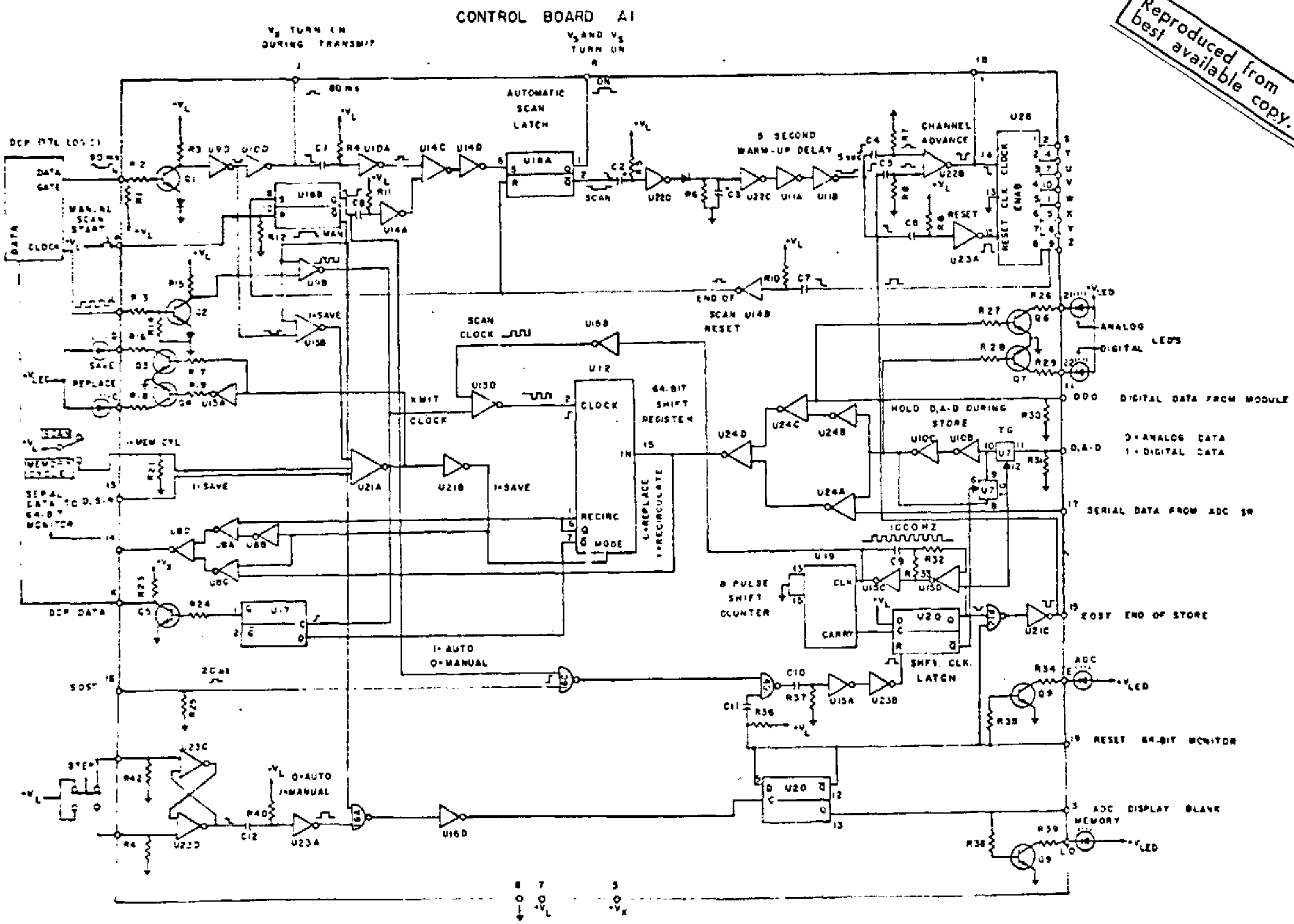

Fig. 2. Control Board A1

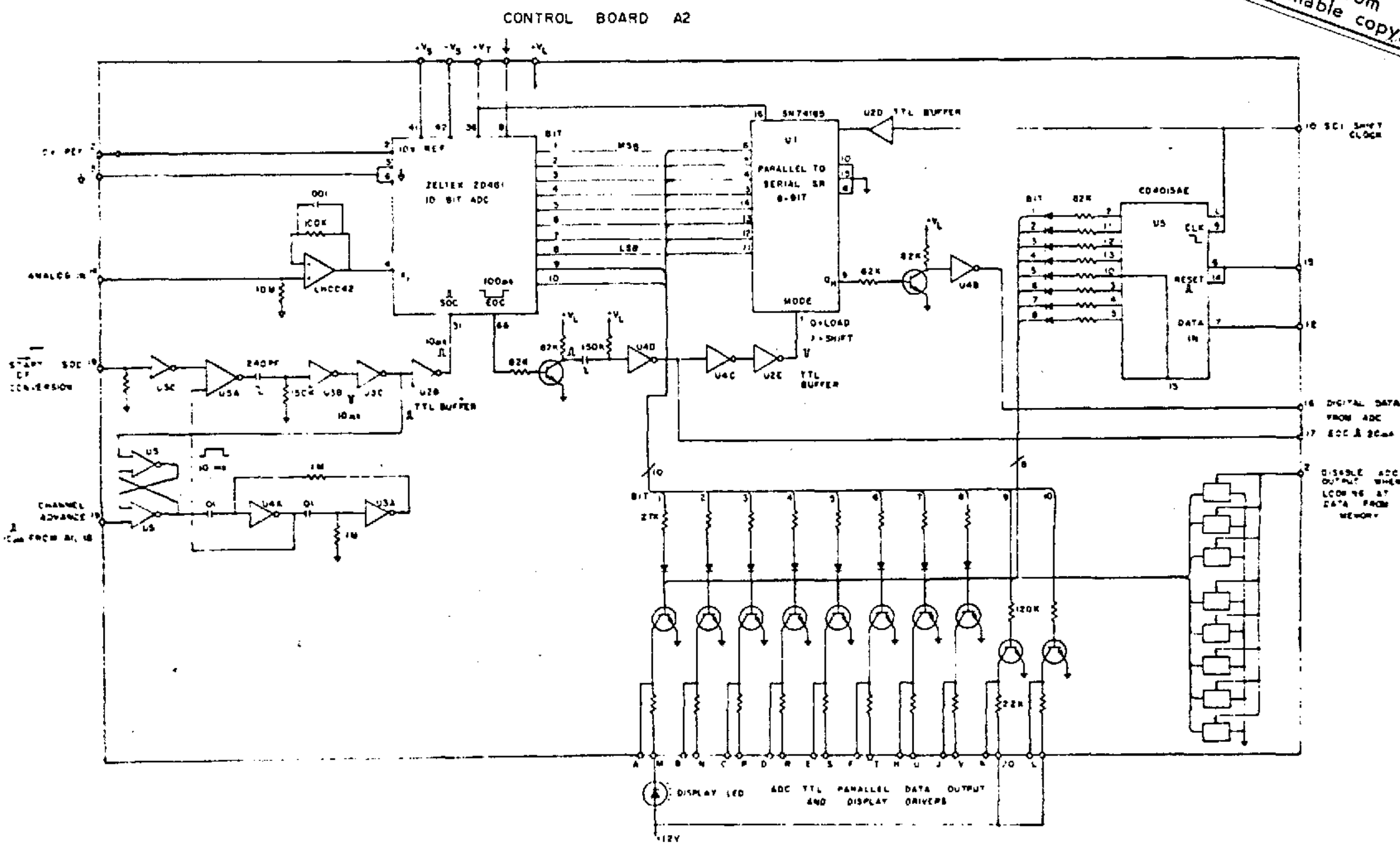

Fig. 3. Control board A2

TIME CLOCK

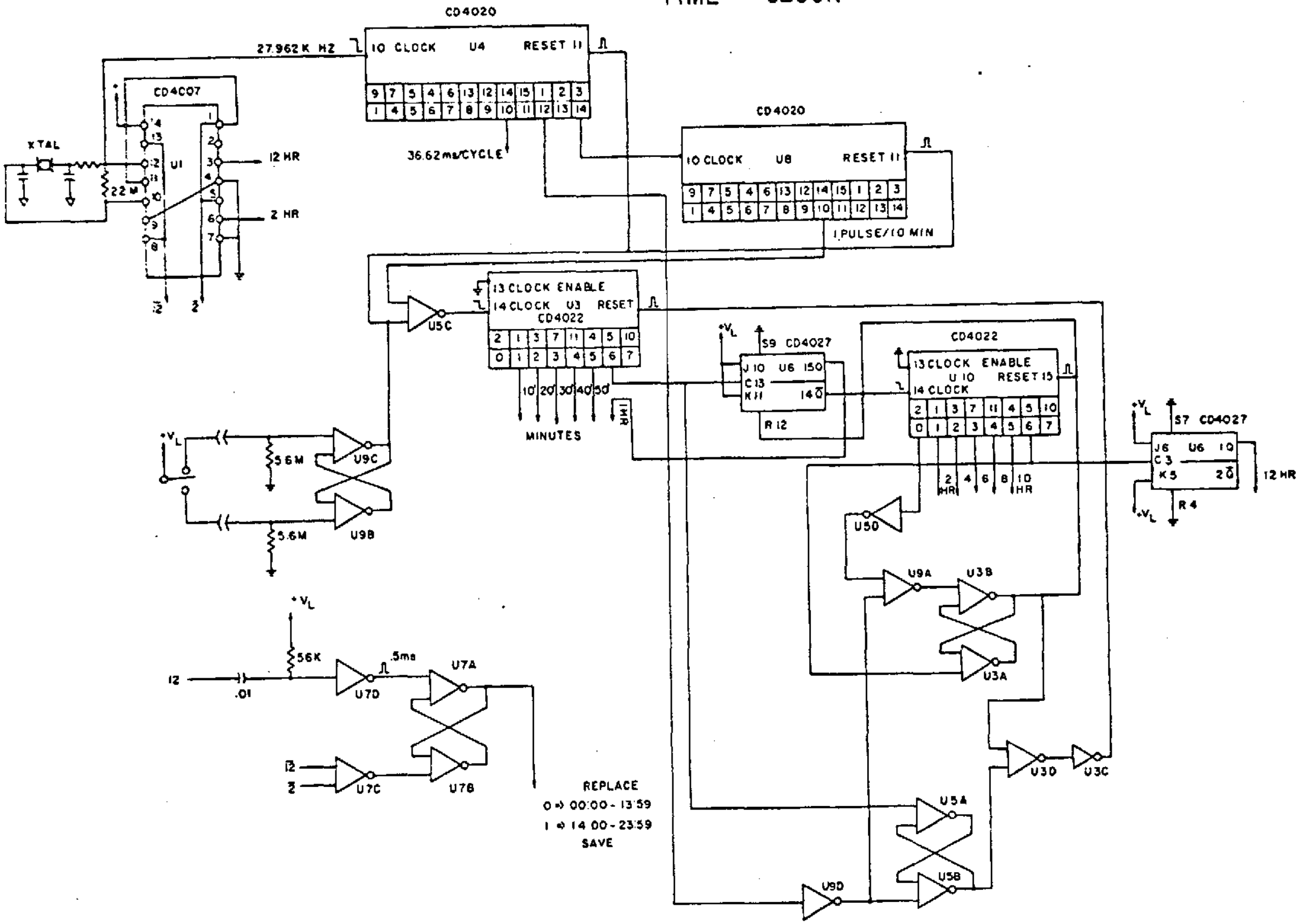

Fig. 4. Time Clock

RADIATION MODULES

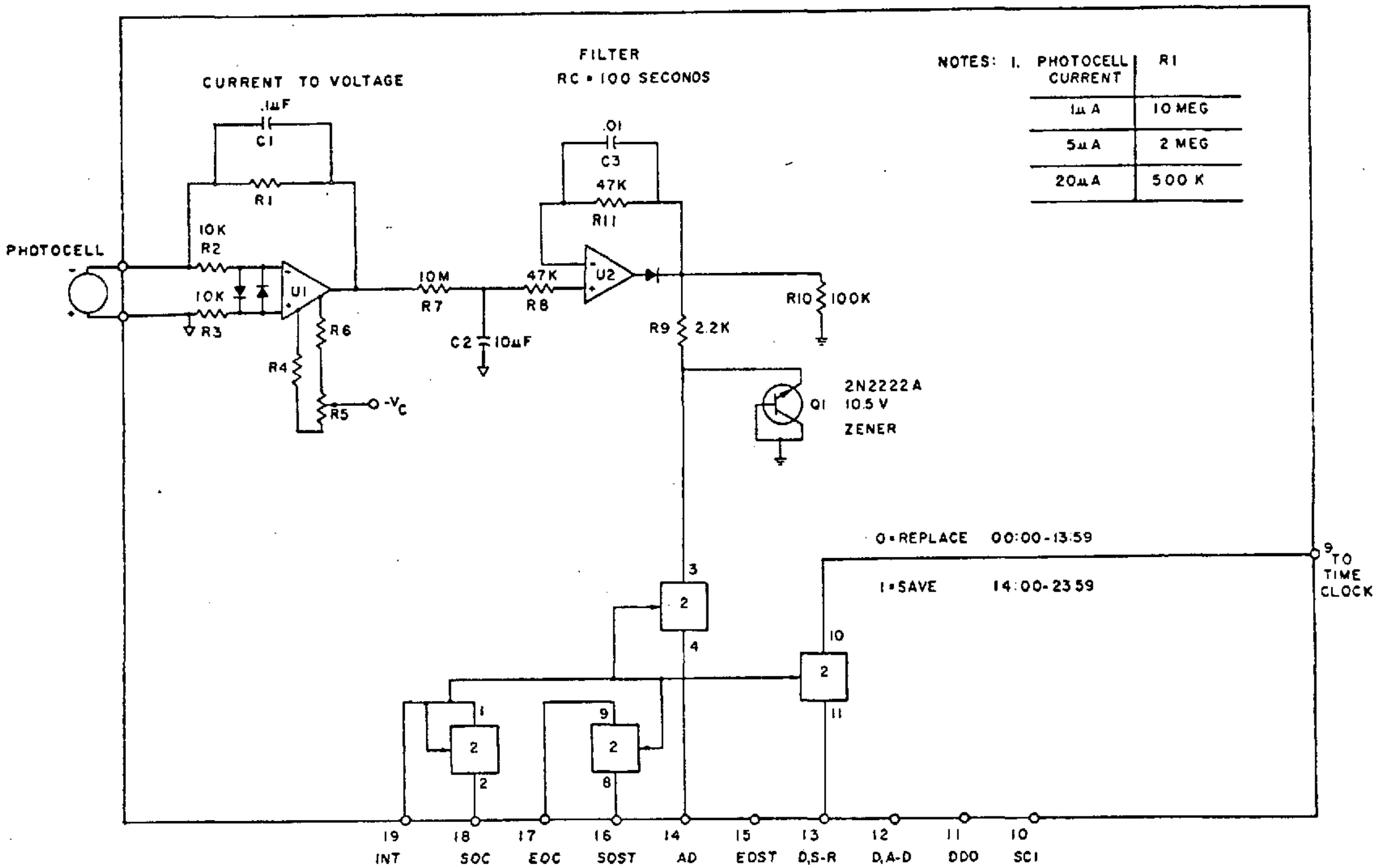

Fig. 5. Radiation Modules

MAX-MIN-INSTANTANEOUS TEMPERATURE

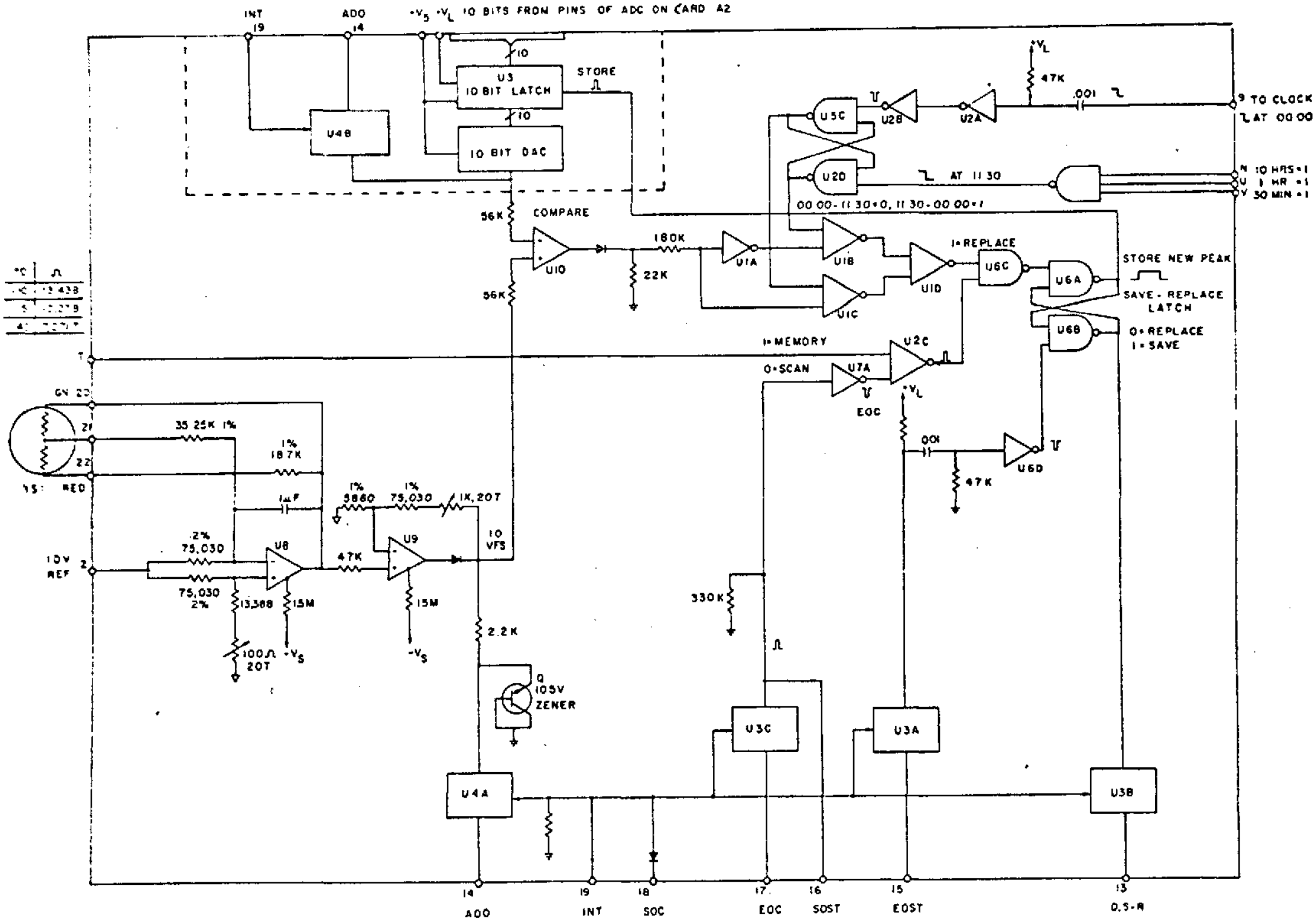

Fig. 6. Max-Min-Instantaneous Temperature

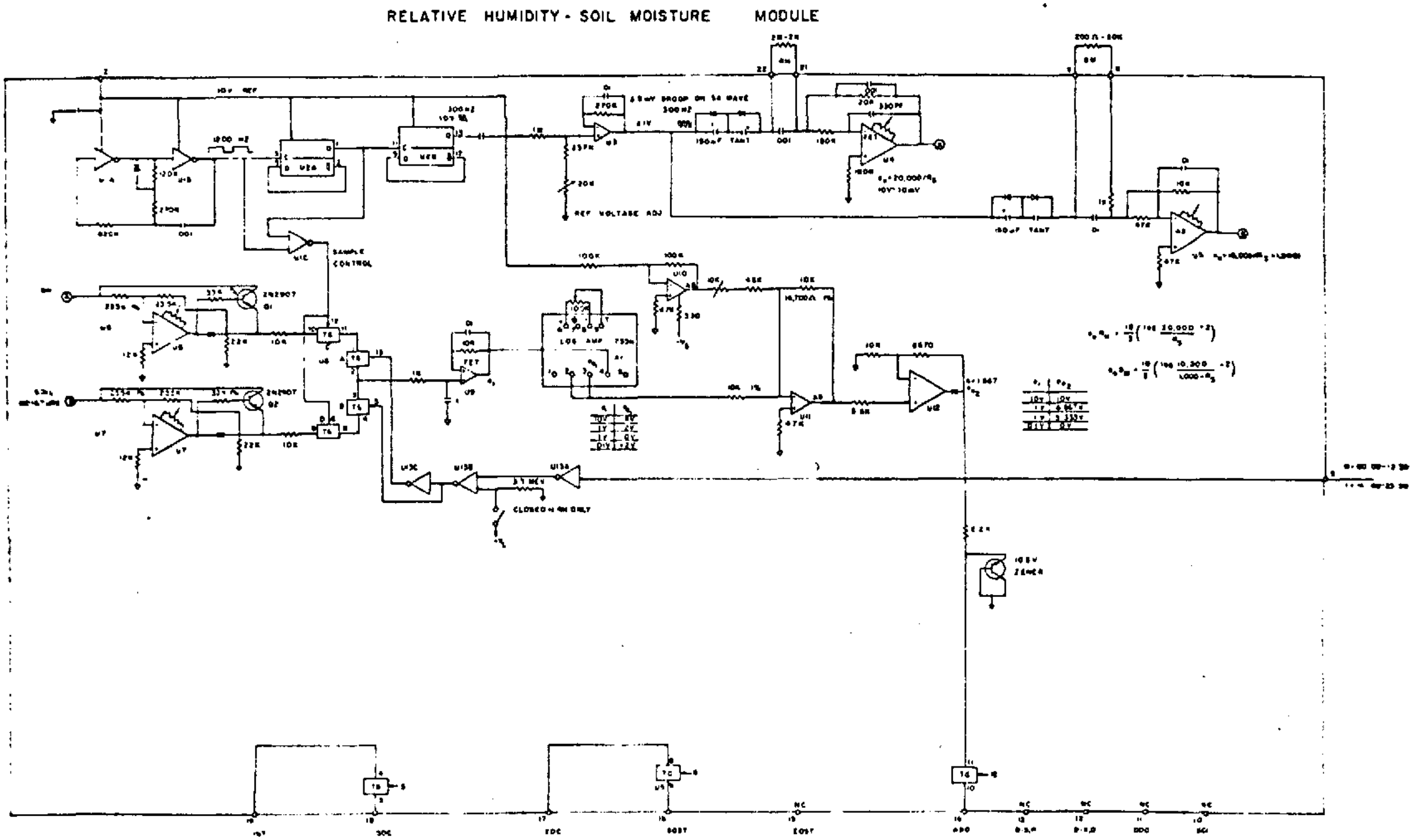

Fig. 7. Relative Humidity-Soil Moisture Module

HOURS FREE MOISTURE

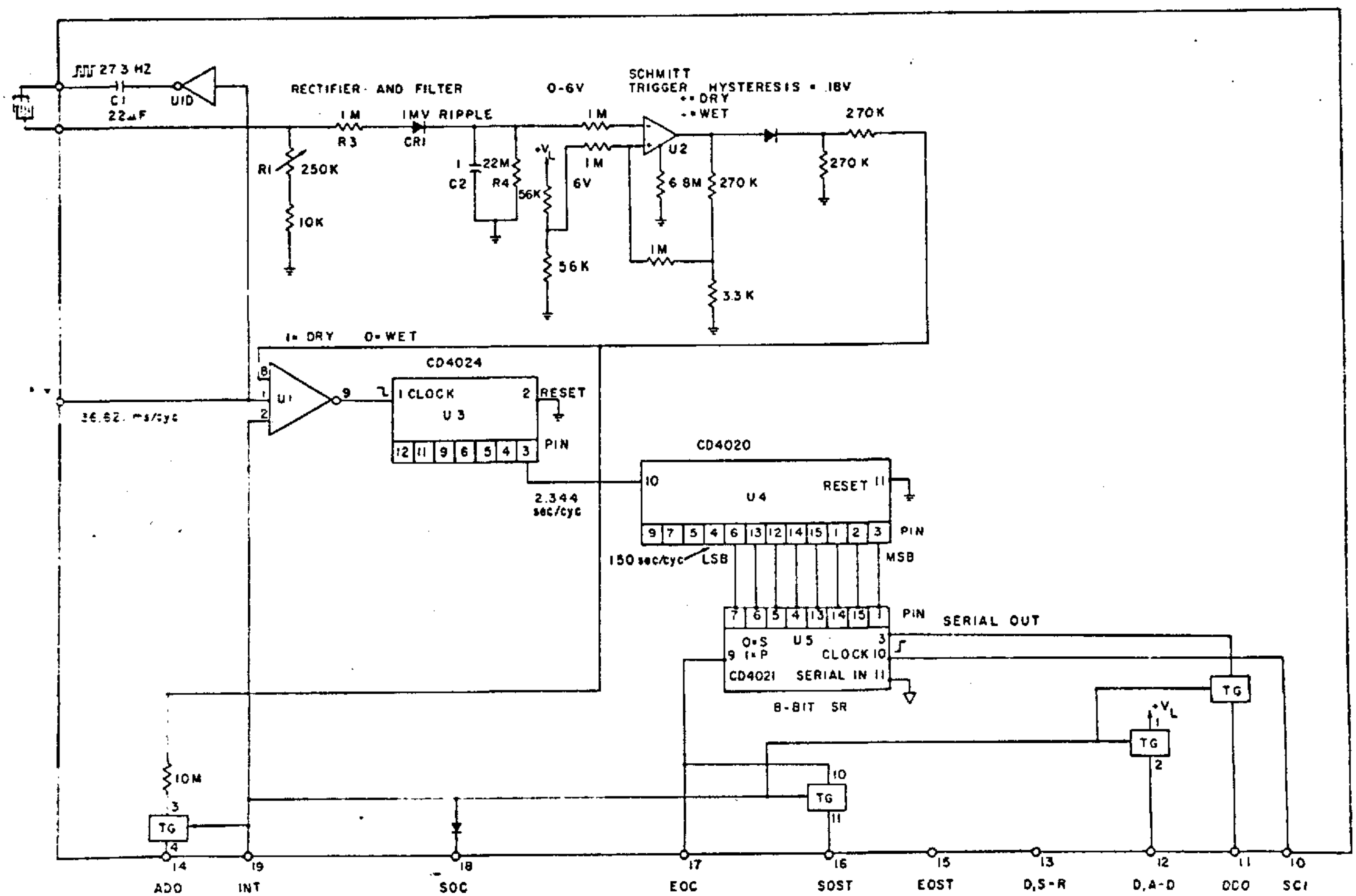

Fig. 8. Hours free moisture

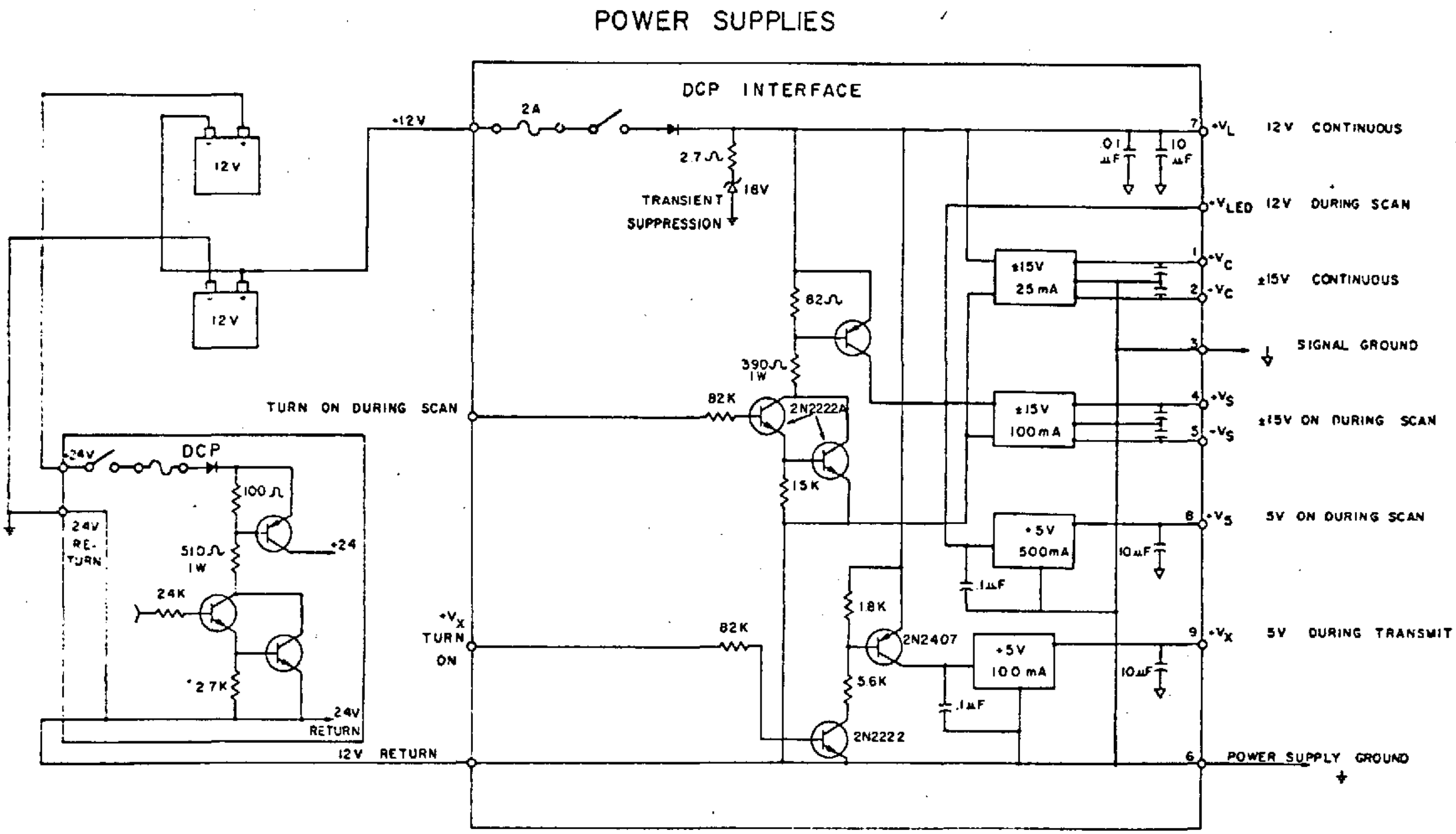

Fig. 9. Power Supplies

N74-27810

Appendix D

Master's Thesis: Predicting Soil Moisture and Wheat Vegetative Growth from ERTS-1 Imagery

PREDICTING SOIL MOISTURE AND WHEAT VEGETATIVE GROWTH FROM ERTS-1 IMAGERY

by

JOHN WAYNE KRUPP

B.S., Kansas State University, 1972

A MASTER'S THESIS

submitted in partial fulfillment of the

requirements for the degree

MASTER OF SCIENCE

Department of Agricultural Engineering

KANSAS STATE UNIVERSITY
Manhattan, Kansas

1974

Approved by:

____
Major Professor

ACKNOWLEDGEMENTS

The National Aeronautics and Space Administration provided much appreciated financial support for this research project. The author is also grateful to Dr. E. T. Kanemasu and Dr. D. H. Lenhert, committee members, for their advice and cooperation, and a special thanks goes to Dr. Harry L. Manges, my major professor, for his patience, advice and encouragement in coursework as well as research.

TABLE OF CONTENTS

LIST OF TABLES

LIST OF FIGURES

INTRODUCTION

An expanding population has brought about an awareness that there are only limited resources on the Earth. This realization comes at a time when resource use is greater than ever before. Adequate informational techniques are necessary for improved resource development. These techniques can aid in wise resource management.

The magnitude of the data required for improved resource management has led to the development of automatic recognition techniques for agriculture. These systems utilize remote sensing from aircraft and spacecraft. Earth Resources Technology Satellite program is a major step in combining space and remote sensing technologies into a system for developing and demonstrating the techniques for efficient management of the Earth's resources (NASA Earth Resources Technology Satellite Data Users Handbook, 1972).

Over 400 million acres of land are irrigated in the world (Israelsen and Hansen, 1967). Some of the water applied is needlessly lost by excess applications. Irrigation scheduling can help to better conserve this valuable resource. One method of scheduling irrigation requires the determination of crop water use (evapotranspiration). Actual evapotranspiration is dependent upon potential evapotranspiration and a crop coefficient. One possible approach to predicting the crop coefficient is the use of a plant's actual growth which may be determined by its reflection of solar radiation from the plant canopy (Myers _et al._, 1966). If this method is to be used, the relationship between reflectance, soil moisture and vegetative growth must be established.

The purpose of this research is to evaluate reflectance for prediction of soil moisture and vegetative growth, and to determine the feasibility of using vegetative growth to evaluate the winter wheat crop coefficient.

REVIEW OF LITERATURE

Remote Sensing

Remote sensing refers to the acquiring of data at a distance by detecting the radiant energy which the object either reflects or emits. Detection devices can be field spectrometers and cameras or instruments designed for installation in aircraft and space vehicles.

Albedo is the ratio of the entire solar radiation spectrum reflected from a body to the total incident radiation (Ashburn and Weldon, 1956), while reflectance is the ratio of reflected radiation to the total incident radiation at a specific wavelength. At any specified wavelength, Reflectance + Absorptance + Transmittance = 1. Transmittance of any opaque material is zero; thus a decrease in reflectance will cause an equal increase in absorption.

Physical Properties that Affect Reflectance

Soil Factors

The albedo of various soil surfaces was compiled by Kondrat'yev (1965). The soils had extremely variable albedos. The variability was attributed to the different soil color, soil moisture content, organic matter and particle size. The soil moisture content was considered the most important factor. He pointed out that a decrease in albedo with an increase in moisture was due to water's low albedo. Bowers (1971) indicated that the relationship between soil moisture and reflectance is precise enough to utilize reflectance techniques to measure surface moisture (Fig. 1). However, due to the soil color, a calibration is necessary for each soil type.

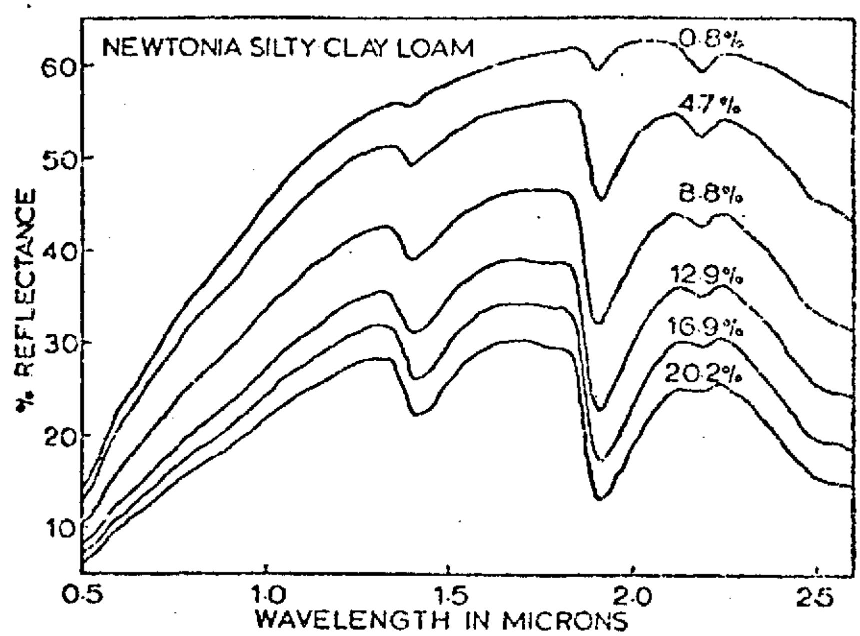

Fig. 1. Reflectance from Newtonia Silty Clay Loam at Different Soil Moisture Percentages (Figure reproduced from Bowers, 1971).

Allen and Sewell (1973) concluded that the use of infrared films and electronic scanner detectors could detect fallow soil moisture over a range of 1 to 24 percent dry weight. Their prediction equations for both the surface soil moisture and soil moisture at the 4 inch depth had regression coefficients (R^2) of at least 0.94.

Organic matter also influences reflectance. A study by Bowers (1971) shows that an oxidized soil sample compared to the check or control sample has a greater reflectance. He also states that some of the change could have been due to oxidation of the carbonates, although in one soil no carbonate was detected.

Bowers (1971) and Myers and Allen (1968) also reported that particle size has an effect on reflectance. In most cases an increase in particle size decreased the reflectance. This was due to the fine particles filling the volume more completely, thus a more even surface. Coarse aggregates, having an irregular shape, formed a large number of pores and cracks in the surface. When the soil surface was wet and pulverized there was very little difference in reflectance from soils, instead the real contrast was at a low moisture content.

Vegetative Factors

The main factor that causes variation in reflectance from crop canopies is leaf density or leaf area index. Leaf area index is defined as the ratio of the leaf area to soil area. Stanhill *et al*. (1968) reported that leaf area index is linearly correlated to albedo or shortwave reflection. The plant albedo increases with increasing plant development to a maximum at full plant canopy. The suggested model indicates internal trapping of radiation, which decreases albedo. Internal trapping is almost complete after the second reflection with hardly any effect by height after a minimum value. In the near infrared region, reflectance increased 17 percent with two leaf layers and only slightly more for each additional leaf layer. When the crop cover is incomplete all of the soil factors mentioned previously, including soil color, soil moisture, particle size and organic matter, caused variation in reflectance. In addition, leaf reflectance also is affected by stand geometry and leaf morphology, most significantly in the near infrared region (Gates, 1965), as well as the variety and relative maturity of the crop (Remote Multispectral Sensing in Agriculture, 1970).

A comparison of different varieties of a crop by Interpretation of Remote Multispectral Imagery of Agricultural Crops (1967) and Remote Multispectral Sensing in Agriculture (1967) indicated that the spectral responses were statistically different. These differences could also have been attributed to variations in crop canopy or leaf area index and crop maturity. In mid-season it could have been due to weed infestations, diseases or farming practices.

Variations of reflectance were found with spectral bands. In the visible region, the striking feature of the leaf spectrum was the high absorptance from 0.4 to 0.5 μ, the reduced absorptance from 0.5 to 0.6 μ, the high absorptance from 0.6 to 0.7 μ and the low transmittance in the entire region (Fig. 2). This was mainly due to the chlorophyll and carotene absorption that predominates in this region (Remote Sensing, 1970). Sinclair, et al. (1973) reported that cell walls scatter the light diffusively, but the chlorophyll or other pigments are present to absorb the light. The absorbing process is a dominate factor in influencing the spectral response in the visible region. If water deficits occur, the metabolic

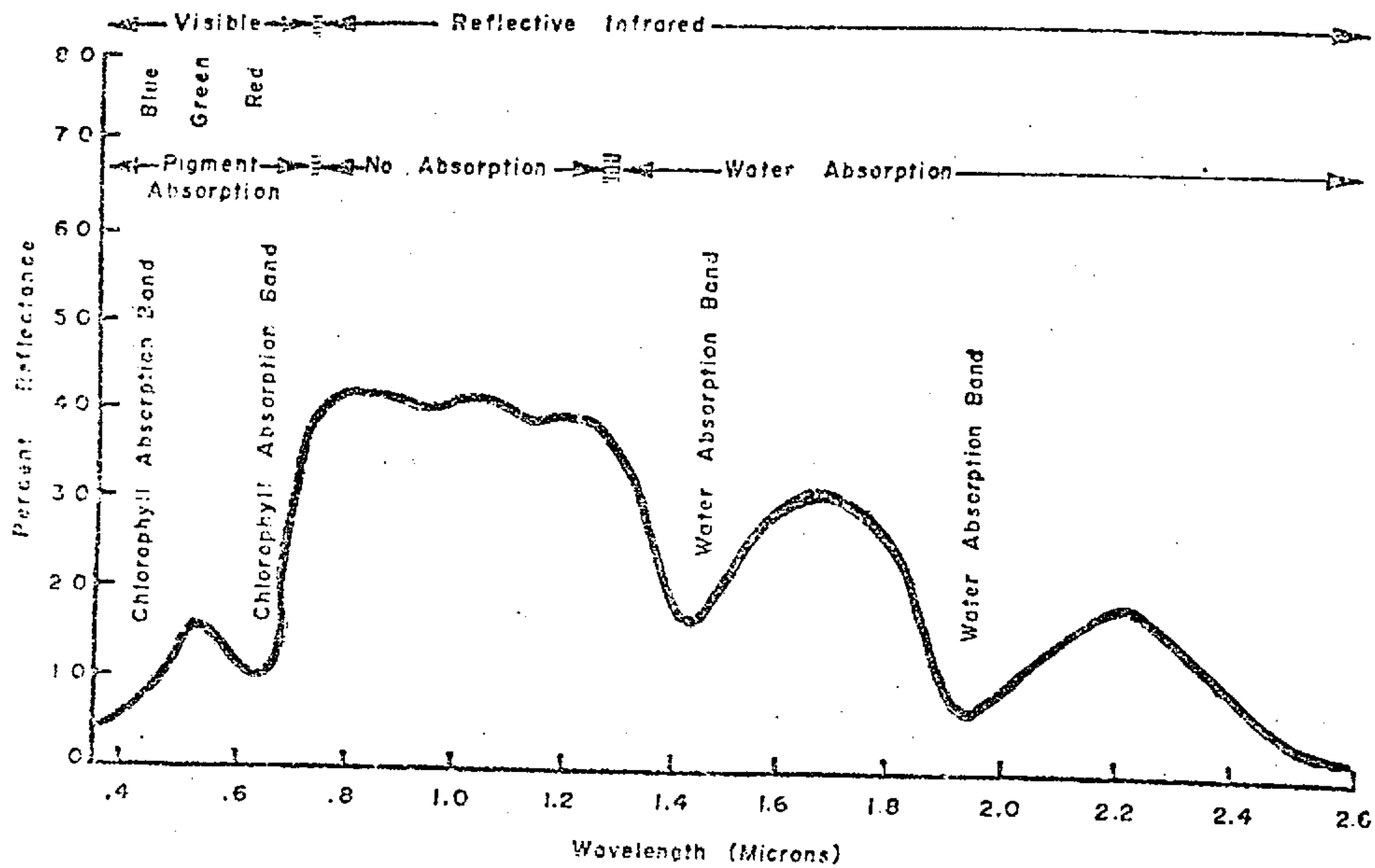

Fig. 2. Characteristic Spectral Reflectance Curve of a Green Leaf (Figure reproduced from Remote Multispectral Sensing in Agriculture, 1970).

processes slow down resulting in the breakdown of carbohydrates and protein within the plant cell. As the stress becomes more severe, accelerated migration of soluble leaf phosphorous and nitrogen compounds to the stem occurs. The loss of chlorophyll accompanying the breakdown and migration results in higher reflectance (David, 1969). Therefore, reflectance is related to the amount of plant pigments. Other factors may result in the loss of chlorophyll such as leaf maturity, salinity, disease or mineral deficiencies. Severe nitrogen deficiences increase reflection (Remote Sensing, 1970), but differences in available nitrogen produce differences in vegetative growth (Bhangoo, 1956, Bolaria, 1956, and Monteith, 1959).

In the near infrared region (0.7 to 1.3 μ) reflectance is caused by the lack of pigment absorption and by the lack of absorption by liquid water (Remote Sensing, 1970). Sinclair, et al. (1973) suggested that reflectance had to occur at interfaces within the leaf where total or critical reflectance was possible. The requirements for total or critical reflectance are that the radiation pass from a material with a high index of refraction to a material with a low index of refraction and that the angle of incidence must be sufficiently large. The increase in reflectance as the leaves become more nitrogen deficient suggests that the leaves are thicker since reflectance increases exponentially as leaf thickness increases. Moisture stress causes physiological changes in the leaf that cause the infrared reflectance to decrease with an increase in moisture stress. The low absorption or high reflectance in this region is a distinctive feature of vegetative. Remote Sensing (1970) reports that of the total incident radiation which strikes a leaf, about 50 percent is reflected, 45 percent is transmitted and the remaining is absorbed. Sinclair et al. (1973) provide a more detailed explanation of the reflectance of an individual leaf in both the visible and near infrared regions.

Sun angle and attenuation are two factors that affect reflection from an object. At low sun angles the reflectance of an object increases compared to a large sun angle. Attenuation is defined by Remote Sensing (1970) as including losses from a beam of radiation by either atmospheric absorption or scattering. In the visible region absorption plays only a minor role compared to scattering. Scattering is caused by interaction between radiation and small particles (dust or water droplets usually in the form of a cloud or haze).

Estimating Soil Moisture

A large amount of time and effort has been expended in the research of transpiration and evaporation with only recent applications in the modeling of evapotranspiration for management of irrigated land. This comes at a time when studies indicate that the timing of irrigations and the amount of water applied have changed very little (Jensen et al., 1971). If a model is to be used on a practical basis for irrigation scheduling, necessary information must be relatively simple to obtain.

Jensen et al. (1971) have developed a computerized model to estimate soil moisture depletion. One of the model's primary objectives is the orientation for the user instead of the researcher. To calculate the potential evaporative flux, the Penman combination equation is used (Penman, 1963). The meteorological data necessary to evaluate the equation include minimum and maximum daily air temperatures, daily solar radiation, dew point temperature at 8 AM and daily wind run.

The crop coefficient used in the computer model represents the effects of the resistance of water movement from the soil to the evaporating surfaces, the resistance to the diffusion of water vapor from the surfaces to the atmosphere and the amount of available energy compared to the reference crop (Jensen, 1968). Thus the crop coefficient is limited by the available soil moisture as well as the daily meteorological conditions and stage of plant growth. For each separate crop a coefficient must be developed for the model. A more detailed explanation can be obtained from Jensen *et al.* (1971).

Ritchie and Burnett (1971) and Ritchie (1972) determined a nonlinear relationship between the leaf area index of a crop and the ratio of the plant's evapotranspiration to the potential evapotranspiration. They reported that while an adequate supply of water is available in the soil, plant factors influence evapotranspiration rates.

INVESTIGATION

Objectives

This work was concerned with problems dealing with utilizing remote sensing data. The objectives of the study were: (1) to evaluate reflectance for prediction of soil moisture and vegetative growth, (2) to determine the feasibility of using vegetative growth to evaluate the winter wheat crop coefficient, and (3) to evaluate the winter wheat crop coefficient in the mathematical model by Jensen et al. (1971) for irrigation scheduling.

Equipment

ERTS-1 satellite revolves in a circular orbit around the Earth every 103 minutes at 914 km above sea level. The satellite travels over the research area in midmorning in a north to south direction. It passes over any location on the Earth's surface once every 18 days at the same time of day.

The Multispectral Scanner (MSS) is a line-scanning device that operates in two bands of the visible spectrum and two in the near infrared. Band 4 included the spectrum between 0.5 and 0.6 μ, band 5 between 0.6 and 0.7 μ, band 6 between 0.7 and 0.8 μ and band 7 between 0.8 and 1.1 μ. Fig. 3 shows the 4 bands with the energy emitted in the solar and thermal spectrum. An oscillating mirror in the MSS causes light energy from a 185 km swath to be swept across the focus of a small telescope. At the focus is a four-by-six array of 24 optical fibers (6 for each band). The fibers carry the energy from the light through spectral filters to detectors that convert it to an electrical signal. An area of 79 meters square is contained in each

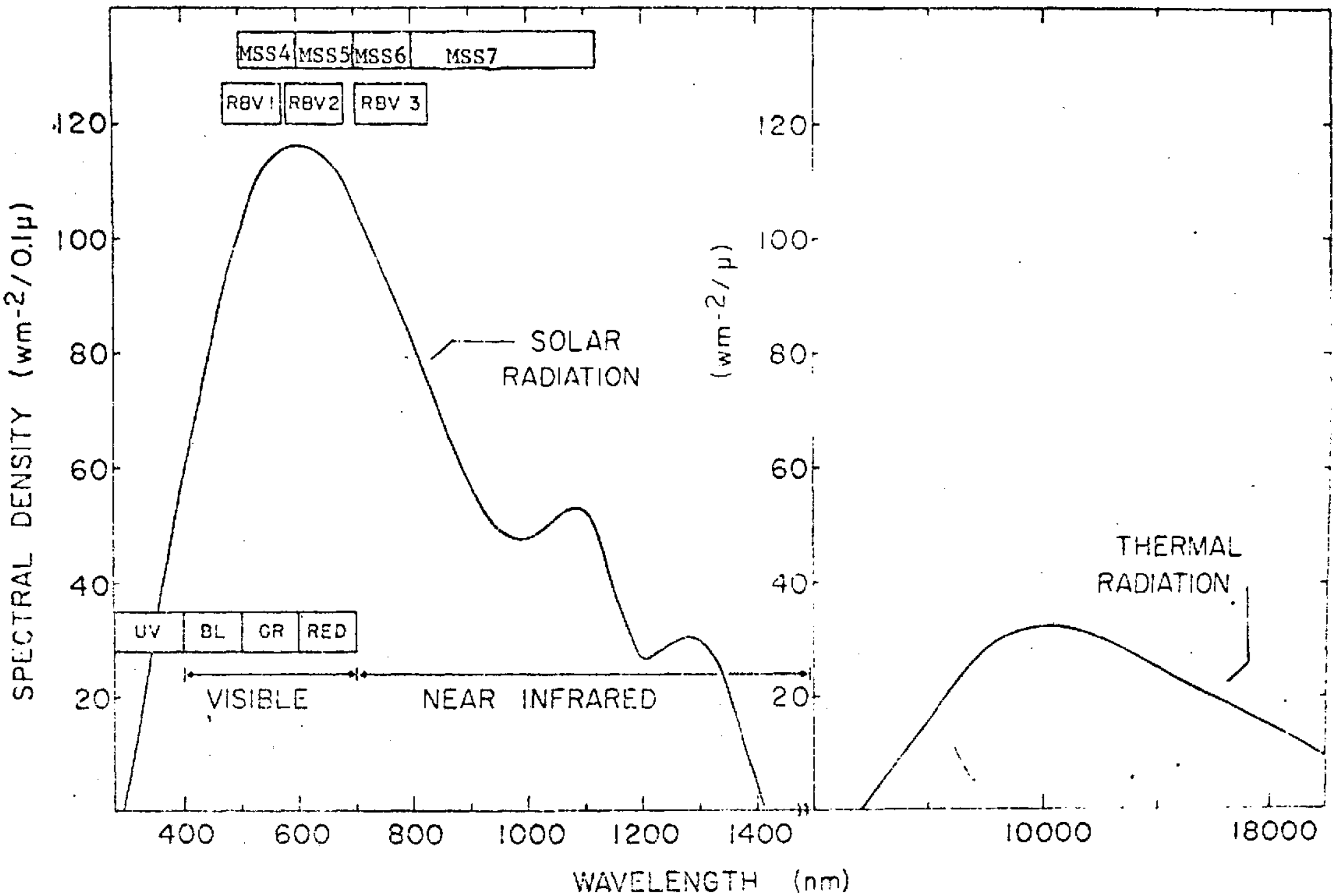

Fig. 3. Energy Emitted in the Solar and Thermal Spectrum.

fiber. The MSS image covers 185 km square with 4 images per area. The imagery is relayed to ground stations and then is processed into photographs at Goddard Space Flight Center in Greenbelt, Maryland. The resolution capability reveals surface features at a scale of 1:250,000 and information at a scale of 1:30000. Further details of the equipment aboard the ERTS-1 satellite are given by NASA Earth Resources Technology Satellite Data Users Handbook (1972).

Methods of Procedure

The research was conducted on winter wheat fields approximately 30 kilometers northwest of Garden City, Kansas. Two soil moisture treatments, one dryland wheat field (A) located 38° 9.6' North latitude and 101° 5.9' West longitude and one irrigated field (B) 38° 8.5' North latitude and 101° 4.9' West longitude, were used with approximately 60 hectares in each. Field B was irrigated by a center pivot sprinkler system. The two fields were located within 3 km of each other. The area's normal annual precipitation is 43.6 cm with about 70 percent of the precipitation during September through June.

The two fields were located on Ulyssess-Richfield silt loam with an average organic matter of 1.5 percent and soil pH of 6.9. The exchangeable potassium was in excess of 560 kg per hectare. Available phosphorus in field A was 117 kg per hectare and in field B was 64 kg per hectare. Particle size analyses revealed that both field's soils contained an average of 50 percent silt and 20 percent clay.

Field A had been in fallow the previous year. Scout wheat was planted at a seeding rate of 29 kg per hectare on September 15, 1972. The grain drill used had a 25.4 cm spacing between rows. By May 24, 1973, the wheat was completely headed and was harvested on July 5.

Since field B had been in wheat the previous season, the field was preirrigated. Anhydrous ammonia at a rate of 90 kg of nitrogen per hectare was applied to the field. On September 22, 1972, Eagle wheat was seeded at a rate of 50 kg per hectare with a row spacing of 30.48 cm. According to Variety Tests with Fall-Planted Small Grains (1971), Eagle wheat was a selection of Scout with nearly identical vegetative characteristics. Water was applied with the center pivot irrigation system on May 23 (3.05 cm) and June 2 (3.05 cm). Harvest of the wheat was completed on July 5.

Data Collection

Both fields A and B were divided into four square equally sized plots with a sampling area in the center of each plot. An additional sampling area was also set up in two of the plots in field A where the corners had been double drilled. This gave a total of six sampling areas in field A and four in field B. By the use of random sampling techniques, the areas were broken down into one meter squares, where the leaf area index and soil moisture were measured.

The soil samples were gathered at the surface and at intervals of 0 to 15, 15 to 30, 30 to 60, 60 to 91, 91 to 121, 121 to 152 and 152 to 182 cm with a soil sampling tube. The samples were later dried in an oven at 105°C until they reached a constant weight. Then the soil moistures were calculated.

The leaf area was determined by measuring the length and breadth of each leaf from randomly selected plants in the one square meter and using the following equation (Teare and Peterson, 1971):

$$LA = -0.64 + 0.813\ X \qquad (1)$$

where:

LA = leaf area (cm^2)

X = product of length times breadth of leaf (cm^2).

The leaf area index is the total leaf area divided by the land surface area. Both soil moisture and leaf area index data were obtained within one day of the flights over.

The meteorological data were from the Garden City Experiment Station. These data included maximum and minimum temperatures, dew point temperatures and wind run. Also the field capacity, permanent wilting point and bulk density for Ulyssess-Richfield silt loam were obtained from the experiment station. This information was determined by laboratory measurements and may not describe the test fields accurately. Solar radiation was obtained from the Dodge City Weather Service while rainfall readings were taken near the research area.

Data Analysis

Using a negative transparency from ERTS-1, the general area of fields (A and B) was located. Then the specific fields were found by the use of computer printed gray scales. From the gray scales the coordinates were located and the numerical values were stripped off the magnetic tapes. To prevent any overlapping outside of the research area, one row of data points around the edge of the fields was eliminated. The mean and standard deviation of the remaining data of the four bands were calculated (Tables 1 and 2). Also the mean and standard deviation of point by point ratios were determined (Tables 1 and 2). Stepwise Deletion Multiple Regression (1973) was used to evaluate the relationship between reflectance, soil moisture and leaf area index.

The meteorological data, as well as the soil moistures on March 22, were used in the computer model of evapotranspiration (Appendix, Table 11) developed by Jensen *et al.* (1971). The original wheat crop coefficient

Table 1. ERTS-1 Data for Field A.

Date		MSS4	MSS5	MSS6	MSS7	MSS4/5	MSS4/7	MSS5/7
9/22/72	Mean	34.75	37.89	38.64	19.55	0.918	1.779	1.939
	S.D.*	1.41	1.90	2.18	0.86	0.040	0.068	0.080
3/22/73	Mean	33.26	32.29	45.87	25.25	1.031	1.318	1.280
	S.D.*	1.28	1.58	1.74	0.69	0.040	0.055	0.069
5/14/73	Mean	29.74	24.50	48.11	28.08	1.218	1.064	0.877
	S.D.*	1.69	2.12	1.79	1.66	0.066	0.101	0.104
6/1/73	Mean	33.43	29.48	52.32	29.87	1.138	1.121	0.990
	S.D.*	1.72	2.42	1.84	1.04	0.062	0.083	0.104
6/19/73	Mean	41.14	49.33	55.26	28.70	0.835	1.436	1.722
	S.D.*	1.62	2.07	1.49	0.92	0.033	0.074	0.090
7/7/73	Mean	59.46	78.53	77.68	36.36	0.758	1.636	2.161
	S.D.*	2.14	4.25	2.72	1.49	0.030	0.061	0.115

*Standard deviation.

Table 2. ERTS-1 Data for Field B.

Date		MSS4	MSS5	MSS6	MSS7	MSS4/5	MSS4/7	MSS5/7
9/22/72	Mean	37.05	40.41	40.96	20.78	0.919	1.786	1.947
	S.D.*	1.62	2.54	2.37	1.02	0.038	0.094	0.128
3/22/73	Mean	33.54	32.99	41.47	22.57	1.019	1.488	1.463
	S.D.*	1.09	1.91	2.15	0.96	0.049	0.073	0.088
5/14/73	Mean	27.63	19.22	56.66	36.78	1.454	0.760	0.532
	S.D.*	1.60	2.68	3.56	3.18	0.132	0.109	0.129
6/1/73	Mean	26.93	20.03	48.66	31.61	1.355	0.858	0.638
	S.D.*	1.32	2.23	3.43	2.54	0.111	0.083	0.094
6/19/73	Mean	36.68	37.94	52.00	29.97	0.971	1.227	1.270
	S.D.*	1.21	3.11	2.05	1.56	0.060	0.079	0.131
7/7/73	Mean	54.46	73.87	77.48	38.24	0.739	1.425	1.932
	S.D.*	2.30	4.37	3.39	1.31	0.033	0.060	0.100

*Standard deviation.

curves were evaluated first. Then curves developed by regression analysis from the leaf area index data were used as the crop coefficient curves. From the computer model, soil moisture depletions were predicted.

RESULTS

Prediction of Vegetative Growth

ERTS-1 passes over any location on the Earth's surface once every 18 days at the same time of day, but some dates had high percentages of cloud cover. Neither aerial nor ground data were collected on those days (Table 3). These data (Table 4) were used as a means for determining vegetative growth with Stepwise Deletion Multiple Regression (1973). The July 7 data were not used because of the alteration of the natural vegetative growth by harvesting the wheat. The wheat threshed straw provided a stubble mulch compared to the uncut wheat. The equations that best describe vegetative growth were:

$$LAI = 2.92MSS4/5 - 2.63 \quad , \quad R^2 = 0.95 \qquad (2)$$

$$LAI = -0.065MSS5 + 2.66 \quad , \quad R^2 = 0.86 \qquad (3)$$

$$LAI = -1.22MSS5/7 + 2.08 \quad , \quad R^2 = 0.85 \qquad (4)$$

where

LAI = Leaf area index

MSS4/5 = Ratio of band 4 to band 5

MSS5 = Band 5

MSS5/7 = Ratio of band 5 to band 7

R^2 = Regression coefficient.

For the predicted values of leaf area index to have meaning, it is necessary that a minimum or maximum value of MSS4/5, MSS5 and MSS5/7 be set so that the predicted leaf area index is never negative.

The general trend from equation 2 indicates that as the ratio of band 4 to band 5 increases the leaf area index increases linearly. This

Table 3. Weather Conditions at Flight Time Over Test Fields.

Date	Weather Condition	Data Acquired*
September 4, 1972	Cloudy	
September 22, 1972	Clear	X
October 10, 1972	Partly Cloudy	
October 28, 1972	Cloudy	
November 15, 1972	Cloudy	
December 3, 1972	Partly Cloudy	
December 21, 1972	Partly Cloudy	
January 8, 1973	Cloudy	
January 26, 1973	Cloudy	
February 13, 1973	Rain	
March 3, 1973	Foggy	
March 21, 1973	Clear	X
April 8, 1973	Heavy Snow	
April 26, 1973	Rain	
May 14, 1973	Clear	X
June 1, 1973	Clear	X
June 19, 1973	Clear	X
July 7, 1973	Clear	X

*Indicates both ERTS-1 and field data taken.

Table 4. Leaf Area Index Data for Fields A and B.

Date	Field A		Field B	
	Mean	Standard Deviation	Mean	Standard Deviation
9/22/72	0.00	0.00	0.00	0.00
12/21/72	0.33	0.00	0.12	0.07
3/22/73	0.37	0.10	0.44	0.07
5/14/73	0.97	0.26	1.53	0.39
6/1/73	0.89	0.25	1.23	0.36
6/18/73	0.00	0.00	0.00	0.00
7/7/73	0.00	0.00	0.00	0.00

means that reflectance due to plant growth in band 4 increases faster than band 5 since the vegetation reflects less radiation in band 5. Equation 2 (Fig. 4) best describes leaf area index because of its high regression coefficient. The ratio appears to have cancelled any soil moisture variations.

Equation 3 shows a linear relationship between leaf area index and band 5. From the equation it appears soil moisture is not significant in band 5. Of the three equations presented, an error in band data would have the least effect on leaf area index as represented by the low coefficient of the band in equation 3. Equation 4 uses the ratio of band 5 and band 7 to evaluate leaf area index with no significant variation from soil moisture. The reflectance due to vegetation of band 7 increases at a much faster rate than band 5 as plant growth continues, causing a decrease in the ratio.

Prediction of Soil Moisture

The Stepwise Deletion Multiple Regression (1973) was used to help interpret the aerial and ground truth data available (Tables 5 and 6). The information for field B on March 22 was eliminated since rain fell before the soil moisture could be measured. Again the July 7 data were not used due to the stubble mulch caused by harvesting the wheat crop. The equations determined were:

$$SM2 = 164.44 - 4.00MSS4 - 24.08LAI \quad , \quad R^2 = 0.93 \qquad (5)$$

$$SM2 = 80.70 - 1.41MSS6 + 10.00LAI \quad , \quad R^2 = 0.80 \qquad (6)$$

$$SM2 = 77.92 - 2.56MSS7 + 20.36LAI \quad , \quad R^2 = 0.79 \qquad (7)$$

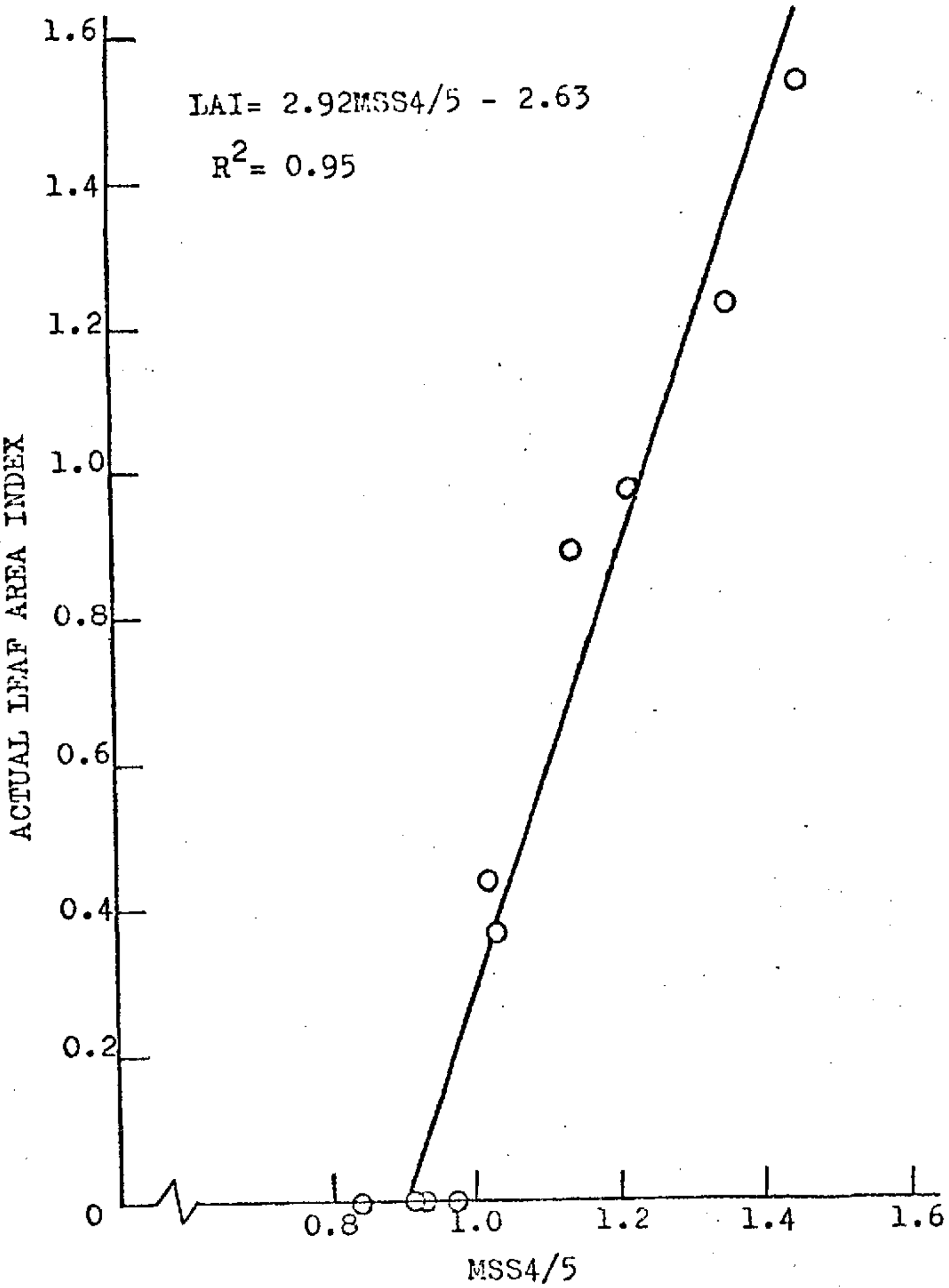

Fig. 4. Prediction of Leaf Area Index.

Table 5. Soil Moisture Percentages† for Field A.

Date		Soil Moisture at Increments (cm)							
		Surface	0-15	15-30	30-61	61-91	91-122	122-152	152-183
9/22/72	Mean	10.43	22.97	23.70	21.35	17.65	14.35	12.85	13.55
	S.D.*	2.18	0.99	2.58	0.93	3.10	1.87	0.75	0.97
12/21/72	Mean	34.30	30.40	27.70	26.50	24.30	21.10	15.70	13.80
	S.D.*	0.0	0.0	0.0	0.0	0.0	0.0	0.0	0.0
3/22/73	Mean	8.13	22.98	25.42	23.82	20.70	16.63	14.62	14.98
	S.D.*	2.59	1.27	1.81	1.26	2.02	2.70	2.61	2.61
5/14/73	Mean	3.82	16.92	17.20	19.12	20.35	20.03	18.52	16.45
	S.D.*	0.75	1.87	1.61	1.15	1.61	1.52	1.99	2.40
6/1/73	Mean	2.87	11.12	13.45	15.22	15.72	15.95	16.38	15.97
	S.D.*	0.84	1.50	0.63	1.22	2.04	2.19	2.00	2.28
6/19/73	Mean	0.85	6.35	9.80	11.12	10.13	11.08	12.47	13.32
	S.D.*	0.44	0.73	1.55	1.31	1.68	1.41	2.06	2.01
7/7/73	Mean	1.77	15.65	11.45	12.92	14.15	15.20	16.33	17.33
	S.D.*	0.21	1.73	0.89	0.39	1.00	2.30	2.65	2.51

†Soil moisture percentages on dry weight basis

*Standard deviation

Table 6. Soil Moisture Percentages† for Field B.

Date		Soil Moisture at Increments (cm)							
		Surface	0-15	15-30	30-61	61-91	91-122	122-152	152-183
9/22/72	Mean	8.35	22.40	20.75	16.93	13.43	13.00	14.70	16.05
	S.D.*	1.81	1.30	0.34	2.99	2.81	4.13	3.62	2.40
12/21/72	Mean	16.28	30.10	26.27	24.90	19.25	14.83	15.70	16.70
	S.D.*	3.71	5.60	2.11	3.19	2.83	3.41	2.75	2.88
3/22/73	Mean	19.00	27.05	23.97	24.15	20.02	14.78	15.00	15.97
	S.D.*	6.44	4.11	1.68	4.16	3.49	4.56	3.43	3.18
5/14/73	Mean	5.58	21.20	16.33	18.15	18.38	17.73	16.70	16.90
	S.D.*	0.93	3.27	2.06	3.53	3.85	3.75	3.85	2.58
6/1/73	Mean	25.10	25.47	18.93	15.48	13.88	13.68	15.55	16.62
	S.D.*	12.43	4.10	5.16	3.70	2.85	2.40	4.12	2.81
6/19/73	Mean	2.28	9.63	9.23	11.98	10.78	11.18	11.48	13.50
	S.D.*	1.13	2.19	1.73	3.88	3.02	1.72	1.68	1.91
7/7/73	Mean	2.60	17.20	9.40	11.43	11.10	10.50	10.38	13.15
	S.D.*	1.25	1.81	2.23	1.53	0.67	1.39	1.27	1.64

†Soil moisture percentages on dry weight basis.

*Standard deviation.

where:

SM2 = Soil moisture dry weight at 0 to 15 cm (%)

LAI = Leaf area index

MSS4 = Band 4

MSS6 = Band 6

MSS7 = Band 7

MSS4/5 = Ratio of band 4 to band 5

R^2 = Regression coefficient.

The soil moisture equation 5 indicates that an increase in leaf area index, with soil moisture remaining constant, decreases the reflectance in band 4. This could be caused by the reflectance of the soil being greater than the plant reflectance. Thus as the leaf area increased, more surface was covered by the plant canopy causing a decrease in reflectance monitored. The fact that soil moisture increases absorption is reaffirmed by equations 5, 6 and 7. Equation 5 is the best equation due to its high regression coefficient.

Equations 6 and 7 indicate that the reflectance of the plant is greater than the reflectance of the soil. An error in band reading or leaf area index would cause the least change in soil moisture in equation 6 due to the small coefficients.

Upon substituting equation 2 into equation 5, soil moisture at 0 to 15 cm depth became:

$$SM2 = 101.11 - 4.00MSS4 - 70.31MSS4/5 \qquad (8)$$

Table 7 and Fig. 5 show a comparison of soil moisture predicted by equation 8 with the measured soil moisture. Equation 8 was developed for soil factors pretaining to the fields. Different soil factors would require a new equation to be developed for soil moisture. These factors include soil type, organic matter, particle size and cultural practices.

Table 7. Predicted Soil Moisture Percentages at 0 to 15 cm from ERTS-1 Data.

Date	Field A				Field B			
	MSS4	MSS4/5	Predicted[a] SM2	Actual SM2	MSS4	MSS4/5	Predicted[a] SM2	Actual SM2
9/22/72	34.75	0.918	24.24	22.97	37.05	0.919	14.80	22.40
3/22/73	33.26	1.031	22.25	22.98	33.54	1.019	21.85	27.05[b]
5/14/73	29.74	1.218	23.09	16.92	27.63	1.454	14.91	21.20
6/1/73	33.43	1.138	13.86	11.12	26.93	1.355	24.69	25.47
6/19/73	41.14	0.835	-----[c]	6.35	36.68	0.971	12.66	9.63

[a]Calculated by SM2 = 101.11 - 4.00MSS4 - 70.31MSS4/5.

[b]Precipitation fell after ERTS-1 flight but before measurement.

[c]A negative value is predicted which has no meaning.

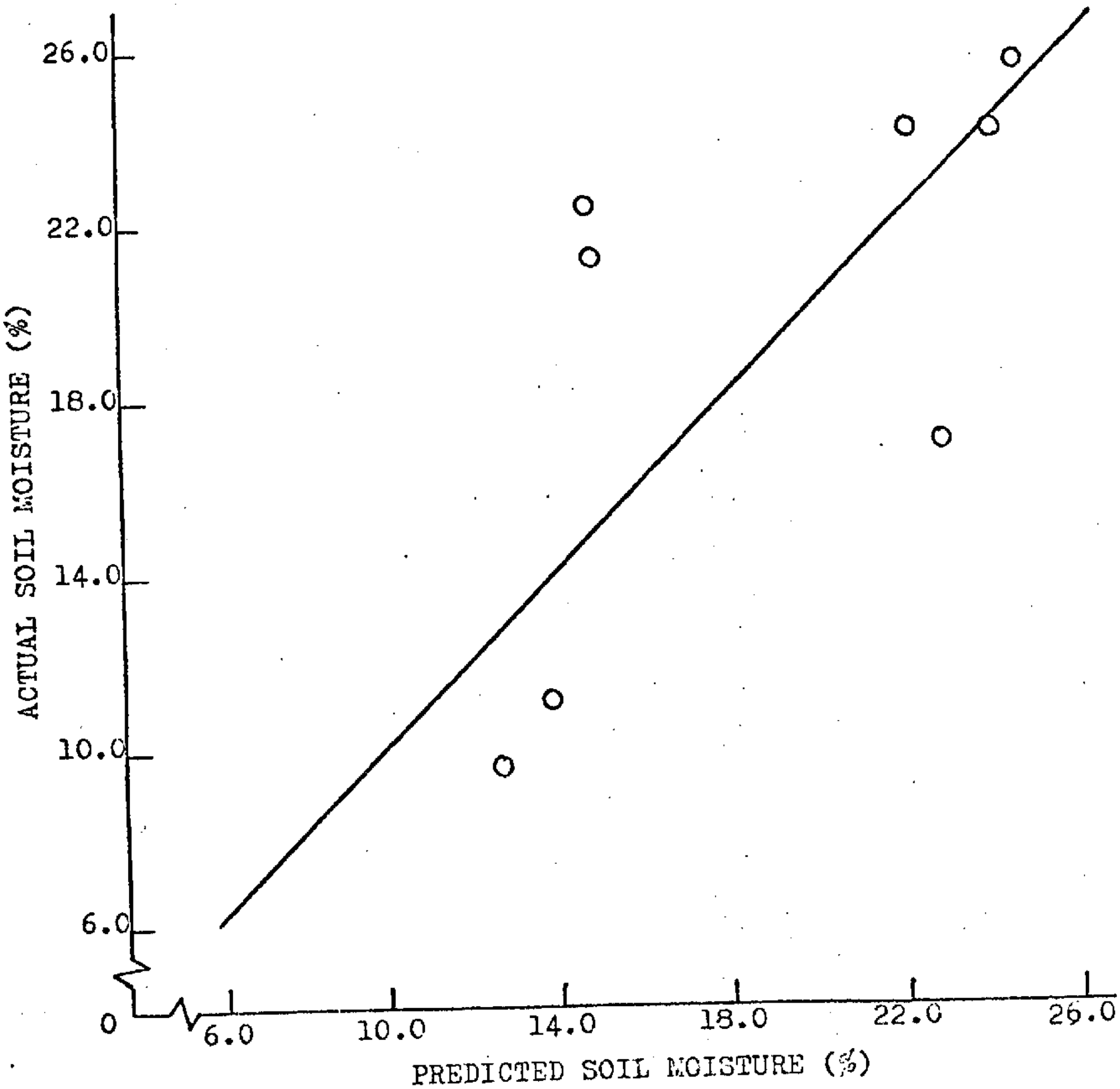

Fig. 5. Actual and Predicted Soil Moisture Percentages at 0 to 15 cm.

Soil Moisture Model

The original wheat crop coefficient curve developed by Jensen et al. (1971) was:

$$Y = 0.233 - 0.0114X + 0.000484X^2 - 0.00000289X^3 \quad (9)$$

$$Y = 1.022 + 0.00853D - 0.000726D^2 + 0.00000444D^3 \quad (10)$$

where:

Y = Wheat crop coefficient

X = Percent of crop cover

D = Days after 100 percent crop cover.

Equations 9 and 10 in conjunction with climatic data (Table 8) and soil moisture information (Tables 5, 6 and 9), were used in the computer model developed by Jensen et al. (1971). The soil moisture depletion for both fields in most cases was overestimated (Table 10).

Regression analysis of leaf area index data for field A (Fig. 6) was used as the new winter wheat crop coefficient curve (Fig. 7). The equations of the curve were:

$$Y = 0.005 + 0.0165X - 0.000467X^2 + 0.00000402X^3 \quad (11)$$

$$Y = 0.998 - 0.00297D - 0.000747D^2 \quad (12)$$

where:

Y = Wheat crop coefficient

X = Percent of crop cover

D = Days after 100 percent crop cover.

Fig. 8 and Table 10 represent the results from the computer model with equations 11 and 12 on dryland (Field A) compared to the actual measured values. The actual soil moisture values compared very closely with predicted values of the model until near maturity of the wheat crop on June 19. At

Table 8. Climatic Data.

Month	Day	Minimum Temp. (°F)	Maximum Temp. (°F)	Solar Radiation (cal/cm^2 day)	Dew Point Temp. (°F)	Wind Run (miles/day)	Rainfall (inches)
March	20	28	52	561.5	28	144	
	21	31	53	492.6	36	113	
	22	39	56	505.9	36	327	
	23	39	63	33.8	39	157	1.10
	24	36	49	108.2	36	167	
	25	35	40	90.2	35	415	
	26	35	42	468.6	35	284	
	27	35	55	205.5	35	127	.70
	28	42	51	163.4	42	200	
	29	32	50	91.1	32	160	
	30	32	39	47.7	32	166	1.00
	31	32	37	214.9	32	325	
April	1	30	45	588.5	30	239	
	2	30	58	428.7	34	79	
	3	31	54	429.0	32	187	
	4	31	48	642.3	31	274	
	5	22	54	634.0	30	163	
	6	31	63	627.3	28	164	
	7	37	70	44.7	35	124	0.25
	8	24	37	381.6	24	378	
	9	17	33	596.2	17	262	
	10	19	35	664.7	19	192	
	11	26	53	625.2	37	123	
	12	31	64	400.6	38	68	
	13	37	62	595.8	40	102	
	14	46	66	470.8	57	273	
	15	58	78	216.5	58	387	
	16	25	61	642.3	31	220	
	17	35	60	652.1	39	158	
	18	46	76	643.9	48	209	
	19	45	77	596.8	42	336	
	20	36	60	693.4	23	219	
	21	38	72	672.7	37	259	
	22	36	65	612.9	38	98	
	23	33	67	655.0	42	78	
	24	46	73	162.5	50	117	0.80
	25	44	57	107.9	45	115	
	26	34	48	221.9	36	181	
	27	31	48	200.5	36	122	
	28	38	66	666.9	43	153	
	29	45	82	635.9	45	167	
	30	49	78	368.8	49	134	

Table 8. Continued.

Month	Day	Minimum Temp. (°F)	Maximum Temp. (°F)	Solar Radiation (cal/cm^2 day)	Dew Point Temp. (°F)	Wind Run (miles/day)	Rainfall (inches)
May	1	44	73	156.6	45	176	
	2	35	46	633.8	37	178	
	3	32	58	704.2	36	90	
	4	40	71	688.0	41	165	
	5	50	79	503.6	45	319	
	6	47	79	702.9	47	207	
	7	48	77	520.8	50	185	1.25
	8	42	68	682.7	44	160	
	9	48	79	706.0	45	109	
	10	44	77	698.4	45	106	
	11	50	77	681.7	48	140	
	12	46	70	674.5	40	144	
	13	42	68	672.1	37	67	
	14	38	65	728.4	42	59	
	15	38	66	727.4	38	84	
	16	45	78	718.4	39	123	
	17	42	71	568.8	42	127	
	18	48	88	708.2	46	77	
	19	54	87	705.3	49	102	
	20	54	84	633.4	52	109	
	21	57	86	689.5	61	201	
	22	51	85	611.9	50	148	
	23	51	68	672.9	53	79	
	24	54	80	738.7	50	79	
	25	47	72	641.0	47	143	
	26	55	80	488.7	56	249	
	27	46	68	107.2	37	266	
	28	50	53	624.3	48	490	
	29	40	73	674.8	42	208	
	30	46	70	406.9	44	125	
	31	42	62	751.1	44	43	
June	1	48	77	623.8	60	133	
	2	57	82	659.7	56	247	
	3	53	86	645.8	53	192	
	4	53	80	599.6	54	94	
	5	47	68	667.5	48	133	
	6	50	79	736.5	46	70	
	7	51	88	729.0	49	78	
	8	56	94	719.4	53	87	
	9	57	97	739.9	56	98	
	10	60	92	734.1	58	182	
	11	62	90	707.2	59	277	

Table 8. Continued.

Month	Day	Minimum Temp. (°F)	Maximum Temp. (°F)	Solar Radiation (cal/cm^2 day)	Dew Point Temp. (°F)	Wind Run (miles/day)	Rainfall (inches)
June	12	64	91	498.0	60	210	
	13	64	82	627.2	66	102	
	15	59	89	737.1	52	216	
	16	57	94	743.0	46	215	
	17	53	84	740.3	49	121	
	18	48	95	757.4	32	239	
	19	54	78	695.6	35	170	
	20	45	79	738.7	41	113	
	21	52	85	683.0	54	85	
	22	55	86	725.5	51	62	
	23	57	91	723.3	51	84	
	24	64	98	729.4	46	126	
	25	61	98	663.5	49	186	
	26	63	101	701.2	51	130	
	27	62	102	690.7	50	156	
	28	63	93	594.5	61	106	0.90
	29	64	87	646.0	66	97	
	30	65	88	647.8	68	82	
July	1	66	94	668.4	68	146	
	2	70	102	613.5	63	197	
	3	67	92	639.6	63	75	
	4	66	102	661.3	65	160	
	5	62	95	702.4	62	94	
	6	65	97	715.1	62	102	
	7	68	101	714.1	64	170	

Table 9. Soil Moisture Information.*

Depth (cm)	Field Capacity (%)	Permanent Wilting Point (%)	Bulk Density (gm/cm^3)
0-30	28.5	14.5	1.29
30-61	28.0	14.0	1.37
61-91	27.5	13.5	1.39
91-122	27.0	13.0	1.16
122-152	26.5	12.5	1.16
152-183	26.0	12.0	1.16

*Obtained from the Garden City Experiment Station.

Table 10. Soil Moisture Depletion Using the Model Developed by Jensen *et al.*

Date	Field A (cm)			Field B (cm)			
	Actual[a]	Jensen[b]	Revised 1[c]	Actual[a]	Jensen[b]	Revised 1[c]	Revised 2[d]
3/21/73	17.65			19.28			
5/14/73	19.84	25.07	19.35	23.44	26.14	20.80	26.52
6/1/73	27.74	31.24	27.86	27.15	29.24	26.56	32.66
6/19/73	37.52	32.16	34.65	37.77	27.61	31.52	37.90
7/7/73	28.68	31.29	34.51	34.21	26.75	31.70	38.07

[a]Actual field measurements of soil moisture depletion.

[b]Original wheat crop coefficient suggested by Jensen *et al.*

[c]Wheat crop coefficient using leaf area index of Field A.

[d]Wheat crop coefficient using leaf area index of Field B.

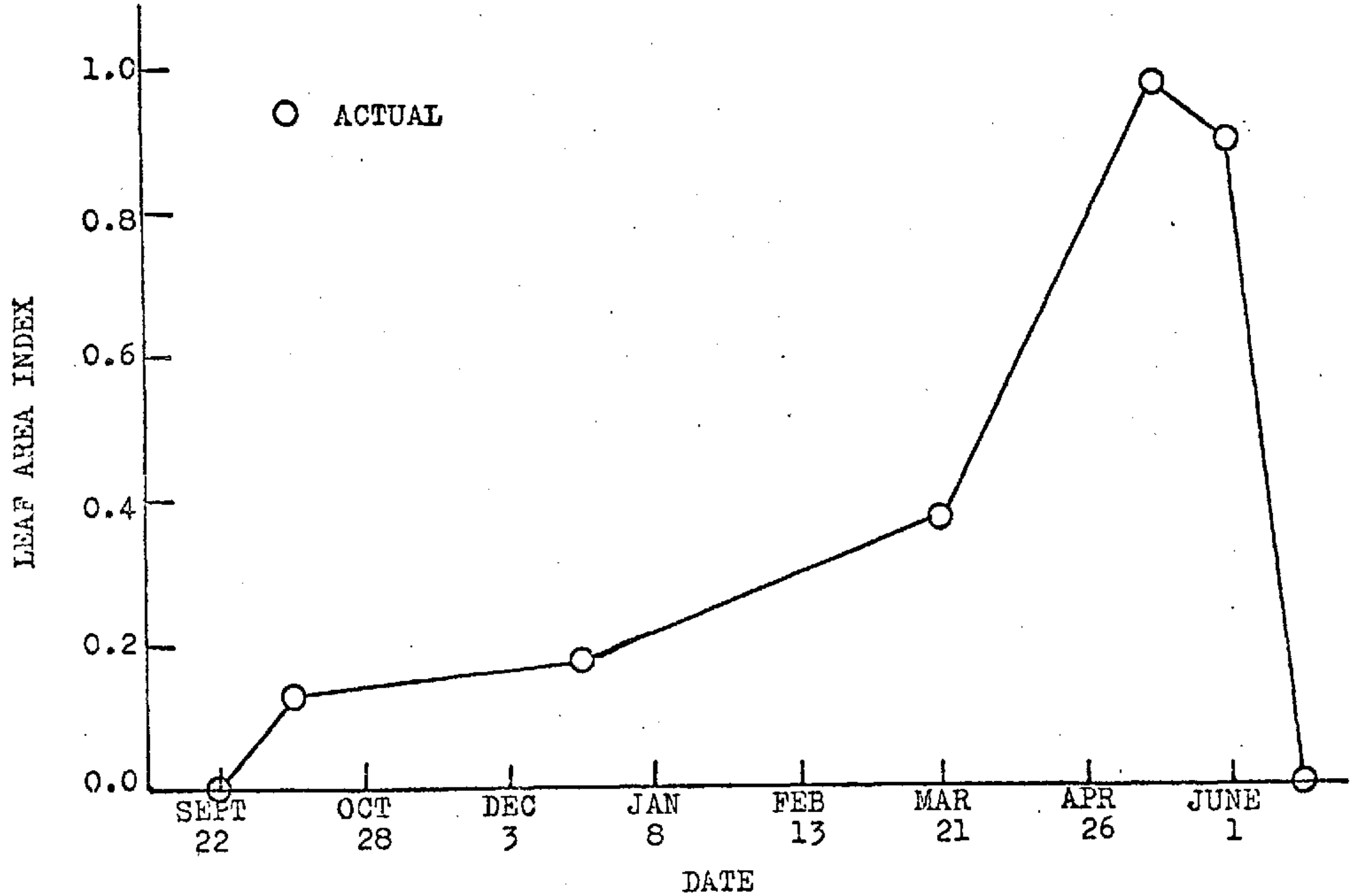

Fig. 6. Measured Leaf Area Index from Field A.

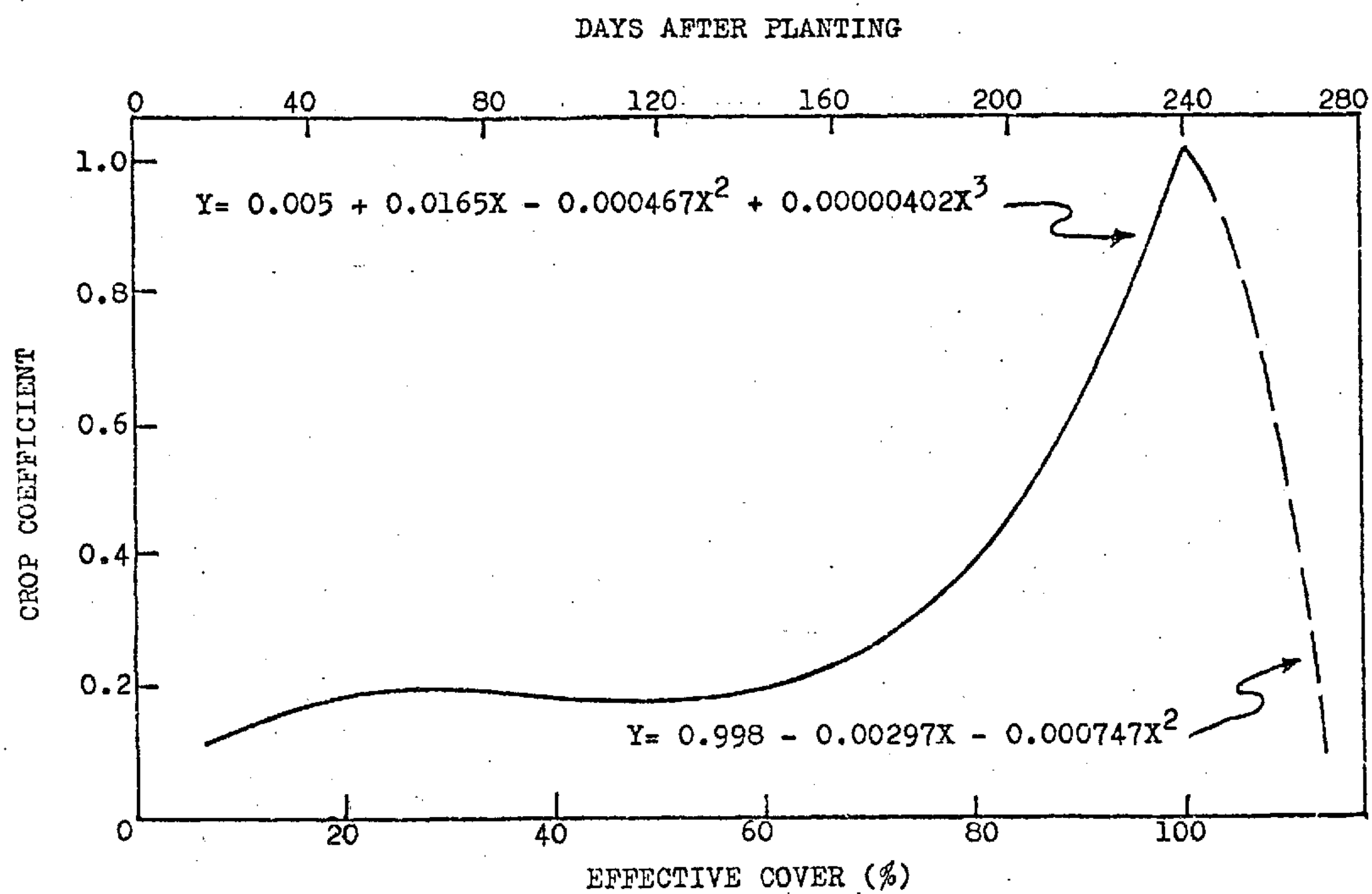

Fig. 7. Winter Wheat Crop Coefficient.

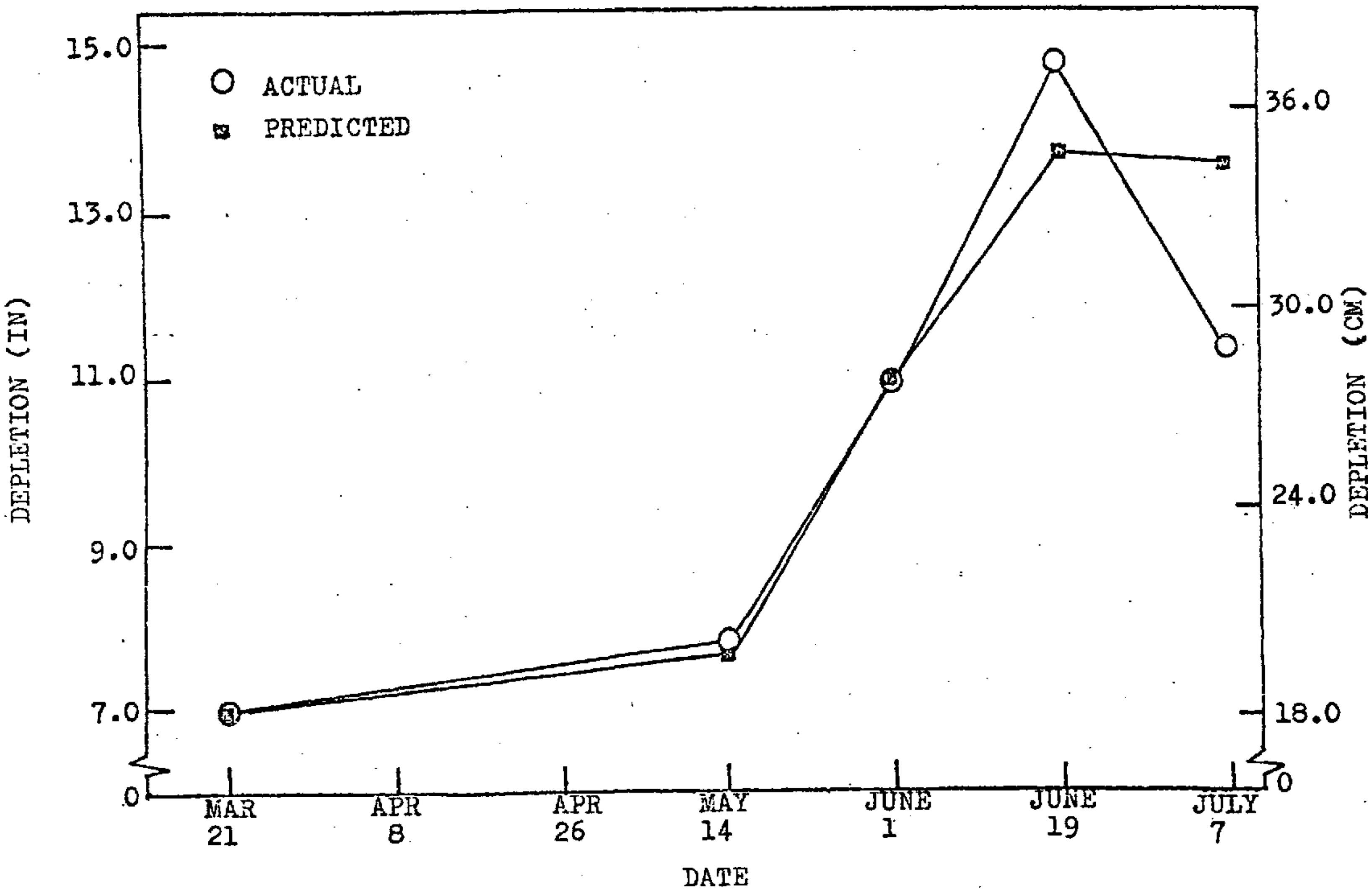

Fig. 8. Soil Moisture Depletion Measured and Predicted for Field A.

this date soil moisture depletion was underestimated, but still the difference in values were insignificant compared to the available moisture. After the June 19 date, comparison became difficult due to the discrepancy of actual soil moisture increasing 8.84 cm while rainfall only totaled 2.29 cm.

Fig. 9 and Table 10 show the results of the irrigated Field (B) using equations 11 and 12. The computer model consistently underestimates the evapotranspiration. For the time period up to June 1, the differences were not significant in relation to the available soil moisture, which included an irrigation on May 23 of 3.05 cm. By June 19 the two had considerably different values with another unexplained increase of 3.56 cm in soil moisture and only 2.29 cm of rainfall.

Regression analysis was used to develop a third wheat crop coefficient curve from the leaf area index of Field B (Fig. 10). The equations for the curve were:

$$Y = 0.0109X - 0.000288X^2 + 0.00000333X^3 \qquad (13)$$

$$Y = 1.52 - 0.000834D^2 \qquad (14)$$

where:

Y = Wheat crop coefficient

X = Percent of crop cover

D = Days after 100 percent crop cover.

The computer model's results using equations 13 and 14 indicate that the soil moisture depletion was overestimated meaning the crop coefficient used was too large.

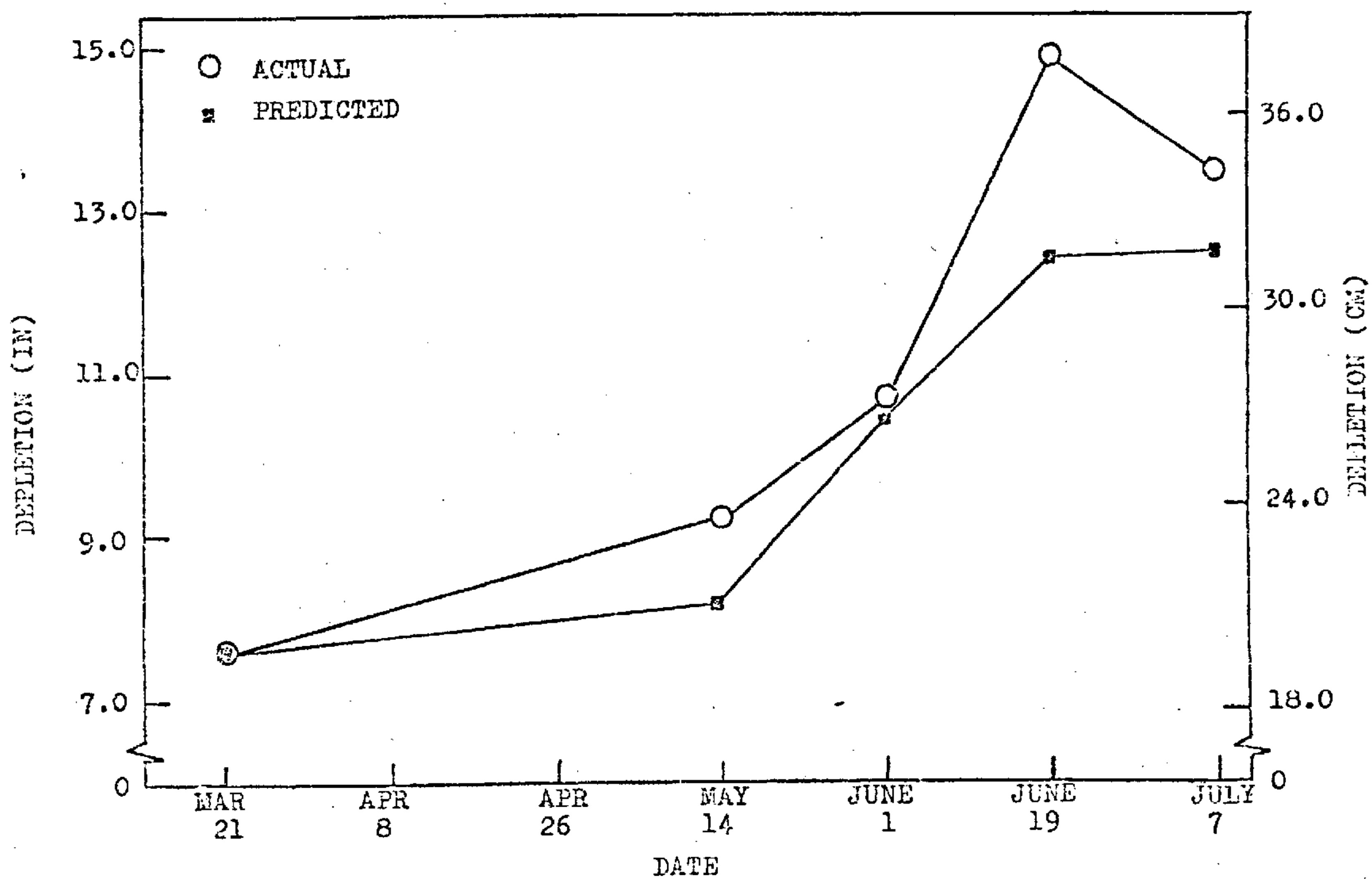

Fig. 9. Soil Moisture Depletion Measured and Predicted for Field B.

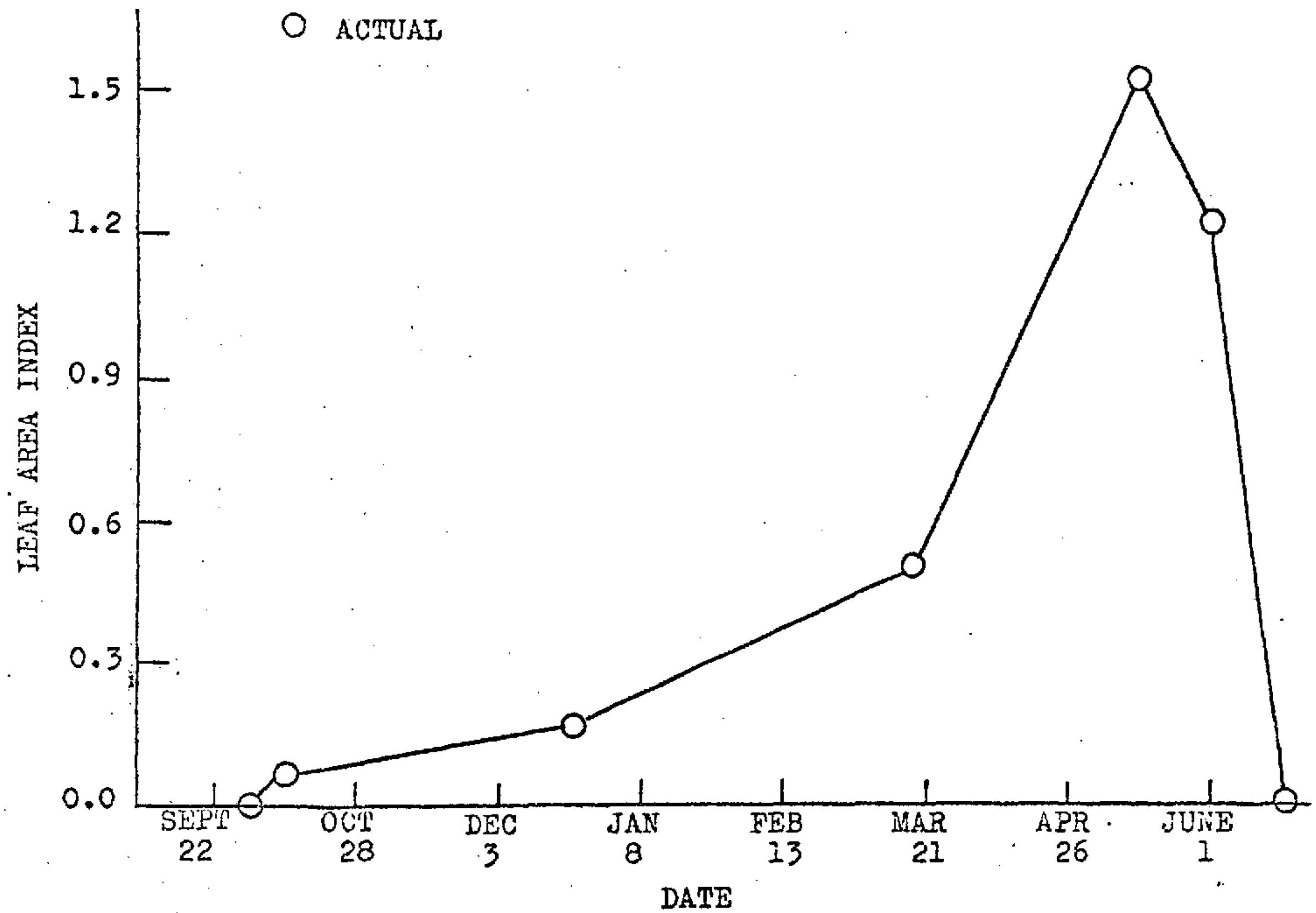

Fig. 10. Measured Leaf Area Index from Field B.

DISCUSSION

The computer model of irrigation scheduling developed by Jensen et al., (1971) uses a crop coefficient which represents the effects of the resistance of the water movement from the soil to the evaporating surfaces, the resistance of the diffusion of water vapor from the surfaces to the atmosphere and the amount of available energy compared to the reference crop. The model predicts percent effective cover by assuming that it is equal to days after planting divided by the days from planting to heading for small grains. This proves to be a poor assumption for winter wheat.

An alternative to this method of crop coefficient determination would be the direct use of wheat vegetative growth or more specifically leaf area index. If a leaf area index versus the crop coefficient curve was developed, vegetative growth would then indicate a specific value for the crop coefficient at a certain point in time. This would eliminate problems due to seasonal variation of weather conditions such as an early fall or late spring.

From this study it appears that a further step can be taken to utilize remote sensing. The winter wheat leaf area index has been described, with high correlation, by reflectance readings. These readings could be used as a direct input into a computer model instead of the original percent of effective cover.

If remote sensing data were available within hours after flight over an area, the following procedure might occur. Data direct from the remote sensing device would be fed into the computer containing an irrigation scheduling model. Meteorological data and a weather forecast for the prediction period would be the other inputs. From a leaf area index curve averaged over many years and the value from the remote sensor, the growth of the crop could be estimated for the prediction period. Knowing the growth or water use, the computer model would then be able to predict the irrigation requirement necessary. This process could be handled by one manager for large areas of irrigated wheat land.

CONCLUSIONS

Results from this study indicate:

1. Vegetative growth was best predicted by a linear relationship between leaf area index and the ratio of band 4 to band 5. All significant soil moisture effects were cancelled by the ratio.
2. Soil moisture at a depth of 0 to 15 cm, with specific soil factors, was predicted by band 4 and leaf area index with a high regression coefficient.
3. Vegetative growth, measured by leaf area index, was one of the necessary inputs in evaluating the winter wheat crop coefficient from March to maturity.

SUMMARY

A realization that wise resource management is necessary comes at a time when resource use is greater than ever before and the population is still increasing. With the use of remote sensing large quantities of data are available for resource management. These large quantities of data have led to the development of automatic recognition techniques in agriculture. Earth Resources Technology Satellite program provides a system for developing and demonstrating the techniques for efficient resource management.

With the large amount of irrigated land in the world, excess irrigation applications means large quantities of water needlessly lost. This valuable resource could be better utilized through the use of irrigation scheduling. Irrigation scheduling predicts the consumptive use (evapotranspiration). The actual evapotranspiration is dependent upon potential evapotranspiration and a crop coefficient which may be predicted by the plant's actual growth. The plant's growth can be determined by reflection of solar radiation from the plant canopy.

The objectives of this study were to evaluate reflectance for prediction of soil moisture and vegetative growth; and to determine the feasibility of using the plant's actual growth for use in determining the winter wheat crop coefficient curve and using it in a computer model developed by Jensen _et al_. (1971).

The study was conducted on winter wheat fields located northwest of Garden City, Kansas. Two soil moisture treatments were used, one dryland wheat field and one irrigated wheat field. Both fields were on Ulyssess-Richfield silt loam.

ERTS-1 satellite passes over any location on the Earth's surface once every 18 days at the same time of day. The satellite contains a line scanning device (Multispectral Scanner) that operates in two bands of the visible region and two in the near infrared region. Band 4 includes the spectrum between 0.5 and 0.6 μ, band 5 between 0.6 and 0.7 μ, band 6 between 0.7 and 0.8 μ and band 7 between 0.8 and 1.1 μ.

The ground truth data were gathered within one day of the aerial flights by ERTS-1. The ground truth data included soil moisture at various depths, leaf area index measurements and rainfall readings. The meteorological data were from the Garden City Experiment Station with the exception of solar radiation which was obtained from the Dodge City Weather Service.

Stepwise Deletion Multiple Regression (1973) was used to formulate equations with the use of reflectance data for vegetative growth and soil moisture. The equation that best described the relationship between reflectance and vegetative growth was:

$$LAI = 2.92 MSS4/5 - 2.63 \quad , \quad R^2 = 0.95 \tag{2}$$

where:

LAI = Leaf area index

MSS4/5 = Ratio of band 4 to band 5

R^2 = Regression coefficient

Soil moisture at a depth of 0 to 15 cm was best predicted by;

$$SM2 = 101.11 - 4.00 MSS4 - 70.31 MSS4/5 \tag{8}$$

where:

SM2 = Soil moisture dry weight at 0 to 15 cm (%)

MSS4 = Band 4

MSS4/5 = Ratio of band 4 to band 5.

The best winter wheat crop coefficient curve was developed by regression analysis on the leaf area index data of the dryland field (A). The crop coefficient curve was:

$$Y = 0.005 + 0.0165X - 0.000467X^2 - 0.00000402X^3 \qquad (11)$$

$$Y = 0.998 - 0.00297D - 0.000747D^2 \qquad (12)$$

where:

Y = Wheat crop coefficient

X = Percent of crop cover

D = Days after 100 percent crop cover.

Meteorological data, starting soil moistures and crop coefficient curve were used in the computer model by Jensen et al. (1971). From results obtained, vegetative growth provides a feasible method for evaluating the winter wheat crop coefficient from at least March through maturity. Within the limits specified by Jensen et al. (1971), the model and modified coefficient proved to be a good estimator of soil moisture.

SUGGESTIONS FOR FUTURE RESEARCH

The research on evapotranspiration modeling and determining the crop coefficient by leaf area index should be expanded to include other crops and the whole growing season as well as increasing the number of test fields. More frequent sampling of soil moisture and leaf area index may be helpful. The neutron probe method for determining soil moisture measurement would provide a more representative indication due to the increased area of sampling. Continued research in using remote sensing for predicting vegetative growth with an emphasis on its use as an input in evaluating the crop coefficient in an evapotranspiration model may prove beneficial.

Additional research in the area of detecting soil moistures at depths greater than 15 cm with thermal energy could prove productive.

REFERENCES

Allen, W. H. and J. I. Sewell. 1973. Remote sensing of fallow soil moisture by photography and infrared line scanner. Transactions ASAE. 16(4): 700-706.

Angstrom, A. 1925. The albedo of various surfaces of the ground. Geografiska Annaler. (7):323.

Ashburn, E. V. and R. G. Weldon. 1956. Reflectance of Spectral Diffuse Desert Surfaces. Optical Society of America Journal. (46):583.

Bauer, Kenneth G. and John A. Dutton. 1962. Albedo variations measured from an airplane over several types of surfaces. Journal of Geophysical Research. 67(6):2367-2376.

Bhangoo, M. S. 1956. Fractionation of total supplies of nitrogen, phosphorus and potassium in certain Kansas surface soils and subsoils and their effect on the yield and composition of wheat. Kansas State University Library. Manhattan, Kansas.

Bolaria, T. S. 1956. Cold hardiness, growth and yield of winter wheat as influenced by mineral nutrients. Kansas State University Library. Manhattan, Kansas.

Bowers, S. A. 1971. Reflection of radiant energy from soils. Kansas State University Library. Manhattan, Kansas.

Carlson, Richard E. 1971. Remote detection of moisture stress: Field and laboratory experiments. Iowa State University Library. Ames, Iowa.

Cole, F. W. 1970. Introduction to meteorology. New York. John Wiley and Sons, Inc.

Coulson, L. 1966. Effects of reflection properties of natural surfaces in aerial reconnaissance. Applied Optics. (5):905-917.

David, W. P. 1969. Remote sensing of crop water deficits and its potential applications. Texas A&M University Remote Sensing Center Technical Report RSC-06.

Earing, Dianne L. and I. William Ginsberg. 1969. A spectral discrimination technique for agricultural applications. Sixth International Symposium on Remote Sensing of Environment Proceedings.

Economic Research Service. 1965. Agricultural application of remote sensing--The potential from space platforms. U.S. Dept. of Agri. Bulletin 328.

Fritschen, L. J. 1967. Net and solar radiation relations over irrigated field crops. Agri. Meteorology. (4):55-62.

Frits, Sigmund. 1948. The albedo of the ground and atmosphere. Meteorological Society Bulletin. (29):303.

Fry, A. W. and Alfred S. Gray. 1970. Sprinkler irrigation handbook. Glendora, California. Rain Bird Sprinkler Mfg. Corporation.

Gates, David M. 1965. Characteristics of soil and vegetated surfaces to reflected and emitted radiation. Third Symposium on Remote Sensing of Environment Proceedings.

Gates, David M. and R. J. Hanks. 1967. Plant factors affecting evapotranspiration. Irrigation of Agricultural Lands. American Society of Agronomy Monograph No. 11.

Geiger, Rudolf. 1965. The climate near the ground. Cambridge, Massachusetts. Harvard University Press.

George, Theodore A. 1970. Unmanned spacecraft for surveying earth's resources. Princeton University Conference on Aerospace Methods for Revealing and Evaluating Earth's Resources.

Heermann, D. F. and H. R. Gardner. 1970. Evapotranspiration model for dryland crops for the Great Plains. Evapotranspiration in the Great Plains Seminar.

Hoffer, Roger M., Roger A. Holmes and J. Ralph Shay. 1966. Vegetative, soil and photographic factors affecting tone in agricultural remote multispectral sensing. Fourth Symposium on Remote Sensing of Environment Proceedings.

Interpretation of remote multispectral imagery of agricultural crops. 1967. Purdue University Agri. Exp. Sta. Bulletin 831.

Israelsen, Orson W. and Vaughn E. Hansen. 1967. Irrigation principles and practices. New York. John Wiley and Sons, Inc.

Jensen, M. E. 1968. Water consumption by agricultural plants. Water Deficits and Plant Growth. (2):1-22.

__________ and J. L. Wright. 1970. Irrigation-oriented et models for the Great Plains. Evapotranspiration in the Great Plains Seminar.

____________________ and B. J. Pratt. 1971. Estimating soil moisture depletion from climate, crop and soil data. Transactions of ASAE. 14(5):954-959.

Kanemasu, E. T. 1973. Energy from solar and thermal radiation. (Private Communication).

Kohnke, Helmut. 1968. Soil physics. New York. McGraw-Hill Book Company.

Kondrat'yev, K. Y. 1965. Actinomentry NASATT F9712. National Aeronautics and Space Administration, Washington, D.C.

Lowry, W. P. 1969. Weather and life. New York. Academic Press.

Luxmoore, R. J., R. J. Millington and H. Marcellos. 1971. Soybean canopy structure and some radiant energy relations. Agronomy Journal. (63):111-114.

Monteith, J. L. 1959. The reflection of short-wave radiation by vegetation. Quarterly Journal of the Royal Meteorological Society. (85):386-392.

__________ and G. Szeicz. 1961. The radiation balance of bare soil and vegetation. Royal Meteorological Society of London (87):159-170.

Myers, Victor I. and William A. Allen. 1968. Electrical sensing as non-destructive testing and measuring techniques in agriculture. Applied Optics. (7):1819.

Myers, V. I., C. L. Wiegand, M. D. Heilman and J. R. Thomas. 1966. Remote sensing in soil and water conservation research. Southern Plains Branch Soil and Water Conservation Research Div. Agri. Research Service U.S. Dept. of Agri.

NASA Earth Resources Technology Satellite Data Users Handbook. 1972. Goddard Space Flight Center Document 71SD4249.

Nicodemus, F. E. 1965. Directional reflectance and emissivitiy of an opaque surface. Applied Optics. (4):767-773.

Penman, H. L. 1963. Vegetation and hydrology. Commonwealth Bureau of Soils Technical Communication No. 53.

__________, D. E. Angus and C. H. M. Van Bavel. 1967. Microclimatic factors affecting evaporation and transpiration. Irrigation of Agricultural Lands. American Society of Agronomy Monograph No. 11.

Remote multispectral sensing in agriculture. 1967. Purdue University Agri. Exp. Sta. Bulletin 844.

Remote multispectral sensing in agriculture. 1970. Purdue University Agri. Expt. Sta. and Purdue University Bulletin 873.

Remote Sensing. 1970. Washington, D.C. National Academy of Sciences.

Rijks, D. A. 1967. Water use by irrigated cotton in Sudan. I. Reflection of short-wave radiation. Journal of Applied Ecology. (4):561-568.

Ritchie, J. T. 1971. Dryland evaporative flux in a subhumid climate: I. Micrometeorological influences. Agronomy Journal. (63):51-55.

__________. 1972. Model for predicting evaporation from a row crop with incomplete cover. Water Resources Research. 8(5):1204-1213.

__________ and Earl Burnett. 1971. Dry land evaporative flux in a sub humid climate: II. Plant influences. Agronomy Journal (63):56-62.

Savage, R. G. 1949. Moisture determinations in hay yield. Sci. Agri. (29):305-329.

Sewell, John I., William H. Allen and Robert S. Pile. 1971. Visible and near infrared remote-sensing of soil moisture levels. Transactions ASAE. 14(6):1163-1166.

Sinclair, T. R., R. M. Hoffer and M. M. Schreiber. 1971. Reflectance and internal structure of leaves from several crops during a growing season. Agronomy Journal. (63):863-868.

__________, M. M. Schreiber and R. M. Hoffer. 1973. Diffuse reflectance hypothesis for the pathway of solar radiation through leaves. Agronomy Journal 65(2):276-283.

Stanhill, G., G. J. Hofstede and J. D. Kalma. 1966. Radiation balance of natural and agricutlrual vegetation. Quarterly Journal of the Royal Meteorological Society. (92):128-140.

__________, J. H. Cox and S. Moreshet. 1968. The effect of crop and climate factors on the radiation balance of an irrigated maize crop. Journal of Applied Ecology. (5):707-720.

Stepwise deletion multiple regression (STEPDEL) description 4. 1973. Kansas State University Statistical Laboratory. Manhattan, Kansas.

Teare, I. D. and C. J. Peterson. 1971. Surface area of chlorophyll-containing tissue of the inflorescence of triticum aestivum l. Crop Science. 2(5):627-628.

Variety tests with fall-planted small grains. 1971. Kansas State University Agri. Exp. Sta. Report 180.

Werner, Hal D., Fred A. Schmer, Maurice L. Horton and Fred A. Waltz. 1971. Application of remote sensing techniques to monitoring soil moisture. Seventh International Symposium on Remote Sensing of Environment Proceedings.

Winkler, Erhard M. 1966. Moisture measurements in glacial soils from airphotos. Ecology. 47(1):156-158.

APPENDIX

Table 11. Computer Model of Evapotranspiration by Jensen *et al*.

```
$JOB            JK,TIME=(5),PAGES=20
      REAL METH1,IRR
C**   "IRRIGATE" WITH 1971 REVISIONS BY PRATT, JENSEN & HEERMANN
C********     PLUS  KSU MODIFICATIONS FOR IBM 360/50
C** MAIN PROGRAM
      COMMON A(4,5), CTR(4),TXR(4),ND(4,30).
     1X(15,4,30),DESC(5),DATE(4),CROP(3),AIRR(2),FIRC(15),
     2N(4),NDB(4),RSO(4),RODAY(4),WI(5,100),C(8,8),RREG(4,20),M(30)
      COMMON /NEW/  M(4),MON(13),ID,NCP,NDE,NOP,B(4,6),ETAP(4),TP(4).
     1DT1(4),DT2(4),FCT(4),ETP5
      DIMENSION CW(4)
      DATA METH1 /'RREG'/
C     READ NUMBER OF REGIONS
C** READ CROP COEFFICIENTS BEFORE EFFECTIVE COVER, C(1,1) TO C(8,4)
C** II=CROP NO.  JJ=NO. OF TERM IN POLYNOMIAL EQUATION
   16 FORMAT (5X,F15.3,3F20.3)
   17 FORMAT(1H ,4F15.8)
      DO 18 II=1,8
   15 READ(5,16)(C(II,JJ),JJ=1,4)
   18 WRITE(6,17)(C(II,JJ),JJ=1,4)
C** READ CROP COEFFICIENTS AFTER EFFECTIVE COVER, C(1,5) TO C(8,8)
      DO 21 II=1,8
   20 READ (5,16) (C(II,JJ),JJ=5,8)
   21 WRITE(6,17)(C(II,JJ),JJ=5,8)
      READ (5,1) NREG,RNRD
    1 FORMAT  (5X,I5,1X,A4)
C     READ REGIONAL DATA
      DO 2 I=1,NREG
      READ (5,3) (A(I,J), J=1,5), CTR(I),TXR(I),CW(I)
    3 FORMAT(5X,5A4,3F7.3)
      READ (5,103)  ETAP(I),TP(I),DT1(I),DT2(I)
  103 FORMAT  (5X,F5.2,3F5.0)
    2 READ (5,104)  (B(I,J),J=1,6)
  104 FORMAT  (5X,6E10.2)
C     READ CLIMATIC DATA - NUM. OF DAYS PLUS THREE PREVIOUS DAYS
      DO 7 I=1,NREG
      READ(5,11)N(I),NDB(I), FCT (I),RSO(I)
   11 FORMAT (5X,2I5,F5.2 ,F5.0)
      K=N(I) +3
C** IF RNRD=METH1 THEN RAIN IS READ BY REGION RATHER THAN BY FARM
C** I=REGION.  K=NO OF DAY.  K=4 IS FIRST DAY OF ANALYSIS PERIOD.
C**  K=1 IS FIRST DAY OF THREE PREVIOUS DAYS.
      IF (RNRD.EQ.METH1) GO TO 12
      DO 4 J=1,K
    4 READ( 5,5) ND(I,J),X (1,I,J),X (2,I,J),X(3,I,J),X(4,I,J),X(5,I,J)
      GO TO 7
   12 DO 9 J=1,K
    8 READ (5,25) ND(I,J),X(1,I,J),X(2,I,J),X(3,I,J),X(4,I,J),X(5,I,J)
     1,RREG(I,J)
    7 CONTINUE
   25 FORMAT  (5X,I5,6F5.0)
      WRITE(6,9)
    9 FORMAT(1H1)
    5 FORMAT(5X,I5,5F5.0)
      DO 6  I=1,NREG
      K=N(I)+3
 2889 FORMAT(1H ,4F15.8)
      WRITE(6,2889)C(1,1),C(1,2),C(1,3),C(1,4)
      CALL EVAP (I,K)
      WRITE(6,2889)C(1,1),C(1,2),C(1,3),C(1,4)
```

Table 11. Continued.

```
      CALL VAPOR(I,K,CW)
      WRITE(6,2389)C(1,1),C(1,2),C(1,3),C(1,4)
    6 CALL PRINTR(I,K)
      WRITE(6,2389)C(1,1),C(1,2),C(1,3),C(1,4)
      CALL FARMS(NREG,METH1,RNRD)
      WRITE(6,2389)C(1,1),C(1,2),C(1,3),C(1,4)
      CALL PRINTS(NREG,METH1,RNRD)
      WRITE(6,2389)C(1,1),C(1,2),C(1,3),C(1,4)
  999 STOP
      END

      SUBROUTINE FARMS (NREG,METH1,RNRD)
C     SUBROUTINE TO CALCULATE IRRIGATION DATES
      REAL METH1,IRR
      COMMON A(4,5), CTR(4),TXP(4),ND(4,30),
     1X(16,4,30),DESC(5),DATE(4),CROP(3),AIRR(2),FORC(15),
     2N(4),NDB(4),KSU(4),MODAY(4),W1(5,100),C(8,8),PREG(4,30),R(30)
      COMMON /NEW/  W(4),MON(13),ID,NCR,NDE,NDP,B(4,6),ETAP(4),TP(4),
     1DT1(4),DT2(4),FCT(4),ETP5
      DIMENSION DPAKSU(6),AIRKSU(6),NXDKSU(6)
      DIMENSION D(8),        SUMR(30),ET(30),DPL(30),D1(8)
      DIMENSION  ETRSET(8,30),ETSET(8,30),AKC11(8,30),AKCSET(8,30),
     1RSET(4,8,30),AETFLD(8),CROPST (8,3 ), DPLSET(8,30)
C     D ARRAY -LOWER LIMIT FOR CROP COEFFS.
C     D1ARRAY-UPPER LIMIT FOR CROP COEFFS.
      DATA D1/1.1,1.1,1.1,1.1,1.1,1.1,1.0,0.87/
      DATA NCROPS/8/,D/7*0.1,.87/
      DATA    SUMR,ET,DPL/30*0.0,30*0.0,30*0.0/
C     READ DATE
      READ( 5,14) (DATE(K),K=1,4)
      N4=1
      F=0.9
      DO 100 I=1,NREG
      WRITE(6 ,13)(A(I,J),J=1,5)
   13 FORMAT(1H1,' REGION:  ',5A4,//)
   14 FORMAT(5X,15A4)
      READ( 5,10)LL
   10 FORMAT(25X,I5)
      M=N(I) +3
      NN=N(I)
      DO 100 L=1,LL
      READ(5 ,10)NFN
      READ(5 ,14)(DESC(K),K=1,5)
      WRITE(6 ,15)(DESC(K),K=1,5),(DATE(K),K=1,4)
   15 FORMAT('1FARM:',5A4,3X,'DATE OF COMPUTATION: ',4A4,/)
      WRITE (6,16)
   16 FORMAT  ('0',T11,'|',T18,'|***** SOIL MOISTURE DEPLETION ******|--
     1---- IRRIGATIONS -------| INCHES |',/,' ',T11,'|',T18,'|',T28,'|',
     2          T37,'|',T48,'|',T55,'|',T64,                  '|   IF   |  WITH
     3  |    TO   |',/,
     4 ' CROP-FLD | COEF | TO DATE | TYPE-O | OPTIMUM  | RATE |  LAST',' 
     5  | RAIN=0 |  RAIN  | APPLY  | REG FM FLD')
   24 DO 110 NF=1,NFN
      IF(RNRD.EQ.METH1) GO TO 1
      GO TO 2
    1 DO 26 J=1,M
   26 R(J)=PREG(I,J)
    2 READ(5,17)NCP,CROP(1),CROP(2),CROP(3),NDP,NDE,IOH,E,AVM
   17 FORMAT(5X,I2,2A4,A2,3I5,2F5.2)
      IF (RNRD.EQ.METH1) GO TO 23
```

Table 11. Continued.

```
      READ(5,18)(AIRR(J),J=1,2),DPA,N5,(R(J),J=4,M )
   18 FORMAT (5X,2A3,F4.1,I4,10F4.2/20F4.2)
      READ(5,19) DPL(NF),SUMR(NF),(R(J),J=1,3)
   19 FORMAT(5F10.2)
      GOTO 22
   23 READ (5,20)(AIRR(J),J=1,2),DPA,N5,IRR
   20 FORMAT  (5X,2A3,F4.1,I4,F4.1)
      READ  (5,19) DPL(NF),SUMR(NF)
      IF (N5.GE.1)  R(N5+3)=R(N5+3)+IRR
   22 CONTINUE
      AKC=0.0
      AKC1=0.0
      PCT=0.0
      DT=0.0
C
C**  J=4 REPRESENTS FIRST DAY OF THE PERIOD FOR WHICH ANALYSIS IS BEING
C**  RUN
      DO 98 J=4,M
      ET(J)=0.0
      ETR=0.0
      RX= R(J)
      SUMR(NF)= SUMR(NF)+R(J)
      IF(J-N5-3)76,75,76
C** DPL AND SUMR ARE SET TO ZERO ON THE DAY OF IRRIGATION
   75 DPL(NF)=0.0
      SUMR(NF)=0.0
      GO TO 99
   76 IF(NDB(I)-NDP)109,176,176
  176 IF(NDB(I)-NDH)29,29,109
   29 IF(NDB(I)+J-4-NDE) 30,30,31
   30 PCT=100.0*(NDB(I)+J-4-NDP)/(NDE-NDP)
      AKC1=C(NCR,1)+C(NCR,2)*PCT+C(NCR,3)*PCT**2+C(NCR,4)*PCT**3
      IF(AKC1-D1(NCR))231,232,232
  232 AKC1=D1(NCR)
  231 AV=(1.0-DPL(NF)/AVM)*100.0
      IF(AV)130,131,131
  130 AV=0.0
  131 AV3=1.0+AV
      AKC=AKC1*ALOG(AV3)/ALOG(101.0)
      GO TO 32
   31 DT=NDB(I)+J-4-NDE
      PCT=100.
      AV=(1.0-DPL(NF)/AVM)*100.0
      AKC1=C(NCR,5)+C(NCR,6)*DT+C(NCR,7)*DT**2+C(NCR,8)*DT**3
      IF(AKC1-D(NCR))88,235,235
  235 IF(AKC1-D1(NCR))242,241,241
  241 AKC1=D1(NCR)
      GO TO 242
   88 AKC1=D(NCR)
  242 IF(AV)233,234,234
  233 AV=0.0
  234 AV3=1.0+AV
      AKC=AKC1*ALOG(AV3)/ALOG(101.0)
   32 ET(J)=AKC*X(16,I,J)
      IF(AKC-F) 38,121,121
   38 IF(R(J-1))42,42,43
   43 ETR=0.8*(F-AKC)*X(16,I,J)
      R(J-1)=R(J-1)-ETR
      IF(R(J-1))49,121,121
   49 R(J-2)=R(J-2)+R(J-1)
```

Table 11. Continued.

```
          R(J-1)=0.0
       45 IF(R(J-2))46,121,121
       46 R(J-3)=R(J-3)+R(J-2)
          R(J-2)=0.0
       40 IF(R(J-3))53,121,121
       53 ETR=ETR+R(J-3)
          R(J-3)=0.0
          GO TO 121
       42 IF(R(J-2))44,44,47
       47 ETR=0.5*(F-AKC)*X(16,I,J)
          R(J-2)=R(J-2)-ETR
          GO TO 45
       44 IF(R(J-3))121,121,48
       48 ETR=0.3*(F-AKC)*X(16,I,J)
          R(J-3)=R(J-3)-ETR
          GO TO 40
      121 IF(ETR)50,51,51
       50 ETR=0.0
       51 ET(J)=ET(J)+ETR
       91 DPL(NF)=DPL(NF)+ET(J)-RX
          IF(DPL(NF))115,99,99
      115 DPL(NF)=0.0
       99 CONTINUE
          ETRSET(NF,J)=ETR
          ETSET(NF,J)=ET(J)
          AKC11(NF,J)=AKC1
          AKCSET(NF,J)=AKC
          DO 890 NM=1,4
      890 RSET(NM,NF,J)=R(J-NM+1)
          DPLSET(NF,J)=DPL(NF)
       98 CONTINUE
          SUMET=0.0
          DO 57 J=4,M
       57 SUMET=SUMET + ET(J)
          RDIF=M-3
          AET=SUMET/RDIF
          AETFLD(NF)=AET
          DO 880 J=1,3
      880 CROPST(NF,J)=CROP(J)
          MBD=NDB(I)+N(I)
          IF (NDB(I)+N(I)+3-NDE)  250,250,255
      250 PCT=100.0*(NDB(I)+N(I)+2-NDP)/(NDE-NDP)
          AKC5 = C(NCR,1)+C(NCR,2)*PCT+C(NCR,3)*PCT**2+C(NCR,4)*PCT**3
          GO TO 260
      255 DT=NDB(I)+N(I)+3-NDE
          PCT=100.0
          AKC5 = C(NCR,5)+C(NCR,6)*DT+C(NCR,7)*DT**2+C(NCR,8)*DT**3
      260 IF  (AKC5 .LT. D(NCR)) AKC5=D(NCR)
          IF (AKC5 .GT. D1(NCR)) AKC5=D1(NCR)
          AJJ5=NDB(I)+N(I)+3
          IF (AJJ5 .GT. TP(I)) GO TO 7034
          DLT=DT1(I)
          GO TO 7341
     7034 DLT=DT2(I)
     7341 ETP5=  (ETAP(I)/(EXP(((AJJ5-TP(I))/DLT)**2)))*FCT(I)
          ETA5 = AKC5*ETP5
          DPLA = DPL(NF)
C**        SUBSCRIPT  J=1 IS 20%D  --  J=2 IS 30%D  --  J=3 IS 40%D
C**      -   J=4 IS 50%D  --  J=5 IS 60%D
          NPCT=100.0*(NDB(I)+N(I)+2-NDP)/(NDE+33.-NDP)
```

Table 11. Continued.

```
      IF(NPCT-100)248,248,249
  249 NPCT=100.0
  248 CONTINUE
                            DO 108 J=1,5
                            RJJ=J+1
      DPAKSU(J)=NPCT*AVM*RJJ*.001
                            IPC=(J+1)*10
      AVW=DPAKSU(J)-DPL(NF)
      CALL SCHED (NDD,AVW,NDH,NXD,NXDP,I,DPLA,AVM,D,D1)
      CALL DATEE (NXD,IX,IY,NDH)
      CALL DATEE (NXDP,JX,JY,NDH)
   59 IF (DPAKSU(J) - DPL(NF)) 60,61,61
   60 AIR = DPL(NF)/E
      GO TO 63
   61 AIR = DPAKSU(J)/E
   63 IF (J .GT. 1) GO TO 65
      WRITE (6,64)  CROP,AKC5,DPL(NF),DPAKSU(J),ETA5,AIRR,MON(IX),IY,MON
     1   (JX),JY,AIR,   I,L,NF
   64 FORMAT  ('0',2A4,A2,F5.2,F9.2,5X,'20% D',2F9.2,' | ',2A3,2(2X,A4,I
     23),' | ',F4.1,I7,2I4)
      GO TO 108
   65 WRITE (6,68)  IPC,DPAKSU(J),ETA5,AIRR,MON(IX),IY,MON(JX),JY,AIR
   68 FORMAT  (' ',T31,I2,'% D',2F9.2,' | ',2A3,2(2X,A4,I3),
     1    ' | ',F4.1,I7,2I4)
  108 CONTINUE
  109 CONTINUE
      W1(1,N4)=DPL(NF)
      W1(2,N4)=SUMR(NF)
      W1(3,N4)=R(M-2)
      W1(4,N4)=R(M-1)
      W1(5,N4)=R(M)
      N4=N4+1
  110 CONTINUE
      WK = (NDB(I) + N(I) - 53)/7
      PP = 14.*(B(I,1)+B(I,2)*WK+  B(I,3)*WK**2+  B(I,4)*WK**3 +
     1   B(I,5)*WK**4 + B(I,6)*WK**5)
      IF (PP .LT. 0.0) PP=0.0
      WRITE (6,163) PP,I,L
  163 FORMAT  ('0PROBABLE RAIN NEXT TWO WEEKS=',F5.2,2X,'INCHES',30X,2I2
     1   )
      WRITE  (6,801)
  801 FORMAT  ('-***TABLE OF DAILY VALUES***')
      DO 830 NF=1,NFN
      WRITE  (6,803)(CROPST(NF,K),K=1,3)
  803 FORMAT  ('0',2A4,A2,/,
     1          '0  DAY        ETR        ET        SO      AKC1      AKC',
     2        RX    R(J-1)  R(J-2)  R(J-3)     DPL',/)
      DO 820 J=4,M
      WRITE  (6,802) ND(I,J),(TRSET(NF,J),ETSET(NF,J),X(16,I,J),
     1AKC11(NF,J),AKCSET(NF,J),(RSET(NM,NF,J),NM=1,4),DPLSET(NF,J)
  802 FORMAT  (' ',I5,2X,F8.4,F8.3,8F8.2)
  820 CONTINUE
      WRITE (6,821) AETFLD(NF)
  821 FORMAT  (13X,'AET=',F7.3)
  830 CONTINUE
  100 CONTINUE
C
C**   NDB(1)= NO. OF FIELDS FOR WHICH ANALYSIS WAS RUN
      NDB(1)=N4-1
   81 RETURN
```

Table 11. Continued.

```
      END

      SUBROUTINE EVAP(I,K)
C     SUBROUTINE TO CALCULATE EVAPOTRANSPIRATION POTENTIAL
      REAL METH1
      COMMON A(4,5), CTR(4),TXR(4),NO(4,30),
     1X(16,4,30),DESC(5),DATE(4),CROP(3),AIRR(2),FORC(15),
     2N(4),NDB(4),RSO(4),MODAY(4),W1(5,100),C(8,8),RREG(4,30),R(30)
      DO 10 J=4,K
      X(6,I,J)= (X(1,I,J) + X(2,I,J))/2.0
   15 X(7,I,J)=  CTR(I)*( X(6,I,J)-TXR(I)) *X(3,I,J)* 0.000673
   10 CONTINUE
      RETURN
      END

      SUBROUTINE VAPOR(I,K,CW)
C     SUBROUTINE TO CALCULATE HEAT FLUX,EO POTENTIAL, NET RADIATION
      REAL METH1
      COMMON A(4,5), CTR(4),TXR(4),NO(4,30),
     1X(16,4,30),DESC(5),DATE(4),CROP(3),AIRR(2),FORC(15),
     2N(4),NDB(4),RSO(4),MODAY(4),W1(5,100),C(8,8),RREG(4,30),R(30)
      COMMON /NEW/  W(4),MON(13),ID,NCS,NDE,NDP,B(4,6),ETAP(4),TP(4),
     1DT1(4),DT2(4),FCT(4),ETP5
      DIMENSION CW(4)
      DO 30 J=4,K
      IF(X(4,I,J).EQ.0)GOTO 35
      X(8,I,J)= X(5,I,J)/24.0
      VPS1= -0.6959+0.2946*X(2,I,J)-0.005195*X(2,I,J)**2+0.000089*
     1X(2,I,J)**3
      VPS2= -0.6959+0.2946*X(1,I,J)-0.005195*X(1,I,J)**2+0.000089*
     1X(1,I,J)**3
      X(9,I,J) = (VPS1+VPS2)/2.0
      X(10,I,J)=-0.6959+ 0.2946*X(4,I,J)-0.005195*X(4,I,J)**2 +
     10.000089* X(4,I,J)**3
      X(11,I,J )=(X(6,I,J)-(X(1,I,J-1)+X(2,I,J-1)+X(1,I,J-2)+X(2,I,J
     1-2)+X(1,I,J-3)+X(2,I,J-3))/6.0)*5
      T1= 0.041 + 0.0125*X(6,I,J)-4.534*X(6,I,J)**2/10**5
      T2= 0.959 -0.0125*X(6,I,J)+4.534*X(6,I,J)**2/10**5
      X(12,I,J)= ((X(1,I,J)-32)/1.8 + 273)/100.0
      X(13,I,J)= ((X(2,I,J)-32)/1.8 + 273)/100.0
      Y= X(10,I,J)
      JJ=NDB(I) + J - 4
      EMT=0.325+0.045*SIN(30*(JJ/30.-1.5)*3.1416/180.)
      X(14,I,J)= (EMT -0.044*SQRT(Y))*11.71*(X(13,I,J)**4+X(12,I,J)
     1**4)*0.5
      X(15,I,J)= 0.77*X(3,I,J)-(1.22* X(3,I,J)/RSO(I)-0.13)*X(14,I,J)
   30 X(16,I,J)=(T1*(X(15,I,J)-X(11,I,J))+T2*15.36*(.75+CW(I)*
     1X(5,I,J))*(X(9,I,J)-X(10,I,J)))*0.000673
      AJJ5=NDB(I)+N(I)+3
      IF (AJJ5 .GT. TP(I)) GO TO 34
      DLT=DT1(I)
      GO TO 341
   34 DLT=DT2(I)
  341 ETP5=  (ETAP(I)/(EXP(((AJJ5-TP(I))/DLT)**2)))*FCT(I)
   35 RETURN
      END

      SUBROUTINE PRINTR(I,K)
C     SUBROUTINE TO PRINT REGIONAL DATA
      REAL METH1
```

Table 11. Continued.

```
      COMMON A(4,5), CTR(4),TXR(4),ND(4,30),
     1X(16,4,30),DESC(5),DATE(4),CROP(3),AIRR(2),FORC(15),
     2N(4),NDB(4),RSD(4),MODAY(4),W1(5,100),C(8,8),PREG(4,30),P(30)
      COMMON /NEW/  W(4),MON(13),ID,NCR,NDE,NDP,B(4,6),ETAP(4),TP(4),
     1DT1(4),DT2(4),FCT(4),ETP5
      JJ=NDB(I)
      CALL DATEE (JJ,MN,NID,336)
      WRITE(6,10) (A(I,J),J=1,5),MON(MN),NID
   10 FORMAT(1H-,5X,'REGION:',5A4,5X,'BEGINNING DATE=',A4,I3)
      WRITE(6,15)
   15 FORMAT(1H-,'    DAY   TAVG      RS    UA       VPS      VPU      RN        G
     1    ETP      EO')
      WRITE(6,27)
   27 FORMAT(1H )
      DO 20 J=4,K
      WRITE(6,25)ND(I,J),X(6,I,J),X(3,I,J),X(8,I,J),X(9,I,J),X(10,I,J)
     1,X(15,I,J),X(11,I,J),X(7,I,J),X(16,I,J)
   20 CONTINUE
   35 WRITE(6,40)    ETP5
   40 FORMAT(1H ,'FORECAST :  POTENTIAL ET NEXT 5 DAYS=',F5.2)
   25 FORMAT(1H ,I5,F7.1,F6.0,F6.1,F7.1,F8.1,F7.0,F8.1,2F7.2)
      RETURN
      END

      SUBROUTINE ETAVG(II,ETA,MBD,I,D,D1.AVM,DPL)
      COMMON A(4,5), CTR(4),TXR(4),ND(4,30),
     1X(16,4,30),DESC(5),DATE(4),CROP(3),AIRR(2),FORC(15),
     2N(4),NDB(4),RSD(4),MODAY(4),W1(5,100),C(8,8),PREG(4,30),P(30)
      COMMON /NEW/  W(4),MON(13),ID,NCR,NDE,NDP,B(4,6),ETAP(4),TP(4),
     1DT1(4),DT2(4),FCT(4),ETP5
      DIMENSION D(8),D1(8)
      AI=II
      AV=(1.0-DPL/AVM)*100.
      IF (AV .GT. 0.0) GO TO 300
      AV=0.0
  300 AV3=1+AV
    5 IF (II .GT. NDE) GO TO 2
      AP=NDP
      AE=NDE
      PCT=100.*(AI-AP)/(AE-AP)
      AKC1=C(NCR,1)+C(NCR,2)*PCT+C(NCR,3)*PCT**2+C(NCR,4)*PCT**3
      GO TO 1
    2 DT=II-NDE
      AKC1=C(NCR,5)+C(NCR,6)*DT+C(NCR,7)*DT**2+C(NCR,8)*DT**3
    1 IF (AKC1 .LT. D(NCR)) AKC1=D(NCR)
      IF (AKC1 .GT. D1(NCR)) AKC1=D1(NCR)
      IF(II .GT. TP(I)) GO TO 7
      DLT=DT1(I)
      GO TO 8
    7 DLT=DT2(I)
    8 AKC=AKC1*ALOG(AV3)/ALOG(101.0)
      ETA=AKC * (ETAP(I)/(EXP(((AI-TP(I))/DLT)**2)))
      IF (II-MBD .LT. 5) ETA=ETA*FCT(I)
      RETURN
      END

      SUBROUTINE DATES (II,MN,IID,NDM)
C     CALCULATES MONTH AND DAY FROM JULIAN DAY
      DIMENSION NMD (12)
      DATA NMD/0,31,60,91,121,152,182,213,244,274,305,335/
```

Table 11. Continued.

```
      DO 10 J=2,12
      IF (II .LE. NMO(J)) GO TO 12
   10 CONTINUE
      J=13
   12 MN=J-1
      IID = II-NMO(J-1)
      IF (II .LT. NDH) GO TO 14
      MN=13
      IID = 0
   14 RETURN
      END

      BLOCK DATA
      COMMON /NEW/  W(4),MON(13),ID,NCR,NDE,NDP,B(4,6),ETAP(4),TP(4),
     1DT1(4),DT2(4),FCT(4),ETP5
      DATA MON  /'JAN','FEB','MAR','APR','MAY','JUN','JUL','AUG','SEP',
     1  'OCT','NOV','DEC','NONE'/
      END

      SUBROUTINE SCHED(MBD,AVW,NDH,NXD,NXDP,I,DPL,AVM,D,D1)
      COMMON A(4,5), CTR(4),TXR(4),ND(4,30),
     1X(16,4,30),DESC(5),DATE(4),CROP(3),AIRR(2),FORC(15),
     2N(4),NDB(4),RSD(4),MODAY(4),X1(5,100),C(8,8),RLEG(4,30),F(30)
      COMMON /NEW/  W(4),MON(13),ID,NCR,NDE,NDP,B(4,6),ETAP(4),TP(4),
     1DT1(4),DT2(4),FCT(4),ETP5
      DIMENSION D(8),D1(8)
C     CHECK TO SEE IF THE FIELD NEEDS IRRIGATING AT BEGINNING OF DAY
      IF (AVW.LE.0.0) GO TO 10
      BD=MBD
C     CALCULATING ESTIMATED DATE OF IRRIGATION WITHOUT PROB PRECIP
      DO 1 II=MBD,NDH
      CALL ETAVG (II,ETA,MBD,I,D,D1,AVM,DPL)
      AVW=AVW-ETA
      IF (AVW.LE.0.0) GO TO 2
    1 CONTINUE
C     IF AN IRRIGATION IS NOT REQUIRED BEFORE HARVEST
      GO TO 12
    2 NXD=II
      NXDP=NXD
C     CHECK IF RAINFALL PROBABILITY IS TO BE USED
C     B(I,1)=0 IF RAINFALL PROBABILITY IS NOT DESIRED
      IF (ABS(B(I,1)) .LT. 0.00001) GO TO 11
C     DETERMINE NUMBER OF DAYS FOR EXPECTED PRECIPITATION
      WK=(MBD-53)/7
   16 AI=II
      T=AI-BD
      BD=BD+T
      IF (T .LE. 14. )  GO TO 15
      BD=BD-T+14.
      T=14.
   15 AVW=AVW+PAMT(T,WK,I)
      L=II+1
      DO 3 II=L,NDH
      CALL ETAVG(II,ETA,MBD,I,D,D1,AVM,DPL)
      AVW=AVW-ETA
      IF (AVW .LE. 0.0 )  GO TO 4
    3 CONTINUE
C     IRRIGATION NOT REQUIRED BEFORE HARVEST
      GO TO 13
C      CHECKING IF EACH EXTENDED IRRIGATION DATE USING PROBABILITIES
```

Table 11. Continued.

```
      DO 10 J=2,12
      IF (II .LE. NND(J)) GO TO 12
   10 CONTINUE
      J=13
   12 MN=J-1
      IID = II-NND(J-1)
      IF (II .LT. NDH) GO TO 14
      MN=13
      IID = 0
   14 RETURN
      END

      BLOCK DATA
      COMMON /NEW/  W(4),MON(13),ID,NCR,NDE,NDP,B(4,6),ETAP(4),TP(4),
     1DT1(4),DT2(4),FCT(4),ETP5
      DATA MON  /'JAN','FEB','MAR','APR','MAY','JUN','JUL','AUG','SEP',
     1  'OCT','NOV','DEC','NONE'/
      END

      SUBROUTINE SCHED(MBD,AVW,NDH,NXD,NXDP,I,DPL,AVM,D,D1)
      COMMON A(4,5), CTR(4),TXR(4),ND(4,30),
     1X(16,4,30),DESC(5),DATE(4),CROP(3),AIRR(2),FORC(15),
     2N(4),NDB(4),RSO(4),MODAY(4),W1(5,100),C(8,3),RKEG(4,30),F(30)
      COMMON /NEW/  W(4),MON(13),ID,NCR,NDE,NDP,B(4,6),ETAP(4),TP(4),
     1DT1(4),DT2(4),FCT(4),ETP5
      DIMENSION D(8),D1(8)
C     CHECK TO SEE IF THE FIELD NEEDS IRRIGATING AT BEGINNING OF DAY
      IF (AVW.LE.0.0) GO TO 10
      BD=MBD
C     CALCULATING ESTIMATED DATE OF IRRIGATION WITHOUT PROB PRECIP
      DO 1 II=MBD,NDH
      CALL ETAVG (II,ETA,MBD,I,D,D1,AVM,DPL)
      AVW=AVW-ETA
      IF (AVW.LE.0.0) GO TO 2
    1 CONTINUE
C     IF AN IRRIGATION IS NOT REQUIRED BEFORE HARVEST
      GO TO 12
    2 NXD=II
      NXDP=NXD
C     CHECK IF RAINFALL PROBABILITY IS TO BE USED
C     B(I,1)=0 IF RAINFALL PROBABILITY IS NOT DESIRED
      IF (ABS(B(I,1)) .LT. 0.00001) GO TO 11
C     DETERMINE NUMBER OF DAYS FOR EXPECTED PRECIPITATION
      WK=(MBD-53)/7
   16 AI=II
      T=AI-BD
      BD=BD+T
      IF (T .LE. 14. )  GO TO 15
      BD=BD-T+14.
      T=14.
   15 AVW=AVW+PAMT(T,WK,I)
      L=II+1
      DO 3 II=L,NDH
      CALL ETAVG(II,ETA,MBD,I,D,D1,AVM,DPL)
      AVW=AVW-ETA
      IF (AVW .LE. 0.0 )  GO TO 4
    3 CONTINUE
C     IRRIGATION NOT REQUIRED BEFORE HARVEST
      GO TO 13
C      CHECKING IF EACH EXTENDED IRRIGATION DATE USING PROBABILITIES
```

Table 11. Continued.

```
C       OF RAIN RESULTS IN FURTHER EXTENSION OF IRRIGATION PERIOD
      4 IF (II-1 .EQ. NXDP) GO TO 11
        WK=WK+T/7
        NXDP=II
        GO TO 16
C       SITUATION WHERE FIELD NEEDS IRRIGATION AT THE BEGINNING DATE
     10 NXD=MBD
        NXDP=NXD
        GO TO 11
C       SITUATION WHERE AN IRRIGATION IS NOT REQUIRED BEFORE HARVEST
     12 NXD=NDH
     13 NXDP=NDH
     11 RETURN
        END

        FUNCTION PAMT(T,WK,I)
C   FUNCTION FOR PROBABLE PRECIPITATION
        COMMON /NEW/  W(4),MON(13),ID,NCR,NDE,NDP,B(4,6),ETAP(4),TP(4),
       1DT1(4),DT2(4),FCT(4),ETP5
        PAMT       =T*(B(I,1)+B(I,2)*WK+B(I,3)*WK*WK+B(I,4)*
       1     WK**3+B(I,5)*WK**4+B(I,6)*WK**5)
        RETURN
        END

        SUBROUTINE  PRINTS  (NREG,METH1,RNRD)
C SUBROUTINE TO RETAIN INFORMATION IN "SAVE" FOR NEXT RUN
        REAL METH1
        COMMON A(4,5), CTR(4),TXR(4),ND(4,30),
       1X(16,4,30),DESC(5),DATE(4),CROP(3),AIRR(2),EORC(15),
       2N(4),NOB(4),PSO(4),MODAY(4),W1(5,100),C(8,8),RREG(4,30),F(20)
        COMMON /NEW/  W(4),MON(13),ID,NCR,NDE,NDP,B(4,6),ETAP(4),TP(4),
       1DT1(4),DT2(4),FCT(4),ETP5
        WRITE(6,11) NOB(1)
     11 FORMAT(1H1,' NO. OF FIELDS =',I5)
        DO 40 I=1,NREG
        K1=N(I)+3
        K=K1-2
        IF (RNRD.EQ.METH1) GO TO 15
        WRITE(7,10) (ND(I,J),X(1,I,J),X(2,I,J),X(3,I,J),X(4,I,J),
       1X(5,I,J),J=K,K1)
        WRITE(6,10) (ND(I,J),X(1,I,J),X(2,I,J),X(3,I,J),X(4,I,J),
       1X(5,I,J),J=K,K1)
     10 FORMAT(5X,I5,5F5.0)
        GO TO 40
     15 WRITE (7,20) (ND(I,J),X(1,I,J),X(2,I,J),X(3,I,J),X(4,I,J),X(5,I,J)
       1,RREG(I,J),J=K,K1)
        WRITE (6,20) (ND(I,J),X(1,I,J),X(2,I,J),X(3,I,J),X(4,I,J),X(5,I,J)
       1,RREG(I,J),J=K,K1)
     40 CONTINUE
     20 FORMAT  (5X,I5,5F5.0,F5.2)
        K=NOB(1)
        DO 50 J=1,K
        WRITE(7,55) W1(1,J),W1(2,J),W1(3,J),W1(4,J),W1(5,J)
        WRITE(6,55) W1(1,J),W1(2,J),W1(3,J),W1(4,J),W1(5,J)
     50 CONTINUE
     55 FORMAT(5F10.2)
        RETURN
        END

$ENTRY
```

PREDICTING SOIL MOISTURE AND WHEAT VEGETATIVE GROWTH FROM ERTS-1 IMAGERY

by

JOHN WAYNE KRUPP

B.S., Kansas State University, 1972

AN ABSTRACT OF A MASTER'S THESIS

submitted in partial fulfillment of the

requirements for the degree

MASTER OF SCIENCE

Department of Agricultural Engineering

KANSAS STATE UNIVERSITY
Manhattan, Kansas

1974

ABSTRACT

Wise resource management techniques are necessary if the population of the Earth is to continue to expand. The Earth Resources Technology Satellite program combines remote sensing in space with efficient resource management. Water is a valuable resource needlessly lost by excessive irrigation applications. If needless loss of water is to be lessened, determination of evapotranspiration will be necessary. Actual evapotranspiration is dependent upon potential evapotranspiration and a crop coefficient. One method of predicting the crop coefficient is to use the plant's vegetative growth which may be determined by reflection from the plant canopy.

The relationship between soil moisture, vegetative growth and solar reflectance was studied. Vegetative growth was evaluated by leaf area index with the equation:

$$LAI = 2.92 MSS4/5 - 2.63 \quad , \quad R^2 = 0.95$$

where:

LAI = Leaf area index

MSS4/5 = Ratio of band 4 (0.5-0.6 μ) to band 5 (0.6-0.7 μ)

R^2 = Regression coefficient.

It appears that the ratio eliminated soil moisture effects. At a depth of 0 to 15 cm soil moisture was predicted by:

$$SM2 = 101.11 - 4.00 MSS4 - 70.31 MSS4/5$$

where:

SM2 = Soil moisture dry weight at 0 to 15 cm (%)

MSS4 = Band 4 (0.5-0.6 μ)

MSS4/5 = Ratio of band 4 (0.5-0.6 μ) to band 5 (0.6-0.7 μ).

The equations of the wheat crop coefficient for the evapotranspiration model of Jensen and associates, developed by using leaf area index of dryland wheat, were:

$$Y = 0.005 + 0.0165X - 0.000467X^2 - 0.00000402X^3$$

$$Y = 0.998 - 0.00297D - 0.000747D^2$$

where:

Y = Wheat crop coefficient

X = Percent of crop cover

D = Days after 100 percent crop cover.

This method of evaluating the crop coefficient provided reasonable estimates of soil moisture depletion.

Appendix E

Computer Program to Generate the Mean and Standard Deviation for the Interior of a Field

```
      $JOB
            DIMENSION LINE(010),NCELL(010),SLOPE(010),THETA(010),ALINE(010)
            DIMENSION B(010),ACELL(010)
            INTEGER*4 DATE,TAPE
            INTEGER*4 SEG,DX
            INTEGER*2 XDATA(5,64,64)
            INTEGER*4 HICELL
            DIMENSION CELL(7)
            DIMENSION IFREQ(128,16)
            DIMENSION AMIN(16),AMAX(16),SUM(16),PROD(16,16),R(16)
            DIMENSION RAVE(16),RSTD(16),RCOR(16,16),AN(4)
            REAL FIELD/' ALL'/
            NREAD=9
            NTERM=13
            D=1.0
            NCN=0
            NWIND=0
            NSEG=0
            MAXC=64
            MAXL=64
             READ 444,D,NSW,NSWI
        444 FORMAT(F5.2,I1,I1)
          5 READ(5,500,END=999) NDATE,NTAPE,NID1,NID2,NCELLB
        500 FORMAT(I4,1X,I5,2A4,2X,I5)
        100 CONTINUE
            IF(NSWI.EQ.1) GO TO 101
            READ(5,1000,END=999)SEG,NPTS,(LINE(I),NCELL(I),I=1,4),NFILE,NC,
           1NTAPEA,FIELD
       1000 FORMAT(I1,I1,4(I4,I3),1X,I1,I1,2X,I4,3X,A3)
            PRINT 1102,SEG,NPTS,(LINE(I),NCELL(I),I=1,4),NFILE,NC,NTAPEA,FIELD
       1102 FORMAT(1H ,'SEG=',I2,'PTS=',I2,4(I5,1X,I4,1X),'FILE=',I2,'NC=',
           1I2,'TAPE=',I5,'FIELD=',A4)
            GO TO 202
        101 CONTINUE
            READ(5,1003,END=999)SEG,NPTS,(LINE(I),NCELL(I),I=1,8),NFILE,NC,
           1NTAPEA,FIELD
       1003 FORMAT(I1,I1,8(I4,I3),2X,I1,I1,1X,I4,1X,A3)
            PRINT 1101,SEG,NPTS,(LINE(I),NCELL(I),I=1,8),NFILE,NC,NTAPEA,FIELD
       1101 FORMAT(1H ,'SEG=',I2,'PTS=',I2,8(I5,1X,I4,1X),'FILE=',I2,'NC=',
           1I2,'TAPE=',I5,'FIELD=',A4)
        202 CONTINUE
            IF(NTAPEA.NE.NDATE) GO TO 991
            IF(NCN.EQ.1) GO TO 10
            NO=0
            DO 220 I=1,NTERM
            DO 190 J=1,128
        190 IFREQ(J,I)=0
            AMIN(I)=128
            AMAX(I)=0.
            SUM(I)=0.
            DO 210 J=1,NTERM
            PROD(I,J)=0.
        210 CONTINUE
        220 CONTINUE
            IF(SEG.EQ.NSEG) GO TO 870
         10 READ(NREAD) DATE,TAPE,ID1,ID2,LINET,NCELLT
            IF(DATE.NE.NDATE) GO TO 990
            IF(TAPE.NE.NTAPE) GO TO 990
            IF(ID1.NE.NID1) GO TO 990
            IF(ID2.NE.NID2) GO TO 990
```

```
      READ(NREAD) XDATA
  370 CONTINUE
      NCN=NC
      NSEG=SEG
      IF(LINE(1).LT.LINET) GO TO 994
      IF(LINE(1).GT.(LINET+64)) GO TO 10
      NCB=NCELLB+64*(SEG-1)+64*NCELL(1)/77
      PRINT,NCELLB,SEG,NCELL(1),NCB
      IF(NCELLT.GT.NCB) GO TO 995
      IF(NCELLT.LT.(NCB-63)) GO TO 10
      DO 800 I=1,NPTS
      LINE(I)=LINE(I)-LINET+1
      CELL(I)=64.*NCELL(I)/77.
  800 CONTINUE
      DO 900 I=1,NPTS
      II=I+1
      IF(I.EQ.NPTS) II=1
      DX=LINE(II)-LINE(I)
      DY1=CELL(II)-CELL(I)
      DX1=FLOAT(DX)
      IF(DX.EQ.0) GO TO 880
      SLOPE(I)=DY1/DX1
      THETA(I)=ATAN2(DY1,DX1)
      GO TO 890
  880 SLOPE(I)=999.
      THETA(I)=ATAN2(DY1,.001)
  890 CONTINUE
      B(I)=CELL(I)-SLOPE(I)*LINE(I)-D/COS(THETA(I))
   900 CONTINUE
      AAMIN=100000.
      AAMAX=0.
      DO 910 I=1,NPTS
      II=I+1
      IF(I.EQ.NPTS) II=1
      DS=SLOPE(I)-SLOPE(II)
      ALINE(I)=(B(II)-B(I))/DS
      ACELL(I)=(B(II)*SLOPE(I)-B(I)*SLOPE(II))/DS
      IF(AAMIN.LT.ALINE(I)) GO TO 909
      MINI=I
      AAMIN=ALINE(I)
  909 IF(AAMAX.LT.ALINE(I)) AAMAX=ALINE(I)
   910 CONTINUE
      LINMIN=IFIX(AAMIN+1.)
      LINMAX=IFIX(AAMAX)
      I=MINI-1
      II=MINI+1
      IF(I.EQ.0) I=NPTS
      IF(II.GT.NPTS) II=1
      IF(LINMIN.LT.1) LINMIN=1
      IF(LINMAX.GT.MAXL) LINMAX=MAXL
      IF(LINMIN.GT.LINMAX) GO TO 2100
      DO 1100 J=LINMIN,LINMAX
      IF(J.GT.IFIX(ALINE(II)))    II=II+1
      IF(J.GT.IFIX(ALINE(I)))    I=I-1
      IF(I.EQ.0) I=NPTS
      IF(II.GT.NPTS) II=1
      III=I+1
      IF(III.GT.NPTS) III=III-NPTS
      LOCELL=IFIX(SLOPE(III)*J+B(III)+1)
      HICELL=IFIX(SLOPE(II)*J+B(II))
```

```
          CCELL=SLOPE(II)*J+B(II)
          BCELL=SLOPE(III)*J+B(III)+1
          IF(LOCELL.LT.1) LOCELL=1
          IF(HICELL.GT.MAXC) HICELL=MAXC
          IF(LOCELL.GT.HICELL) GO TO 1105
          DO 1104 L=LOCELL,HICELL
          XDATA(1,L,J)=1
          NO=NO+1
          DO 240 K=1,4
          KK=K+1
          NA=XDATA(KK,L,J)
          AN(K)=FLOAT(NA)
   240    CONTINUE
          R(1)=AN(1)
          R(2)=AN(2)
          R(3)=AN(3)
          R(4)=AN(4)
          R(5)=AN(3)-AN(1)
          R(6)=2.*AN(4)-AN(1)
          R(7)=AN(3)-AN(2)
          R(8)=2.*AN(4)-AN(2)
          R(9)=AN(1)/AN(2)
          R(10)=AN(1)/AN(3)
          R(11)=AN(1)/AN(4)
          R(12)=AN(2)/AN(3)
          R(13)=AN(2)/AN(4)
          DO 250 K=1,NTERM
          RA=R(K)
          NA=INT(RA)
          IF(RA.LT.AMIN(K)) AMIN(K)=RA
          IF(RA.GT.AMAX(K)) AMAX(K)=RA
          IF(K.LT.9) GO TO 242
          NA=INT(10.*RA)
   242    IF(NA.LE.0) NA=1
          IF(NA.GT.128) NA=128
          IFREQ(NA,K)=IFREQ(NA,K)+1
          SUM(K)=SUM(K)+RA
          DO 250 KA=1,K
          PROD(KA,K)=PROD(KA,K)+R(K)*R(KA)
   250    CONTINUE
   1104   CONTINUE
   1105   CONTINUE
   1100   CONTINUE
   2100   CONTINUE
          IF(NO.LE.1) GO TO 992
          IF(NCN.EQ.1) GO TO 100
          RO=FLOAT(NO)
          DO 320 I=1,NTERM
          RAVE(I)=SUM(I)/RO
          RSTD(I)=SQRT((PROD(I,I)-RO*RAVE(I)*RAVE(I))/(RO-1.))
          DO 321 J=1,I
          RCOR(J,I)=0.
          IF(RSTD(I) .EQ.0.) GO TO 321
          IF(RSTD(J) .EQ.0.) GO TO 321
          RCOR(J,I)=(PROD(J,I)/RO-RAVE(J)*RAVE(I))/(RSTD(I)*RSTD(J))
   321    CONTINUE
   320    CONTINUE
   102    FORMAT(1H1,'NUMBER OF POINTS = ',I5,'IN FIELD ',A4, 'WITH INSET OF
         1 ',F3.1,'UNITS, TAPE =',I4,'-',I5,2A4,' INITIAL LINE = ',I4,' CEL
         2L = ',I4)
```

```
      WRITE(6,102) NO,FIELD,D,DATE,TAPE,ID1,ID2,LINET,NCELLT
      PRINT 103
  103 FORMAT('0',10X,'MSS4',4X,'MSS5',4X,'MSS6',4X,'MSS7',3X,'MSS6-4  2M
     1SS7-4 MSS6-5 2MSS7-5  MSS4/5  MSS4/6  MSS4/7  MSS5/6  MSS5/7')
      PRINT 104,(RAVE(I),I=1,13)
  104 FORMAT('0','MEANS',3X,16F8.3)
      PRINT 105,(AMIN(I),I=1,13)
  105 FORMAT('0','MINIMUMS',16F8.3)
      PRINT 106,(AMAX(I),I=1,13)
  106 FORMAT('0','MAXIMUMS',16F8.3)
      PRINT 107,(RSTD(I),I=1,13)
  107 FORMAT('0','STD DEV ',16F8.3)
      PRINT 116
  116 FORMAT('-','CORRELATION COEFFICIENTS')
      PRINT 111, (RCOR(01,I),I=01,NTERM)
  111 FORMAT('0','MSS4',4X,16F8.5)
      PRINT 112, (RCOR(02,I),I=02,NTERM)
  112 FORMAT('0','MSS5',12X,15F8.5)
      PRINT 113, (RCOR(03,I),I=03,NTERM)
  113 FORMAT('0','MSS6',20X,14F8.5)
      PRINT 114, (RCOR(04,I),I=04,NTERM)
  114 FORMAT('0','MSS7',28X,13F8.5)
      PRINT 115, (RCOR(05,I),I=05,NTERM)
  115 FORMAT('0','MSS6-4',34X,12F8.5)
      PRINT 121, (RCOR(06,I),I=06,NTERM)
  121 FORMAT('0','2MSS7-4',41X,11F8.5)
      PRINT 122, (RCOR(07,I),I=07,NTERM)
  122 FORMAT('0','MSS6-5',50X,10F8.5)
      PRINT 123, (RCOR(08,I),I=08,NTERM)
  123 FORMAT('0','2MSS7-5',57X,09F8.5)
      PRINT 124, (RCOR(09,I),I=09,NTERM)
  124 FORMAT('0','MSS4/5',66X,8F8.5)
      PRINT 125, (RCOR(10,I),I=10,NTERM)
  125 FORMAT('0','MSS4/6',74X,7F8.5)
      PRINT 126, (RCOR(11,I),I=11,NTERM)
  126 FORMAT('0','MSS4/7',82X,6F8.5)
      PRINT 127, (RCOR(12,I),I=12,NTERM)
  127 FORMAT('0','MSS5/6',90X,5F8.5)
      PRINT 128, (RCOR(13,I),I=13,NTERM)
  128 FORMAT('0','MSS5/7',98X,4F8.5)
      IF(NSW.EQ.0) GO TO 399
      WRITE(7,130) FIELD,DATE,(RAVE(I),I=1,13)
      WRITE(7,131) FIELD,DATE,(RSTD(I),I=1,13)
      WRITE(7,132) FIELD,DATE,(AMIN(I),I=1,13)
      WRITE(7,134) FIELD,DATE,(AMAX(I),I=1,13)
  130 FORMAT('1',A3,I4,8F5.2,5F4.2)
  131 FORMAT('2',A3,I4,8F5.2,5F4.2)
  132 FORMAT('3',A3,I4,4F5.2,4F6.2,5F4.2)
  134 FORMAT('4',A3,I4,8F5.2,5F4.2)
  399 CONTINUE
      PRINT 108,FIELD,DATE,TAPE,ID1,ID2,LINET,NCELLT
  108 FORMAT(1H1,'HISTOGRAM',3X,'FIELD =',A4,'TAPE =',I4,'-',I5,2A4,
     1' INITIAL LINE = ',I4,' CELL = ',I4)
      LMIN=MIN1 (AMIN(1),AMIN(2),AMIN(3),AMIN(4),AMIN(5),AMIN(6),
     1AMIN(7),AMIN(8),AMIN(9)*10.,AMIN(10)*10.,AMIN(11)*10.,
     2AMIN(12)*10.,AMIN(13)*10.)
      LMAX=MAX1(AMAX(1),AMAX(2),AMAX(3),AMAX(4),AMAX(5),AMAX(6),
     1AMAX(7),AMAX(8),AMAX(9)*10.,AMAX(10)*10.,AMAX(11)*10.,
     2AMAX(12)*10.,AMAX(13)*10.)
      IF(LMIN.LE.0) LMIN=1
```

```
      IF(LMAX.GT.128) LMAX=128
      DO 400 I=LMIN,LMAX
400   PRINT 109,I,(IERRO(I,J),J=1,NTERM)
109   FORMAT(1H,I5,16(3X,I5))
      WRITE(6,1001)LINMIN,FIELD,DATE,TAPE,ID1,ID2
1001  FORMAT('1','MINIMUM LINE NO = ',I8,3X,'FIELD =',A4,'TAPE =',
     1I4,'-',I5,2A4)
      DO 1110 J=1,MAXL
      WRITE(6,1002)(XDATA(1,I,J),I=1,MAXC)
1002  FORMAT(' ',64I1)
1110  CONTINUE
      NWIND=0
      GO TO 100
991   WRITE(6,120) NTAPEA,NDATE
120   FORMAT('0','FIELD CARD REQUESTS TAPE ',I4,' BUT TAPE USED IS ',I4)
      GO TO 100
990   WRITE(6,503) NDATE,NTAPE,NID1,NID2,DATE,TAPE,ID1,ID2
503   FORMAT('1','TAPE REQUESTED(',I4,'-',I5,2A4,') DIDNOT MATCH TAPE MO
     1UNTED(',I4,'-',I5,2A4,')')
      GO TO 999
992   IF(NCN.EQ.1) GO TO 100
      WRITE(6,119) FIELD
119   FORMAT(1H1,'FIELD ',A4,' TOO SMALL')
      GO TO 100
994   IF(NCELLT.LT.NCELLB) GO TO 10
995   WRITE(6,110) LINE(1),LINET,NCB,NCELLT
110   FORMAT(1H ,'ERROR TAPE TOO FAR:LINE =',I5,'TAPELINE=',I5,'CELL =',
     1I5,'TAPE CELL = ',I5)
      IF(NWIND.EQ.1) GO TO 999
      REWIND NREAD
      NWIND=1
      GO TO 10
999   RETURN
      END
```

```
$JOB
      DIMENSION LINE(010),NCELL(010),SLOPE(010),THETA(010),ALINE(010)
      DIMENSION B(010),ACELL(010)
      INTEGER*4 DATE,TAPE
      INTEGER*4 SEG,DX
      INTEGER*2 XDATA(5,64,64)
      INTEGER*4 HICELL
      DIMENSION CELL(7)
      DIMENSION IFREQ(128,16)
      DIMENSION AMIN(16),AMAX(16),SUM(16),PROD(16,16),R(16)
      DIMENSION RAVE(16),RSTD(16),RCOR(16,16),AN(4)
      REAL FIELD/' ALL'/
      NREAD=9
      NTERM=13
      D=1.0
      NCN=0
      NWIND=0
      NSEG=0
      MAXC=64
      MAXL=64
       READ 444,D,NSW,NSWI
444   FORMAT(F5.2,I1,I1)
  5   READ(5,500,END=999) NDATE,NTAPE,NID1,NID2,NCELLB
500   FORMAT(I4,1X,I5,2A4,2X,I5)
100   CONTINUE
      IF(NSWI.EQ.1) GO TO 101
      READ(5,1000,END=999)SEG,NPTS,(LINE(I),NCELL(I),I=1,4),NFILE,NC,
     1NTAPEA,FIELD
 1000 FORMAT(I1,I1,4(I4,I3),1X,I1,I1,2X,I4,3X,A3)
      PRINT 1102,SEG,NPTS,(LINE(I),NCELL(I),I=1,4),NFILE,NC,NTAPEA,FIELD
1102  FORMAT(1H ,'SEG=',I2,'PTS=',I2,4(I5,1X,I4,1X),'FILE=',I2,'NC=',
     1I2,'TAPE=',I5,'FIELD=',A4)
      GO TO 202
101   CONTINUE
      READ(5,1003,END=999)SEG,NPTS,(LINE(I),NCELL(I),I=1,8),NFILE,NC,
     1NTAPEA,FIELD
 1003 FORMAT(I1,I1,8(I4,I3),2X,I1,I1,1X,I4,1X,A3)
      PRINT 1101,SEG,NPTS,(LINE(I),NCELL(I),I=1,8),NFILE,NC,NTAPEA,FIELD
1101  FORMAT(1H ,'SEG=',I2,'PTS=',I2,8(I5,1X,I4,1X),'FILE=',I2,'NC=',
     1I2,'TAPE=',I5,'FIELD=',A4)
202   CONTINUE
      IF(NTAPEA.NE.NDATE) GO TO 991
      IF(NCN.EQ.1) GO TO 10
      NO=0
      DO 220 I=1,NTERM
      DO 190 J=1,128
190   IFREQ(J,I)=0
      AMIN(I)=128
      AMAX(I)=0.
      SUM(I)=0.
      DO 210 J=1,NTERM
      PROD(I,J)=0.
210   CONTINUE
220   CONTINUE
      IF(SEG.EQ.NSEG) GO TO 970
 10   READ(NREAD) DATE,TAPE,ID1,ID2,LINET,NCELLT
      IF(DATE.NE.NDATE) GO TO 990
      IF(TAPE.NE.NTAPE) GO TO 990
      IF(ID1.NE.NID1) GO TO 990
      IF(ID2.NE.NID2) GO TO 990
```

Appendix F

Computer Program and Flow Chart to Create

Contour Plots on Calcomp Plotter

CONTUR

CREATE CONTOUR PLOT ON CALCOMP PLOTTER

Programmer: Jay Alloway, Kansas State University Computing Center, May 1973.

Language: FORTRAN IV for 360/370 with calls to CALCOMP plot subprogram PLOT.

Purpose: This subroutine prepares a contour plot from a rectangular grid of uniformally spaced values.

Calling sequence:

```
CALL CONTUR (GRID, ROW, COL, CU, NV, XLEN, YLEN)
```

where

GRID contains the values (REAL*4) to be plotted. These could be reflection intensities, levels of radiation, etc at equally spaced points.

ROW is the number of rows to be plotted down the paper and the size of the first dimension of GRID. ROW is integer.

COL is the number of columns to be plotted across the paper and is the second dimension of GRID. COL is integer.

CU is a vector (REAL*4) containing the desired contours.

NV is the number of contours in the CU vector.

XLEN is the length (REAL*4) of the x-axis (down the paper) in inches.

YLEN is the length (REAL*4) of the y-axis (across the paper) in inches.

NOTE: CONTUR assumes the pen is located at location (0.0, 0.0) when called and does not reorigin before returning. Location (0.0, 0.0) is GRID(1,1). Location (XLEN, YLEN) is GRID(ROW,COL).

Method: CONTUR looks at the grid point by point forming a square at each point consisting of the points to the right, below, and right and below the point is question. Except for two cases where two lines may be drawn, only one contour line may appear in a square. CONTUR assumes a uniform media within a square. The line drawing technique outlines flat (equal contour) areas. There is a total of (ROW-1)*(COL-1) squares in GRID.

```
      SUBROUTINE CONTUR (X,N,M,CU,NC,XSIZE,YSIZE)
C
C     SUBROUTINE CONTUR CREATES A CONTOUR PLOT ON THE CALCOMP PLOTTER
C     FROM AN ARRAY OF POINTS.
C
C     WRITTEN BY JAY ALLOWAY, KANSAS STATE UNIVERSITY COMPUTING CENTER
C     IN MAY 1973.
C
      DIMENSION X(N,M), CU(NC)
      LOGICAL*1 ISW
      INTEGER UP, DOWN
      DATA TOL, UP, DOWN /1E-7,3,2/
C
C     CALL CONTUR (GRID, ROW, COL, CU, NV, XLEN, YLEN)
C       WHERE  GRID  CONTAINS THE VALUES TO BE PLOTTED.
C              ROW   IS AN INTEGER GIVING THE NUMBER OF ROWS TO BE
C                    PLOTTED AND THE 1ST DIMENSION OF GRID.
C              COL   IS AN INTEGER GIVING THE NUMBER OF COLUMNS TO BE
C                    PLOTTED AND THE 2ND DIMENSION GO GRID.
C              CU    CONTAINS VALUES OF THE DESIRED CONTOURS.
C              NV    IS THE NUMBER OF CONTOURS IN CU.
C              XLEN  IS THE LENGTH OF THE X-AXIS (ROWS).
C              YLEN  IS THE LENGTH OF THE Y-AXIS (COLUMNS).
C
C
C     DEFINE BASIC FUNCTIONS NEEDED
C
      XLOC(AI) = (AI/AN)*XSIZE
      YLOC(AJ) = (AJ/AM)*YSIZE
      AINC(AS,AE) = (C-AS)/(AE-AS)
      EQUAL(PT) = ABS(C-PT)
      BETWEN(AS,AE) = (C-AS)*(C-AE)
C
C     INITIALIZE CONSTANTS
C
      NX = N-1
      MX = M-1
      AN = NX
      AM = MX
C
C     LOOP THROUGH ROWS
C
      DO 215 IX=1,NX,2
      I = IX
      ISW = .FALSE.
      GO TO 15
   10 I = IX+1
      IF (I.GT.NX) GO TO 215
      ISW = .TRUE.
   15 IP1 = I+1
      AIM1 = I-1
      AI = I
C
C     LOOP THROUGH COLUMNS
C
      DO 210 JX=1,MX
      J = JX
C     FOR FASTER PLOTTING, PLOT EVERY OTHER ROW BACKWARDS
      IF (ISW) J = M-JX
      JP1 = J+1
```

```
      AJM1 = J-1
      AJ = J
C     GET VALUES OF CORNERS OF SQUARE
      A1 = X(I,J)
      A2 = X(I,JP1)
      A3 = X(IP1,J)
      A4 = X(IP1,JP1)
C
C     LOOP THROUGH CONTOURS
C
      DO 205 K=1,NC
      C = CU(K)
C     PLOT BEST CURVE THROUGH THIS SQUARE
      IF (EQUAL(A1).GT.TOL) GO TO 70
      IF (EQUAL(A2).GT.TOL) GO TO 35
      IF (EQUAL(A3).GT.TOL) GO TO 20
      IF (EQUAL(A4).LE.TOL) GO TO 205
      CALL PLOT (XLOC(AI),YLOC(AJM1),UP)
      CALL PLOT (XLOC(AIM1),YLOC(AJ),DOWN)
      GO TO 205
   20 XX = XLOC(AIM1)
      CALL PLOT (XX,YLOC(AJM1),UP)
      YY = YLOC(AJ)
      IF (EQUAL(A4).LE.TOL) GO TO 30
      IF (BETWEN(A3,A4).LE.0.0) GO TO 25
      CALL PLOT (XX,YY,DOWN)
      GO TO 205
   25 CALL PLOT (XLOC(AI),YLOC(AJM1+AINC(A3,A4)),DOWN)
      CALL PLOT (XX,YY,DOWN)
      GO TO 205
   30 CALL PLOT (XLOC(AI),YY,DOWN)
      GO TO 205
   35 XX = XLOC(AIM1)
      YY = YLOC(AJM1)
      IF (EQUAL(A4).GT.TOL) GO TO 45
      IF (EQUAL(A3).GT.TOL) GO TO 40
      CALL PLOT (XX,YY,UP)
      CALL PLOT (XLOC(AI),YLOC(AJ),DOWN)
      GO TO 205
   40 IF (BETWEN(A2,A3).GT.0.0) GO TO 205
      CALL PLOT (XX,YY,UP)
      DIFF = AINC(A2,A3)
      CALL PLOT (XLOC(AIM1+DIFF),YLOC(AJ-DIFF),DOWN)
      CALL PLOT (XLOC(AI),YLOC(AJ),DOWN)
      GO TO 205
   45 IF (EQUAL(A3).LE.TOL) GO TO 60
      IF (BETWEN(A2,A4).GT.0.0) GO TO 50
      IF (BETWEN(A3,A4).GT.0.0) GO TO 55
      CALL PLOT (XLOC(AI),YLOC(AJM1+AINC(A3,A4)),UP)
      CALL PLOT (XLOC(AIM1),YLOC(AJM1),DOWN)
      CALL PLOT (XLOC(AIM1+AINC(A2,A4)),YLOC(AJ),DOWN)
      GO TO 205
   50 IF (BETWEN(A2,A3).GT.0.0) GO TO 205
      IF (BETWEN(A3,A4).GT.0.0) GO TO 205
      CALL PLOT (XX,YY,UP)
      DIFF = AINC(A2,A3)
      CALL PLOT (XLOC(AIM1+DIFF),YLOC(AJ-DIFF),DOWN)
      CALL PLOT (XLOC(AI),YLOC(AJM1+AINC(A3,A4)),DOWN)
      GO TO 205
   55 IF (BETWEN(A2,A3).GT.0.0) GO TO 205
```

```
      CALL PLOT (XX,YY,UP)                                              CNTR1210
      DIFF = AINC(A2,A3)                                                CNTR1220
      CALL PLOT (XLOC(AIM1+DIFF),YLOC(AJ-DIFF),DOWN)                    CNTR1230
      CALL PLOT (XLOC(AIM1+AINC(A2,A4)),YLOC(AJ),DOWN)                  CNTR1240
      GO TO 205                                                         CNTR1250
   60 CALL PLOT (XX,YY,UP)                                              CNTR1260
      IF (BETWEN(A2,A4).LE.0.0) GO TO 65                                CNTR1270
      CALL PLOT (XLOC(AI),YY,DOWN)                                      CNTR1280
      GO TO 205                                                         CNTR1290
   65 CALL PLOT (XLOC(AIM1+AINC(A2,A4)),YLOC(AJ),DOWN)                  CNTR1300
      CALL PLOT (XLOC(AI),YY,DOWN)                                      CNTR1310
      GO TO 205                                                         CNTR1320
   70 IF (EQUAL(A2).GT.TOL) GO TO 105                                   CNTR1330
      IF (EQUAL(A4).GT.TOL) GO TO 85                                    CNTR1340
      IF (EQUAL(A3).GT.TOL) GO TO 75                                    CNTR1350
      CALL PLOT (XLOC(AI),YLOC(AJM1),UP)                                CNTR1360
      CALL PLOT (XLOC(AIM1),YLOC(AJ),DOWN)                              CNTR1370
      GO TO 205                                                         CNTR1380
   75 CALL PLOT (XLOC(AI),YLOC(AJ),UP)                                  CNTR1390
      IF (BETWEN(A1,A3).GT.0.0) GO TO 80                                CNTR1400
      CALL PLOT (XLOC(AIM1+AINC(A1,A3)),YLOC(AJM1),DOWN)                CNTR1410
   80 CALL PLOT (XLOC(AIM1),YLOC(AJ),DOWN)                              CNTR1420
      GO TO 205                                                         CNTR1430
   85 IF (EQUAL(A3).LE.TOL) GO TO 100                                   CNTR1440
      IF (BETWEN(A1,A3).GT.0.0) GO TO 90                                CNTR1450
      IF (BETWEN(A3,A4).GT.0.0) GO TO 95                                CNTR1460
      CALL PLOT (XLOC(AIM1+AINC(A1,A3)),YLOC(AJM1),UP)                  CNTR1470
      CALL PLOT (XLOC(AIM1),YLOC(AJ),DOWN)                              CNTR1480
      CALL PLOT (XLOC(AI),YLOC(AJM1+AINC(A3,A4)),DOWN)                  CNTR1490
      GO TO 205                                                         CNTR1500
   90 IF (BETWEN(A1,A4).GT.0.0) GO TO 205                               CNTR1510
      IF (BETWEN(A3,A4).GT.0.0) GO TO 205                               CNTR1520
      CALL PLOT (XLOC(AIM1),YLOC(AJ),UP)                                CNTR1530
      DIFF = AINC(A1,A4)                                                CNTR1540
      CALL PLOT (XLOC(AIM1+DIFF),YLOC(AJM1+DIFF),DOWN)                  CNTR1550
      CALL PLOT (XLOC(AI),YLOC(AJM1+AINC(A3,A4)),DOWN)                  CNTR1560
      GO TO 205                                                         CNTR1570
   95 IF (BETWEN(A1,A4).GT.0.0) GO TO 205                               CNTR1580
      CALL PLOT (XLOC(AIM1+AINC(A1,A3)),YLOC(AJM1),UP)                  CNTR1590
      DIFF = AINC(A1,A4)                                                CNTR1600
      CALL PLOT (XLOC(AIM1+DIFF),YLOC(AJM1+DIFF),DOWN)                  CNTR1610
      CALL PLOT (XLOC(AIM1),YLOC(AJ),DOWN)                              CNTR1620
      GO TO 205                                                         CNTR1630
  100 IF (BETWEN(A1,A4).GT.0.0) GO TO 205                               CNTR1640
      CALL PLOT (XLOC(AI),YLOC(AJM1),UP)                                CNTR1650
      DIFF = AINC(A1,A4)                                                CNTR1660
      CALL PLOT (XLOC(AIM1+DIFF),YLOC(AJM1+DIFF),DOWN)                  CNTR1670
      CALL PLOT (XLOC(AIM1),YLOC(AJ),DOWN)                              CNTR1680
      GO TO 205                                                         CNTR1690
  105 IF (EQUAL(A3).GT.TOL) GO TO 130                                   CNTR1700
      IF (EQUAL(A4).LE.TOL) GO TO 120                                   CNTR1710
      IF (BETWEN(A1,A2).GT.0.0) GO TO 110                               CNTR1720
      IF (BETWEN(A2,A4).GT.0.0) GO TO 115                               CNTR1730
      CALL PLOT (XLOC(AIM1),YLOC(AJM1+AINC(A1,A2)),UP)                  CNTR1740
      CALL PLOT (XLOC(AI),YLOC(AJM1),DOWN)                              CNTR1750
      CALL PLOT (XLOC(AIM1+AINC(A2,A4)),YLOC(AJ),DOWN)                  CNTR1760
      GO TO 205                                                         CNTR1770
  110 IF (BETWEN(A1,A4).GT.0.0) GO TO 205                               CNTR1780
      IF (BETWEN(A2,A4).GT.0.0) GO TO 205                               CNTR1790
      CALL PLOT (XLOC(AI),YLOC(AJM1),UP)                                CNTR1800
```

```
      DIFF = AINC(A1,A4)
      CALL PLOT (XLOC(AIM1+DIFF),YLOC(AJM1+DIFF),DOWN)
      CALL PLOT (XLOC(AIM1+AINC(A2,A4)),YLOC(AJ),DOWN)
      GO TO 205
  115 IF (BETWEN(A1,A4).GT.0.0) GO TO 205
      CALL PLOT (XLOC(AI),YLOC(AJM1),UP)
      DIFF = AINC(A1,A4)
      CALL PLOT (XLOC(AIM1+DIFF),YLOC(AJM1+DIFF),DOWN)
      CALL PLOT (XLOC(AIM1),YLOC(AJM1+AINC(A1,A2)),DOWN)
      GO TO 205
  120 XX = XLOC(AI)
      CALL PLOT (XX,YLOC(AJM1),UP)
      IF (BETWEN(A1,A2).GT.0.0) GO TO 125
      CALL PLOT (XLOC(AIM1),YLOC(AJM1+AINC(A1,A2)),DOWN)
  125 CALL PLOT (XX,YLOC(AJ),DOWN)
      GO TO 205
  130 IF (EQUAL(A4).GT.TOL) GO TO 145
      IF (BETWEN(A1,A2).GT.0.0) GO TO 135
      IF (BETWEN(A1,A3).GT.0.0) GO TO 140
      CALL PLOT (XLOC(AIM1+AINC(A1,A3)),YLOC(AJM1),UP)
      CALL PLOT (XLOC(AI),YLOC(AJ),DOWN)
      CALL PLOT (XLOC(AIM1),YLOC(AJM1+AINC(A1,A2)),DOWN)
      GO TO 205
  135 IF (BETWEN(A2,A3).GT.0.0) GO TO 205
      IF (BETWEN(A1,A3).GT.0.0) GO TO 205
      CALL PLOT (XLOC(AIM1+AINC(A1,A3)),YLOC(AJM1),UP)
      DIFF = AINC(A2,A3)
      CALL PLOT (XLOC(AIM1+DIFF),YLOC(AJ-DIFF),DOWN)
      CALL PLOT (XLOC(AI),YLOC(AJ),DOWN)
      GO TO 205
  140 IF (BETWEN(A2,A3).GT.0.0) GO TO 205
      CALL PLOT (XLOC(AIM1),YLOC(AJM1+AINC(A1,A2)),UP)
      DIFF = AINC(A2,A3)
      CALL PLOT (XLOC(AIM1+DIFF),YLOC(AJ-DIFF),DOWN)
      CALL PLOT (XLOC(AI),YLOC(AJ),DOWN)
      GO TO 205
  145 IF (BETWEN(A1,A3).LE.0.0) GO TO 170
      IF (BETWEN(A1,A2).LE.0.0) GO TO 150
      IF (BETWEN(A3,A4).GT.0.0) GO TO 205
      CALL PLOT (XLOC(AI),YLOC(AJM1+AINC(A3,A4)),UP)
      DIFF = AINC(A1,A4)
      CALL PLOT (XLOC(AIM1+DIFF),YLOC(AJM1+DIFF),DOWN)
      CALL PLOT (XLOC(AIM1+AINC(A2,A4)),YLOC(AJ),DOWN)
      GO TO 205
  150 IF (BETWEN(A2,A4).GT.0.0) GO TO 155
      CALL PLOT (XLOC(AIM1),YLOC(AJM1+AINC(A1,A2)),UP)
      DIFF = AINC(A2,A3)
      CALL PLOT (XLOC(AIM1+DIFF),YLOC(AJ-DIFF),DOWN)
      CALL PLOT (XLOC(AIM1+AINC(A2,A4)),YLOC(AJ),DOWN)
      GO TO 205
  155 IF ((ABS(A4-A1).GT.ABS(A3-A2))) GO TO 160
      IF (BETWEN(A2,A3).GT.0.0) GO TO 205
      DIFF = AINC(A2,A3)
      XX = XLOC(AIM1+DIFF)
      YY = YLOC(AJ-DIFF)
      GO TO 165
  160 IF (BETWEN(A1,A4).GT.0.0) GO TO 205
      DIFF = AINC(A1,A4)
      XX = XLOC(AIM1+DIFF)
      YY = YLOC(AJM1+DIFF)
```

```
  165 CALL PLOT (XLOC(AI),YLOC(AJM1+AINC(A3,A4)),UP)                    CNTR2410
      CALL PLOT (XX,YY,DOWN)                                            CNTR2420
      CALL PLOT (XLOC(AIM1),YLOC(AJM1+AINC(A1,A2)),DOWN)                CNTR2430
      GO TO 205                                                         CNTR2440
  170 IF (BETWEN(A1,A2).GT.0.0) GO TO 185                               CNTR2450
      IF (BETWEN(A1,A4).GT.0.0) GO TO 175                               CNTR2460
      CALL PLOT (XLOC(AIM1+AINC(A1,A3)),YLOC(AJM1),UP)                  CNTR2470
      DIFF = AINC(A1,A4)                                                CNTR2480
      CALL PLOT (XLOC(AIM1+DIFF),YLOC(AJM1+DIFF),DOWN)                  CNTR2490
      CALL PLOT (XLOC(AIM1),YLOC(AJM1+AINC(A1,A2)),DOWN)                CNTR2500
      GO TO 205                                                         CNTR2510
  175 CALL PLOT (XLOC(AIM1),YLOC(AJM1+AINC(A1,A2)),UP)                  CNTR2520
      IF ((C-A1).GT.TOL) GO TO 180                                      CNTR2530
      CALL PLOT (XLOC(AIM1+AINC(A2,A4)),YLOC(AJ),DOWN)                  CNTR2540
      CALL PLOT (XLOC(AI),YLOC(AJM1+AINC(A3,A4)),UP)                    CNTR2550
      CALL PLOT (XLOC(AIM1+AINC(A1,A3)),YLOC(AJM1),DOWN)                CNTR2560
      GO TO 205                                                         CNTR2570
  180 CALL PLOT (XLOC(AIM1+AINC(A1,A3)),YLOC(AJM1),DOWN)                CNTR2580
      CALL PLOT (XLOC(AI),YLOC(AJM1+AINC(A3,A4)),UP)                    CNTR2590
      CALL PLOT (XLOC(AIM1+AINC(A2,A4)),YLOC(AJ),DOWN)                  CNTR2600
      GO TO 205                                                         CNTR2610
  185 IF (BETWEN(A3,A4).GT.0.0) GO TO 190                               CNTR2620
      CALL PLOT (XLOC(AIM1+AINC(A1,A3)),YLOC(AJM1),UP)                  CNTR2630
      DIFF = AINC(A2,A3)                                                CNTR2640
      CALL PLOT (XLOC(AIM1+DIFF),YLOC(AJ-DIFF),DOWN)                    CNTR2650
      CALL PLOT (XLOC(AI),YLOC(AJM1+AINC(A3,A4)),DOWN)                  CNTR2660
      GO TO 205                                                         CNTR2670
  190 IF (BETWEN(A2,A4).GT.0.0) GO TO 205                               CNTR2680
      IF ((ABS(A4-A1).GT.ABS(A3-A2))) GO TO 195                         CNTR2690
      IF (BETWEN(A2,A3).GT.0.0) GO TO 205                               CNTR2700
      DIFF = AINC(A2,A3)                                                CNTR2710
      XX = XLOC(AIM1+DIFF)                                              CNTR2720
      YY = YLOC(AJ-DIFF)                                                CNTR2730
      GO TO 200                                                         CNTR2740
  195 IF (BETWEN(A1,A4).GT.0.0) GO TO 205                               CNTR2750
      DIFF = AINC(A1,A4)                                                CNTR2760
      XX = XLOC(AIM1+DIFF)                                              CNTR2770
      YY = YLOC(AJM1+DIFF)                                              CNTR2780
  200 CALL PLOT (XLOC(AIM1+AINC(A1,A3)),YLOC(AJM1),UP)                  CNTR2790
      CALL PLOT (XX,YY,DOWN)                                            CNTR2800
      CALL PLOT (XLOC(AIM1+AINC(A2,A4)),YLOC(AJ),DOWN)                  CNTR2810
C                                                                       CNTR2820
C     END OF LOOPS                                                      CNTR2830
C                                                                       CNTR2840
  205 CONTINUE                                                          CNTR2850
  210 CONTINUE                                                          CNTR2860
      IF (.NOT.ISW) GO TO 10                                            CNTR2870
  215 CONTINUE                                                          CNTR2880
      RETURN                                                            CNTR2890
      END                                                               CNTR2900
```

JAY ALLOWAY

F-8

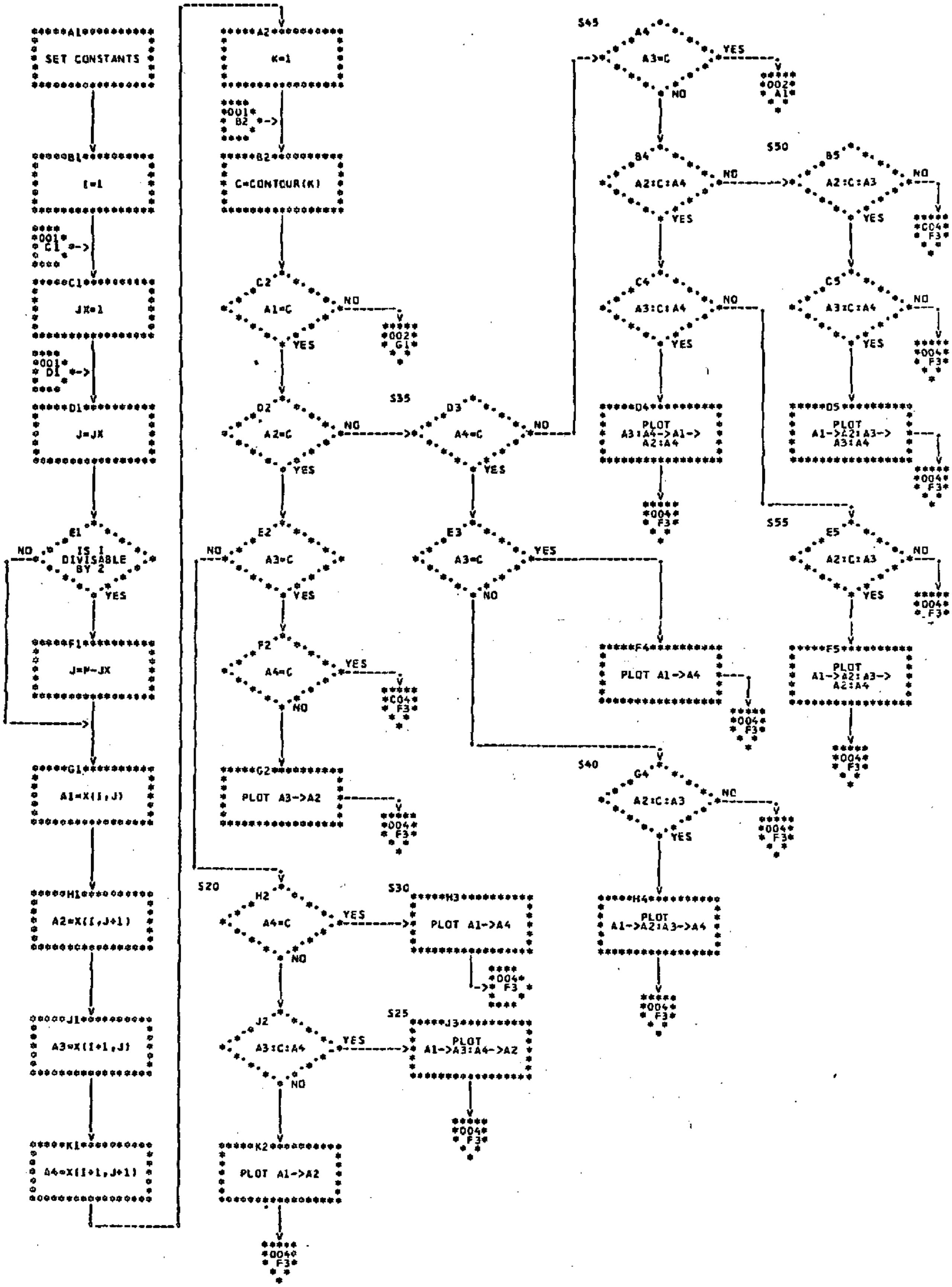

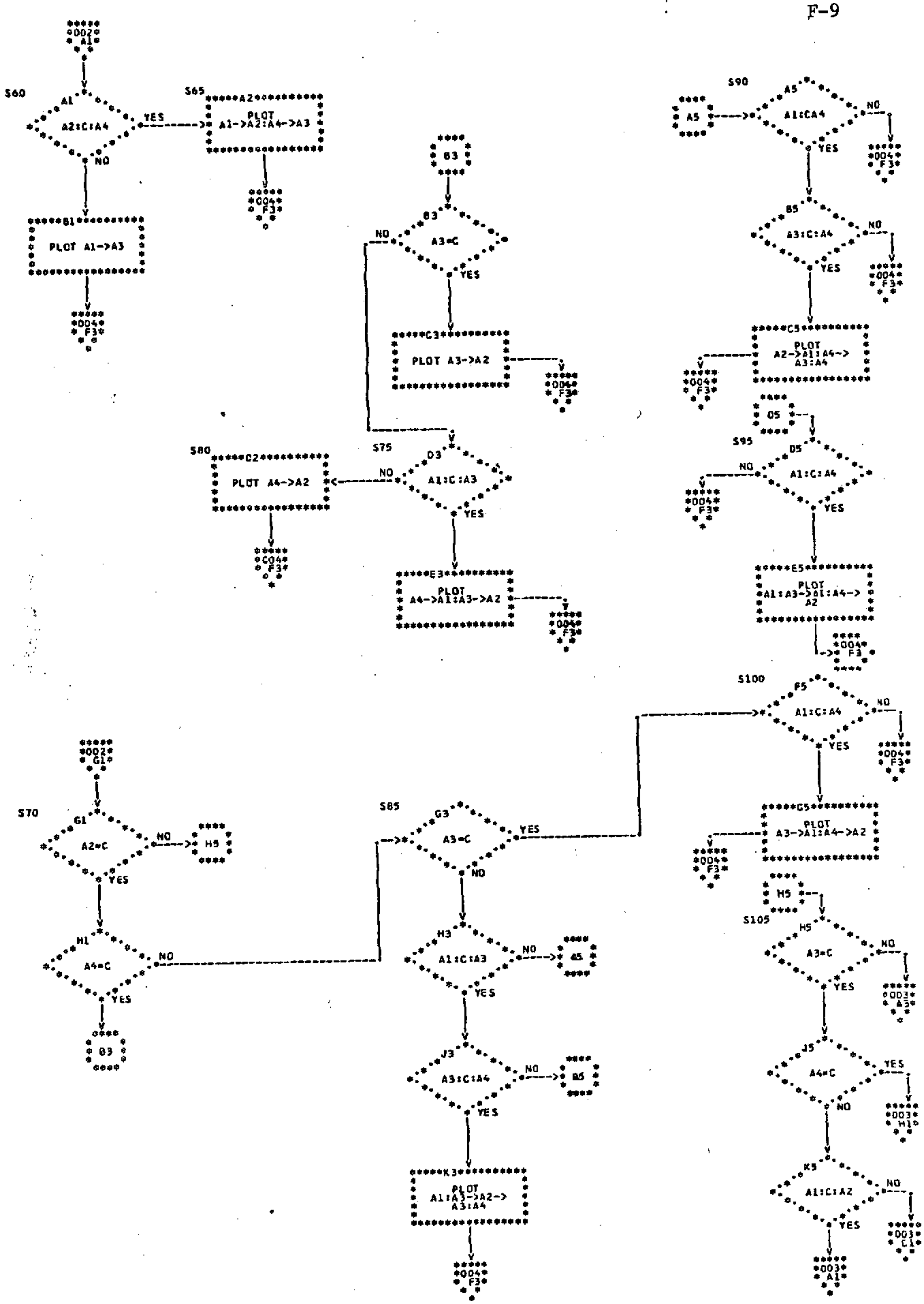
S60
A1
A2:C:A4
YES
NO
S65
A2
PLOT A1->A2:A4->A3
B1
PLOT A1->A3
B3
A3=C
C3
PLOT A3->A2
S80
D2
PLOT A4->A2
S75
D3
A1:C:A3
E3
PLOT A4->A1:A3->A2
S90
A5
A1:CA4
B5
A3:C:A4
C5
PLOT A2->A1:A4->A3:A4
S95
D5
A1:C:A4
E5
PLOT A1:A3->A1:A4->A2
S100
F5
A1:C:A4
G5
PLOT A3->A1:A4->A2
S70
G1
A2=C
H5
H1
A4=C
S85
G3
A3=C
H3
A1:C:A3
J3
A3:C:A4
K3
PLOT A1:A3->A2->A3:A4
S105
H5
A3=C
J5
A4=C
K5
A1:C:A2

JAY ALLOWAY

E-10

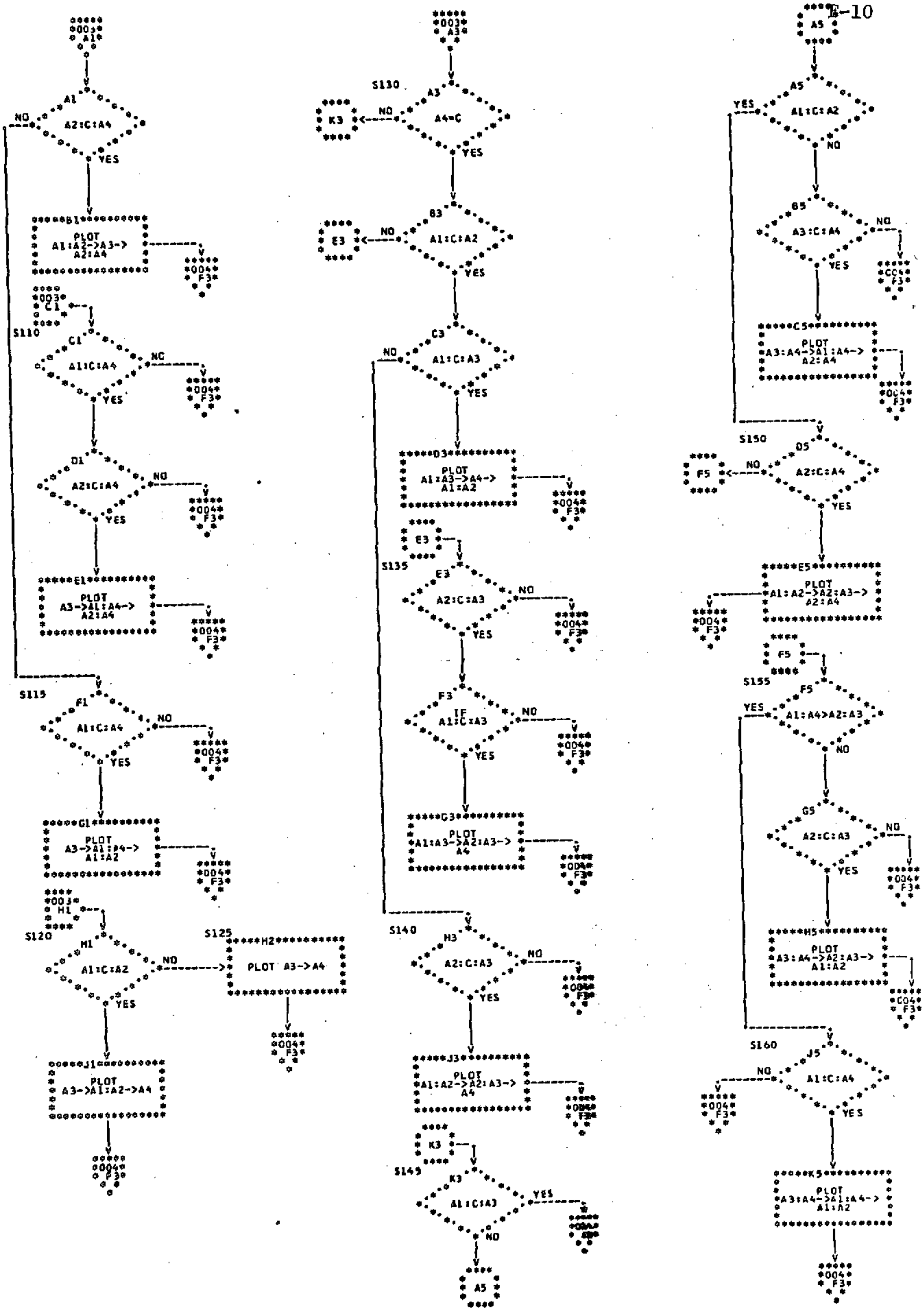

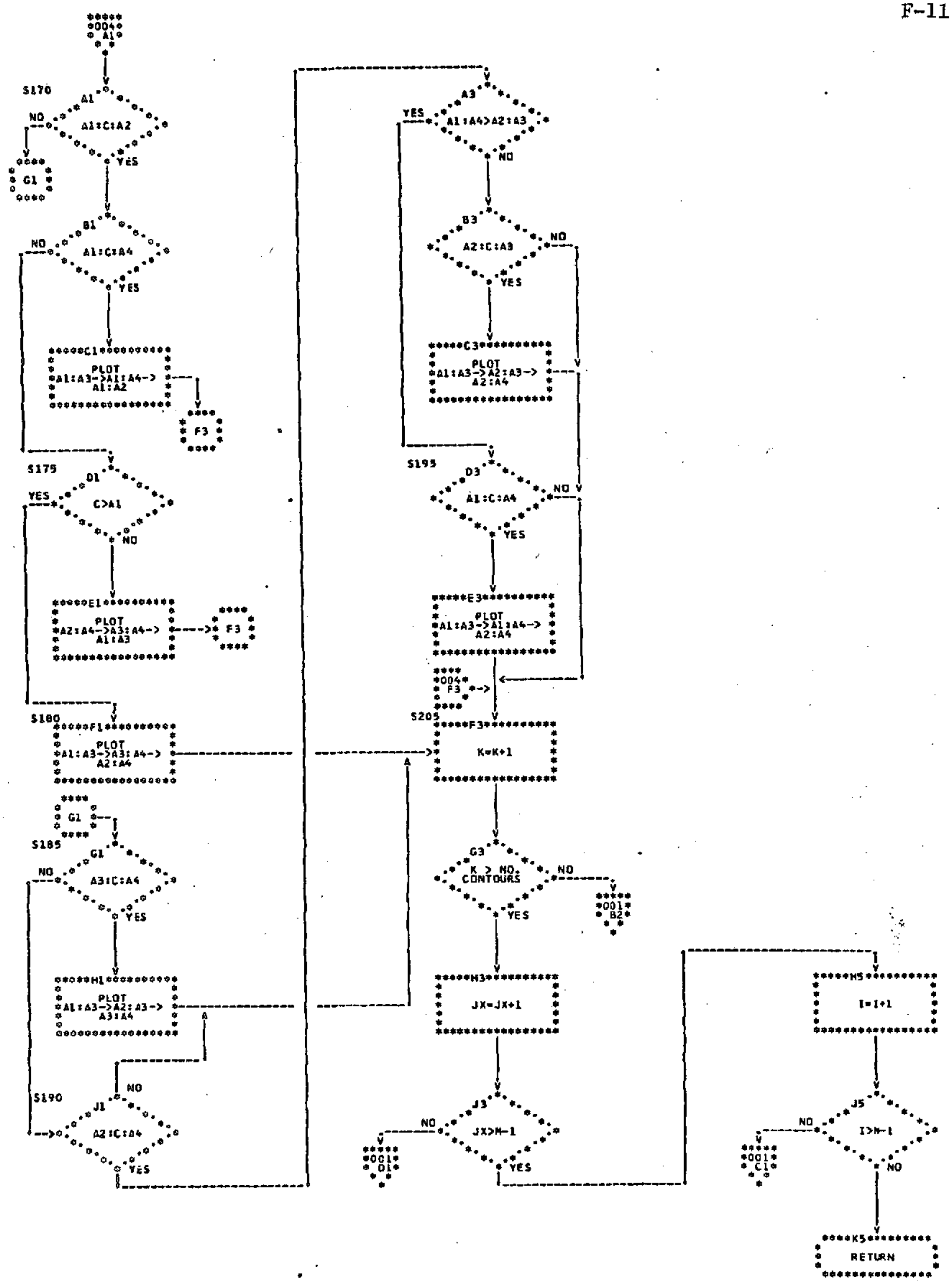
004 A1
S170
A1
A1:C:A2
NO
YES
G1
B1
A1:C:A4
C1
PLOT
A1:A3->A1:A4->
A1:A2
F3
S175
D1
C>A1
E1
PLOT
A2:A4->A3:A4->
A1:A3
S180
F1
PLOT
A1:A3->A3:A4->
A2:A4
S185
G1
A3:C:A4
H1
PLOT
A1:A3->A2:A3->
A3:A4
S190
J1
A2:C:A4
A3
A1:A4>A2:A3
B3
A2:C:A3
C3
PLOT
A1:A3->A2:A3->
A2:A4
S195
D3
A1:C:A4
E3
PLOT
A1:A3->A1:A4->
A2:A4
004 F3
S205
F3
K=K+1
G3
K > NO. CONTOURS
001 B2
H3
JX=JX+1
J3
JX>M-1
001 D1
H5
I=I+1
J5
I>N-1
001 C1
K5
RETURN

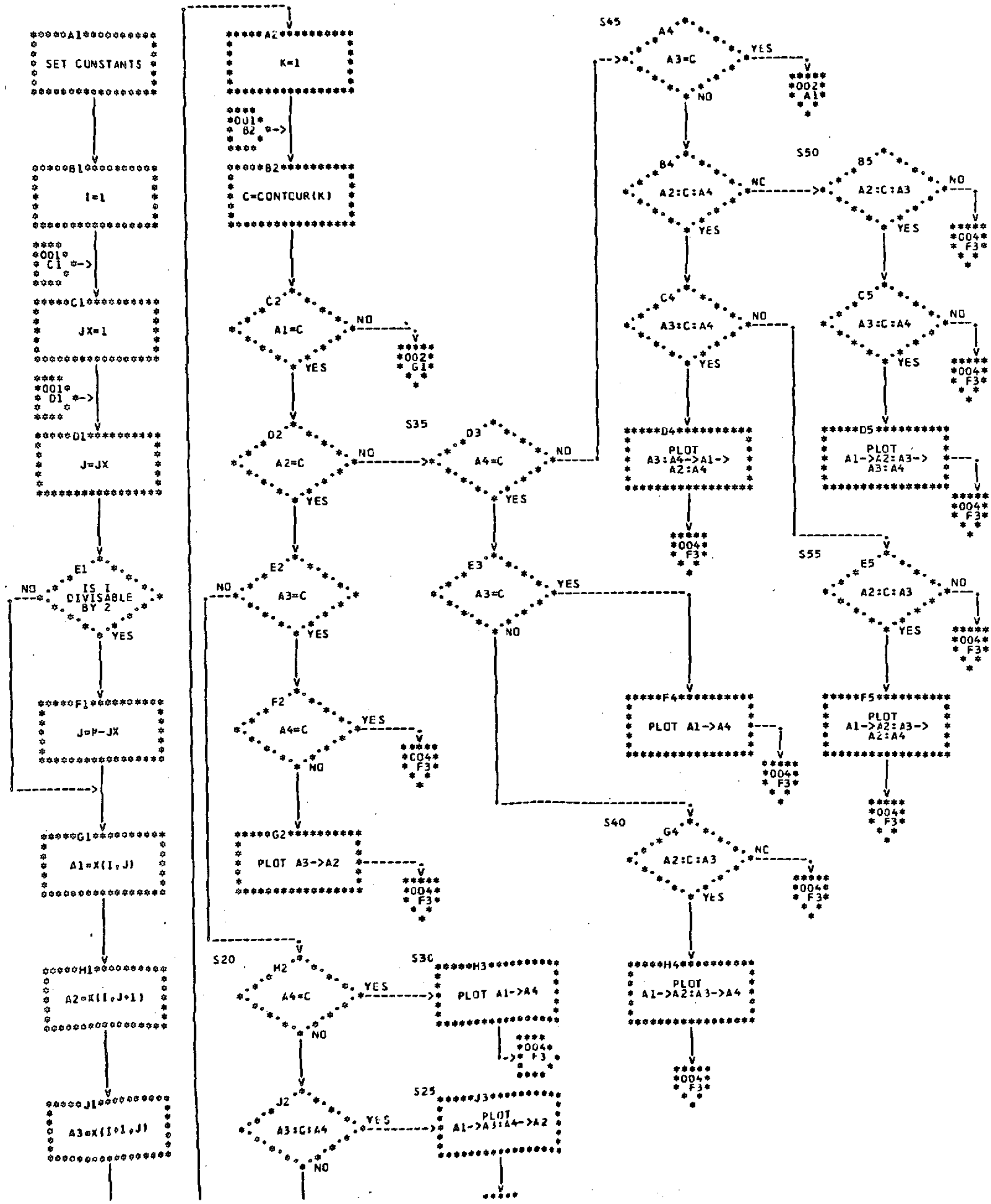
A1
SET CONSTANTS
B1
I=1
001 C1
C1
JX=1
001 D1
D1
J=JX
E1
IS I DIVISABLE BY 2
NO
YES
F1
J=M-JX
G1
A1=X(I,J)
H1
A2=X(I,J+1)
J1
A3=X(I+1,J)
A2
K=1
001 B2
B2
C=CONTCUR(K)
C2
A1=C
NO
002 G1
YES
D2
A2=C
NO
YES
E2
A3=C
NO
YES
F2
A4=C
YES
004 F3
NO
G2
PLOT A3->A2
004 F3
S20
H2
A4=C
YES
NO
S30
H3
PLOT A1->A4
004 F3
J2
A3:C:A4
YES
NO
S25
J3
PLOT A1->A3:A4->A2
S35
D3
A4=C
NO
YES
E3
A3=C
YES
NO
S45
A4
A3=C
YES
002 A1
NO
B4
A2:C:A4
NC
YES
C4
A3:C:A4
NO
YES
D4
PLOT A3:A4->A1-> A2:A4
004 F3
F4
PLOT A1->A4
004 F3
S40
G4
A2:C:A3
NC
004 F3
YES
H4
PLOT A1->A2:A3->A4
004 F3
S50
B5
A2:C:A3
NO
004 F3
YES
C5
A3:C:A4
NO
004 F3
YES
D5
PLOT A1->A2:A3-> A3:A4
004 F3
S55
E5
A2:C:A3
NO
004 F3
YES
F5
PLOT A1->A2:A3-> A2:A4
004 F3

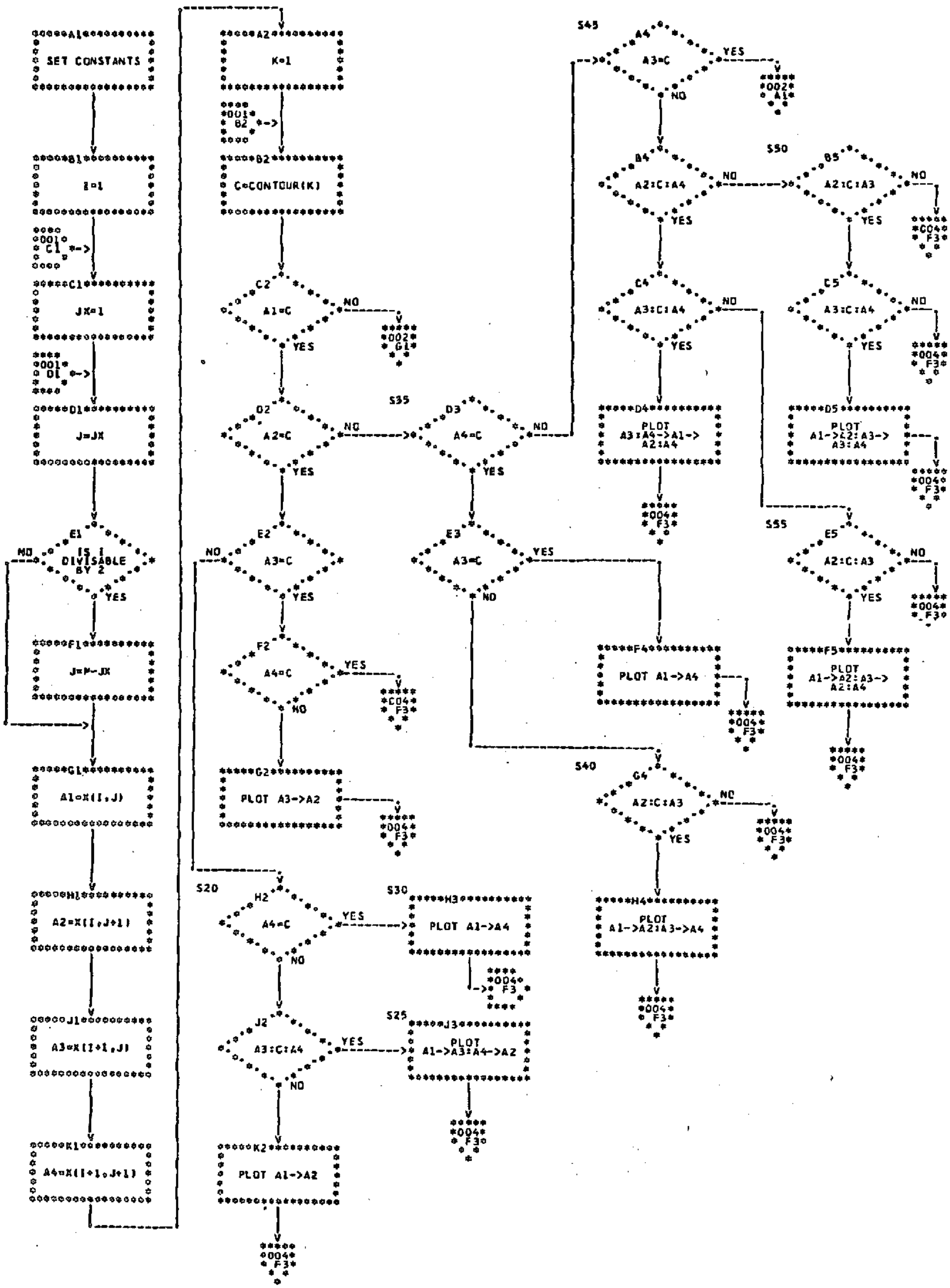
A1 SET CONSTANTS
B1 I=1
C1 JX=1
D1 J=JX
E1 IS I DIVISIBLE BY 2
F1 J=M-JX
G1 A1=X(I,J)
H1 A2=X(I,J+1)
J1 A3=X(I+1,J)
K1 A4=X(I+1,J+1)
A2 K=1
B2 C=CONTOUR(K)
C2 A1=C
D2 A2=C
E2 A3=C
F2 A4=C
G2 PLOT A3->A2
S20 H2 A4=C
J2 A3:C:A4
K2 PLOT A1->A2
S35 D3 A4=C
E3 A3=C
S30 H3 PLOT A1->A4
S25 J3 PLOT A1->A3:A4->A2
S45 A4 A3=C
B4 A2:C:A4
C4 A3:C:A4
D4 PLOT A3:A4->A1->A2:A4
F4 PLOT A1->A4
S40 G4 A2:C:A3
H4 PLOT A1->A2:A3->A4
S50 B5 A2:C:A3
C5 A3:C:A4
D5 PLOT A1->A2:A3->A3:A4
S55 E5 A2:C:A3
F5 PLOT A1->A2:A3->A2:A4
YES
NO

Appendix G

Algorithm to Enhance Variations Within a Category

ENHANCING CATEGORY VARIATIONS[1]

Let u_i, S_i be the mean and covariance of category i, $i = 1, \ldots, k$. Define $B_{ik} = (u_i - u_k)(u_i - u_k)'$. We would like to bring to zero all points from categories other than c_k, enhance all the variation in category c_k, and show this variation about a point away from zero.

The Algorithm

Compute t_i, $i = 1, 2, \ldots, k$, $i \neq k$ where t_i is the eigenvector of $S_i^{-1}(S_k + B_{ik})$ with largest eigenvalue.

Normalize t_i so that

$$t_i'(u_k - u_i) = 1 \quad i = 1, \ldots, k, \; i \neq k.$$

This normalization makes it so that

$$\text{if } x \in c_k, \; E\left[t_i'[x - u_i]\right] = t_i'(u_k - u_i) = 1$$

and

$$\text{if } x \notin c_k, \; x \in c_j \text{ for some j, and } E[t_j'(x - u_j)] = 0$$

For any x compute $t_i'(x - u_i)$. Define $f(x) = \min_{\substack{i \\ i=1,\ldots,k \\ i \neq k}} t_i'(x - u_i)$.

The following theorem and proof show how t_i is determined. In this theorem the covariance S_k of category c_k is used rather than the combined

[1] Private Communication from R.M. Haralick, Remote Sensing Laboratory, University of Kansas, Center for Research, Inc.

covariance S_k, within category c_k, and B_{ik}, between categories c_i and c_k. Hence the theorem obtains t_i from $S_i^{-1} S_k$ rather than from $S_i^{-1}(S_k + B_{ik})$. Inclusion of the between-category variance term B_{ik} makes use of the separation of the category sample means.

Theorem: Let $f: R^N \rightarrow R$ be defined by $f(t) = \frac{V[t'x \mid c_2]}{V[t'x \mid c_1]}$. Then f has a global maximum of e where t is the eigenvector of $S_1^{-1} S_2$ having largest eigenvalue e. (S_i is the covariance matrix for category c_i, $i = 1, 2$).

Proof: To maximize $\frac{V[t'x \mid c_2]}{V[t'x \mid c_1]}$, we will maximize $V[t'x \mid c_2]$ under the constraint $V[t'x \mid c_1] = k$.

Consider $g(t) = V[t'x \mid c_2] - e\,(V[t'x \mid c_1] - k)$.

$$= E\left[\,\|t'x - E[t'x \mid c_2]\|^2 \;\middle|\; c_2\right] - e\left(E\left[\,\|t'x - E[t'x \mid c_1]\|^2 \;\middle|\; c_1\right] - k\right)$$

Expanding the norm and letting $u_2 = E[x \mid c_2]$ and $u_1 = E[x \mid c_1]$, we obtain

$$g(t) = E\left[(x - u_2)'t\ t'(x - u_2) \mid c_2\right] - e\left(E\left[(x - u_1)'t\ t'(x - u_1) \mid c_1\right] - k\right)$$

$$= E\left[\text{trace}\ \ (t t'\,(x - u_2)\,(x - u_2)' \mid c_2\right]$$

$$- e\left(E\left[\ \text{trace}\ (t t'\,(x - u_1)\,(x - u_1)' \mid c_1\right] - k\right)$$

Since trace is a linear operator, we may interchange the expectation with the trace.

$$g(t) = \text{trace}\left(E\,[t t' (x - u_2)(x - u_2)' \mid c_2]\right) - c\left(\text{trace}\, E\,[t t' (x - u_1)(x - u_1)' \mid c_1] - k\right)$$

$$= \text{trace}\,(t t'\, E\,[x - u_2)(x - u_2)' \mid c_2]) - c\left(\text{trace}\, t t'\, E\,[(x - u_1)(x - u_1)' \mid c_1] - k\right)$$

$$= \text{trace}\,(t t' S_2) - c\,(\text{trace}\, t t' S_1 - k)$$

$$= t' S_2 t - c\,(t' S_1 t - k)$$

Let $t = \begin{pmatrix} t_1 \\ t_2 \\ \vdots \\ t_N \end{pmatrix}$, $S_2 = \left(s_{ji}^{(2)}\right)$, and $S_1 = \left(s_{ji}^{(1)}\right)$

$$g(t_1, \ldots, t_N) = \sum_{i=1}^{N} t_i \sum_{j=1}^{N} t_j \left(s_{ji}^{(2)} - c\, s_{ji}^{(1)}\right) + c\,k$$

A necessary condition for g to be maximized is for $\frac{\partial g}{\partial t_n} = 0$, $n = 1, \ldots, N$.

Expanding the summation for g so that we can take partial derivatives easily,

$$g\,(t_1, \ldots, t_N) = \sum_{\substack{i=1 \\ i \neq n}}^{N} t_i \sum_{\substack{j=1 \\ j \neq n}}^{N} t_j \,(s_{ji}^{(2)} - c\, s_{ji}^{(1)})$$

$$+ t_n \sum_{\substack{j=1 \\ j \neq n}}^{N} t_j \,(s_{jn}^{(2)} - c\, s_{jn}^{(1)})$$

$$+ \sum_{\substack{i=1 \\ i \neq n}}^{N} t_i\, t_n\, (s_{ni}^{(2)} - c\, s_{ni}^{(1)}) + c\,k$$

$$+ t_n t_n (s^{(2)}_{nn} - e\, s^{(1)}_{nn})$$

Hence,

$$\frac{\partial g}{\partial t_N} = \sum_{\substack{j=1 \\ j\neq n}}^{N} t_j (s^{(2)}_{jn} - e\, s^{(1)}_{jn}) + \sum_{\substack{i=1 \\ i\neq n}}^{N} t_i (s^{(2)}_{ni} - e\, s^{(1)}_{ni})$$

$$+ 2t_n (s^{(2)}_{nn} - e\, s^{(1)}_{nn})$$

$$= 2 \left\{ \sum_{i=1}^{N} (s^{(2)}_{ni} - e\, s^{(1)}_{ni})\, t_i \right\}, \text{ by symmetry of } S_1 \text{ and } S_2.$$

Setting $\frac{\partial g}{\partial t_N} = 0$, we have

$$\sum_{i=1}^{N} (s^{(2)}_{ni} - e\, s^{(1)}_{ni})\, t_i = 0, \; n = 1, 2, \ldots, N;$$

or in matrix form

$$(S_2 - e S_1)\, t = 0.$$

Hence, $S_2 t = e S_1 t$ or $S_1^{-1} S_2 t = e t$ so that it is necessary for t to be an eigen-

vector of $S_1^{-1} S_2$ having corresponding eigenvalue e.

To see which eigenvector, we will evaluate f(t) for those cases when t is an

eigenvector of $S_1^{-1} S_2$.

$$f(t) = \frac{t'S_2t}{t'S_1t} \text{ and } S_1^{-1}S_2t = e\,t.$$

$$f(t) = \frac{t'S_2t}{t'S_1\frac{S_1^{-1}S_2t}{e}} = \frac{t'S_2t}{t'S_1S_1^{-1}S_2t} = e\,\frac{t'S_2t}{t'S_2t} = e$$

Therefore it should be that eigenvector of $S_1^{-1}S_2$ with largest eigenvalue e.

Appendix H

Computer Programs to Implement the Algorithm of Appendix G

```
C
C     THIS PROGRAM IS AN IMPLENTATION OF AN ALGORITHM TO ENCHANCE CATEGORY
C     VARIATIONS.  PERIODIC REFERENCES ARE MADE TO A PAPER ENTITLED ENCHANCING
C     CATEGORY VARIATION FROM WHICH THE ALGORITHM COMES FROM AND WILL BE REFERED
C     TO AS THE ECV PAPER.
C
      REAL  IAA,IAB,IAC,IAD,IAAS,IABS,IACS,IADS
      REAL  IABM,IBCM,ICDM,IACM,IBDM,IADM
      INTEGER*2  CATEG,CLEN,COL,ROW,MCOLL,MROWL,CAT,HOWRED
      INTEGER*2  X(5,128,128),FLAG(100)
      DIMENSION B(10),WORKV1(4),WORKV2(4)
      DIMENSION  BUIK(4,4)
      DIMENSION  FMT(15)
      DIMENSION  S(5,4,4)
      DIMENSION  SI(4,4)
      DIMENSION  SK(4,4)
      DIMENSION  SKA(4,4)
      DIMENSION  TI(4,4)
      DIMENSION  U(4,2)
      DIMENSION  UA(4)
      DIMENSION  UCATEG(4)
      DIMENSION  U1(4),U2(4)
C
C     THE FIRST DATA CARD CONTAINS THE NUMBER OF THE CATEGORY OF INTEREST,
C     THE NUMBER OF CATEGORIES, THE NUMBER OF COLUMNS AND ROWS IN THE INPUT
C     MATRIX, AND A NUMBER FOR THE READ TYPE FOR THE INPUT MATRIX.
      READ (5,200) CATEG,CLEN,MCOLL,MROWL,NREAD,HOWRED
      WRITE (6,211) CATEG,CLEN,MCOLL,MROWL,NREAD,HOWRED
C
C     READ THE FORMAT FOR READING IN THE INPUT MATRIX X.
      READ (5,210) FMT
C
C     INITIALIZE THE INPUT MATRIX X.
      DO  121  K=1,128
      DO 120  J=1,128
      X(1,J,K)=1
      DO 120 I=2,5
      X(I,J,K)=0
  120 CONTINUE
  121 CONTINUE
C
C     READ IN THE MATRIX DATA IN THE FORM X(CAT,ROW,COL).
      IF (HOWRED.NE.1) GO TO 450
      READ (NREAD) X
      GO TO 451
  450 READ (NREAD,FMT) (((X(I,J,K),I=1,5),J=1,MROWL),K=1,MCOLL)
C
C     GO THROUGH THE INPUT DATA FOR EACH CATEGORY.
  451 DO 100 CAT=1,CLEN
      NUMBER=0
      IAA=0
      IAB=0
      IAC=0
      IAD=0
      IAAS=0
      IABS=0
      IACS=0
      IADS=0
      IABM=0
      IBCM=0
```

```
      ICDM=0
      IACM=0
      IBDM=0
      IADM=0
C   GO THROUGH THE INPUT MATRIX TO GET EACH DATA POINT IN THE CATEGORY.
      DO 101 COL=1,MCOLL
      DO 102 ROW=1,MROWL
      IF (X(1,ROW,COL).NE.CAT)  GO TO 102
      NUMBER=NUMBER+1
      I1=X(2,ROW,COL)
      I2=X(3,ROW,COL)
      I3=X(4,ROW,COL)
      I4=X(5,ROW,COL)
      IAA=IAA+I1
      IAB=IAB+I2
      IAC=IAC+I3
      IAD=IAD+I4
      IAAS=IAAS+I1*I1
      IABS=IABS+I2*I2
      IACS=IACS+I3*I3
      IADS=IADS+I4*I4
      IABM=IABM+I1*I2
      IBCM=IBCM+I2*I3
      ICDM=ICDM+I3*I4
      IACM=IACM+I1*I3
      IBDM=IBDM+I2*I4
      IADM=IADM+I1*I4
  102 CONTINUE
  101 CONTINUE
      FLAG(CAT)=0
C   THIS TEST IS TO PREVENT DIVISION BY ZERO.
      IF(NUMBER.NE.0)  GO TO 400
      FLAG(CAT)=1
      GO TO 100
C   FORM THE MEAN FOR EACH BAND.
  400 AN=IAA/NUMBER
      BN=IAB/NUMBER
      CN=IAC/NUMBER
      DN=IAD/NUMBER
      WRITE (6,202) AN,BN,CN,DN,CAT,NUMBER
C   FORM THE MEAN MATRIX
      U(1,CAT)=AN
      U(2,CAT)=BN
      U(3,CAT)=CN
      U(4,CAT)=DN
C   FORM THE COVARIANCE MATRIX
      S(CAT,1,1)=IAAS/NUMBER-AN*AN
      S(CAT,1,2)=IABM/NUMBER-AN*BN
      S(CAT,1,3)=IACM/NUMBER-AN*CN
      S(CAT,1,4)=IADM/NUMBER-AN*DN
      S(CAT,2,1)=S(CAT,1,2)
      S(CAT,3,1)=S(CAT,1,3)
      S(CAT,4,1)=S(CAT,1,4)
      S(CAT,2,2)=IABS/NUMBER-BN*BN
      S(CAT,2,3)=IBCM/NUMBER-BN*CN
      S(CAT,2,4)=IBDM/NUMBER-BN*DN
      S(CAT,3,2)=S(CAT,2,3)
      S(CAT,4,2)=S(CAT,2,4)
      S(CAT,3,3)=IACS/NUMBER-CN*CN
      S(CAT,3,4)=ICDM/NUMBER-CN*DN
```

```
      S(CAT,4,3)=S(CAT,3,4)
      S(CAT,4,4)=IADS/NUMBER-DN*DN
  100 CONTINUE
      DO 105 J=1,4
      UCATEG(J)=U(J,CATEG)
      DO 106 K=1,4
      SK(J,K)=S(CATEG,J,K)
  106 CONTINUE
  105 CONTINUE
      WRITE (6,203) CATEG
      WRITE (6,204) (UCATEG(I),(SK(I,J),J=1,4),I=1,4)
      DO 103 CAT=1,CLEN
      IF (CAT.EQ.CATEG)  GO TO 103
      IF(FLAG(CAT).EQ.1)  GO TO 103
      DO 104 J=1,4
      U1(J)=U(J,CAT)
      U2(J)=U1(J)
      DO 107 K=1,4
      SI(J,K)=S(CAT,J,K)
  107 CONTINUE
  104 CONTINUE
      WRITE (6,205) CAT
      WRITE (6,206) (U1(I),(SI(I,J),J=1,4),I=1,4)
C
C    SUBTRACT THE MEAN MATRIX.
      CALL GMSUB(U1,UCATEG,UA,4,1)
C
C    U1 NOW BECOMES THE TRANSPOSE OF UA.
      CALL GMTRA (UA,U1,4,1)
C
C    FORM THE PRODUCT WHICH IS B(IK) IN THE ECV PAPER.
      CALL GMPRD (UA,U1,BUIK,4,1,4)
C
C    ADD THE SK MATRIX AND B MATRIX WHICH WAS JUST FORMED.
      CALL GMADD (SK,BUIK,SKA,4,4)
C
C    FORM THE INVERSE OF THE SI MATRIX.
      CALL MINV (SI,4,DET,WORKV1,WORKV2)
C
C    FORM THE PRODUCT S(I)INV*(S(K)+B(I,K)).
      CALL GMPRD (SI,SKA,TI,4,4,4)
C
C    FORM THE EIGENVALUES AND EIGENVECTORS.
      K=0
      DO 113 J=1,4
      DO 113 I=1,J
      K=K+1
  113 B(K)=TI(I,J)
C
      CALL EIGEN (B,TI,4,0)
C    FORM A SCALAR TO NORMALIZE THE EIGENVECTOR.
      SCALA1=-TI(1,1)*UA(1)-TI(2,1)*UA(2)-TI(3,1)*UA(3)-TI(4,1)*UA(4)
      WRITE (6,223) SCALA1,B(1)
      IF (SCALA1.NE.0) GO TO 401
      WRITE (6,212) CAT,(TI(I,1),I=1,4)
      GO TO 103
  401 DO 114 I=1,4
C    FORM THE NORMALIZED EIGENVECTOR.
  114 TI(I,1)=TI(I,1)/SCALA1
      WRITE (6,201) CAT,(TI(I,1),I=1,4)
```

```
      WRITE (7,215) (U2(J),J=1,4),CAT
      WRITE (7,215) (TI(I,1),I=1,4),CAT
  103 CONTINUE
C     CAT IS USED TO IDENTIFY THE CATEGORY IN DIFFERENT LOOPS THROUGH THE
C     PROGRAM AND ALSO AS A SUBSCRIPT FOR ARRAYS.
C     CATEG IS THE CATEGORY TO BE ENHANCED.
C     CLEN IS THE NUMBER OF CATERGORIES.
C     COL & ROW ARE USED AS SUBSCRIPT VARIABLES IN A LOOP TO GET THE DATA
C     FROM THE INPUT MATRIX WITH MCOLL AND MROWL BEING THE LIMITS OF COL AND
C     ROW IN THE LOOP.
C     HOWRED IS CODE FOR READING INPUT DATA; IF 1, READ FROM DISK UNFORMATED.
C     IAA IS THE SUMMATION OF THE VALUES IN BAND 1.
C     IAB IS THE SUMMATION OF THE VALUES IN BAND 2.
C     IAC IS THE SUMMATION OF THE VALUES IN BAND 3.
C     IAD IS THE SUMMATION OF THE VALUES IN BAND 4.
C     IAAS-IADS ARE THE SUMMATIONS OF THE SQUARES OF THE INPUT NUMBERS.
C     IABM-IADM ARE THE SUMMATIONS OF THE CROSS PRODUCTS OF THE INPUT NUMBERS.
C     I1-I4 ARE THE INPUT VALUES IN EACH LIGHT BAND.
C     NCOLL IS THE NUMBER OF COLUMNS IN THE DATA MATRIX.
C     NREAD IS USED TO SPECIFY INPUT TYPE.
C     NROWL IS THE NUMBER OF ROWS IN THE DATA MATRIX.
C     NUMBER IS THE NUMBER OF VALUES IN A CATEGORY.
C
  200 FORMAT   (I3,3X,I3,3X,I3,3X,I3,3X,I3,3X,I3)
  201 FORMAT ('0',3X,'CATEGORY IS ',I2,6X,'TI=',E14.7,3X,E14.7,3X,E14.7,
     13X,E14.7)
  202 FORMAT (' ','AN=',F6.2,'  BN=',F6.2,'  CN=',F6.2,'  DN=',F6.2,'  C
     1ATEGORY IS ',I2,'  NUMBER=',I6)
  203 FORMAT ('-',3X,'CATEGORY IS ',I2,10X,'UCATEG',10X,'SK MATRIX')
  204 FORMAT ('0',27X,F6.2,12X,F6.2,5X,F6.2,5X,F6.2,5X,F6.2)
  205 FORMAT ('-',3X,'CATEGORY IS ',I2,10X,'U1',14X,'SI MATRIX')
  206 FORMAT ('0',27X,F6.2,13X,F6.2,5X,F6.2,5X,F6.2,5X,F6.2)
  210 FORMAT (20A4)
  211 FORMAT (' ',3X,'CATEG=',I2,'  CLEN=',I2,'  MCOLL=',I2,'  MROWL=',I
     12,'  NREAD=',I2,'  HOWRED=',I2)
  212 FORMAT (' ',3X,'FOR CATEGORY=',I2,' THE SCALAR IS ZERO.',10X,'TI='
     1,4(3X,E14.7))
  215 FORMAT (E14.7,3X,E14.7,3X,E14.7,3X,E14.7,3X,I2,10X)
  223 FORMAT ('0',20X,'SCALA1=',F8.4,10X,'EIGENVALUE IS ',E14.7)
C
C     B, WORKV1, AND WORKV2 ARE VORK AREA VECTORS.
C     BUIK REFERS TO THE B(IK) IN THE ECV PAPER.
C     FLAG IS USED FOR A CONDITION CODE, WHEN A CATEGORY IS NOT USED.
C     FMT IS READ IN AS THE FORMAT OF THE INPUT MATRIX X.
C     S REFERS TO THE COVARIANCE MATRIX IN THE ECV PAPER.
C     SI REFERS TO THE S(I) MATRIX IN THE ECV PAPER.
C     SK REFERS TO THE S(K) IN THE ECV PAPER.
C     SKA IS THE SUM OF S(K) AND B(IK) IN THE ECV PAPER.
C     TI IS THE EIGENVECTOR WITH THE LARGEST EIGENVALUE.
C     U IS A MATRIX USED TO FIND THE MEAN.
C     UA IS THE DIFFERENCE OF U(I) AND U(K).
C     UCATEG REFERS TO THE U(I) IN THE ECV PAPER.
C     U1 AND U2 REFERS TO THE U(I) IN THE ECV PAPER.
C     X IS THE INPUT MATRIX STORAGE AREA.
      STOP
      END
//GO.SYSIN DD *
//GO.FT18F001  DD    DSN=COBLA2.ASHLAND.SEP19-72,DISP=SHR
  1     2     4     4     5
(I2,I2,I2,I2,I2)
```

```
C     THIS PROGRAM USES THE EIGENVECTORS AND MEAN VECTORS, FORMED IN AN EARLIER
C     PROGRAM, TO FIND MINIMUM VALUES FOR THE INPUT MATRIX.
      INTEGER   COUNT,FLAG,HOWRED,VECLEN
      INTEGER*2 COL,DEPTH,ROW
      INTEGER*2 CAT(99),CAT2(128,128),XDATA(5,128,128)
      DIMENSION AMEAN(99,4),DIFF(99,4),EVECT(99,4)
      DIMENSION FMT1(15),FMT2(15),FMT3(15),FMT4(15),FMT5(15)
      DIMENSION PROD(99),PROD2(128,128)
C     THE FIRST DATA CARD CONTAINS: CODE FOR TYPE OF INPUT AND OUTPUT,
C     THE DIMENSIONS OF THE INPUT DATA, AND THE NUMBER OF INPUT DATA BLOCKS.
      READ (5,200) NREAD,ROW,COL,DEPTH,NWRITE,NUMX,HOWRED
      WRITE (6,402) NREAD,ROW,COL,DEPTH,NWRITE,NUMX,HOWRED
C     READ THE INPUT AND OUTPUT FORMATS.
      READ (5,201) FMT1
      READ (5,201) FMT2
      READ (5,201) FMT3
      READ (5,201) FMT4
      READ (5,201) FMT5
      WRITE (6,411) FMT1
      WRITE (6,412) FMT2
      WRITE (6,413) FMT3
      WRITE (6,414) FMT4
      WRITE (6,415) FMT5
      VECLEN=ROW-1
      NUM=0
  100 COUNT=1
      NUM=NUM+1
C     READ THE EIGENVECTORS, THE MEAN, THE ASSOCIATED CATEGORY NUMBER, AND A FLAG.
  102 READ (NREAD,FMT1) (AMEAN(COUNT,I2),I2=1,VECLEN)
      READ (NREAD,FMT2) (EVECT(COUNT,I2),I2=1,VECLEN),CAT(COUNT),FLAG
C     PUT 999 IN COLUMNS 73-75 ON THE LAST DATA CARD AFTER CAT.
C     FLAG IS USED FOR ESCAPING FROM THE READ LOOP WHEN THE LAST EIGENVECTOR
C     IS READ.
      IF (FLAG.EQ.999) GO TO 151
      COUNT=COUNT+1
      GO TO 102
C
C     READ DATA IN THE FORM X(ROW,COL,DEPTH).
  151 IF (HOWRED.NE.1) GO TO 150
      READ (NREAD) XDATA
      GO TO 101
  150 READ(NREAD,FMT3)(((XDATA(I1,I2,I3),I1=1,ROW),I2=1,COL),I3=1,DEPTH)
  101 DO 300 K1=1,DEPTH
      DO 301 K3=1,COL
C     SET VALUE USED IN FINDING THE MINIMUM VALUE.
      PROD2(K1,K3)=999
      DO 302 I=1,COUNT
C     CALCULATE THE DIFFERENCE (DIFF) FOR EACH POINT.
      DO 303 K2=1,VECLEN
      DIFF(I,K2)=XDATA(K2+1,K3,K1)-AMEAN(I,K2)
  303 CONTINUE
C     CALCULATE THE SCALAR PRODUCTS.
      PROD(I)=0
      DO 305 J=1,VECLEN
  305 PROD(I)=PROD(I)+EVECT(I,J)*DIFF(I,J)
C     FIND MINIMUM PROD.
      IF (PROD(I).NE.PROD2(K1,K3)) GO TO 103
C     IF THE SCALAR IS EQUAL TO ANOTHER SCALAR FOR A POINT, PRINT BUT DON'T
C     CHANGE PROD2 OR CAT2.
      WRITE (6,401)
```

```
      WRITE (6,400) PROD(I),CAT(I),K1,K3,CAT2(K1,K3),I
      GO TO 302
  103 IF (PROD(I).GT.PROD2(K1,K3)) GO TO 302
C     SAVE THE MINIMUM PROD2 AND THE RESPECTIVE CATEGORY.
      PROD2(K1,K3)=PROD(I)
      CAT2(K1,K3)=CAT(I)
  302 CONTINUE
  301 CONTINUE
  300 CONTINUE
      WRITE (6,403) NUM
      WRITE (NWRITE,FMT4) ((PROD2(I2,I1),I1=1,COL),I2=1,DEPTH)
      WRITE (6,404)
      WRITE (NWRITE,FMT5) ((CAT2(I2,I1),I1=1,COL),I2=1,DEPTH)
      IF (NUM.NE.NUMX) GO TO 100
C
C     AMEAN IS THE MEAN VECTORS.
C     CAT IS A VECTOR WITH CATEGORY IDENTIFICATION FROM THE FIRST PROGRAM.
C     CAT2 IS USED TO STORE THE CATEGORY ASSOCIATED WITH THE MINIMUM PROD.
C     COL IS A DIMENSION OF THE INPUT MATRIX XDATA.
C     COUNT IS THE NUMBER OF EIGENVECTORS AND MEAN VECTORS.
C     DEPTH IS A DIMENSION OF THE INPUT MATRIX XDATA.
C     DIFF IS A VECTOR OF THE INPUT DATA MINUS THE MEANS.
C     EVECT IS THE EIGENVECTORS.
C     FLAG IS USED TO STOP A READ LOOP.
C     FMT1 IS THE FORMAT FOR READING AMEAN.
C     FMT2 IS THE FORMAT FOR READING EVECT, CAT, AND THE FLAG.
C     FMT3 IS THE FORMAT FOR READING THE INPUT DATA (XDATA).
C     FMT4 IS THE OUTPUT FORMAT FOR PROD2.
C     FMT5 IS THE OUTPUT FORMAT FOR CAT2.
C     HOWRED IS CODE FOR READING INPUT DATA, IF 1, READ FROM DISK FORMAT 40A2.
C     NREAD IS A CODE FOR THE TYPE OF INPUT.
C     NUM IS USED TO TEST FOR THE LAST DATA BLOCK.
C     NUMX IS THE NUMBER OF INPUT DATA BLOCKS.
C     NWRITE IS CODE FOR THE TYPE OF OUTPUT.
C     PROD IS THE SCALAR PRODUCT OF THE EVECT VECTOR AND DIFF VECTOR.
C     PROD2 IS USED TO STORE THE MINIMUM PRODUCT (PROD).
C     ROW IS A DIMENSION OF THE INPUT MATRIX XDATA.
C     VECLEN IS USED AS A LIMIT FOR LOOPS AND IS THE NUMBER OF LIGHT BANDS.
C     XDATA IS THE INPUT DATA.
C
  200 FORMAT (I3,3X,I3,3X,I3,3X,I3,3X,I3,3X,I3,3X,I3)
  201 FORMAT (20A4)
  400 FORMAT (' ',3X,'PROD=',F6.2,'   CAT=',I2,'   CAT2(',I2,',',I2,')=',
     1I2,'   I=',I2)
  401 FORMAT ('0',10X,'THERE ARE TWO EQUAL MINIMUM VALUES.')
  402 FORMAT ('1',3X,'NREAD=',I2,3X,'ROW=',I2,3X,'COL=',I2,3X,'DEPTH=',I
     12,3X,'NWRITE=',I2,3X,'NUMX=',I2,'   HOWRED=',I2)
  403 FORMAT ('0',6X,'MINIMUM F(X) MATRIX FROM DATA SET NUMBER',I3)
  404 FORMAT (' ',6X,'CATEGORY MATRIX')
  411 FORMAT (' ','        FMT1    ',20A4)
  412 FORMAT (' ','        FMT2    ',20A4)
  413 FORMAT (' ','        FMT3    ',20A4)
  414 FORMAT (' ','        FMT4    ',20A4)
  415 FORMAT (' ','        FMT5    ',20A4)
      STOP
      END

//GO.SYSIN DD*
```

```
//GO.FT18F001  DD    DSN=COBLA2.ASHLAND.SEP19-72,DISP=SHR
  5     5     4     4     6     1
(E14.7,3X,E14.7,3X,E14.7,3X,E14.7,15X)
(E14.7,3X,E14.7,3X,E14.7,3X,E14.7,3X,I2,2X,I3,5X)
(I2,I2,I2,I2,I2)
(' ',E14.7,3X,E14.7,3X,E14.7,3X,E14.7)
(' ',I2,3X,I2,3X,I2,3X,I2)
 0.1770000E+02    0.2250000E+02    0.1520000E+02    0.3050000E+02
 0.6687719E-01    0.1727624E-01   -0.5513757E-02   -0.8726493E-02    2  999
 22420 731
 220311828
 217191934
 214231227
 219231730
 2 9141224
 136301425
 23223 931
 213271133
 129281826
 127231533
 13224 934
 213222530
 216232237
 132251429
 13423 934
/*
```